TECHNICAL REPORT

ISO/TR 10400

First edition
2007-12-15

Petroleum and natural gas industries — Equations and calculations for the properties of casing, tubing, drill pipe and line pipe used as casing or tubing

Industries du pétrole et du gaz naturel — Équations et calculs relatifs aux propriétés des tubes de cuvelage, des tubes de production, des tiges de forage et des tubes de conduites utilisés comme tubes de cuvelage et tubes de production

Reference number
ISO/TR 10400:2007(E)

ISO copyright office
Case postale 56 • CH-1211 Geneva 20
Tel. + 41 22 749 01 11
Fax + 41 22 749 09 47
E-mail copyright@iso.org
Web www.iso.org

Published in Switzerland

Contents

Page

Foreword

ISO (the International Organization for Standardization) is a worldwide federation of national standards bodies (ISO member bodies). The work of preparing International Standards is normally carried out through ISO technical committees. Each member body interested in a subject for which a technical committee has been established has the right to be represented on that committee. International organizations, governmental and non-governmental, in liaison with ISO, also take part in the work. ISO collaborates closely with the International Electrotechnical Commission (IEC) on all matters of electrotechnical standardization.

International Standards are drafted in accordance with the rules given in the ISO/IEC Directives, Part 2.

The main task of technical committees is to prepare International Standards. Draft International Standards adopted by the technical committees are circulated to the member bodies for voting. Publication as an International Standard requires approval by at least 75 % of the member bodies casting a vote.

In exceptional circumstances, when a technical committee has collected data of a different kind from that which is normally published as an International Standard ("state of the art", for example), it may decide by a simple majority vote of its participating members to publish a Technical Report. A Technical Report is entirely informative in nature and does not have to be reviewed until the data it provides are considered to be no longer valid or useful.

Attention is drawn to the possibility that some of the elements of this document may be the subject of patent rights. ISO shall not be held responsible for identifying any or all such patent rights.

ISO/TR 10400 was prepared by Technical Committee ISO/TC 67, *Materials, equipment and offshore structures for petroleum, petrochemical and natural gas industries*, Subcommittee SC 5, *Casing, tubing and drill pipe*.

This first edition of ISO/TR 10400 cancels and replaces ISO 10400:1993, which has been technically revised.

Introduction

Performance design of tubulars for the petroleum and natural gas industries, whether it is formulated by deterministic or probabilistic calculations, compares anticipated loads to which the tubular may be subjected to the anticipated resistance of the tubular to each load. Either or both the load and resistance may be modified by a design factor.

Both deterministic and probabilistic (synthesis method) approaches to performance properties are addressed in this Technical Report. The deterministic approach uses specific geometric and material property values to calculate a single performance property value. The synthesis method treats the same variables as random and thus arrives at a statistical distribution of a performance property. A performance distribution in combination with a defined lower percentile determines the final design equation.

Both the well design process itself and the definition of anticipated loads are currently outside the scope of standardization for the petroleum and natural gas industries. Neither of these aspects is addressed in this Technical Report. Rather, this text serves to identify useful equations for obtaining the resistance of a tubular to specified loads, independent of their origin. This Technical Report provides limit state equations (see annexes) which are useful for determining the resistance of an individual sample whose geometry and material properties are given, and design equations which are useful for well design based on conservative geometric and material parameters.

Whenever possible, decisions on specific constants to use in a design equation are left to the discretion of the reader.

Petroleum and natural gas industries — Equations and calculations for the properties of casing, tubing, drill pipe and line pipe used as casing or tubing

1 Scope

This Technical Report illustrates the equations and templates necessary to calculate the various pipe properties given in International Standards, including

— pipe performance properties, such as axial strength, internal pressure resistance and collapse resistance,

— minimum physical properties,

— product assembly force (torque),

— product test pressures,

— critical product dimensions related to testing criteria,

— critical dimensions of testing equipment, and

— critical dimensions of test samples.

For equations related to performance properties, extensive background information is also provided regarding their development and use.

Equations presented here are intended for use with pipe manufactured in accordance with ISO 11960 or API 5CT, ISO 11961 or API 5D, and ISO 3183 or API 5L, as applicable. These equations and templates may be extended to other pipe with due caution. Pipe cold-worked during production is included in the scope of this Technical Report (e.g. cold rotary straightened pipe). Pipe modified by cold working after production, such as expandable tubulars and coiled tubing, is beyond the scope of this Technical Report.

Application of performance property equations in this Technical Report to line pipe and other pipe is restricted to their use as casing/tubing in a well or laboratory test, and requires due caution to match the heat-treat process, straightening process, yield strength, etc., with the closest appropriate casing/tubing product. Similar caution should be exercised when using the performance equations for drill pipe.

This Technical Report and the equations contained herein relate the input pipe manufacturing parameters in ISO 11960 or API 5CT, ISO 11961 or API 5D, and ISO 3183 or API 5L to expected pipe performance. The design equations in this Technical Report are not to be understood as a manufacturing warrantee. Manufacturers are typically licensed to produce tubular products in accordance with manufacturing specifications which control the dimensions and physical properties of their product. Design equations, on the other hand, are a reference point for users to characterize tubular performance and begin their own well design or research of pipe input properties.

This Technical Report is not a design code. It only provides equations and templates for calculating the properties of tubulars intended for use in downhole applications. This Technical Report does not provide any guidance about loads that can be encountered by tubulars or about safety margins needed for acceptable design. Users are responsible for defining appropriate design loads and selecting adequate safety factors to develop safe and efficient designs. The design loads and safety factors will likely be selected based on historical practice, local regulatory requirements, and specific well conditions.

All equations and listed values for performance properties in this Technical Report assume a benign environment and material properties conforming to ISO 11960 or API 5CT, ISO 11961 or API 5D and ISO 3183 or API 5L. Other environments may require additional analyses, such as that outlined in Annex D.

Pipe performance properties under dynamic loads and pipe connection sealing resistance are excluded from the scope of this Technical Report.

Throughout this Technical Report tensile stresses are positive.

2 Conformance

2.1 Normative references

In the interests of worldwide application of this Technical Report, ISO/TC 67 has decided, after detailed technical analysis, that certain of the normative documents listed in Clause 3 and prepared by ISO/TC 67 or other ISO Technical Committees are interchangeable in the context of the relevant requirement with the relevant document prepared by the American Petroleum Institute (API), the American Society for Testing and Materials (ASTM) or the American National Standards Institute (ANSI). These latter documents are cited in the running text following the ISO reference and preceded by or, for example, “ISO XXXX or API YYYY”. Application of an alternative normative document cited in this manner will lead to technical results different from the use of the preceding ISO reference. However, both results are acceptable and these documents are thus considered interchangeable in practice.

2.2 Units of measurement

In this Technical Report, data are expressed in both the International System (SI) of units and the United States Customary (USC) system of units. For a specific order item, it is intended that only one system of units be used, without combining data expressed in the other system.

For data expressed in the SI, a comma is used as the decimal separator and a space as the thousands separator. For data expressed in the USC system, a dot (on the line) is used as the decimal separator and a space as the thousands separator.

3 Normative references

The following referenced documents are indispensable for the application of this document. For dated references, only the edition cited applies. For undated references, the latest edition of the referenced document (including any amendments) applies.

ISO 3183:2007, *Petroleum and natural gas industries — Steel pipe for pipeline transportation systems*

ISO 10405, *Petroleum and natural gas industries — Care and use of casing and tubing*

ISO 11960:2004, *Petroleum and natural gas industries — Steel pipes for use as casing or tubing for wells*

ISO 11961, *Petroleum and natural gas industries — Steel drill pipe*

ISO 13679, *Petroleum and natural gas industries — Procedures for testing casing and tubing connections*

ANSI-NACE International Standard TM0177, *Laboratory Testing of Metals for Resistance to Sulfide Stress Cracking and Stress Corrosion Cracking in H_2S Environments*

API 5B, *Threading, Gauging and Thread Inspection of Casing, Tubing, and Line Pipe Threads (US Customary Units)*

API RP 579, *Recommended Practice for Fitness-for-Service*, January 2000

API RP 5C1, *Recommended Practice for Care and Use of Casing and Tubing*

API RP 5C5, *Recommended Practice on Procedures for Testing Casing and Tubing Connections*

API 5CT, *Specification for Casing and Tubing*

API 5D, *Specification for Drill Pipe*

API 5L:2004, *Specification for Line Pipe*

BS 7910, *Guide to methods for assessing the acceptability of flaws in metallic structures*

4 Terms and definitions

For the purposes of this document, the following terms and definitions apply.

4.1
Cauchy stress
true stress
force applied to the surface of a body divided by the current area of that surface

4.2
coefficient of variance
dimensionless measure of the dispersion of a random variable, calculated by dividing the standard deviation by the mean

4.3
design equation
equation which, based on production measurements or specifications, provides a performance property useful in design calculations

NOTE A design equation can be defined by applying reasonable extremes to the variables in a limit state equation to arrive at a conservative value of expected performance. When statistically derived, the design equation corresponds to a defined lower percentile of the resistance probability distribution curve.

4.4
deterministic
approach which assumes all variables controlling a performance property are known with certainty

NOTE Pipe performance properties generally depend on one or more controlling parameters. A deterministic equation uses specific geometric and material property values to calculate a single performance property value. For design formulations, this value is the expected minimum.

4.5
ductile rupture
failure of a tube due to internal pressure and/or axial tension in the plastic deformation range

4.6
e
Euler's constant
2,718 281 828

4.7
effective stress
combination of pressure and axial stress used in this Technical Report to simplify equations

NOTE Effective stress as used in this Technical Report does not introduce a distinct, physically defined stress quantity. Effective stress is a dependent quantity, which is determined as a combination of axial stress, internal pressure, external pressure and pipe dimensions, and provides a convenient grouping of these terms in some equations. The effective stress is sometimes called the Lubinski fictitious stress.

4.8
engineering strain
dimensionless measure of the stretch of a deforming line element, defined as the change in length of the line element divided by its original length

4.9
engineering stress
force applied to the surface of a body divided by the original area of that surface

4.10
fracture pressure
internal pressure at which a tube fails due to propagation of an imperfection

4.11
inspection threshold
maximum size of a crack-like imperfection which is defined to be acceptable by the inspection system

4.12
J-integral
measure of the intensity of the stress-strain field near the tip of a crack

4.13
label 1
dimensionless designation for the size or specified outside diameter that may be used when ordering pipe

4.14
label 2
dimensionless designation for the mass per unit length or wall thickness that may be used when ordering pipe

4.15
limit state equation
equation which, when used with the measured geometry and material properties of a sample, produces an estimate of the failure value of that sample

NOTE A limit state equation describes the performance of an individual sample as closely as possible, without regard for the tolerances to which the sample was built.

4.16
logarithmic strain
dimensionless measure of the stretch of a deforming line element, defined as the natural logarithm of the ratio of the current length of the line element to its original length

NOTE Alternatively, the logarithmic strain can be estimated as the natural logarithm of one plus the engineering strain.

4.17
mass
label used to represent wall thickness of tube cross section for a given pipe size

4.18
pipe body yield
stress state necessary to initiate yield at any location in the pipe body

4.19
principal stress
stress on a principal plane for which the shear stress is zero

NOTE For any general state of stress at any point, there exist three mutually perpendicular planes at that point on which shearing stresses are zero. The remaining normal stress components on these three planes are principal stresses. The largest of these three stresses is called the maximum principal stress.

4.20
probabilistic method
approach which uses distributions of geometric and material property values to calculate a distribution of performance property values

4.21
synthesis method
probability approach which addresses the uncertainty and likely values of pipe performance properties by using distributions of geometric and material property values

NOTE These distributions are combined with a limit state equation to determine the statistical distribution of a performance property. The performance distribution in combination with a defined lower percentile determines the final design equation.

4.22
template
procedural guide consisting of equations, test methods and measurements for establishing design performance properties

4.23
TPI
threads per inch

NOTE 1 thread per inch = 0,039 4 threads per millimetre; 1 thread per millimetre = 25,4 threads per inch.

4.24
true stress-strain curve
plot of Cauchy stress (ordinate) vs. logarithmic strain (abscissa)

4.25
yield
permanent, inelastic deformation

4.26
yield stress bias
ratio of actual yield stress to specified minimum yield stress

5 Symbols

A hand-tight standoff

A_c empirical constant in historical API collapse equation

A_{crit} area of the weaker connection component at the critical cross section

A_{gbtj} critical dimension on guided bend test jig, denoted as dimension A in ISO 3183 or API 5L

A_{jc} area of the coupling cross section; $A_{jc} = \pi/4\ (W^2 - d_1^2)$

A_{jp} area of the pipe cross section under the last perfect thread

A_p area of the pipe cross section; $A_p = \pi/4\ (D^2 - d^2)$

$A_{p\ ave}$ average area of the pipe cross section; $A_{p\ ave} = \pi/4\ [D_{ave}^2 - (D_{ave} - 2\ t_{c\ ave})^2]$

A_s cross-sectional area of the tensile test specimen in square millimetres (square inches), based on specified outside diameter or nominal specimen width and specified wall thickness, rounded to the nearest 10 mm^2 (0.01 in^2), or 490 mm^2 (0.75 in^2) whichever is smaller

A_x maximum diameter at the extreme-line pin seal tangent point

a for a limit state equation, the maximum actual depth of a crack-like imperfection; for a design equation, the maximum depth of a crack-like imperfection that could likely pass the manufacturer's inspection system

a_N imperfection depth associated with a specified inspection threshold, i.e. the maximum depth of a crack-like imperfection that could reasonably be missed by the pipe inspection system. For example, for a 5 % imperfection threshold inspection in a 12,7 mm (0.500 in) wall thickness pipe, a_N = 0,635 mm (0.025 in)

$a_{t/D}$ average value of t/D ratios used in the regression

B specified inside diameter of the extreme-line connection, in accordance with API 5B

B_c empirical constant in historical API collapse equation

B_f maximum bearing face diameter, special bevel, in accordance with ISO 11960 or API 5CT

b Weibull shape parameter

C_c empirical constant in historical API collapse equation

C_{iR} random variable that represents model uncertainty

c tube curvature, the inverse of the radius of curvature to the centreline of the pipe

D specified pipe outside diameter

D_{ac} average outside diameter after cutting

D_{ave} average pipe outside diameter

D_{bc} average outside diameter before cutting

D_i inside diameter of extreme-line box upset, in accordance with API 5B

D_{max} maximum pipe outside diameter

D_{min} minimum pipe outside diameter

D_p extreme-line pin critical section outside diameter; $D_p = H_x + \delta - \varphi$

D_4 major diameter, in accordance with API 5B

d pipe inside diameter, $d = D - 2t$

d_b inside diameter of the critical section of the extreme-line box; $d_b = I_x + 2h_x - \Delta + \theta$

d_{iu} inside diameter of pin upset, in accordance with ISO 11960 or API 5CT

d_j extreme-line specified joint inside diameter, made up

d_{ou} inside diameter at end of upset pipe

d_{wall} inside diameter based on $k_{wall}\, t$; $d_{wall} = D - 2k_{wall}\, t$

d_1 diameter at the root of the coupling thread at the end of the pipe in the power-tight position

E Young's modulus

E_c pitch diameter, at centre of coupling

E_{ec} pitch diameter, at end of coupling

E_s pitch diameter, at plane of seal

E_0 pitch diameter, at end of pipe

E_1 pitch diameter at the hand-tight plane, in accordance with API 5B

E_7 pitch diameter, in accordance with API 5B

ec eccentricity

e_m mass gain due to end finishing

F_a axial force

F_{eff} effective axial force

F_c empirical constant in historical API collapse equation

F_{YAPI} axial force at yield, historical API equation

f degrees of freedom $= N_t - 1$

$f(\bar{x})$ joint probability density function of the variables in $\bar{x}$

f_{rn} root truncation of the pipe thread of API line pipe threads, as follows:
0,030 mm (0.001 2 in) for 27 TPI,
0,046 mm (0.001 8 in) for 18 TPI,
0,061 mm (0.002 4 in) for 14 TPI,
0,074 mm (0.002 9 in) for 11-1/2 TPI,
0,104 mm (0.004 1 in) for 8 TPI

f_u tensile strength of a representative tensile specimen

f_{uc} tensile strength of a representative tensile specimen from the coupling

f_{umn} specified minimum tensile strength

f_{umnc} specified minimum tensile strength of the coupling

f_{umnp} specified minimum tensile strength of the pipe body

f_{up} tensile strength of a representative tensile specimen from the pipe body

f_y yield strength of a representative tensile specimen

f_{yax} equivalent yield strength in the presence of axial stress

f_{ye} equivalent yield stress in the presence of axial stress

f_{ymn} specified minimum yield strength

f_{ymnc} specified minimum yield strength of the coupling

f_{ymnp} specified minimum yield strength of the pipe body

f_{ymx} specified maximum yield strength

f_{yp} yield strength of a representative tensile specimen from the pipe body

G_c empirical constant in historical API collapse equation

G_0 influence coefficient for fracture limit state FAD curve

G_1 influence coefficient for fracture limit state FAD curve

G_2 influence coefficient for fracture limit state FAD curve

G_3 influence coefficient for fracture limit state FAD curve

G_4 influence coefficient for fracture limit state FAD curve

g length of imperfect threads, in accordance with API 5B

$g(\bar{x})$ limit state function

H is the thread height of a round-thread equivalent Vee thread, as follows:
0,815 mm (0.032 1 in) for 27 TPI,
1,222 mm (0.048 1 in) for 18 TPI,
1,755 mm (0.069 1 in) for 14 TPI,
1,913 mm (0.075 3 in) for 11-1/2 TPI,
2,199 6 mm (0.086 60 in) for 10 TPI,
2,749 6 mm (0.108 25 in) for 8 TPI

Ht_{des} decrement factor, as given in Table F.9

Ht_{ult} a decrement factor

H_x maximum extreme-line root diameter at last perfect pin thread

h_B buttress thread height: 1,575 for SI units, 0.062 for USC units

h_n stress-strain curve shape factor

h_s round thread height

h_x minimum box thread height for extreme-line casing, as follows:
1,52 mm (0.060 in) for 6 TPI
2,03 mm (0.080 in) for 5 TPI

I moment of inertia of the pipe cross section; $I = \pi/64\ (D^4 - d^4)$

I_{ave} average moment of inertia of the pipe cross section; $I = \pi/64\ (D_{ave}{}^4 - (D_{ave} - 2\ t_{c\ ave})^4)$

I_B length from the face of the buttress thread coupling to the base of the triangle in the hand-tight position: 10,16 mm (0.400 in) for Label 1: 4-1/2; 12,70 mm (0.500 in) for sizes between Label 1: 5 and Label 1: 13-3/8, inclusive; and 9,52 mm (0.375 in) for sizes greater than Label 1: 13-3/8

I_x minimum extreme-line crest diameter of box thread at Plane H

J distance from end of pipe to centre of coupling in power-tight position, in accordance with API 5B

J_{Ic} fracture resistance of the material

J_{Imat} fracture resistance of the material in a particular environment

J_p polar moment of inertia of the pipe cross section; $J_p = \pi/32\ (D^4 - d^4)$

J_r stress intensity ratio based on the J-Integral

K stress intensity factor at the crack tip

K_{Imat} fracture toughness of a material in a particular environment

K_p ratio of internal pressure stress to yield strength, or $p_i\ D/(2\ f_{ymnp}\ t)$

K_r stress intensity ratio

k_A variable intermediate term in ISO 13679 or API RP 5C5 representation of von Mises yield criterion

k_a burst strength factor, having the numerical value 1,0 for quenched and tempered (martensitic structure) or 13Cr products and 2,0 for as-rolled and normalized products based on available test data; and the default value set to 2,0 where the value has not been measured. The value of k_a can be established for a specific pipe material based on testing

k_B variable intermediate term in ISO 13679 or API RP 5C5 representation of von Mises yield criterion

k_C variable intermediate term in ISO 13679 or API RP 5C5 representation of von Mises yield criterion

k_c constant used in elastic collapse equation

k_{dr} correction factor based on pipe deformation and material strain hardening, having the numerical value $[(1/2)^{n+1} + (1/\sqrt{3})^{n+1})]$

k_e bias factor for elastic collapse

$k_{e\ des}$ down-rating factor for design elastic collapse

k_{el} elongation constant, equal to 1942,57 for SI units and 625 000 for USC units

$k_{e\ uls}$ calibration factor for ultimate elastic collapse, 1,089

k_i factor used to determine minimum wall thickness for transverse impact specimens:
1,00 for full-size specimens
0,75 for three-quarter size specimens
0,50 for one-half size specimens

k_{lsl} length conversion factor, equal to 0,001 for SI units and 1/12 for USC units

k_m mass correction factor, 1,000 for carbon steel, 0,989 for martensitic chromium steel

k_n stress conversion factor, equal to $1{,}18 \times 10^{-4}$ MPa^{-1} for SI units and 8.12×10^{-7} psi^{-1} for USC units

k_{pi} upper quadrant geometry factor in ISO 13679 or API RP 5C5 representation of von Mises yield criterion

k_{po} lower quadrant geometry factor in ISO 13679 or API RP 5C5 representation of von Mises yield criterion

k_{wall} factor to account for the specified manufacturing tolerance of the pipe wall. For example, for a tolerance of −12,5 %, $k_{wall} = 0{,}875$

k_{wpe} mass per unit length conversion factor, equal to 0,024 661 5 for SI units and 10.69 for USC units

k_y bias factor for yield collapse

$k_{y\ des}$ down-rating factor for design yield collapse

$k_{y\ uls}$ calibration factor for ultimate yield collapse, 0,991 1

L length

L_c minimum length of full crest threads from end of pipe, in accordance with API 5B

L_{ef} length of pipe including end finish

L_{et} engaged thread length, [$= L_4 - M$] for nominal make-up, in accordance with API 5B

L_{eu} length from end of pipe to start of taper, in accordance with ISO 11960 or API 5CT

L_{iu} length of pin upset, in accordance with ISO 11960 or API 5CT

L_j length of a standard piece of pipe

L_r load ratio

L_1 length from the end of the pipe to the hand-tight plane, in accordance with API 5B

L_7 length of perfect threads, in accordance with API 5B

M specified outside diameter of the extreme-line connection; length from the face of the coupling to the hand-tight plane for line pipe and for round thread casing and tubing, in accordance with API 5B

M_b bending moment

m_c coupling mass

m_{cB} coupling mass of buttress thread casing

m_{crsb} coupling mass removed by special bevel

m_{csb} coupling mass with special bevel

m_{eu} length of box upset taper, in accordance with ISO 11960 or API 5CT

m_{exu} external upset mass

m_{eiu} external-internal upset mass

m_{irt} integral joint mass removed by threading and recessing

m_{inu} internal upset mass

m_{iu} length of pin upset taper, in accordance with ISO 11960 or API 5CT

m_{prt} pin mass removed by threading

m_{xbu} extreme-line pin upset mass

m_{xpu} extreme-line pin upset mass

m_{xrt} extreme-line mass removed by threading and recessing

m_{rt} mass removed by threading

mu	model uncertainty
N	number of thread turns make-up
N_L	coupling length, in accordance with ISO 11960 or API 5CT
N_t	number of tests
n	dimensionless hardening index used to obtain a curve fit (see B.2.3.3) of the true stress-strain curve derived from the uniaxial tensile test
O_x	minimum diameter at the extreme-line box seal tangent point
ov	ovality
P_j	joint strength
p	thread pitch 3,175 mm (0.125 in) for round thread casing 5,080 mm (0.200 in) for buttress thread casing
p_c	collapse pressure
p_{ci}	collapse pressure in the presence of internal pressure
p_{des}	design collapse pressure
p_{desi}	design collapse pressure corrected for internal pressure
$p_{des\ e}$	collapse pressure corrected for axial stress and internal pressure
p_e	elastic collapse term
p_{ec}	elastic collapse pressure difference
$p_{e\ des}$	design elastic collapse term
$p_{e\ ult}$	ultimate elastic collapse term
p_E	pressure for elastic collapse
p_{ht}	hydrostatic test pressure
p_i	internal pressure
p_{iF}	internal pressure at fracture
p_{iL}	internal pressure at leak
p_{iR}	internal pressure at ductile rupture of an end-capped pipe
p_{iRa}	p_{iR} adjusted for axial load and external pressure
p_{iYAPI}	internal pressure at yield for a thin tube
p_{iYc}	internal pressure at yield for coupling
p_{iYLc}	internal pressure at yield for a capped-end thick tube

p_{iYLo} internal pressure at yield for an open-ended thick tube

p_o external pressure

$p_{o\ ult}$ ultimate external pressure for collapse

p_P pressure for plastic collapse

p_{Pav} pressure for average plastic collapse

p_T pressure for transition collapse

p_{ult} ultimate collapse pressure

p_y yield collapse term

p_{yc} yield collapse pressure difference

$p_{y\ des}$ design yield collapse term

p_{yM} through-wall von Mises yield pressure difference

p_{Yp} pressure for yield strength collapse

$p_{y\ Tresca}$ Tresca yield pressure for collapse

$p_{y\ ult}$ ultimate yield collapse term

$p_{y\ vme}$ von Mises yield pressure for collapse

Q diameter of coupling recess, in accordance with API 5B

r radial coordinate, $(d/2) \leqslant r \leqslant (D/2)$

rs residual stress (compression at ID face is negative)

S distance between flattening plates

S_p standard error of estimate of the regression equation

s_{rn} root truncation of the pipe thread of round threads, 0,36 mm (0.014 in) for 10 TPI, 0,43 mm (0.017 in) for 8 TPI

$s_{t/D}$ standard deviation of t/D ratios used in the regression

T applied torque

T_d taper (on diameter)

t specified pipe wall thickness

t_{ave} actual average pipe wall thickness disregarding crack-like imperfections

$t_{c\ ave}$ actual average pipe wall thickness

$t_{c\ max}$ maximum pipe wall thickness

$t_{c\ min}$ minimum pipe wall thickness

t_{max} actual maximum pipe wall thickness disregarding crack-like imperfections

t_{min} actual minimum pipe wall thickness disregarding crack-like imperfections

t_p tolerance interval corresponding to a confidence level of p that the proportion of the population not included does not exceed

W specified coupling outside diameter, in accordance with ISO 11960 or API 5CT

u_p fractile corresponding to confidence level p

$u_{1-\theta}$ fractile, the deviation from the mean of a standardized normal cumulative distribution that includes the fraction $1 - \theta_p$ of the population

W_L calculated mass of a piece of pipe of length L

w_{ij} upset and threaded mass per unit length

w_{pe} plain-end mass per unit length

w_{tc} threaded and coupled mass per unit length

w_u upset mass per unit length

$\vec{x}$ vector of random variables

Z_p correction factor for variation in t/D from average

Δ taper drop in extreme-line pin perfect thread length
6,43 mm (0.253 in) for 6 TPI
5,79 mm (0.228 in) for 5 TPI

α sensitivity factor

β first-order reliability index

δ extreme-line taper rise between Plane H and Plane J, as follows:
0,89 mm (0.035 in) for 6 TPI
0,81 mm (0.032 in) for 5 TPI

φ one-half of the maximum extreme-line seal interference, $\varphi = (A_x - O_x)/2$

ε_{eng} engineering strain

ε_{el} minimum gauge length extension in 50,8 mm (2.0 in), in percent, rounded to the nearest 0,5 % below 10 % and to the nearest unit percent for 10 % and larger

ε_{ln} logarithmic strain

ε_{ymn} strain at which specified minimum yield strength is determined

μ mean

μ_{ec} mean calculated eccentricity as a percent, [eccentricity = 100 $(t_{c\,max} - t_{c\,min})/t_{c\,ave}$]

μ_{fy} mean calculated f_y as a percent

μ_{ov} mean calculated ovality as a percent, [ovality = 100 $(D_{max} - D_{min})/D_{ave}$]

μ_{rs} mean calculated residual stress (compression at ID face is negative)

ν Poisson's ratio

π circumference of a circle divided by its diameter, assigned a value of 3,141 6

ϕ_f probability of failure

θ one-half of the extreme-line maximum thread interference, $\theta = (H_x - I_x)/2$

θ_p the proportion of the population not included

σ standard deviation

σ_a component of axial stress not due to bending

σ_b component of axial stress due to bending

σ_c true (Cauchy) stress

σ_e equivalent stress

σ_{eff} effective stress

σ_f fibre stress corresponding to the percent of specified yield strength as given in Table 12

σ_h circumferential or hoop stress

σ_{pmx} maximum principal stress

σ_r radial stress

σ_{res} residual stress

σ_{th} threshold stress

σ_{ye} equivalent yield strength in the presence of axial tension

σ_{ymne} equivalent minimum yield strength in the presence of axial tension

τ_{ha} torsional (shear) stress

6 Triaxial yield of pipe body

6.1 General

The criterion for triaxial pipe body yield is that proposed by von Mises. The elastic state leading to incipient yield consists of the superposition of

a) radial and circumferential stress as determined by the Lamé Equations for a thick cylinder,

b) uniform axial stress due to all sources except bending,

c) axial bending stress for a Timoshenko beam,

d) torsional shear stress due to a moment aligned with the axis of the pipe.

Details of the derivation of the design equation can be found in Annex A.

6.2 Assumptions and limitations

6.2.1 General

Equations (1) to (7) are based on the assumptions given in 6.2.2 to 6.2.5.

6.2.2 Concentric, circular cross-sectional geometry

The equations for radial stress, circumferential or hoop stress, bending and torsion presume the pipe cross section to consist of inner and outer surfaces that are circular and concentric.

6.2.3 Isotropic yield

The yield strength of the material of which the pipe is composed is assumed to be independent of direction. An axial sample and a circumferential sample are assumed to possess identical elastic moduli and yield stress in both tension and compression.

6.2.4 No residual stress

For determination of the onset of yield, residual stresses due to manufacturing processes are assumed to be negligible, and are ignored.

6.2.5 Cross-sectional instability (collapse) and axial instability (column buckling)

Particularly in instances where $p_o > p_i$, it is possible for the pipe cross section to collapse due to instability prior to yield. For external pressure greater than internal pressure, see Clause 8 on collapse. Similarly, if $\sigma_{eff} < 0$, it is possible for the pipe to buckle as a column prior to yield, and the bending stress due to buckling should be included in the yield check.

6.3 Data requirements

The following input data are required to complete the calculation for triaxial yield of the pipe body:

c tube curvature, the inverse of the radius of curvature to the centreline of the pipe;

D specified pipe outside diameter;

E Young's modulus;

F_a axial force;

f_{ymn} specified minimum yield strength;

k_{wall} factor to account for the specified manufacturing tolerance of the pipe wall. For example, for a tolerance of −12,5 %, $k_{wall} = 0{,}875$;

p_i internal pressure;

p_o external pressure;

T applied torque;

t specified pipe wall thickness.

6.4 Design equation for triaxial yield of pipe body

The onset of yield is defined as

$$\sigma_e = f_{ymn} \tag{1}$$

where $\sigma_e < f_{ymn}$ corresponds to elastic behaviour, and

f_{ymn} is the specified minimum yield strength;

σ_e is the equivalent stress.

The equivalent stress is defined as

$$\sigma_e = [\sigma_r^2 + \sigma_h^2 + (\sigma_a + \sigma_b)^2 - \sigma_r\sigma_h - \sigma_r(\sigma_a + \sigma_b) - \sigma_h(\sigma_a + \sigma_b) + 3\tau_{ha}^2]^{1/2} \tag{2}$$

with

$$\sigma_r = [(p_i d_{wall}^2 - p_o D^2) - (p_i - p_o) d_{wall}^2 D^2/(4r^2)]/(D^2 - d_{wall}^2) \tag{3}$$

$$\sigma_h = [(p_i d_{wall}^2 - p_o D^2) + (p_i - p_o) d_{wall}^2 D^2/(4r^2)]/(D^2 - d_{wall}^2) \tag{4}$$

$$\sigma_a = F_a/A_p \tag{5}$$

$$\sigma_b = \pm M_b r/I = \pm Ecr \tag{6}$$

$$\tau_{ha} = Tr/J_p \tag{7}$$

where

A_p is the area of the pipe cross section, $A_p = \pi/4\ (D^2 - d^2)$;

c is the tube curvature, the inverse of the radius of curvature to the centreline of the pipe;

D is the specified pipe outside diameter;

d is the pipe inside diameter, $d = D - 2t$;

d_{wall} is the inside diameter based on $k_{wall}\ t$, $d_{wall} = D - 2k_{wall}\ t$;

E is Young's modulus;

F_a is the axial force;

I is the moment of inertia of the pipe cross section, $I = \pi/64\ (D^4 - d^4)$;

J_p is the polar moment of inertia of the pipe cross section, $J_p = \pi/32\ (D^4 - d^4)$;

k_{wall} is the factor to account for the specified manufacturing tolerance of the pipe wall. For example, for a tolerance of –12,5 %, $k_{wall} = 0{,}875$;

M_b is the bending moment;

p_i is the internal pressure;

p_o is the external pressure;

r is the radial coordinate, $(d/2) \leqslant r \leqslant (D/2)$ for σ_a, σ_b and τ_{ha}, $(d_{wall}/2) \leqslant r \leqslant (D/2)$ for σ_r and σ_h;

T is the applied torque;

t is the specified pipe wall thickness;

σ_a is the component of axial stress not due to bending;

σ_b is the component of axial stress due to bending;

σ_e is the equivalent stress;

σ_h is the circumferential or hoop stress;

σ_r is the radial stress;

τ_{ha} is the torsional (shear) stress.

The $\pm$ sign in Equation (6) indicates that the component of axial stress due to bending can be positive (tension) or negative (compression), depending on the location of the point in the cross section. Points in the pipe cross section closer to the centre of tube curvature than the centreline of the pipe experience compressive bending stress. Points in the pipe cross section farther from the centre of tube curvature than the centreline of the pipe experience tensile bending stress.

The variable c has units of radian/length, which are not the norm for the petroleum industry. The more common measure of c in the industry is °/30 m (°/100 ft). If, therefore, the required units for c are radians/metre, and c is expressed in °/30 m (°/100 ft), the right-hand side of Equation (6) should be multiplied by the constant $\pi/(180 \times 30) = 5{,}817\ 8 \times 10^{-4}$ rad-m/°–30 m [$\pi/(180 \times 100) = 1{,}645\ 3 \times 10^{-4}$ rad-ft/°–100 ft].

In the presence of bending, Equation (2) should be evaluated four times, i.e. at the inner and outer radii on both the tensile and compressive sides of the cross section. In the presence of torsion, Equation (2) should be evaluated two times, i.e. at the inner and outer radii. In the absence of both bending and torsion, Equation (2) should be evaluated once, at the minimum value of the radius. In all cases, the maximum computed value of σ_e should be used in Equation (1).

The purpose of the design equation is to determine the stress state which results in the onset of pipe yield when the properties of the pipe are at their worst-case, minimum allowable values. The wall thickness of the pipe at all times accounts for the extreme allowable thin-wall eccentricity which comes about naturally as part of the pipe manufacturing process.

6.5 Application of design equation for triaxial yield of pipe body to line pipe

The pipe body yield strength of line pipe can be calculated by means of equations presented in this clause, minding the limitations given in 6.2.

6.6 Example calculations

6.6.1 Initial yield of pipe body, Lamé Equation for pipe when external pressure, bending and torsion are zero

The Lamé Equations for the radial and hoop stresses of the pipe are based on the three-dimensional equations of equilibrium for a linear elastic cross section. As such, these equations are triaxial equations and provide the most accurate calculation of pipe stresses. Two equations are provided, open-end with zero axial stress, and closed-end with axial stress due to internal pressure acting on the end cap.

6.6.1.1 Yield design equation, special case for capped-end conditions

Initial yield of a capped-end thick tube is a special case of Equations (1) and (2) when external pressure, bending and torsion are zero. The axial stress is generated solely by the action of internal pressure on the ends of the sample (e.g. the capped-end condition.)

A design equation for initial yield of the pipe body with capped-end conditions and using the Lamé Equations for the radial and hoop stresses should be formulated from Equation (2), evaluated at the inner diameter. The resulting design equation is

$$p_{iYLc} = f_{ymn}/\{(3\,D^4 + d_{wall}{}^4)/(D^2 - d_{wall}{}^2)^2 + d^4/(D^2 - d^2)^2 - 2d^2 d_{wall}{}^2/[(D^2 - d^2)\,(D^2 - d_{wall}{}^2)]\}^{1/2} \quad (8)$$

where

D is the specified pipe outside diameter;

d is the pipe inside diameter, $d = D - 2t$;

d_{wall} is the inside diameter based on $k_{wall}\,t$, $d_{wall} = D - 2k_{wall}\,t$;

f_{ymn} is the specified minimum yield strength;

k_{wall} is the factor to account for the specified manufacturing tolerance of the pipe wall. For example, for a tolerance of −12,5 %, $k_{wall} = 0{,}875$;

p_{iYLc} is the internal pressure at yield for a capped-end thick tube;

t is the specified pipe wall thickness.

There is no adjustment to Equation (8) for axial tension, as all axial tension is generated by the action of internal pressure on the (closed) ends of the pipe. The more general case, where axial stress is generated by other than the action of internal pressure on the ends of the pipe, is addressed by the triaxial yield criterion, Equations (1) and (2).

6.6.1.2 Yield design equation, special case for internal pressure with zero axial load

Initial yield of an open-ended thick tube is a special case of Equations (1) and (2) when the uniform axial stress, external pressure, bending and torsion are zero.

A design equation for initial yield of the pipe body with open-end conditions and using the Lamé Equations for the radial and hoop stresses should be formulated from Equation (2) evaluated at the inner diameter. The resulting design equation is

$$p_{iYLo} = f_{ymn}(D^2 - d_{wall}{}^2)/(3\,D^4 + d_{wall}{}^4)^{1/2} \quad (9)$$

where

D is the specified pipe outside diameter;

d_{wall} is the inside diameter based on $k_{wall}\,t$, $d_{wall} = D - 2k_{wall}\,t$;

f_{ymn} is the specified minimum yield strength;

k_{wall} is the factor to account for the specified manufacturing tolerance of the pipe wall. For example, for a tolerance of −12,5 %, $k_{wall} = 0{,}875$;

p_{iYLo} is the internal pressure at yield for an open-end thick tube;

t is the specified pipe wall thickness.

The more general case, where axial stress is non-zero, is addressed by the triaxial yield criterion, Equations (1) and (2).

6.6.2 Initial yield pressure of pipe body, historical API equation

6.6.2.1 General

The Barlow Equation for pipe yield, which is the historical API equation, is based on a one-dimensional (not triaxial) approximate equation of the von Mises yield condition, combined with an approximate expression for the hoop stress in the pipe. In essence, the Barlow Equation approximates the hoop stress and then equates this approximation to the yield strength. This approximation is less accurate than the Lamé Equation of yield discussed in 6.6.1. Because the Barlow Equation neglects axial stress, there is no distinction between pipe with capped ends, pipe with open ends or pipe with tension end load.

6.6.2.2 Historical, one-dimensional yield pressure design equation

Initial yield of a thin tube is defined by the following expression:

$$p_{\text{iYAPI}} = [2f_{\text{ymn}}(k_{\text{wall}}t)/D] \tag{10}$$

where

D is the specified pipe outside diameter;

f_{ymn} is the specified minimum yield strength;

k_{wall} is the factor to account for the specified manufacturing tolerance of the pipe wall. For example, for a tolerance of −12,5 %, $k_{\text{wall}} = 0{,}875$;

p_{iYAPI} is the internal pressure at yield for a thin tube;

t is the specified pipe wall thickness.

This equation is subject to the same assumptions and limitations as the more general expressions from which it may be derived (by methods other than that used by Barlow) (see 6.2).

6.6.3 Pipe body yield strength, historical API equation

6.6.3.1 General

Pipe body yield strength is the axial load required to yield the pipe in the absence of internal and external pressure, bending and torsion. It is taken as the product of the cross-sectional area and the specified minimum yield strength for the particular grade of pipe:

$$F_{\text{YAPI}} = f_{\text{ymn}} A_{\text{p}} \tag{11}$$

where

A_{p} is the area of the pipe cross section, $A_{\text{p}} = \pi/4\ (D^2 - d^2)$;

D is the specified pipe outside diameter;

d is the pipe inside diameter, $d = D - 2t$;

F_{YAPI} is the axial force at yield, historical API equation;

f_{ymn} is the specified minimum yield strength;

t is the specified pipe wall thickness.

6.6.4 Yield in the absence of bending and torsion

If bending and torsion are zero, Equation (2) reduces to

$$\sigma_e = [\sigma_r^2 + \sigma_h^2 + \sigma_a^2 - \sigma_r\sigma_h - \sigma_r\sigma_a - \sigma_h\sigma_a]^{1/2} \quad (12)$$

Consider, for example, the case of a tube being lowered open-ended into a vertical well full of fluid with mass density 1,080 kg/dm^3 (9 lb/gal). The internal and external pressure at any depth are equal, and the bottom of the tube is exposed to an axial compression equal to the product of the fluid pressure and the tube cross-sectional area. Ignoring connections, let the tube be of outside diameter 244,48 mm (9.625 in), of wall thickness 13,84 mm (0.545 in) and have $k_{wall} = 0{,}875$. Assume the mass density of steel is 7,85 kg/dm^3 (0.283 3 lb/in^3). Compute the yield state of the uppermost cross section of the tube when the tube is at a depth of 3 000 m (9 842.5 ft). The tube has a minimum yield stress of 551,6 MPa (80 000 psi).

Table 1 presents the results of the calculation in both SI and USC units.

Table 1 — Example calculations — Yield in the absence of bending and torsion

Term	SI		USC	
	Value	Units	Value	Units
Load				
F_a	1 995 717	N	448 655	lb
p_i	31,73	MPa	4 601	psi
p_o	31,73	MPa	4 601	psi
c	0	°/30 m	0	°/100 ft
T	0	N-m	0	ft-lb
Geometry				
D	244,48	mm	9.625	in
t	13,84	mm	0.545	in
k_{wall}	0,875		0.875	
Material				
E	206 842	MPa	30 000 000	psi
Calculations				
d	216,80	mm	8.535	in
d_{wall}	220,26	mm	8.671	in
A_p	10 028	mm^2	15.55	in^2
I	66 920 762	mm^4	160.8	in^4
J_p	133 841 524	mm^4	321.6	in^4
σ_a	199,01	MPa	28 859	psi
Inner radius				
σ_b	0	MPa	0	psi
σ_h	–31,73	MPa	–4 602	psi
σ_r	–31,73	MPa	–4 602	psi
τ_{ha}	0	MPa	0	psi
σ_e, σ_b+	230,74	MPa	33 461	psi
σ_e, σ_b–	230,74	MPa	33 461	psi
Outer radius				
σ_b	0	MPa	0	psi
σ_h	–31,73	MPa	–4 602	psi
σ_r	–31,73	MPa	–4 602	psi
τ_{ha}	0	MPa	0	psi
σ_e, σ_b+	230,74	MPa	33 461	psi
σ_e, σ_b–	230,74	MPa	33 461	psi

Since both bending and torsion are zero in this example, there is no need to calculate σ_e at both the inner and outer radii of the tube, as yield will always occur at the inner radius. The calculations have been included here for completeness.

As the equivalent stress is less than the yield stress, the tube does not yield at its uppermost cross section.

7 Ductile rupture of the pipe body

7.1 General

The equations for ductile rupture pertain to the actual failure of the pipe body due to internal pressure. While the yield equations of Clause 6 are intended to describe the onset of permanent plastic deformation and not loss of pressure integrity, the rupture equations are intended to describe the ultimate pressure capacity of the pipe at a pressure which fails the pipe body with loss of internal pressure integrity.

The equations for ductile rupture depend on the minimum physical wall thickness, the pipe outer diameter, the maximum depth of imperfections which have a reasonable probability of passing through the inspection process undetected, the fracture toughness of the material, the work hardening of the material and the ultimate tensile strength of the pipe. Yield strength has no direct impact on the ductile rupture pressure except through the correlation of the work hardening parameter n.

The ductile rupture equations can be derived from the mechanics of pipe equilibrium combined with a model of pipe plasticity and a model of the effect of imperfections. The selection of the basic equation, the application of the basic equation to ISO/API tubular products, and the verification of the equation with actual test data are discussed in detail in Annex B. The ductile rupture limit state and design equations consist of three interlinked concepts:

a) an equation for equilibrium-plasticity based rupture of a pipe with known physical wall thickness and diameter;

b) reduction in performance due to wall loss in proportion to depths of imperfections which may not be detected by the manufacturing and inspection system;

c) a criterion for minimum toughness at which ductile rupture applies.

These equations are applicable to direct pressure and axial loading, but do not describe the capacity of the pipe under fatigue loading. The subtraction to the pipe wall for the presence of imperfections and the interrelated role of pipe toughness are based on a fracture mechanics approach relating J_{Ic} toughness measurements of sample pipes to numerically calculated crack-tip intensities (J-Integrals) as a function of imperfection depth. This is explained in detail in Annex B.

7.2 Assumptions and limitations

These equations are applicable only when the pipe material in its environment has sufficient toughness to meet a minimum criterion such that the deformation of the pipe, in its environment, through to rupture is ductile and not brittle, even in the presence of small imperfections.

Bending stresses (for instance, due to buckling or bending due to curvature of the well trajectory) are not included in the equation for ductile rupture pressure. Hence, the ductile rupture equation may not apply to pipe which is buckled (nor to pipe in a dogleg).

7.3 Data requirements

7.3.1 General

The following input data are required to complete the calculation for ductile rupture of the pipe body:

a_N imperfection depth associated with a specified inspection threshold, i.e. the maximum depth of a crack-like imperfection that could reasonably be missed by the pipe inspection system. For example, for a 5 % imperfection threshold inspection in a 12,7 mm (0.500 in) wall thickness pipe, $a_N = 0{,}635$ mm (0.025 in);

D specified pipe outside diameter;

f_{umn} specified minimum tensile strength;

k_a burst strength factor, having the numerical value 1,0 for quenched and tempered (martensitic structure) or 13Cr products and 2,0 for as-rolled and normalized products based on available test data; and the default value set to 2,0 where the value has not been measured. The value of k_a can be established for a specific pipe material based on testing;

k_{wall} factor to account for the specified manufacturing tolerance of the pipe wall. For example, for a tolerance of −12,5 %, $k_{wall} = 0{,}875$;

n dimensionless hardening index used to obtain a curve fit (see B.2.3.3) of the true stress-strain curve derived from the uniaxial tensile test;

t specified pipe wall thickness.

7.3.2 Determination of the hardening index

In the absence of stress-strain information, the following values of n are suggested.

Table 2 — Suggested values for hardening index in ductile rupture equation

API grade	n
H40	0,14
J55	0,12
K55	0,12
M65	0,12
N80	0,10
L80 Type 1	0,10
L80 Chrome	0,10
C90	0,10
C95	0,09
T95	0,09
P110	0,08
Q125	0,07

If the grade of the material is unknown but is not high-hardening, the hardening index can alternatively be determined from the following correlation.

$$n = 0{,}1693 - k_n f_y \quad (13)$$

where f_y has units of MPa (psi) and

f_y is the yield strength of a representative tensile specimen;

k_n is the stress conversion factor, equal to $1{,}18 \times 10^{-4}$ MPa^{-1} for SI units and 8.12×10^{-7} psi^{-1} for USC units;

n is the dimensionless hardening index used to obtain a curve fit (see B.2.3.3) of the true stress-strain curve derived from the uniaxial tensile test.

The effort expended to determine n should be weighed against the fact that the equation for ductile rupture is relatively insensitive to this quantity for commonly used Oil Country Tubular Goods (OCTG). However, if a high-hardening material such as duplex steel is used, it is important to determine n to avoid a non-conservative rupture strength prediction. Values of n for these materials can be as high as 0,30.

7.3.3 Determination of the burst strength factor, k_a

7.3.3.1 General

The burst strength factor k_a quantifies the impact that the material toughness has on ductile rupture when a crack of depth a_N is present. The value of k_a does not need to be determined for each pipe order; instead, it is recommended that k_a be determined for a fixed tubular product line with a fixed process control plan. For a material with high material toughness, k_a will be 1,0 or lower, and the influence the crack has on the ductile rupture pressure will be no greater than the depth of the crack. However, for a pipe material with lower material toughness, k_a can be larger, say 2,0, so that the penalty from having the crack is as though the crack had twice its actual depth.

When k_a has not been determined for the pipe material, use a k_a value of 2,0. The value of k_a has been measured to be 1,0 for quenched and tempered (martensitic structure) pipe and for 13Cr products. The value of k_a can be established for a specific pipe material based on testing. One of two methods presented below can be used to calculate k_a.

7.3.3.2 Analytical method for determining k_a

The following procedure should be used.

a) Construct a finite element model of a pipe with three separate cases of crack depth: zero, 5 %, and 12,5 %. Model the crack as an infinitely long, longitudinal crack on the ID of the pipe. In the finite element model, use the specified pipe wall thickness (do not reduce the pipe wall for manufacturing eccentricity) and a typical stress-strain curve for the material being analysed.

b) Use the finite element model to simulate applying internal pressure to the pipe model in order to calculate the value of the J-integral of the pipe as a function of internal pressure (see B.7.2 for examples).

c) Experimentally measure the critical J_{1c} value of the pipe material in air. J_{1c} is a parameter similar to K_{1c}, but based on a different type of test. See ASTM E1152-95 [1] for the precisely defined test methodology.

d) Terminate each of the finite element J-integral curves at the critical value of J_{1c} measured in the test. The internal pressure corresponding to this terminal point (where the J-integral equals J_{1c}) represents the rupture pressure in the presence of the crack, for a material with toughness reflected by J_{1c}.

e) Next, divide the rupture pressure for pipe with a crack depth 5 % by the rupture pressure for pipe with no crack, using the finite element results combined with the J_{1c} measurement. Next, set this ratio equal to $(1\text{-}k_a a/t)$ where a/t is the ratio of the crack depth to the specified pipe wall thickness (i.e. 5 % in this case). Solve this equation for the value of k_a.

f) Repeat the above calculation using the finite element model results for the crack with 12,5 % depth.

g) Average the two values of k_a from steps e) and f) and use the average in the rupture equation.

7.3.3.3 Experimental method for determining k_a

An alternative way to measure k_a in lieu of the J_{1c} measurement and the finite element calculation is to conduct full-scale pipe burst tests using a pipe with no measurable crack-like imperfection, another pipe with a crack-like imperfection of 5 % depth, and another pipe with a crack-like imperfection of 12,5 % depth. Then construct the ratios of the rupture pressures as described above and calculate k_a. The limitation and difficulty with this approach is that it is not valid unless the imperfection is sharp, and crack-like. A mechanical or EDM notch is not adequate for this purpose. This means that the crack-like imperfection needs to be generated either as part of the pipe manufacturing process or else through fatigue precracking. In general, the finite element approach combined with the J_{1c} measurement is easier to pursue.

7.3.3.4 Sensitivity of k_a

It turns out that k_a is a weakly sensitive parameter in regard to the grade of the pipe; that is, k_a primarily depends on the manufacturing process and does not vary much by grade within a fixed process. This is understandable since k_a only represents a potential amplification of the pipe's response to the presence of the crack while being loaded to rupture. Because of this, it is recommended that k_a only be determined for a specific grade of product and not for specific sizes or orders of product.

7.4 Design equation for capped-end ductile rupture

Minimum ductile rupture of a tube is defined by:

$$p_{iR} = 2k_{dr}f_{umn}(k_{wall}t - k_a a_N)/[D - (k_{wall}t - k_a a_N)] \quad (14)$$

where

a_N is the imperfection depth associated with a specified inspection threshold, i.e. the maximum depth of a crack-like imperfection that could reasonably be missed by the pipe inspection system. For example, for a 5 % imperfection threshold inspection in a 12,7 mm (0.500 in) wall thickness pipe, $a_N = 0{,}635$ mm (0.025 in);

D is the specified pipe outside diameter;

f_{umn} is the specified minimum tensile strength;

k_a is the burst strength factor, having the numerical value 1,0 for quenched and tempered (Martensitic structure) or 13Cr products and 2,0 for as-rolled and normalized products based on available test data; and the default value set to 2,0 where the value has not been measured. The value of k_a can be established for a specific pipe material based on testing;

k_{dr} is the correction factor based on pipe deformation and material strain hardening, having the numerical value $[(1/2)^{n+1} + (1/\sqrt{3})^{n+1})]$;

k_{wall} is the factor to account for the specified manufacturing tolerance of the pipe wall. For example, for a tolerance of –12,5 %, $k_{wall} = 0{,}875$;

n is the dimensionless hardening index used to obtain a curve fit (see B.2.3.3) of the true stress-strain curve derived from the uniaxial tensile test;

p_{iR} internal pressure at ductile rupture of an end-capped pipe;

t specified pipe wall thickness.

The value selected for k_{dr} renders p_{iR} the average of rupture pressures predicted using Tresca's yield condition and von Mises' yield condition.

The factor k_{wall} addresses minimum pipe body wall thickness without considering imperfections. This value may be adjusted if minimum wall is guaranteed by a particular process or purchasing agreement.

Crack-like imperfections are accounted for by a_N. The term $k_a a_N$ represents a further reduction in minimum wall thickness associated with crack-like imperfections which are outside the sensitivity setting of the inspection equipment and assumed coincident with the location of minimum wall thickness. This stacking of minimum wall thickness and a crack-like imperfection depends on the frequency of occurrence of thin wall and the frequency of occurrence of sharp-bottomed imperfections approaching the depth of the inspection threshold.

For the deterministic calculation of rupture pressure, it is necessary to calculate a conservative ductile rupture design pressure. In this case, the frequency of occurrence of the imperfection is set to 100 % and the imperfection depth equals the inspection threshold.

For the probabilistic calculation of rupture pressure (see Annex B), the depth of the imperfection still equals the depth of the inspection threshold, but the calculation takes account of the actual frequency of occurrence of thin wall and the actual frequency of occurrence of sharp-bottomed imperfections with depth comparable to the inspection threshold.

7.5 Adjustment for the effect of axial tension and external pressure

7.5.1 General

The ductile rupture strength Equation (14) was developed for the situation of an end-capped pipe, where the axial tension is determined by the internal pressure acting on the closed inner pipe surface area. This is a special case of a more general situation where a pipe may reach a maximum internal pressure load, that is a rupture load, under the simultaneous action of arbitrary external pressure and arbitrary axial tension or compression. The combined loads together determine when the pipe is going to yield and how it will plastically deform towards the point of rupture. A fundamental criterion when this rupture load is attained can still be expressed, but this will now be a more involved equation governed by the formulation of the von Mises or Tresca yield surface in terms of axial stress, radial stress and hoop stress.

Moreover, rupture is the prevailing failure mechanism only if the axial tension is not too large. For large axial tension and smaller internal over-pressure, a maximum axial load (a precursor to necking and axial splitting of the pipe) is reached before the maximum pressure phenomenon occurs.

Below, equations for both rupture and necking under combined loads are described, together with a criterion to identify which phenomenon occurs first. The equation is given in terms of "effective axial tension" associated with "effective axial stress" defined in A.1.3.2.4. For effective axial tension, these approximate equations are very accurate when compared to the exact theoretical equation [24]; performance against combined loading test data is given in B.6.2.

For negative values of effective axial tension, i.e. effective axial compression, the pipe can buckle as a column, depending on the quality of lateral support. If buckling is adequately suppressed, the equation for rupture under combined loads is valid also for effective axial compression. However, for higher values of effective axial compression, it is the phenomenon of local buckling of the pipe wall ("wrinkling") that presents the governing failure mechanism. Therefore, there exists a value of effective axial compression that limits the validity of the exact combined loading rupture equation.

7.5.2 Design equation for ductile rupture under combined loads

In the presence of external pressure and axial tension or compression different from capped-end conditions, the general equation for ductile rupture is

$$p_{iRa} = p_o + \min[1/2(p_M + p_{ref\,T}), p_M] \quad (15)$$

with

$$p_M = p_{ref\,M}\,[1 - k_R\,(F_{eff}/F_{uts})^2]^{1/2} \quad (16)$$

where

$$F_a = \pi\,t\,(D - t)\,\sigma_a \quad (17)$$

$$F_{eff} = F_a + p_o\,\pi\,t\,(D - t) - p_M\,t\,(D - t)/[(k_{wall}\,t - k_a\,a_N)\,(D - k_{wall}\,t + k_a\,a_N)]\,\pi/4\,[D - 2\,(k_{wall}\,t - k_a\,a_N)]^2 \quad (18)$$

$$F_{uts} = \pi\,t\,(D - t)\,f_{umn} \quad (19)$$

$$p_{uts} = 2\,f_{umn}\,(k_{wall}\,t - k_a\,a_N)/[D - (k_{wall}\,t - k_a\,a_N)] \quad (20)$$

$$p_{ref} = ½\,(p_{ref\,M} + p_{ref\,T}),\ \text{used in Fig. 1} \quad (21)$$

$$p_{ref\,M} = (2/\sqrt{3})^{1+n}\,(1/2)^n\,p_{uts} \quad (22)$$

$$p_{ref\,T} = (1/2)^n\,p_{uts} \quad (23)$$

$$k_R = (4^{1-n} - 1)/3^{1-n} \quad (24)$$

and

a_N is the imperfection depth associated with a specified inspection threshold, i.e. the maximum depth of a crack-like imperfection that could reasonably be missed by the pipe inspection system. For example, for a 5 % imperfection threshold inspection in a 12,7 mm (0.500 in) wall thickness pipe, a_N = 0,635 mm (0.025 in);

D is the specified pipe outside diameter;

F_a is the axial force;

f_{umn} is the specified minimum tensile strength;

F_{eff} is the effective axial load, i.e. for perfect pipes the axial load additional to the end-cap forces induced by internal and external pressures;

k_a is the burst strength factor, having the numerical value 1,0 for quenched and tempered (Martensitic structure) or 13Cr products and 2,0 for as rolled and normalized products based on available test data; and the default value set to 2,0 where the value has not been measured. The value of k_a can be established for a specific pipe material based on testing;

k_{wall} is the factor to account for the specified manufacturing tolerance of the pipe wall. For example, for a tolerance of –12,5 %, k_{wall} = 0,875;

n is the dimensionless hardening index used to obtain a curve fit (see B.2.3.3) of the true stress-strain curve derived from the uniaxial tensile test;

p_{iR} is the internal pressure at ductile rupture of an end-capped pipe;

p_{iRa} is p_{iR} adjusted for axial load and external pressure;

p_o is the external pressure;

t is the specified pipe wall thickness.

Equation (15) is illustrated in Figure 1, together with the exact formulation.

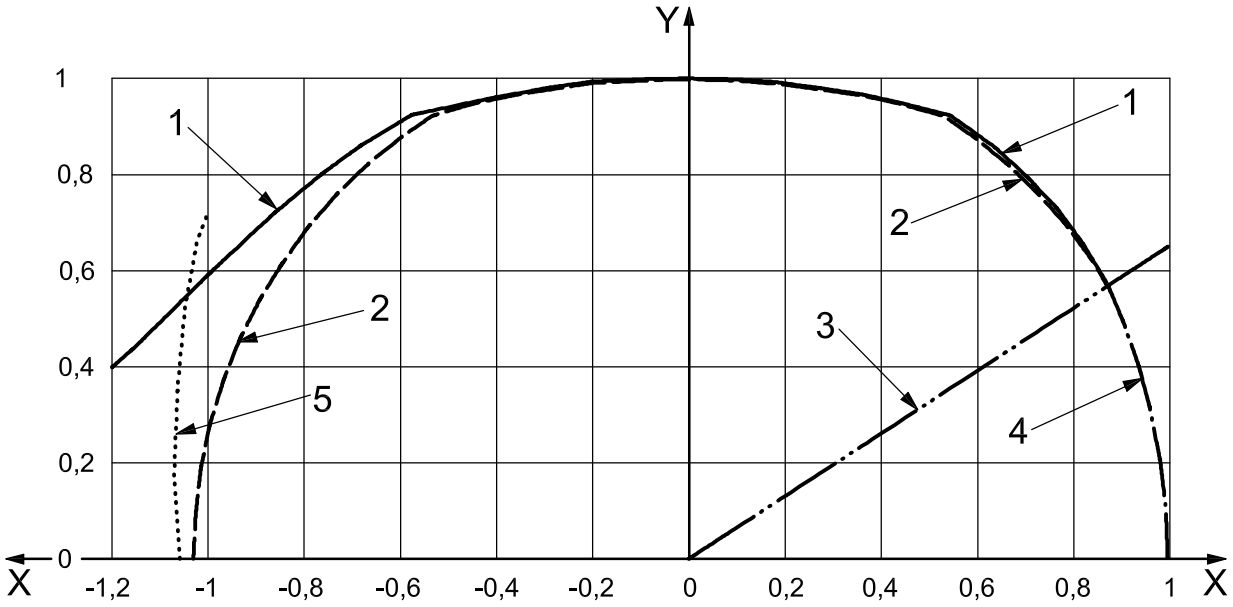

Key

X effective axial tension (F_{eff}/F_{uts})

Y pressure differential $(p_i - p_o)/p_{ref}$

1 rupture (exact)

2 rupture [Equation (15)]

3 transition

4 necking [Equation (26)]

5 wrinkling

Figure 1 — Illustration of the effect of effective axial tension and external pressure on ductile rupture

Under capped-end conditions, the effective axial load is zero and Equation (15) reduces to Equation (14).

The rupture equation is valid, i.e. rupture occurs before necking, when

$$F_{eff}/F_{uts} \leqslant (\sqrt{3}/2)^{1-n} \tag{25}$$

7.5.3 Design equation for ductile necking under combined loads

In the presence of internal and external pressure, the general equation for ductile necking is

$$F_{eff} = F_{uts}\sqrt{[1 - k_N\,[(p_i - p_o)/p_{ref\,M}]^2]} \tag{26}$$

where

$$F_a = \pi\, t\, (D - t)\, \sigma_a \tag{27}$$

$$F_{\text{eff}} = F_{\text{a}} + p_{\text{o}}\,\pi\,t\,(D-t) - p_{\text{M}}\,t\,(D-t)/[(k_{\text{wall}}\,t - k_{\text{a}}\,a_{\text{N}})\,(D - k_{\text{wall}}\,t + k_{\text{a}}\,a_{\text{N}})]\;\pi/4\;[D - 2\,(k_{\text{wall}}\,t - k_{\text{a}}\,a_{\text{N}})]^2 \quad (28)$$

$$F_{\text{uts}} = \pi\,t\,(D-t)\,f_{\text{umn}} \quad (29)$$

$$p_{\text{uts}} = 2\,f_{\text{umn}}\,(k_{\text{wall}}\,t - k_{\text{a}}\,a_{\text{N}})/[D - (k_{\text{wall}}\,t - k_{\text{a}}\,a_{\text{N}})] \quad (30)$$

$$p_{\text{ref M}} = (2/\sqrt{3})^{1+n}(1/2)^{n}\,p_{\text{uts}} \quad (31)$$

$$k_{\text{N}} = 4^{1-n} - 3^{1-n} \quad (32)$$

Under zero pressure conditions, the effective axial load equals the true axial load, and Equation (26) for the maximum axial load reduces to the ultimate tensile strength.

The necking equation is valid, i.e. necking occurs before rupture, when

$$(p_{\text{i}} - p_{\text{o}})/p_{\text{ref M}} \leqslant (1/2)^{1-n} \quad (33)$$

7.5.4 Boundary between rupture and necking

Comparing Equations (15) and (26) reveals that the necking criterion is reached earlier than the rupture criterion when

$$F_{\text{eff}}/F_{\text{uts}} \geqslant (3/2)\,(p_{\text{i}} - p_{\text{o}})/p_{\text{uts}} \quad (34)$$

and this criterion (also shown in Figure 1) describes the boundary between rupture and necking.

7.5.5 Axisymmetric wrinkling under combined loads

Figure 1 shows that in the axial compression range, i.e. for negative values of the effective axial load, Equation (15) is conservative when compared to both the exact rupture equation and the local pipe wall buckling limit, called wrinkling. Although it would be easy to construct an equation such as Equation (16) with a different factor k_{R} that would better fit the exact rupture curve in the effective axial compression range, it is perceived such a separate equation would not have great practical impact.

7.6 Example calculations

7.6.1 Ductile rupture of an end-capped pipe

For an end-capped pipe under pressure load, the effective axial load is zero and Equations (13) and (14) are the same. Moreover, if burst tests are performed on end-capped pipes with an additional axial load applied at the closed pipe ends, this is a situation where the effective axial load is given and Equation (15) can be used directly to calculate the rupture pressure for any value of effective axial load.

Compute the ductile rupture pressure of a 177,8 mm (7 in) tube with wall thickness 11,51 mm (0.453 in) made of P110 material. The tube is end-capped, and no additional axial load is present. Use the hardening index suggested in Table 2 and assume an inspection threshold of 5 % of the wall thickness.

The following table presents the results of the calculation in both SI and USC units.

Table 3 — Example calculations — Ductile rupture of an end-capped pipe

Term	SI		USC	
	Value	Units	Value	Units
Load				
F_{eff}	0	N	0	lb
Geometry				
D	177,8	mm	7	in
t	11,51	mm	0.453	in
k_{wall}	0,875		0.875	
Material				
E	206 842	MPa	30 000 000	psi
f_{umn}	862	MPa	125 000	psi
Calculations				
n	0,08		0.08	
a_N	0,575	mm	0.022 7	in
k_a	1		1	
p_{iR}	99,7	MPa	14 460	psi

7.6.2 Ductile rupture for a given true axial load

If the true axial load on the pipe is given, the pressure differential p_M cannot be calculated directly from Equation (15), because the effective axial load is a function of p_M. The solution can be found by solving for p_M iteratively, or by rewriting Equation (15) as a quadratic equation in the unknown p_M.

Compute the ductile rupture pressure of a 177,8 mm (7 in) tube with wall thickness 11,51 mm (0.453 in) made of P110 material. The axial compressive load is 889 600 N (200 000 lb). Use the hardening index suggested in Table 2 and assume an inspection threshold of 5 % of the wall thickness.

The following table presents the results of the calculation in both SI and USC units.

Table 4 — Example calculations — Ductile rupture for a given true axial load

Term	SI		USC	
	Value	Units	Value	Units
Load				
F_a	−889 600	N	−200 000	lb
p_o	0	MPa	0	psi
Geometry				
D	177,8	mm	7	in
t	11,51	mm	0.453	in
k_{wall}	0,875		0.875	
k_a	1		1	
Material				
E	206 842	MPa	30 000 000	psi
f_{umn}	862	MPa	125 000	psi
Calculations				
n	0,08		0.08	
a_N	0,575 8	mm	0.022 7	in
F_{uts}	5 180 423	N	1 164 663	lb
p_{uts}	97,22	MPa	14 100	psi
$P_{ref\ T}$	91,98	MPa	13 340	psi
$P_{ref\ M}$	107,43	MPa	15 581	psi
k_R	0,939 01		0.939 01	
p_M	92,47	MPa	13 412	psi
p_{iRa}	92,22	MPa	13 376	psi

8 External pressure resistance

8.1 General

The collapse design equation is intended for load cases when the external fluid pressure exceeds internal fluid pressure. A convenient, theoretically rigorous equation for cross-sectional collapse of a tube that accounts for realistic imperfections does not currently exist. The approach taken here combines theoretical, numerical and statistical tools.

The equations in Clause 8 are taken directly from Reference [2]. The collapse equations presented here were originally developed in USC units, and should only be used in these units.

8.2 Assumptions and limitations

The following limitation applies to the design equations for external pressure resistance:

— the axial tension correction does not include the non-uniform axial stress component due to bending. Including bending is a design issue left to the individual user.

8.3 Data requirements

The following input data are required to complete the calculation for collapse of the pipe body:

D specified pipe outside diameter,

f_{ymn} specified minimum yield strength,

t specified pipe wall thickness.

8.4 Design equation for collapse of pipe body

8.4.1 General

The minimum collapse strength for pipe with no axial force or internal pressure is given by a series of equations, depending on the specified minimum yield strength and cross-sectional dimensions of the tube body.

8.4.2 Yield strength collapse pressure equation

The yield strength collapse pressure is not a true collapse pressure, but rather the external pressure, p_{Yp}, that generates minimum yield stress, f_{ymn}, on the inside wall of a tube as calculated by Equation (35).

$$p_{Yp} = 2 f_{ymn} [(D/t) - 1]/[(D/t)^2] \quad (35)$$

where

D is the specified pipe outside diameter;

f_{ymn} is the specified minimum yield strength;

p_{Yp} is the pressure for yield strength collapse;

t is the specified pipe wall thickness.

Equation (35) for yield strength collapse pressure is applicable for D/t values up to the value of D/t corresponding to the intersection with the plastic collapse Equation (37). This intersection is calculated by Equation (36) as follows:

$$(D/t)_{yp} = \{[(A_c - 2)^2 + 8(B_c + C_c/f_{ymn})]^{1/2} + (A_c - 2)\}/[2(B_c + C_c/f_{ymn})] \quad (36)$$

where

A_c is the empirical constant in historical API collapse equation;

B_c is the empirical constant in historical API collapse equation;

C_c is the empirical constant in historical API collapse equation;

f_{ymn} is the specified minimum yield strength.

The parameters used to calculate collapse pressures depend on the pipe yield strength and on the axial load, as explained in later subclauses.

The applicable D/t ratios for yield strength collapse are shown in Table 5.

Table 5 — Yield collapse pressure equation range

Grade [a]	D/t range [b]
H40	16.40 and less
–50	15.24 and less
J55, K55	14.81 and less
–60	14.44 and less
–70	13.85 and less
C75, E75	13.60 and less
L-N-80	13.38 and less
C90	13.01 and less
C95, T95, X95	12.85 and less
–100	12.70 and less
P105, G105	12.57 and less
P110	12.44 and less
–120	12.21 and less
Q125	12.11 and less
–130	12.02 and less
S135	11.92 and less
–140	11.84 and less
–150	11.67 and less
–155	11.59 and less
–160	11.52 and less
–170	11.37 and less
–180	11.23 and less

[a] Grades indicated without letter designation are not API grades but are grades in use or grades being considered for use and are shown for information purposes.

[b] The D/t range values were calculated from Equations (36), (44) or (49), (45) or (50), and (46) or (51).

8.4.3 Plastic collapse pressure equation

The minimum collapse pressure for the plastic range of collapse is calculated by Equation (37):

$$p_P = f_{ymn}\,[A_c/(D/t) - B_c] - C_c \qquad (37)$$

where

A_c is the empirical constant in historical API collapse equation;

B_c is the empirical constant in historical API collapse equation;

C_c is the empirical constant in historical API collapse equation;

D is the specified pipe outside diameter;

f_{ymn} is the specified minimum yield strength;

p_P is the pressure for plastic collapse;

t is the specified pipe wall thickness.

The equation for minimum plastic collapse pressure is applicable for D/t values ranging from $(D/t)_{yp}$, Equation (36) for yield strength collapse pressure, to the intersection with Equation (39) for transition collapse pressure $(D/t)_{pt}$. Values for $(D/t)_{pt}$ are calculated by means of Equation (38):

$$(D/t)_{pt} = [f_{ymn}\,(A_c - F_c)]/[C_c + f_{ymn}\,(B_c - G_c)] \tag{38}$$

where

A_c is the empirical constant in historical API collapse equation;

B_c is the empirical constant in historical API collapse equation;

C_c is the empirical constant in historical API collapse equation;

F_c is the empirical constant in historical API collapse equation;

f_{ymn} is the specified minimum yield strength;

G_c is the empirical constant in historical API collapse equation.

The factors and applicable D/t range for the plastic collapse equation are shown in Table 6.

Table 6 — Equation factors and D/t range for plastic collapse

Grade [a]	A_c	B_c	C_c psi	D/t **range** [b]
H40	2.950	0.046 5	754	16.40 to 27.01
–50	2.976	0.051 5	1 056	15.24 to 25.63
J55, K55	2.991	0.054 1	1 206	14.81 to 25.01
–60	3.005	0.056 6	1 356	14.44 to 24.42
–70	3.037	0.061 7	1 656	13.85 to 23.38
C75, E75	3.054	0.064 2	1 806	13.60 to 22.91
L-N-80	3.071	0.066 7	1 955	13.38 to 22.47
C90	3.106	0.071 8	2 254	13.01 to 21.69
C95, T95, X95	3.124	0.074 3	2 404	12.85 to 21.33
–100	3.143	0.076 8	2 553	12.70 to 21.00
P105, G105	3.162	0.079 4	2 702	12.57 to 20.70
P110	3.181	0.081 9	2 852	12.44 to 20.41
–120	3.219	0.087 0	3 151	12.21 to 19.88
Q125	3.239	0.089 5	3 301	12.11 to 19.63
–130	3.258	0.092 0	3 451	12.02 to 19.40
S135	3.278	0.094 6	3 601	11.92 to 19.18
–140	3.297	0.097 1	3 751	11.84 to 18.97
–150	3.336	0.102 1	4 053	11.67 to 18.57
–155	3.356	0.104 7	4 204	11.59 to 18.37
–160	3.375	0.107 2	4 356	11.52 to 18.19
–170	3.412	0.112 3	4 660	11.37 to 17.82
–180	3.449	0.117 3	4 966	11.21 to 17.47

[a] Grades indicated without letter designation are not API grades but are grades in use or grades being considered for use and are shown for information purposes.

[b] The D/t range values and equation factors were calculated from Equations (36), (38), (44) or (49), (45) or (50), (46) or (51), (47) or (52), and (48) or (53).

8.4.4 Transition collapse pressure equation

The minimum collapse pressure for the plastic to elastic transition zone p_T is calculated by Equation (39):

$$p_T = f_{ymn}\,[F_c/(D/t) - G_c] \tag{39}$$

where

D is the specified pipe outside diameter;

F_c is the empirical constant in historical API collapse equation;

f_{ymn} is the specified minimum yield strength;

G_c is the empirical constant in historical API collapse equation;

p_T is the pressure for transition collapse;

t is the specified pipe wall thickness.

The equation for p_T is applicable for D/t values from $(D/t)_{pt}$, Equation (38) for plastic collapse pressure, to the intersection $(D/t)_{te}$ with Equation (41) for elastic collapse. Values for $(D/t)_{te}$ are calculated by Equation (40):

$$(D/t)_{te} = [2 + B_c/A_c]/[3(B_c/A_c)] \tag{40}$$

where

A_c is the empirical constant in historical API collapse equation;

B_c is the empirical constant in historical API collapse equation.

The factors and applicable D/t range for the transition collapse pressure equation are shown in Table 7.

Table 7 — Equation factors and D/t range for transition collapse

Grade [a]	F_c	G_c	D/t range [b]
H40	2.063	0.032 5	27.01 to 42.64
–50	2.003	0.034 7	25.63 to 38.83
J55, K55	1.989	0.036 0	25.01 to 37.21
–60	1.983	0.037 3	24.42 to 35.73
–70	1.984	0.040 3	23.38 to 33.17
C75, E75	1.990	0.041 8	22.91 to 32.05
L-N-80	1.998	0.043 4	22.47 to 31.02
C90	2.017	0.046 6	21.69 to 29.18
C95, T95, X95	2.029	0.048 2	21.33 to 28.36
–100	2.040	0.049 9	21.00 to 27.60
P105, G105	2.053	0.051 5	20.70 to 26.89
P110	2.066	0.053 2	20.41 to 26.22
–120	2.092	0.056 5	19.88 to 25.01
Q125	2.106	0.058 2	19.63 to 24.46
–130	2.119	0.059 9	19.40 to 23.94
S135	2.133	0.061 5	19.18 to 23.44
–140	2.146	0.063 2	18.97 to 22.98
–150	2.174	0.066 6	18.57 to 22.11
–155	2.188	0.068 3	18.37 to 21.70
–160	2.202	0.070 0	18.19 to 21.32
–170	2.231	0.073 4	17.82 to 20.60
–180	2.261	0.076 9	17.47 to 19.93

[a] Grades indicated without letter designation are not API grades but are grades in use or grades being considered for use and are shown for information purposes.

[b] The D/t range values and equation factors were calculated from Equations (36), (38), (44) or (49), (45) or (50), (46) or (51), (47) or (52), and (48) or (53).

8.4.5 Elastic collapse pressure equation

The minimum collapse pressure for the elastic range of collapse is calculated by Equation (41):

$$p_E = 46.95 \times 10^6/[(D/t)\ (D/t - 1)^2] \tag{41}$$

where

D is the specified pipe outside diameter;

p_E is the pressure for elastic collapse;

t is the specified pipe wall thickness.

The applicable D/t range for elastic collapse is shown in Table 8.

Table 8 — D/t range for elastic collapse

Grade [a]	D/t range [b]
H40	42.64 and greater
–50	38.83 and greater
J55, K55	37.21 and greater
–60	35.73 and greater
–70	33.17 and greater
C75, E75	32.05 and greater
L-N-80	31.02 and greater
C90	29.18 and greater
C95, T95, X95	28.36 and greater
–100	27.60 and greater
P105, G105	26.89 and greater
P110	26.22 and greater
–120	25.01 and greater
Q125	24.46 and greater
–130	23.94 and greater
S135	23.44 and greater
–140	22.98 and greater
–150	22.11 and greater
–155	21.70 and greater
–160	21.32 and greater
–170	20.60 and greater
–180	19.93 and greater

[a] Grades indicated without letter designation are not API grades but are grades in use or grades being considered for use and are shown for information purposes.

[b] The D/t range values were calculated from Equations (40), (44) or (49), and (45) or (50).

8.4.6 Collapse pressure under axial tension stress

The collapse resistance of casing in the presence of an axial stress is calculated by modifying the yield stress to an axial stress equivalent grade according to Equation (42):

$$f_{yax} = \{[1 - 0.75(\sigma_a/f_{ymn})^2]^{1/2} - 0.5\ \sigma_a/f_{ymn}\} f_{ymn} \quad (42)$$

where

f_{yax} is the equivalent yield strength in the presence of axial stress;

f_{ymn} is the specified minimum yield strength;

σ_a is the component of axial stress not due to bending.

Collapse resistance equation factors and D/t ranges for the axial stress equivalent grade are then calculated by means of Equations (36), (38), (40), (44) or (49), (45) or (50), (46) or (51), (47) or (52), and (48) or (53). Using equation factors for the axial stress equivalent grade, collapse resistance under axial stress is calculated by means of Equations (35), (37), (41) and (39).

API collapse resistance equations are not valid for the yield strength of axial stress equivalent grade (f_{yax}) less than 24 000 psi.

Equation (42) is based on the Hencky-von Mises maximum strain energy of distortion theory of yielding.

8.4.7 Effect of internal pressure on collapse

The external pressure equivalent of external pressure and internal pressure is determined by means of Equation (43). The equation is based on the internal pressure acting on the inside diameter and the external pressure acting on the outside diameter.

$$p_{ci} = p_c + (1 - 2\ t/D)\ p_i \tag{43}$$

where

D is the specified pipe outside diameter;

p_c is the collapse pressure;

p_{ci} is the collapse pressure in the presence of internal pressure;

p_i is the internal pressure;

t is the specified pipe wall thickness.

The value p_c is the collapse resistance calculated neglecting internal pressure, but accounting for any axial load as described in 8.4.6. Equation (43) was taken from Reference [56].

8.5 Equations for empirical constants

8.5.1 General

The following equations may be used to calculate the empirical constants in the historical API collapse equations. There are two versions of each equation, one each for SI (8.5.2) and USC (8.5.3) units.

8.5.2 SI units

$$A_c = 2{,}876\ 2 + 0{,}154\ 89 \times 10^{-3} f_{ymn} + 0{,}448\ 09 \times 10^{-6} f_{ymn}^2 - 0{,}162\ 11 \times 10^{-9} f_{ymn}^3 \tag{44}$$

$$B_c = 0{,}026\ 233 + 0{,}73402 \times 10^{-4} f_{ymn} \tag{45}$$

$$C_c = -3{,}212\ 5 + 0{,}030\ 867 f_{ymn} - 0{,}15204 \times 10^{-5} f_{ymn}^2 + 0{,}778\ 10 \times 10^{-9} f_{ymn}^3 \tag{46}$$

$$F_c = 3{,}237 \times 10^5\ [(3\ B_c/A_c)/(2 + B_c/A_c)]^3/\{f_{ymn}\ [(3\ B_c/A_c)/(2 + B_c/A_c) - B_c/A_c][1 - (3\ B_c/A_c)/(2 + B_c/A_c)]^2\} \tag{47}$$

$$G_c = F_c\ B_c/A_c \tag{48}$$

where

A_c is the empirical constant in historical API collapse equation;

B_c is the empirical constant in historical API collapse equation;

C_c is the empirical constant in historical API collapse equation;

F_c is the empirical constant in historical API collapse equation;

f_{ymn} is the specified minimum yield strength;

G_c is the empirical constant in historical API collapse equation.

8.5.3 USC units

$$A_c = 2.876\,2 + 0.106\,79 \times 10^{-5} f_{ymn} + 0.213\,01 \times 10^{-10} f_{ymn}^2 - 0.531\,32 \times 10^{-16} f_{ymn}^3 \quad (49)$$

$$B_c = 0.026\,233 + 0.506\,09 \times 10^{-6} f_{ymn} \quad (50)$$

$$C_c = -465.93 + 0.030\,867 f_{ymn} - 0.104\,83 \times 10^{-7} f_{ymn}^2 + 0.369\,89 \times 10^{-13} f_{ymn}^3 \quad (51)$$

$$F_c = 46.95 \times 10^6 [(3 B_c/A_c)/(2 + B_c/A_c)]^3/\{f_{ymn} [(3 B_c/A_c)/(2 + B_c/A_c) - B_c/A_c][1 - (3 B_c/A_c)/(2 + B_c/A_c)]^2\} \quad (52)$$

$$G_c = F_c B_c/A_c \quad (53)$$

where

A_c is the empirical constant in historical API collapse equation;

B_c is the empirical constant in historical API collapse equation;

C_c is the empirical constant in historical API collapse equation;

F_c is the empirical constant in historical API collapse equation;

f_{ymn} is the specified minimum yield strength;

G_c is the empirical constant in historical API collapse equation.

8.6 Application of collapse pressure equations to line pipe

The collapse pressure equations presented in this clause are empirical relations derived from tests on pipe representative of the casing and tubing inventories listed in ISO 11960 or API 5CT. Application of these relations outside the range of yield strengths and D/t ratios contained in ISO 11960 or API 5CT is not recommended. These equations do not apply to cold expanded pipe because Bauschinger effects significantly reduce collapse resistance.

Some line pipe grades listed in API 5L have a rough casing equivalent in ISO 11960 or API 5CT. However, the API 5L inventory of line pipe contains D/t ratios that often exceed casing D/t ratios significantly.

For line pipe having a yield strength and D/t falling within the limits of the sizes and thicknesses listed in ISO 11960 or API 5CT, application of the equations in this clause should yield reasonable estimates of minimum collapse pressure. Nevertheless, as with the application of any of the equations in this document, sound engineering judgment should prevail.

8.7 Example calculations

Calculate the collapse pressure of size Label 1: 7, mass Label 2: 26, grade P110 casing with axial stress of 11 000 psi and internal pressure 1 000 psi. Wall thickness is 0.362 in.

The following table presents the results of the calculation in both SI and USC units.

Table 9 — Example calculation — Collapse resistance with internal pressure and tension

Term	SI		USC	
	Value	Units	Value	Units
Load				
σ_a	75,842	MPa	11 000	psi
p_i	6,895	MPa	1 000	psi
Geometry				
D	177,80	mm	7.000	in
t	9,19	mm	0.362	in
D/t	19,35			
Material				
f_{ymn}	758	MPa	110 000	psi
Calculations				
f_{yax}	717,7	MPa	104 087	psi
A_c	3.158			
B_c	0.078 9			
C_c	18,444	MPa	2 675	psi
F_c	2.051			
G_c	0.051 2			
Equation	Plastic			
p_c	42,1	MPa	6 110	psi
p_{ci}	48,3	MPa	7 010	psi

9 Joint strength

9.1 General

Joint strength is a measure of the structural integrity of a threaded connection, and does not include consideration of leak resistance. For casing applications, where installation of the tubular string is considered permanent, the limit load can be based on either yield or fracture/pull-out of the connector. For tubing applications, where the tubular string can be repeatedly recovered from and re-installed in the wellbore, the limit load is usually based on yield of the connector.

In this and other clauses, the following abbreviations may be employed:

— BC, buttress thread and coupling;

— BC SC, buttress thread with special clearance coupling;

— EU, external upset end;

— EU SC, external upset end with special clearance coupling;

— LC, long thread and coupling (round thread);

— NU, non-upset end;

— STC, short thread and coupling (round thread);

— XC, extreme-line casing.

9.2 API casing connection tensile joint strength

9.2.1 General

The following tensile joint strength performance properties apply to casing connections manufactured in accordance with API 5B and ISO 11960 or API 5CT.

9.2.2 Round thread casing joint strength

9.2.2.1 General

Round thread casing joint strength is calculated as the minimum of fracture of the pipe under the last perfect thread, of a joint failing by thread jumpout or pullout, or of fracture in the coupling. With certain coupling dimensions, the strength of the coupling can be less than that of the pipe body. The coupling fracture strength is calculated at the root of the coupling thread coincident with the end of the pipe in the power-tight position.

9.2.2.2 Assumptions and limitations

The round thread casing joint strength equation ignores the possible presence of internal and external pressure. The effect of casing curvature on joint strength is also ignored. The coefficients in some of the equations were originally developed in USC units. It is suggested that users perform these calculations in USC units and then convert the result to SI units.

9.2.2.3 Data requirements

The following input data are required to complete the calculation for round thread casing joint strength:

D specified pipe outside diameter, inches;

f_{umnp} specified minimum tensile strength of the pipe body, psi;

f_{ymnp} specified minimum yield strength of the pipe body, psi;

L_{et} engaged thread length, [$= L_4 - M$] for nominal make-up, in accordance with API 5B, inches;

t specified pipe wall thickness, inches.

The following input data are required to complete the calculation for round thread coupling fracture strength:

A hand-tight standoff;

E_1 pitch diameter at the hand-tight plane, in accordance with API 5B;

f_{umc} actual tensile strength of a representative tensile specimen from the coupling, psi;

H is the thread height of a round thread equivalent Vee thread, 2,199 6 mm (0.086 60 in) for 10 TPI, 2,749 6 mm (0.1082 5 in) for 8 TPI;

L_1 length from the end of the pipe to the hand-tight plane, in accordance with API 5B;

s_{rn} root truncation of the pipe thread of round threads, 0,36 mm (0.014 in) for 10 TPI, 0,43 mm (0.017 in) for 8 TPI;

T_d taper (on diameter), 0,062 5 mm/mm (0.062 5 in/in);

W specified coupling outside diameter, in accordance with ISO 11960 or API 5CT.

9.2.2.4 Design equations

Round thread casing joint strength is calculated by taking the minimum of the fracture strength of the pipe threads, the pull-out strength and the fracture strength of the coupling:

$$P_j = 0.95\, A_{jp} f_{umnp} \text{ (fracture strength)} \tag{54}$$

or

$$P_j = 0.95\, A_{jp} L_{et}[(0.74 D^{-0.59} f_{umnp})/(0.5 L_{et} + 0.14 D) + f_{ymnp}/(L_{et} + 0.14 D)] \quad \text{(pull-out strength)} \tag{55}$$

or

$$P_j = 0.95\, A_{jc} f_{umc} \quad \text{(coupling fracture strength)} \tag{56}$$

where

$$A_{jp} = \pi/4\, [(D - 0.142\,5)^2 - d^2] \tag{57}$$

$$A_{jc} = \pi/4\, (W^2 - d_1^2) \tag{58}$$

$$d_1 = E_1 - (L_1 + A) T_d + H - 2 s_{rn} \tag{59}$$

and

A is the hand-tight standoff;

A_{jc} is the area of the coupling cross section, square inches;

A_{jp} is the area of the pipe cross section under the last perfect thread, square inches;

D is the specified pipe outside diameter, inches;

d is the pipe inside diameter, $d = D - 2t$, inches;

d_1 is the diameter at the root of the coupling thread at the end of the pipe in the power-tight position;

E_1 is the pitch diameter at the hand-tight plane, in accordance with API 5B;

f_{umnp} is the specified minimum tensile strength of the pipe body, psi;

f_{umc} is the specified minimum tensile strength of the coupling, psi;

f_{ymnp} is the specified minimum yield strength of the pipe body, psi;

H is the thread height of a round thread equivalent Vee thread, 2,199 6 mm (0.0866 0 in) for 10 TPI, 2,749 6 mm (0.1082 5 in) for 8 TPI;

L_{et} is the engaged thread length, [$= L_4 - M$] for nominal make-up, in accordance with API 5B, inches;

L_1 is the length from the end of the pipe to the hand-tight plane, in accordance with API 5B;

P_j is the joint strength, pounds;

s_{rn} is the root truncation of the pipe thread of round threads, 0,36 mm (0.014 in) for 10 TPI, 0,43 mm (0.017 in) for 8 TPI;

t is the specified pipe wall thickness, inches;

T_d is the taper (on diameter), 0,062 5 mm/mm (0.062 5 in/in);

W is the specified coupling outside diameter, in accordance with ISO 11960 or API 5CT.

9.2.3 Buttress thread casing joint strength

9.2.3.1 General

Buttress thread casing joint strength is calculated as the minimum of the pipe strength and of the coupling fracture strength calculated at the root of the coupling thread coincident with the end of the pipe in the power-tight position.

9.2.3.2 Assumptions and limitations

The buttress thread casing joint strength equations are based on the following assumptions:

— the buttress thread does not fail by pull-out. Note that this assumption is contradicted by some test data for larger D/t ratios;

— the effect of internal and external pressure is ignored;

— the effect of casing curvature is ignored;

— the coefficients in some of the equations were originally developed in USC units. It is suggested that users perform these calculations in USC units and then convert the result to SI units.

9.2.3.3 Data requirements

The following input data are required to complete the calculation for buttress thread casing joint strength:

D specified pipe outside diameter, inches;

E_7 pitch diameter, in accordance with API 5B;

f_{umnc} specified minimum tensile strength of the coupling, psi;

f_{umnp} specified minimum tensile strength of the pipe body, psi;

f_{ymnp} specified minimum yield strength of the pipe body, psi;

h_B buttress thread height: 1,575 for SI units, 0.062 for USC units;

I_B length from the face of the buttress thread coupling to the base of the triangle in the hand-tight position, 10,16 mm (0.400 in) for Label 1: 4-1/2, 12,70 mm (0.500 in) for sizes between Label 1: 5 and Label 1: 13-3/8, inclusive, and 9,52 mm (0.375 in) for sizes greater than Label 1: 13-3/8;

L_7 length of perfect threads, in accordance with API 5B;

t specified pipe wall thickness;

T_d taper (on diameter);

W specified coupling outside diameter, in accordance with ISO 11960 or API 5CT, inches.

9.2.3.4 Design equation

Buttress thread casing joint strength is calculated by taking the minimum of the pipe thread strength and the coupling thread strength:

$$P_j = 0.95 A_p f_{umnp}[1.008 - 0.039\ 6(1.083 - f_{ymnp}/f_{umnp})D] \text{ (pipe thread strength)} \quad (60)$$

or

$$P_j = 0.95 A_{jc} f_{umnc} \text{ (coupling thread strength)} \quad (61)$$

where

A_{jc} is the area of the coupling cross section, $A_{jc} = \pi/4\ (W^2 - d_1{}^2)$, square inches;

A_p is the area of the pipe cross section, $A_p = \pi/4\ (D^2 - d^2)$, square inches;

D is the specified pipe outside diameter, inches;

d is the pipe inside diameter, $d = D - 2t$;

d_1 is the diameter at the root of the coupling thread at the end of the pipe in the power-tight position, inches;

f_{umnc} is the specified minimum tensile strength of the coupling, psi;

f_{umnp} is the specified minimum tensile strength of the pipe body, psi;

f_{ymnp} is the specified minimum yield strength of the pipe body, psi;

P_j is the joint strength, lbs;

t is the specified pipe wall thickness;

W is the specified coupling outside diameter, in accordance with ISO 11960 or API 5CT, inches;

and

$$d_1 = E_7 - (L_7 + I_B)\ T_d + h_B \quad (62)$$

where

E_7 is the pitch diameter, in accordance with API 5B;

h_B is the buttress thread height: 1,575 for SI units, 0.062 for USC units;

I_B is the length from the face of the buttress thread coupling to the base of the triangle in the hand-tight position, 10,16 mm (0.400 in) for Label 1: 4-1/2, 12,70 mm (0.500 in) for sizes between Label 1: 5 and Label 1: 13-3/8, inclusive, and 9,52 mm (0.375 in) for sizes greater than Label 1: 13-3/8;

L_7 is the length of perfect threads, in accordance with API 5B;

T_d is the taper (on diameter), 0,062 5 mm/mm (0.062 5 in/in) for sizes less than or equal to Label 1: 13-3/8, and 0,083 3 mm/mm (0.083 3 in/in) for sizes greater than Label 1: 13-3/8.

9.2.4 Extreme-line casing joint strength

9.2.4.1 General

Extreme-line casing joint strength is based on the dimensions of a critical cross section which can be in the pipe, the pin or the coupling, depending on the dimensions of a specific connection.

9.2.4.2 Assumptions and limitations

The extreme-line casing joint strength equation ignores the possible presence of internal and external pressure. The effect of casing curvature on joint strength is also ignored. The coefficients in some of the equations were originally developed in USC units. It is suggested that users perform these calculations in USC units and then convert the result to SI units.

9.2.4.3 Data requirements

The following input data are required to complete the calculation for extreme-line casing joint strength:

A_x maximum diameter at the extreme-line pin seal tangent point;

D specified pipe outside diameter;

d_j extreme-line specified joint inside diameter, made up;

f_{umn} specified minimum tensile strength;

H_x maximum extreme-line root diameter at last perfect pin thread;

h_x minimum box thread height for extreme-line casing;

I_x minimum extreme-line crest diameter of box thread at Plane H;

M specified outside diameter of the extreme-line connection; length from the face of the coupling to the hand-tight plane for line pipe and for round thread casing and tubing, in accordance with API 5B;

O_x minimum diameter at the extreme-line box seal tangent point;

Δ taper drop in extreme-line pin perfect thread length;

δ extreme-line taper rise between Plane H and Plane J.

9.2.4.4 Design equation

Extreme-line casing joint strength is defined by the following expression:

$$P_j = A_{crit} f_{umn} \tag{63}$$

where

f_{umn} is the specified minimum tensile strength;

A_{crit} is the minimum of

$\pi/4\ (M^2 - d_b^2)$ if box is critical,
$\pi/4\ (D_p^2 - d_j^2)$ if pin is critical,
$\pi/4\ (D^2 - d^2)$ if pipe is critical;

where

A_x is the maximum diameter at the extreme-line pin seal tangent point;

D is the specified pipe outside diameter;

D_p is the extreme-line pin critical section outside diameter, $D_p = H_x + \delta - \varphi$;

d is the pipe inside diameter, $d = D - 2t$;

d_b is the inside diameter of the critical section of the extreme-line box, $d_b = I_x + 2h_x - \Delta + \theta$;

d_j is the extreme-line specified joint inside diameter, made up;

H_x is the maximum extreme-line root diameter at last perfect pin thread;

h_x is the minimum box thread height for extreme-line casing, as follows:
1,52 mm (0.060 in) for 6 TPI,
2,03 mm (0.080 in) for 5 TPI;

I_x is the minimum extreme-line crest diameter of box thread at Plane H;

M is the specified outside diameter of the extreme-line connection, in accordance with API 5B;

O_x is the minimum diameter at the extreme-line box seal tangent point;

P_j is the joint strength;

Δ is the taper drop in extreme-line pin perfect thread length
6,43 mm (0.253 in) for 6 TPI
5,79 mm (0.228 in) for 5 TPI;

δ is the extreme-line taper rise between Plane H and Plane J, as follows:
0,89 mm (0.035 in) for 6 TPI
0,81 mm (0.032 in) for 5 TPI;

φ is one-half of the maximum extreme-line seal interference, $\varphi = (A_x - O_x)/2$;

θ is one-half of the extreme-line maximum thread interference, $\theta = (H_x - I_x)/2$.

9.3 API tubing connection tensile joint strength

9.3.1 General

The following tensile joint strength performance properties apply to tubing connections manufactured in accordance with API 5B and ISO 11960 or API 5CT.

9.3.2 Non-upset tubing joint strength

9.3.2.1 Introduction

Non-upset tubing joint strength is calculated as the product of the yield strength and the area of the pipe cross section under the last perfect thread. The areas of the critical sections of regular tubing couplings and special-clearance couplings are, in all instances, greater than the governing critical areas of the pipe part of the joint and do not affect the strength of the joint.

9.3.2.2 Assumptions and limitations

The non-upset tubing joint strength equation ignores the possible presence of internal and external pressure. The effect of tubing curvature on joint strength is also ignored.

9.3.2.3 Data requirements

The following input data are required to complete the calculation for non-upset tubing joint strength:

D specified pipe outside diameter;

D_4 major diameter, in accordance with API 5B;

f_{ymn} specified minimum yield strength;

h_s round thread height, 1,312 2 mm (0.055 60 in) for 10 TPI, 1,809 8 mm (0.071 25 in) for 8 TPI;

t specified pipe wall thickness.

9.3.2.4 Design equation

The joint strength in tension of non-upset tubing is defined by the following expression:

$$P_j = f_{ymn} \{\pi/4 [(D_4 - 2h_s)^2 - d^2]\} \quad (64)$$

where

D is the specified pipe outside diameter;

d is the pipe inside diameter, $d = D - 2t$;

D_4 is the major diameter, in accordance with API 5B;

f_{ymn} is the specified minimum yield strength;

h_s is the round thread height, 1,312 2 mm (0.055 60 in) for 10 TPI, 1,809 8 mm (0.071 25 in) for 8 TPI;

P_j is the joint strength;

t is the specified pipe wall thickness.

9.3.3 Upset tubing joint strength

9.3.3.1 General

Upset tubing joint strength is calculated as the product of the yield strength and the area of the body of the pipe. The area of the section under the last perfect thread of API upset tubing is greater than the area of the body of the pipe. The areas of the critical sections of regular tubing couplings, special-clearance couplings, and the box of integral-joint tubing are, in all instances, greater than the governing critical areas of the pipe part of the joint and do not affect the strength of the joint.

9.3.3.2 Assumptions and limitations

The upset tubing joint strength equation ignores the possible presence of internal and external pressure. The effect of tubing curvature on joint strength is also ignored.

9.3.3.3 Data requirements

The following input data are required to complete the calculation for upset tubing joint strength:

D specified pipe outside diameter;

f_{ymn} specified minimum yield strength;

t specified pipe wall thickness.

9.3.3.4 Design equation

The joint strength in tension of upset tubing is defined by the following expression:

$$P_j = f_{ymn}\,[\pi/4\,(D^2 - d^2)] \tag{65}$$

where

d is the pipe inside diameter, $d = D - 2t$;

D is the specified pipe outside diameter;

f_{ymn} is the specified minimum yield strength;

P_j is the joint strength;

t is the specified pipe wall thickness.

9.4 Line pipe connection joint strength

Equations for the joint strength of threaded line pipe were developed and presented to the API Committee on Standardization of Tubular Goods by W. O. Clinedinst at the 1976 Standardization Conference. The data and equations are reproduced in Reference [3].

10 Pressure performance for couplings

10.1 General

Internal pressure capacity for threaded and coupled pipe is the same as for plain-end pipe, except where a lower pressure is required to avoid yielding the coupling or leakage due to insufficient internal pressure leak resistance at the E_1 or E_7 plane as calculated below. For integral joint tubing, the box is considered the coupling.

10.2 Internal yield pressure of round thread and buttress couplings

The internal yield pressure for the coupling is calculated from

$$p_{\mathrm{iYc}} = f_{\mathrm{ymnc}}\,(W - d_1)/W \tag{66}$$

where

f_{ymnc} is the specified minimum yield strength of the coupling;

d_1 is the diameter at the root of the coupling thread at the end of the pipe in the power-tight position;

p_{iYc} is the internal pressure at yield for coupling;

W is the specified coupling outside diameter, in accordance with ISO 11960 or API 5CT.

For round thread casing and tubing,

$$d_1 = E_1 - (L_1 + A)T_{\mathrm{d}} + H - 2s_{\mathrm{rn}} \tag{67}$$

where

A is the hand-tight standoff, mm (in);

E_1 is the pitch diameter at the hand-tight plane, in accordance with API 5B;

H is the thread height of a round thread equivalent Vee thread, 2,199 6 mm (0.086 60 in) for 10 TPI, 2,749 6 mm (0.108 25 in) for 8 TPI;

L_1 is the length from the end of the pipe to the hand-tight plane, in accordance with API 5B;

s_{rn} is the root truncation of the pipe thread of round threads, 0,36 mm (0.014 in) for 10 TPI, 0,43 mm (0.017 in) for 8 TPI;

T_{d} is the taper (on diameter), 0,062 5 mm/mm (0.062 5 in/in).

For buttress thread casing,

$$d_1 = E_7 - (L_7 + I_{\mathrm{B}})T_{\mathrm{d}} + h_{\mathrm{B}} \tag{68}$$

where

E_7 pitch diameter, in accordance with API 5B, millimetres or inches;

h_{B} buttress thread height, 1,575 for SI units, 0.062 for USC units;

I_{B} length from the face of the buttress thread coupling to the base of the triangle in the hand-tight position, 10,16 mm (0.400 in) for Label 1: 4-1/2, 12,70 mm (0.500 in) for sizes between Label 1: 5 and Label 1: 13-3/8, inclusive, and 9,52 mm (0.375 in) for sizes greater than Label 1: 13-3/8;

L_7 length of perfect threads, in accordance with API 5B, millimetres or inches;

T_{d} taper (on diameter), 0,062 5 mm/mm (0.062 5 in/in) for sizes less than or equal to Label 1: 13-3/8, 0,083 3 mm/mm (0.083 3 in/in) for sizes greater than Label 1: 13-3/8.

10.3 Internal pressure leak resistance of round thread or buttress couplings

The internal pressure leak resistance at the E_1 or E_7 plane is calculated from Equation (69). Equation (69) is based on the seal being at the E_1 plane for round threads and the E_7 plane for buttress threads where the coupling is the weakest and the internal pressure leak resistance the lowest. Also, Equation (69) is based on the internal leak resistant pressure being equal to the interference pressure between the pipe and coupling threads resulting from make-up and the internal pressure itself, with stresses in the elastic range.

$$p_{iL} = ET_d Np(W^2 - E_s^2)/2E_s W^2 \tag{69}$$

where

E is Young's modulus;

E_s is the pitch diameter, at plane of seal
E_1 for round thread
E_7 for buttress thread casing;

N is the number of thread turns make-up
A for round thread casing and tubing (API 5B)
$A + 1{,}5$ for buttress thread casing smaller than 16
$A + 1$ for buttress thread casing 16 and larger;

p is the thread pitch
3,175 mm (0.125 in) for 8-round thread casing and tubing
2,540 mm (0.100 in) for 10-round thread tubing
5,080 mm (0.200 in) for buttress thread casing;

p_{iL} is the internal pressure at leak;

T_d is the taper (on diameter)
0,062 5 for round thread casing and tubing
0,062 5 for buttress casing smaller than 16
0,083 3 for buttress thread casing 16 and larger;

W is the specified coupling outside diameter, in accordance with ISO 11960 or API 5CT;

where

A is the hand-tight standoff, mm (in);

E_1 is the pitch diameter at the hand-tight plane, in accordance with API 5B;

E_7 is the pitch diameter, in accordance with API 5B.

The interface pressure between the pin and box as a result of make-up is

$$p_1 = ET_d Np(W^2 - E_s^2)(E_s^2 - d^2)/E_s^2(W^2 - d^2) \tag{70}$$

where

E is Young's modulus;

E_s is the pitch diameter, at plane of seal
E_1 for round thread
E_7 for buttress thread casing;

d is the pipe inside diameter, $d = D - 2t$;

N is the number of thread turns make-up
A for round thread casing and tubing (API 5B)
$A + 1{,}5$ for buttress thread casing smaller than 16
$A + 1$ for buttress thread casing 16 and larger;

p is the thread pitch
3,175 mm (0.125 in) for 8-round thread casing and tubing
2,540 mm (0.100 in) for 10-round thread tubing
5,080 mm (0.200 in) for buttress thread casing;

T_d is the taper (on diameter)
0,062 5 for round thread casing and tubing
0,062 5 for buttress casing smaller than 16
0,083 3 for buttress thread casing 16 and larger;

W is the specified coupling outside diameter, in accordance with ISO 11960 or API 5CT;

where

A is the hand-tight standoff;

E_1 is the pitch diameter at the hand-tight plane, in accordance with API 5B;

E_7 is the pitch diameter, in accordance with API 5B;

D is the specified pipe outside diameter;

t is the specified pipe wall thickness.

Subsequent to make-up, internal pressure, p_i, causes a change in the interface pressure by an amount p_2:

$$p_2 = p_i d^2(W^2 - E_s^2)/E_s^2(W^2 - d^2) \tag{71}$$

where

E_s is the pitch diameter, at plane of seal
E_1 for round thread
E_7 for buttress thread casing;

d is the pipe inside diameter, $d = D - 2t$;

p_i is the internal pressure;

W is the specified coupling outside diameter, in accordance with ISO 11960 or API 5CT;

where

E_1 is the pitch diameter at the hand-tight plane, in accordance with API 5B;

E_7 is the pitch diameter, in accordance with API 5B;

D is the specified pipe outside diameter;

t is the specified pipe wall thickness.

Since the external box diameter is always greater than the contact diameter, which in turn is always greater than the internal pipe diameter, p_2 will always be less than p_1. Therefore, when the total interface pressure $p_1 + p_2$ equals the internal pressure p_i, the connection has reached the leak resistance limit p. In other words, if p_i were greater than $p_1 + p_2$, leakage would occur:

$$p_1 + p_2 = p_i = p \tag{72}$$

Substituting the appropriate values for p_1 and p_1 into Equation (72) and simplifying produces Equation (69).

11 Calculated masses

11.1 General

NOTE The dimensional symbols and corresponding numerical values used in the equations for calculation of masses in Clause 11 are given in API 5B and ISO 11960 or API 5CT [see also ISO 3183].

The densities of martensitic chromium steels (L80, Types 9Cr and 13Cr) are different than carbon steels. A mass correction factor of 0,989 may be used for these types.

11.2 Nominal masses

Nominal mass is used in connection with pipe having end finish such as threads and couplings, upset and threaded ends, upset ends, etc., primarily for the purpose of identification in ordering. It is also used generally in the design of casing and tubing strings as the basis for determining joint safety factors in tension.

Nominal mass is approximately equal to the calculated theoretical mass per foot of a 6,10 m (20 ft) length of threaded and coupled pipe, based on the dimensions of the joint in use for the class of product when the particular diameter and wall thickness were introduced. Some nominal masses are based on sharp thread joints that were in use before this specification was adopted. The same nominal masses are used for short thread joints, long thread joints, buttress thread joints, extreme-line joints, and the various proprietary joints offered to the oil industry. Nominal masses for upset drill pipe for weld-on tool joints are based on the calculated mass-per-foot values of the original threaded and coupled drill pipe.

In determining the nominal mass from calculated masses, it would appear that historical rounding was implemented with no definite procedure. Rounding increments of 0,01, 0,05, 0,1 and 0,5 should be used for adding isolated new nominal masses, selecting the increment most compatible with adjacent nominal masses.

11.3 Calculated plain-end mass

Plain-end mass per unit length for ISO 11960 or API 5CT [see also ISO 3183] is calculated by

$$w_{pe} = k_m \, k_{wpe} \, (D - t) \, t \tag{73}$$

where

D is the specified pipe outside diameter, in millimetres or inches;

k_m is the mass correction factor, 1,000 for carbon steel, 0,989 for martensitic chromium steel;

k_{wpe} is the mass per unit length conversion factor, equal to 0,024 661 5 for SI units and 10.69 for USC units;

t is the specified pipe wall thickness, in millimetres or inches;

w_{pe} is the plain-end mass per unit length, in kilograms per metre or pounds per foot.

11.4 Calculated finished-end mass

International Standards use the calculated mass gain (or loss) due to end finishing, e_m, to calculate the theoretical mass of a length of pipe; values of e_m given in International Standards are calculated from Equation (74). For plain-end pipe, $e_m = 0$.

$$e_m = L_j\,(w - w_{pe}) \tag{74}$$

where

e_m is the mass gain due to end finishing, in kilograms or pounds;

L_j is the length of a standard piece of pipe, in metres or feet;

w is the calculated threaded and coupled mass (w_{tc}), upset and threaded mass (w_{ij}), or upset mass (w_u) based on length L_j, in kilograms per metre or pounds per foot;

w_{pe} is the plain-end mass per unit length, in kilograms per metre or pounds per foot.

The finished-end mass of a joint is calculated using Equation (75),

$$W_L = w_{pe}L_{ef} + k_m\,e_m \tag{75}$$

where

e_m is the mass gain due to end finishing, in kilograms or pounds;

k_m is the mass correction factor: 1,000 for carbon steel, 0,989 for martensitic chromium steel;

L_{ef} is the length of pipe including end finish, in metres or feet;

W_L is the calculated mass of a piece of pipe of length L, in kilograms or pounds;

w_{pe} is the plain-end mass per unit length, in kilograms per metre or pounds per foot.

11.5 Calculated threaded and coupled mass

11.5.1 General

The calculated threaded and coupled mass per unit length is based on a length measured from the outer face of the coupling to the end of the pipe, as shown in Figure 2. The mill end of the coupling is assumed to be installed to the power-tight axial position.

$$w_{tc} = \{[L_j - k_{lsl}\,(N_L + 2J)/2]\,w_{pe} + \text{mass of coupling} - \text{mass removed in threading two pipe ends}\}/L_j \tag{76}$$

where

k_{lsl} is the length conversion factor, equal to 0,001 for SI units and 1/12 for USC units;

J is the distance from end of pipe to centre of coupling in power-tight position, in accordance with API 5B, in millimetres or inches;

L_j is the length of a standard piece of pipe, in metres or feet;

N_L is the coupling length, in accordance with ISO 11960 or API 5CT, in millimetres or inches;

w_{tc} is the threaded and coupled mass per unit length;

w_{pe} is the plain-end mass per unit length, in kilograms per metre or pounds per foot.

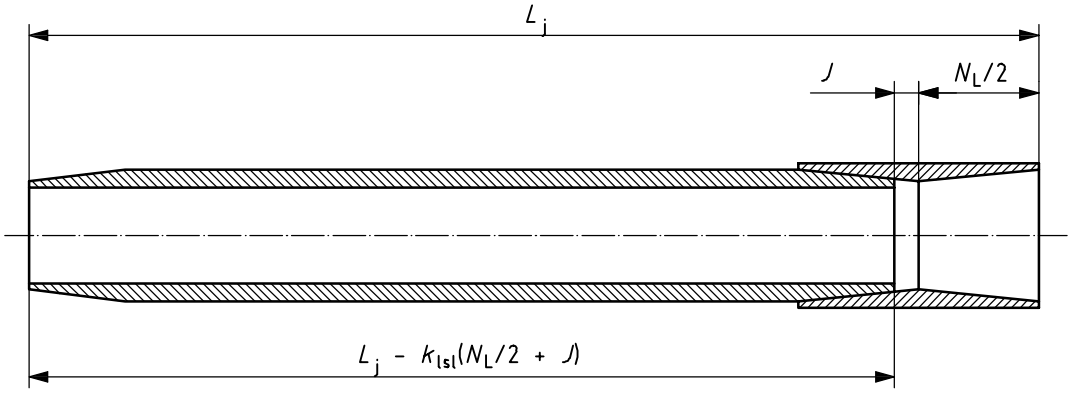

Key

L_j length of standard piece of pipe, in metres or feet

N_L coupling length, in accordance with ISO 11960 or API 5CT, in millimetres or inches

J distance from end of pipe to centre of coupling in power-tight position, in accordance with API 5B

k_{lsl} length conversion factor, equal to 0,001 for SI units and 1/12 for USC units

Figure 2 — Threaded and coupled pipe

11.5.2 Direct calculation of e_m – threaded and coupled pipe

$$e_m = k_{lsl}\,(N_L/2 + J)\,w_{pe} + \text{mass of coupling} - \text{mass removed in threading two pipe ends} \quad (77)$$

where

e_m is the mass gain due to end finishing, in kilograms or pounds;

k_{lsl} is the length conversion factor, equal to 0,001 for SI units and 1/12 for USC units;

J is the distance from end of pipe to centre of coupling in power-tight position, in accordance with API 5B, in millimetres or inches;

N_L is the coupling length, in accordance with ISO 11960 or API 5CT, in millimetres or inches;

w_{pe} is the plain-end mass per unit length, in kilograms per metre or pounds per foot;

and

mass of coupling is determined according to the appropriate part of 11.8 below;

mass removed in threading is determined according to the appropriate part of 11.9 below.

11.6 Calculated upset and threaded mass for integral joint tubing and extreme-line casing

11.6.1 General

The equations originally used by Armco Steel Corporation for calculating the upset and threaded mass values for extreme-line casing shown in the 1963 editions of API casing standards are no longer available due to destruction of some of their records. Calculations using the equations shown here and in 11.9.2, 11.9.4 and 11.10.5 for extreme-line casing result in values substantially in agreement, but not always identical, with those shown in the 1963 API standards.

The calculated upset and threaded mass is based on a standard length as shown in Figure 3.

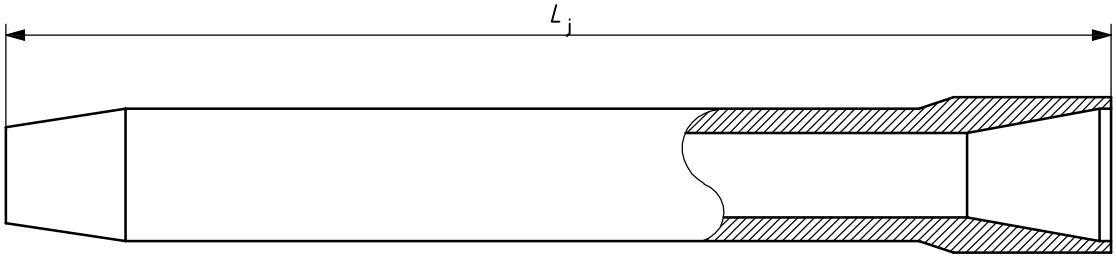

Key

L_j length of standard piece of pipe, in metres or feet

Figure 3 — Upset pipe

$$w_{ij} = w_{pe} + (\text{mass of upsets} - \text{mass removed in threading two ends})/L_j \quad (78)$$

where

L_j length of a standard piece of pipe, meters or feet;

w_{ij} upset and threaded mass per unit length, kilograms per meter or pounds per foot;

w_{pe} plain-end mass per unit length, kilograms per meter or pounds per foot.

11.6.2 Direct calculation of e_m – upset and threaded pipe

$$e_m = \text{mass of upsets} - \text{mass removed threading two pipe ends} \quad (79)$$

where

mass of upsets is determined according to the appropriate part of 11.10 below;

mass removed in threading is determined according to the appropriate part of 11.9 below.

11.7 Calculated upset mass

11.7.1 General

Calculated upset mass of upset drill pipe for weld-on tool joints is necessary for determination of e_m, the mass gain due to end finishing by upsetting.

The calculated upset mass, w_u, is based on a 6,10 m (20 ft) length measured end to end, including the upsets as shown in Figure 4.

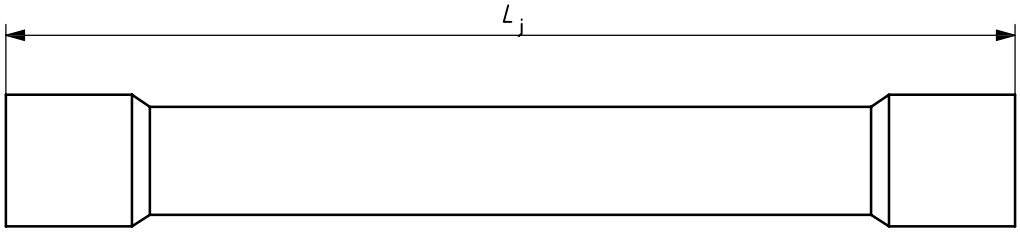

Key

L_j length of standard piece of pipe, in metres or feet

Figure 4 — Upset pipe — Both ends

$$w_u = w_{pe} + (\text{mass of upsets})/L_j \quad (80)$$

where

L_j is the length of a standard piece of pipe, in metres or feet;

w_{pe} is the plain-end mass per unit length, kilograms per metre or pounds per foot;

w_u is the upset mass per unit length, kilograms per metre or pounds per foot.

11.7.2 Direct calculation of e_m – upset pipe

$$e_m = \text{mass of upsets} \quad (81)$$

where mass of upsets is determined according to the appropriate part of 11.10 below.

11.8 Calculated coupling mass

11.8.1 General

Coupling masses are calculated as shown in 11.8.2 for line pipe and round thread casing and tubing, and in 11.8.3 for buttress thread casing.

11.8.2 Calculated coupling mass for line pipe and round thread casing and tubing

11.8.2.1 General

Coupling masses for line pipe are calculated on the basis of the dimensions shown in the 1942 edition of API 5L, which are identical with those shown in the 1971 edition [see also ISO 3183].

Coupling masses for round thread casing are calculated on the basis of the dimensions shown in the 1942 standards except for Label 1: 18-5/8 short and Label 1: 20 long round thread casing, which are based on hand-tight dimensions identical with the 1971 standard values.

Coupling masses shown for Label 1: 18 5/8 long round threads and for Label 1: 16 round threads are based on the old sharp thread form and dimensions. The hand-tight standoff values in the 1971 standards were made one thread turn larger than those in the 1942 standards. Recalculation on the basis of the 1971 hand-tight dimensions would result in slightly different coupling masses.

Non-upset tubing coupling masses are based on 1942 coupling dimensions, except for the Label 1: 1.050, Label 1: 1.315, and Label 1: 1.660 sizes, which were based on coupling dimensions added in 1962. The 1971 dimensions are identical with those from which the present coupling masses were calculated.

External upset tubing coupling masses are based on 1942 coupling dimensions except for the Label 1: 1.050 and Label 1: 1.315 sizes, which were based on coupling dimensions added in 1954. For regular diameter couplings, the dimensions used in calculating masses are identical with those in the 1971 standards. The special clearance coupling masses are based on the diameters introduced in the 1958 standards, which are identical with those in the 1971 standards. In calculating the masses of the special clearance couplings, an allowance is made for the mass removed by the special bevel. However, the masses were calculated several years before special clearance couplings were introduced into the standards in 1958 on the basis of a 12° degree bevel rather than the 20° bevel introduced in the 1962 standard. The masses were not recalculated for the change in bevel dimensions adopted for the special bevel in 1962. The special bevel is also available on regular diameter couplings, but separate listings of masses for these couplings are shown in the standards.

Masses for line pipe couplings and round thread casing and tubing couplings are calculated from Equations (83) to (91), with reference to Figures 5 and 6.

11.8.2.2 Couplings without special bevel mass allowance

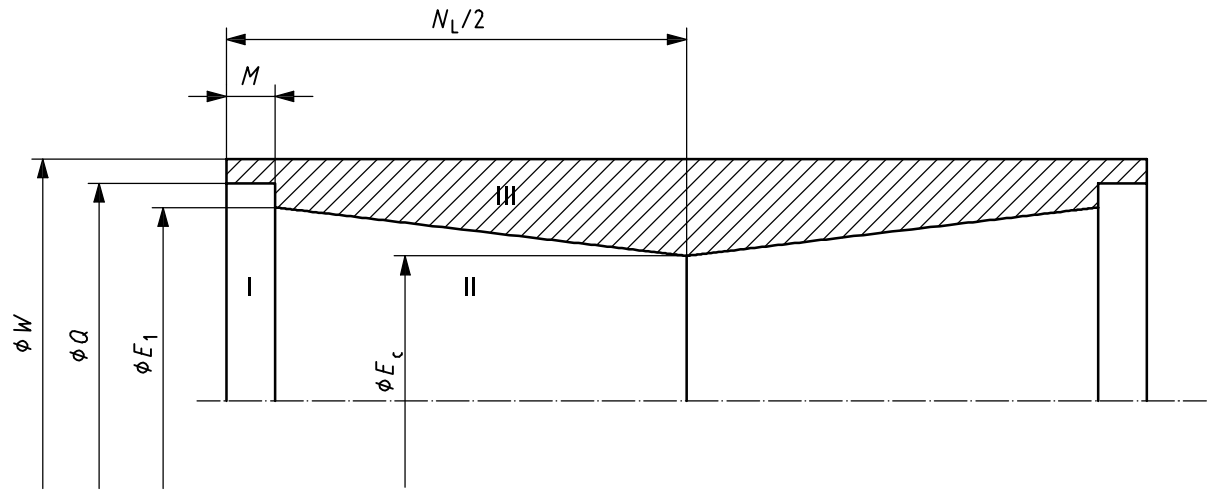

Key

N_L coupling length, in accordance with ISO 11960 or API 5CT, in millimetres or inches

M specified outside diameter of the extreme-line connection, length from the face of the coupling to the hand-tight plane for line pipe and for round thread casing and tubing, in accordance with API 5B

W specified coupling outside diameter, in accordance with ISO 11960 or API 5CT

Q diameter of coupling recess, in accordance with API 5B

E_1 pitch diameter at the hand-tight plane, in accordance with API 5B

E_c pitch diameter, at centre of coupling

I, II, III represent Volumes I, II, III respectively [see Equations (84), (85) and (87)]

Figure 5 — Pipe coupling

$$m_c = 0.566\ 6\ k_m \text{ (Vol. III)} \tag{82}$$

$$E_c = E_1 - (N_L/2 - M)\ T_d \tag{83}$$

$$\text{Vol. I} = 0.785\ 4 M Q^2 \tag{84}$$

$$\text{Vol. II} = 0.261\ 8\ (N_L/2 - M)(E_1^2 + E_1 E_c + E_c^2) \tag{85}$$

$$\text{Vol. (I + II + III)} = 0.785\ 4 N_L\ W^2/2 \tag{86}$$

$$\text{Vol. III} = \text{Vol. (I + II + III)} - \text{Vol. I} - \text{Vol. II.} \tag{87}$$

where

k_m is the mass correction factor: 1.000 for carbon steel, 0.989 for martensitic chromium steel;

m_c is the coupling mass;

T_d is the taper, 0.062 5.

Calculations for coupling masses are expressed in pounds. The final calculated mass is rounded to two decimals with no intermediate rounding in the calculations.

11.8.2.3 Coupling mass removed by special bevel

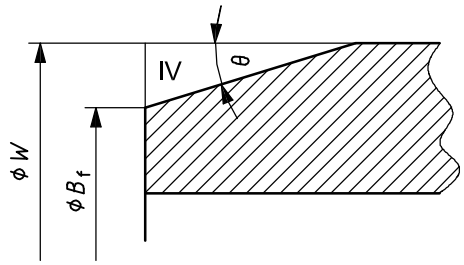

Key

W specified coupling outside diameter, in accordance with ISO 11960 or API 5CT

B_f maximum bearing face diameter, in accordance with dimension b in ISO 11960 or API 5CT

θ angle of bevel

IV represents Volume IV [see Equation (89)]

Figure 6 — Coupling with special bevel

Equation (88), which is used to calculate the mass allowance for the special bevel on special clearance couplings for external upset tubing, is approximate. The exact equation for Vol. IV is shown as Equation (89).

$$\text{Vol. IV} = 0.785\,4\,(W - B_f)\,(W^2 - B_f^2)/2\tan\theta \tag{88}$$

$$\text{Vol. IV} = (W - B_f)\,[0.785W^2 - 0.261\,8\,(B_f^2 + B_f\,W + W^2)]/\tan\theta \tag{89}$$

The coupling mass removed by special bevel, m_{crsb}, is calculated as

$$m_{crsb} = 0.566\,6\,k_m\,(\text{Vol. IV}) \tag{90}$$

where k_m is the mass correction factor: 1.000 for carbon steel, 0.989 for martensitic chromium steel.

11.8.2.4 Coupling mass with special bevel

The mass of a coupling with special bevel is calculated by subtracting the coupling mass removed by the special bevel, Equation (90) above, from the mass of the coupling without a special bevel, Equation (82). Calculations for coupling masses are in pounds. The final calculated mass is rounded to two decimals with no intermediate rounding in the calculations.

$$m_{csb} = m_c - m_{crsb} \tag{91}$$

where

m_c is the coupling mass;

m_{crsb} is the coupling mass removed by special bevel;

m_{csb} is the coupling mass with special bevel.

11.8.3 Calculated coupling mass for buttress thread casing

Coupling masses for buttress thread casing are calculated by Equations (92) to (97), with reference to Figure 7.

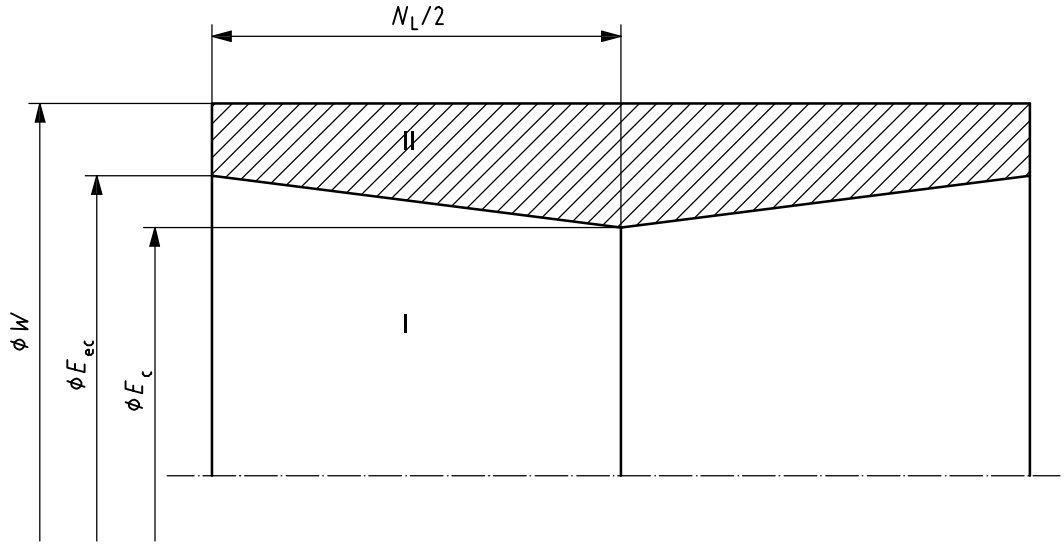

Key

N_L coupling length, in accordance with ISO 11960 or API 5CT, in millimetres or inches

W specified coupling outside diameter, in accordance with ISO 11960 or API 5CT

E_c pitch diameter, at centre of coupling

E_{ec} pitch diameter, at end of coupling

I, II represent Volumes I and II respectively [see Equations (94) and (96)]

Figure 7 — Mass calculations for buttress thread couplings

$$E_c = E_7 - (L_7 + J)\ T_d \tag{92}$$

$$E_{ec} = E_7 + (g + X)\ T_d \tag{93}$$

where

E_7 is the pitch diameter, in accordance with API 5B;

g is the length of imperfect threads, in accordance with API 5B;

J is the distance from end of pipe to centre of coupling in power-tight position, in accordance with API 5B;

L_7 is the length of perfect threads, in accordance with API 5B;

X = 0.300 for sizes less than Label 1: 16
= 0.200 for sizes Label 1: 16 and larger;

T_d is the taper: 0.062 5 for sizes less than Label 1: 16; 0.083 3 for sizes Label 1: 16 and larger.

$$\text{Vol. I} = 0.261\ 8\ (N_L/2)(E_{ec}^2 + E_{ec}E_c + E_c^2) \tag{94}$$

$$\text{Vol. (I + II)} = 0.785\ 4\ (N_L/2)W^2 \tag{95}$$

$$\text{Vol. II} = \text{Vol. (I + II)} - \text{Vol. I} \tag{96}$$

The coupling mass of buttress thread casing, m_{cB}, is calculated as

$$m_{cB} = 0.566\,6\; k_m\, (\text{Vol. II}) \tag{97}$$

where k_m is the mass correction factor: 1.000 for carbon steel, 0.989 for martensitic chromium steel.

Calculations for coupling masses are in pounds. The final calculated mass is rounded to two decimals with no intermediate rounding in the calculations.

11.9 Calculated mass removed during threading

11.9.1 General

The mass removed in threading pipe or pin ends is calculated in accordance with 11.9.2. The mass removed in threading and recessing box ends for extreme-line is calculated in accordance with 11.9.3.

11.9.2 Calculated mass removed during threading pipe or pin ends

The mass removed by threading pipe or pin ends is calculated from Equations (98) to (108) with reference to Figures 8 to 10.

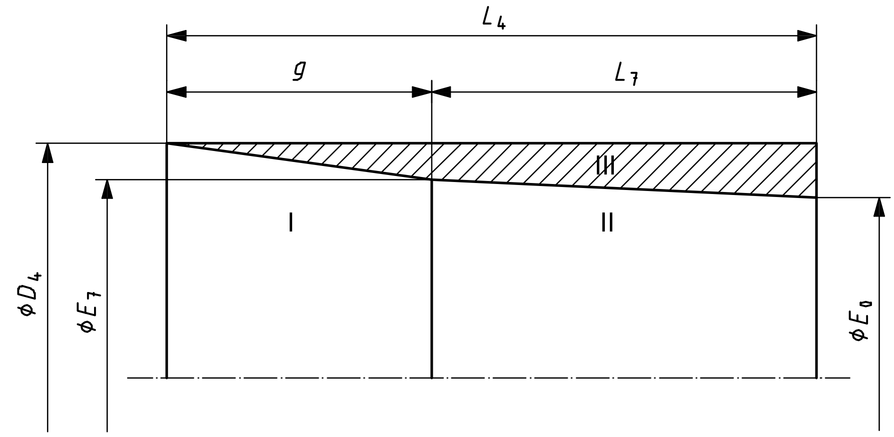

Key

L_4 pin thread length, in accordance with API 5B, in millimetres or inches

D_4 upset outside diameter of upset pipe and pipe outside diameter of non-upset pipe and buttress thread casing, in accordance with API 5B

g length of imperfect threads, in accordance with API 5B

L_7 length of perfect threads, in accordance with API 5B

E_7 pitch diameter, in accordance with API 5B

E_0 pitch diameter, at end of pipe

I, II, III represent Volumes I, II, III respectively [see Equations (99), (100), (102)]

Figure 8 — Round threads and line pipe threads

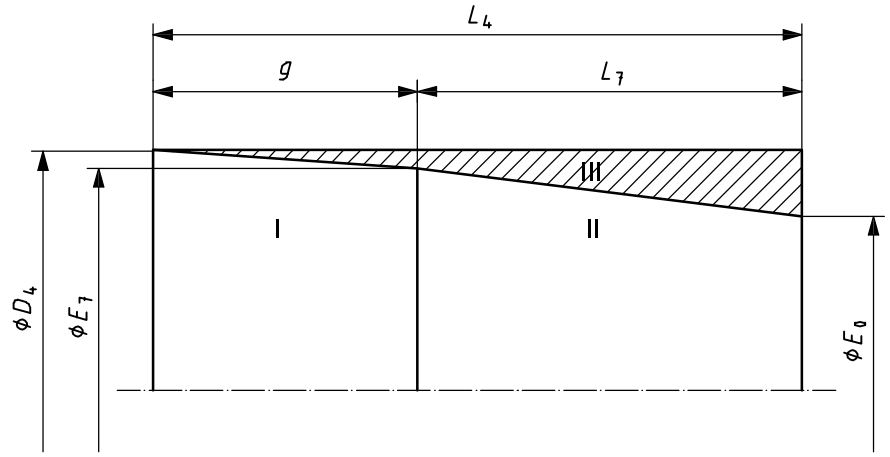

Key

L_4 pin thread length, in accordance with API 5B, in millimetres or inches

D_4 upset outside diameter of upset pipe and pipe outside diameter of non-upset pipe and buttress thread casing, in accordance with API 5B

g length of imperfect threads, in accordance with API 5B

L_7 length of perfect threads, in accordance with API 5B

E_7 pitch diameter, in accordance with API 5B

E_0 pitch diameter, at end of pipe

I, II, III represent Volumes I, II, III respectively [see Equations (99), (100), (102)]

Figure 9 — Buttress threads

$$E_0 = E_7 - L_7\, T_d \tag{98}$$

where

T_d = 0.062 5 for all round threads and for buttress threads in size less than Label 1: 16
= 0.083 3 for buttress threads in sizes Label 1: 16 and larger.

For Figures 8 and 9:

$$\text{Vol. I} = 0.261\,8g\,(D_4^2 + D_4E_7 + E_7^2) \tag{99}$$

$$\text{Vol. II} = 0.261\,8\,(L_4 - g)\,(E_7^2 + E_7E_0 + E_0^2) \tag{100}$$

$$\text{Vol. (I + II + III)} = 0.785\,4L_4D_4^2 \tag{101}$$

$$\text{Vol. III} = \text{Vol. (I + II + III)} - \text{Vol. I} - \text{Vol. II} \tag{102}$$

The mass removed by threading, m_{rt}, is calculated as

$$m_{rt} = 0.283\,3\,k_m\,(\text{Vol. III}) \tag{103}$$

where k_m is the mass correction factor: 1.000 for carbon steel, 0.989 for martensitic chromium steel.

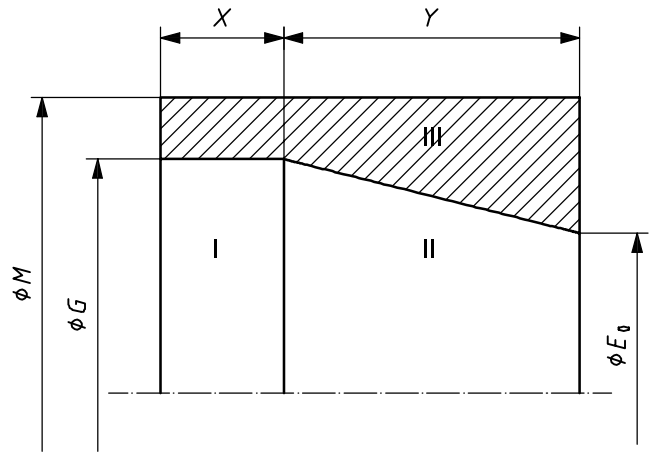

Key

M specified outside diameter of the extreme-line connection, in accordance with API 5B

G internal dimension of extreme-line connection pin beyond thread run-out, in accordance with API 5B

E_0 pitch diameter, at end of pipe

X internal dimension of extreme-line connection entrance threads, in accordance with API 5B

Y internal dimension of extreme-line connection entrance threads, in accordance with API 5B

I, II, III represent Volumes I, II, III respectively [see Equations (104), (105), (107)]

Figure 10 — Extreme-line pin thread

For Figure 10:

X = 0.360 for sizes Label 1: 5-1/2 through Label 1: 7-5/8
= 0.404 for sizes Label 1: 8-5/8 through Label 1: 10-3/4.

Y = 3.230 for sizes Label 1: 5-1/2 through Label 1: 7-5/8
= 5.658 5 for sizes Label 1: 8-5/8 through Label 1: 10-3/4.

E_0 = G – 0.529 for sizes Label 1: 5-1/2 through Label 1: 7-5/8
= G – 0.583 for sized Label 1: 8-5/8 through Label 1: 10-3/4.

$$\text{Vol. I} = 0.785\ 4XG^2 \tag{104}$$

$$\text{Vol. II} = 0.261\ 8Y\ (G^2 + GE_0 + E_0{}^2) \tag{105}$$

$$\text{Vol. (I + II + III)} = 0.785\ 4\ (X + Y)M^2 \tag{106}$$

$$\text{Vol. III} = \text{Vol. (I + II + III)} - \text{Vol. I} - \text{Vol. II} \tag{107}$$

The pin mass removed by threading, m_{prt}, is calculated as

$$m_{prt} = 0.283\ 3\ k_m\ (\text{Vol. III}) \tag{108}$$

where k_m is the mass correction factor: 1.000 for carbon steel, 0.989 for martensitic chromium steel.

11.9.3 Calculated mass removed during threading integral joint tubing box ends

The mass removed by threading and recessing the box ends of integral joint tubing is calculated from Equations (109) to (115), with reference to Figure 11.

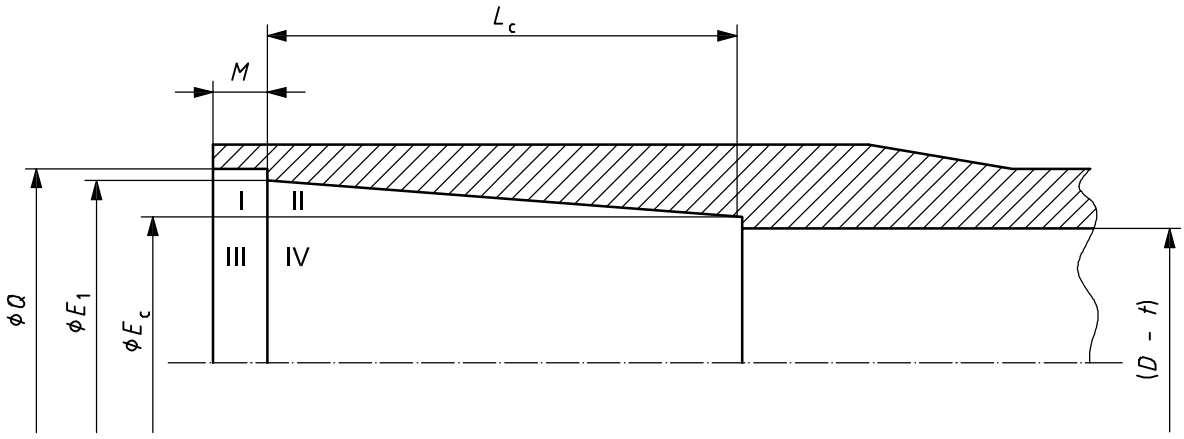

Key

M length from the face of the coupling to the hand-tight plane for line pipe and for ROUND thread casing and tubing, in accordance with API 5B

L_c minimum length of full crest threads from end of pipe, in accordance with API 5B

Q diameter of coupling recess, in accordance with API 5B

E_1 pitch diameter at the hand-tight plane, in accordance with API 5B

E_c pitch diameter, at centre of coupling

D specified pipe outside diameter, in accordance with ISO 11960 or API 5CT

t specified pipe wall thickness, in accordance with ISO 11960 or API 5CT

I, II, III, IV represent Volumes I, II, III IV respectively [see Equations (111) to (114)]

Figure 11 — Integral joint tubing

$$L_c = L_1 + J + A \tag{109}$$

$$E_c = E_1 - L_c\, T_d \tag{110}$$

where

J is the end of pipe to thread run-out in box power-tight.

$$\text{Vol. (I + III)} = 0.785\ 4MQ^2 \tag{111}$$

$$\text{Vol. (II + IV)} = 0.261\ 8L_c\ (E_1^2 + E_1E_c + E_1^2) \tag{112}$$

$$\text{Vol. (III + IV)} = 0.785\ 4\ (M + L_c)(D - t)^2 \tag{113}$$

$$\text{Vol. (I + II)} = \text{Vol. (I + III)} + \text{Vol. (II + IV)} - \text{Vol. (III + IV)} \tag{114}$$

The integral joint mass removed by threading and recessing, m_{irt}, is calculated as

$$m_{irt} = 0.283\ 3\ k_m\ [\text{Vol. (I + II)}] \tag{115}$$

where k_m is the mass correction factor: 1,000 for carbon steel, 0,989 for martensitic chromium steel.

11.9.4 Calculated mass removed during threading extreme-line casing box ends

The mass removed by threading and recessing the box ends of extreme-line casing is calculated from Equations (116) to (123), with reference to Figure 12.

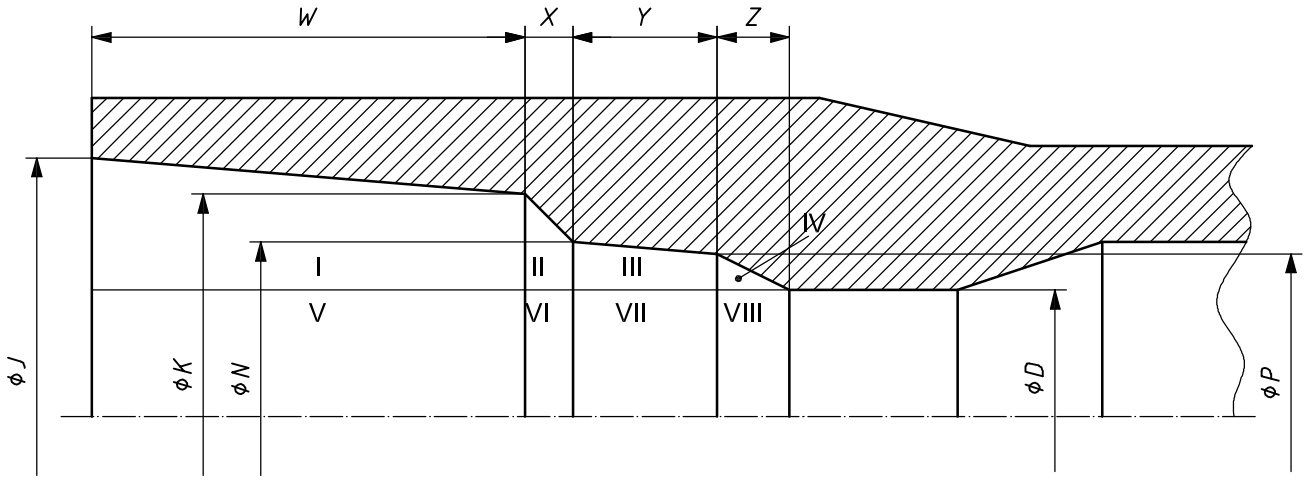

Key

J internal dimension of extreme-line connection, in accordance with API 5B
W internal dimension of extreme-line connection, in accordance with API 5B
K pitch diameter at the hand-tight plane
N for undefined symbols other than the Roman numerals representing areas, see API 5B for extreme-line dimensions
P for undefined symbols other than the Roman numerals representing areas, see API 5B for extreme-line dimensions
D specified pipe outside diameter
X internal dimension of extreme-line connection, in accordance with API 5B
Y internal dimension of extreme-line connection, in accordance with API 5B
Z internal dimension of extreme-line connection, in accordance with API 5B

I, II, III, IV, V, VI, VII, VIII represent Volumes I, II, III, IV, V, VI, VII, VIII respectively [see Equations (117) to (122)]

Figure 12 — Extreme-line casing

where

$$Z = 0.5(P - D) \tag{116}$$

$$\text{Vol. (I + V)} = 0.261\ 8W(J^2 + JK + K^2) \tag{117}$$

$$\text{Vol. (II + VI)} = 0.261\ 8X(K^2 + KN + N^2) \tag{118}$$

$$\text{Vol. (III + VII)} = 0.261\ 8Y(N^2 + NP + P^2) \tag{119}$$

$$\text{Vol. (IV + VIII} = 0.261\ 8Z(P^2 + PD + D^2) \tag{120}$$

$$\text{Vol. (V + VI + VII + VIII)} = 0.785\ 4(W + X + Y + Z)D^2 \tag{121}$$

$$\text{Vol. (I + II + III + IV)} = \text{Vol. (I + V)} + \text{Vol. (II + VI)} + \text{Vol. (III + VII)} + \text{Vol. (IV + VIII)} - \text{Vol. (V + VI + VII + VIII)} \tag{122}$$

The extreme-line mass removed by threading and recessing, m_{xrt}, is calculated as

$$m_{xrt} = 0.283\ 3\ k_m\ [\text{Vol. (I + II + III + IV)}] \quad (123)$$

where k_m is the mass correction factor: 1,000 for carbon steel, 0,989 for martensitic chromium steel.

NOTE Calculations for mass removed in threading, or threading and recessing, are expressed in pounds and are carried to four decimals.

11.10 Calculated mass of upsets

11.10.1 General

The mass added when upsetting pipe or pin ends is calculated in accordance with 11.10.2 to 11.10.4. The mass added for upsets for extreme-line casing is calculated in accordance with 11.10.5.

11.10.2 Calculated mass of external upsets

The mass added by an external upset is calculated by Equations (124) to (128), with reference to Figure 13.

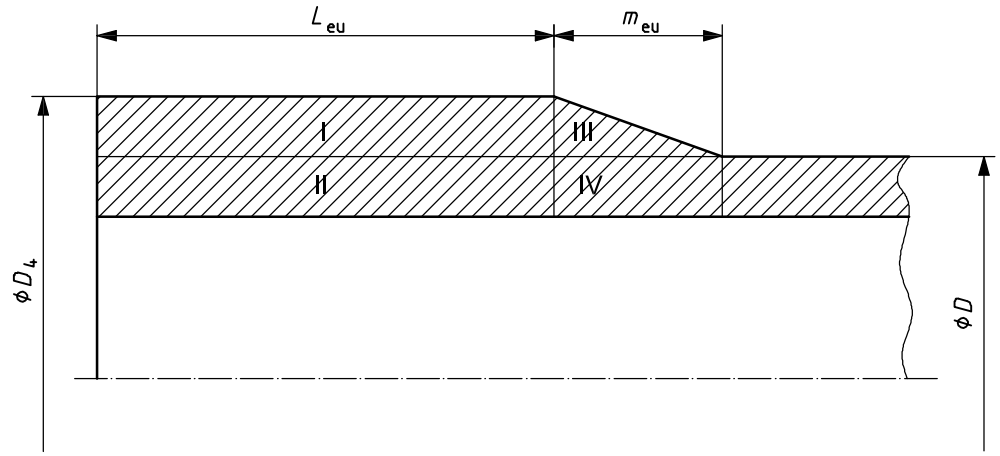

Key

D_4 major diameter, in accordance with API 5B

D specified pipe outside diameter

L_{eu} length from end of pipe to start of taper, in accordance with ISO 11960 or API 5CT

m_{eu} length of box upset taper, in accordance with ISO 11960 or API 5CT

I, II, III, IV represent Volumes I, II, III IV respectively [see Equations (124) to (127)]

Figure 13 — External upset

$$\text{Vol. (I + II)} = 0.785\ 4 L_{eu} D_4^2 \quad (124)$$

$$\text{Vol. (III + IV)} = 0.261\ 8 m_{eu} (D_4^2 + D_4 D + D^2) \quad (125)$$

$$\text{Vol. (II + IV)} = 0.785\ 4\ (L_{eu} + m_{eu}) D^2 \quad (126)$$

$$\text{Vol. (I + III)} = \text{Vol. (I + II)} + \text{Vol. (III + IV)} - \text{Vol. (II + IV)} \quad (127)$$

The external upset mass, m_{exu}, is calculated as

$$m_{exu} = 0.283\ 3\ k_m\ [\text{Vol. (I + III)}] \quad (128)$$

where k_m is the mass correction factor: 1,000 for carbon steel, 0,989 for martensitic chromium steel.

NOTE Calculations for the mass of an external upset are expressed in pounds and carried to four decimals.

11.10.3 Calculated mass of internal upsets

The mass added by an internal upset is calculated by Equations (129) to (133), with reference to Figure 14.

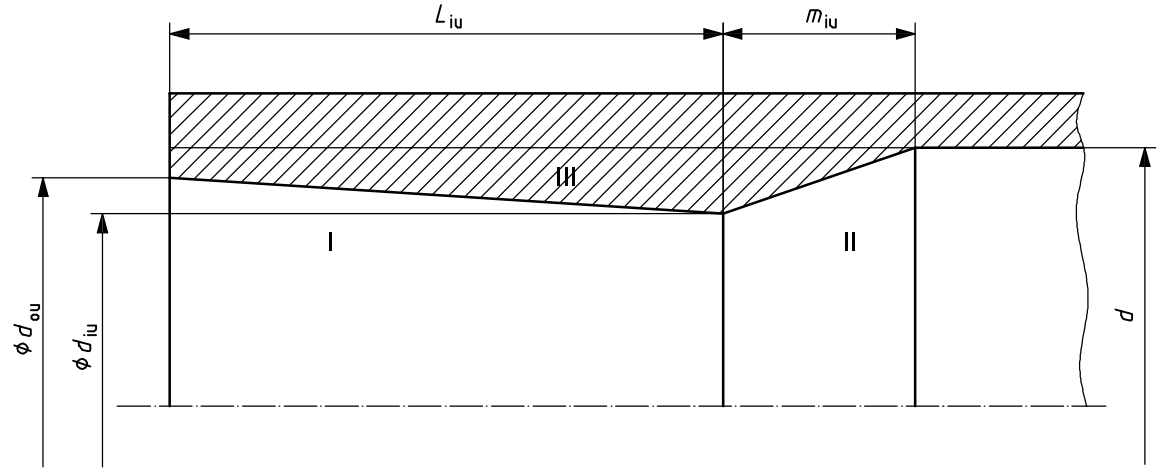

Key

d pipe inside diameter
d_{ou} inside diameter at end of upset pipe
L_{iu} length of pin upset, in accordance with ISO 11960 or API 5CT
d_{iu} inside diameter of pin upset, in accordance with ISO 11960 or API 5CT
m_{iu} length of pin upset taper, in accordance with ISO 11960 or API 5CT

I, II, III represent Volumes I, II, III respectively [see Equations (129) to (132)]

Figure 14 — Internal upset

$$\text{Vol. I} = 0.261\ 8 L_{iu}(d_{ou}^2 + d_{ou}d_{iu} + d_{iu}^2) \quad (129)$$

$$\text{Vol. II} = 0.261\ 8 m_{iu}(d^2 + dd_{iu} + d_{iu}^2) \quad (130)$$

$$\text{Vol. (I + II + III)} = 0.785\ 4 d^2(L_{iu} + m_{iu}) \quad (131)$$

$$\text{Vol. III} = \text{Vol. (I + II + III)} - \text{Vol. I} - \text{Vol. II} \quad (132)$$

The internal upset mass, m_{inu}, is calculated as

$$m_{inu} = 0.283\ 3\ k_m\ (\text{Vol. III}) \quad (133)$$

where k_m is the mass correction factor: 1,000 for carbon steel, 0,989 for martensitic chromium steel.

NOTE Calculations for the mass of an internal upset are expressed in pounds and carried to four decimals.

11.10.4 Calculated mass of external-internal upsets

The mass added by an external-internal upset is calculated as the sum of the mass of an external upset calculated from Equation (128), and the mass of an internal upset calculated from Equation (133).

The external-internal upset mass, m_{eiu}, is calculated as

$$m_{eiu} = m_{inu} + m_{exu} \tag{134}$$

where

m_{exu} is the external upset mass;

m_{inu} is the internal upset mass.

NOTE Calculations for the mass of an external-internal upset are expressed in pounds and carried to four decimals.

11.10.5 Calculated mass of extreme-line upsets

The mass added by the box and pin upsets for extreme-line casing is calculated from Equations (135) to (144) with reference to Figures 15 and 16.

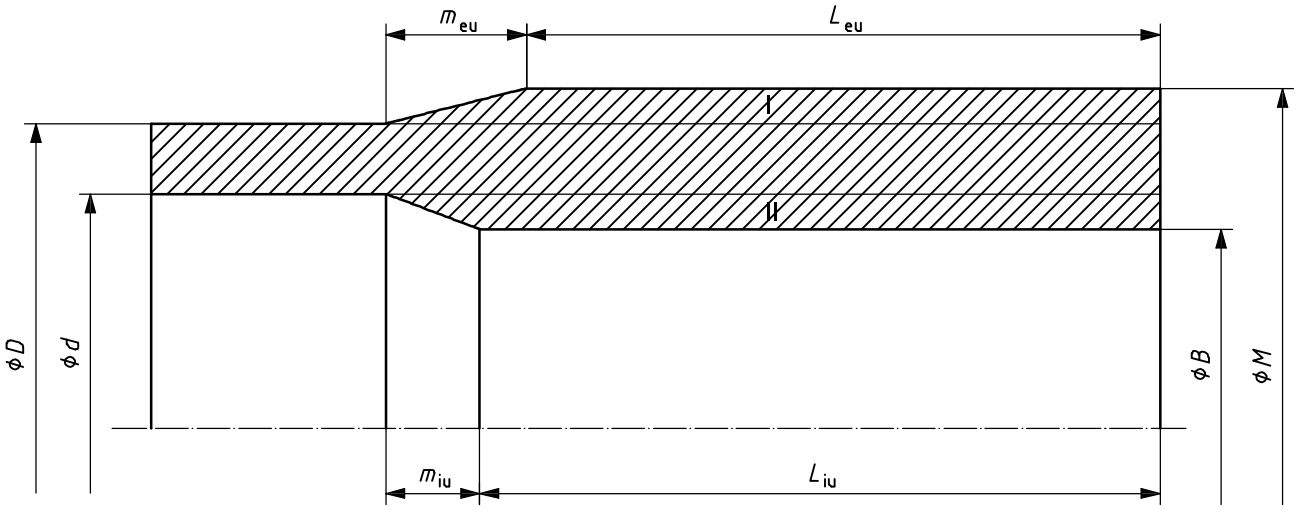

Key

D specified pipe outside diameter

d pipe inside diameter

m_{eu} length of box upset taper, in accordance with ISO 11960 or API 5CT

m_{iu} length of pin upset taper, in accordance with ISO 11960 or API 5CT

L_{iu} length of pin upset, in accordance with ISO 11960 or API 5CT

L_{eu} length from end of pipe to start of taper, in accordance with ISO 11960 or API 5CT

B specified inside diameter of the extreme-line connection, in accordance with API 5B

M specified outside diameter of the extreme-line connection; length from the face of the coupling to the hand-tight plane for line pipe and for round thread casing and tubing, in accordance with API 5B

I, II represent Volumes I, II respectively [see Equations (137) and (138)]

Figure 15 — Pin upset

$$m_{eu} = 6(M - D) \tag{135}$$

$$m_{iu} = 6(d - B) \tag{136}$$

L_{eu} = 8.000 − m_{eu} for Label 1: 5-1/2 through Label 1: 7-5/8
= 10.500 − m_{eu} for Label 1: 8-5/8 through Label 1: 10-3/4

L_{iu} = 6.625 for Label 1: 5-1/2 through Label 1: 7-5/8
= 8.000 for Label 1: 8-5/8 through Label 1: 10-3/4

$$\text{Vol. I} = 0.785\ 4L_{eu}M^2 + 0.261\ 8m_{eu}\ (D^2 + DM + M^2) - 0.785\ 4\ (L_{eu} + m_{eu})D^2 \tag{137}$$

$$\text{Vol. II} = 0.785\ 4\ (L_{iu} + m_{iu})d^2 - 0.785\ 4L_{iu}B^2 - 0.261\ 8m_{iu}\ (d^2 + dB + B^2) \tag{138}$$

The extreme-line pin upset mass, m_{xpu}, is calculated as

$$m_{xpu} = 0.283\ 3\ k_m\ [\text{Vol. (I + II)}] \tag{139}$$

where k_m is the mass correction factor: 1,000 for carbon steel, 0,989 for martensitic chromium steel.

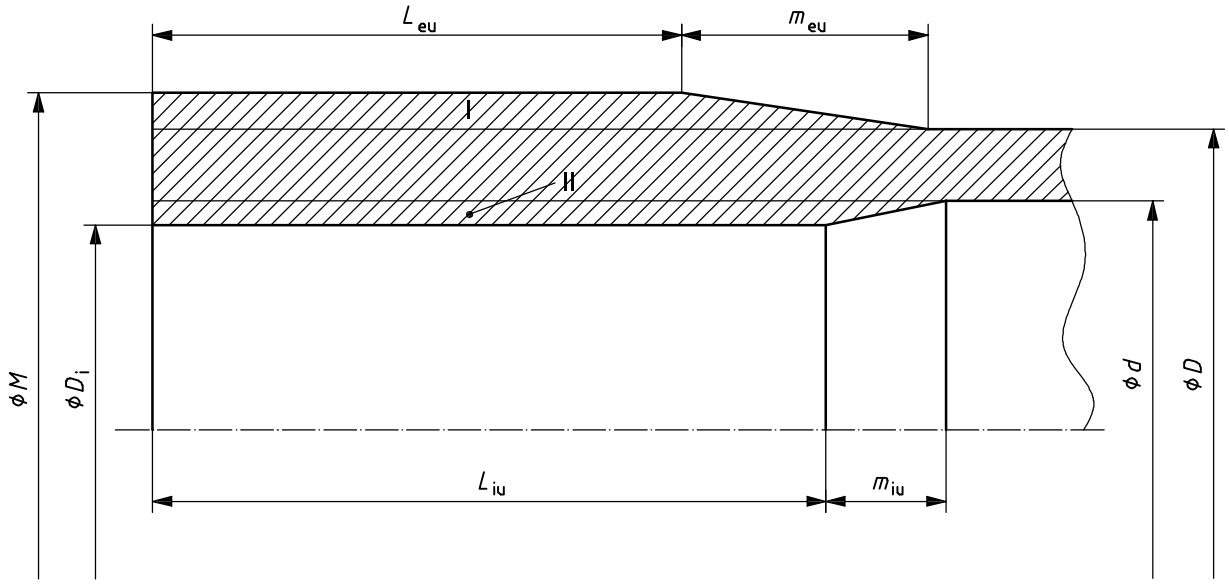

Key

M specified outside diameter of the extreme-line connection; length from the face of the coupling to the hand-tight plane for line pipe and for round thread casing and tubing, in accordance with API 5B

D_i inside diameter of extreme-line box upset, in accordance with API 5B

L_{eu} length from end of pipe to start of taper, in accordance with ISO 11960 or API 5CT

m_{eu} length of box upset taper, in accordance with ISO 11960 or API 5CT

L_{iu} length of pin upset, in accordance with ISO 11960 or API 5CT

m_{iu} length of pin upset taper, in accordance with ISO 11960 or API 5CT

D specified pipe outside diameter

d pipe inside diameter

I, II represent Volumes I, II respectively [see Equations (142) and (143)]

Figure 16 — Box upset

$$m_{eu} = 6(M - D) \tag{140}$$

$$m_{iu} = 6(d - D_i) \tag{141}$$

L_{eu} = 8.000 − m_{eu} for Label 1: 5-1/2 through Label 1: 7-5/8
= 10.500 − m_{eu} for Label 1: 8-5/8 through Label 1: 10-3/4

L_{iu} = 7.000 for Label 1: 5-1/2 through Label 1: 7-5/8
= 8.375 for Label 1: 8-5/8 through Label 1: 10-3/4

$$\text{Vol. I} = 0.785\,4 L_{eu} M^2 + 0.261\,8 m_{eu} (M^2 + MD + D^2) - 0.785\,4 (L_{eu} + m_{eu}) D^2 \tag{142}$$

$$\text{Vol. II} = 0.785\,4 (L_{iu} + m_{iu}) d^2 - 0.785\,4 L_{iu} D_i^2 - 0.261\,8 m_{iu} (D_i^2 + D_i d + d^2) \tag{143}$$

The extreme-line pin upset mass, m_{xbu}, is calculated as

$$m_{xbu} = 0.283\,3\, k_m (\text{Vol. I} + \text{Vol. II}) \tag{144}$$

where k_m is the mass correction factor: 1.000 for carbon steel, 0.989 for martensitic chromium steel.

NOTE Calculations for the masses of the extreme-line box and pin upsets are expressed in pounds and carried to four decimals.

12 Elongation

The minimum elongation over 50,8 mm (2 in) is calculated from

$$\varepsilon_{el} = k_{el} A_s^{0,2} / f_{umn}^{0,9} \tag{145}$$

where

A_s is the cross-sectional area of the tensile test specimen, in square millimetres (square inches), based on specified outside diameter or nominal specimen width and specified wall thickness, rounded to the nearest 10 mm^2 (0.01 in^2), or 490 mm^2 (0.75 in^2), whichever is smaller;

ε_{el} is the minimum gauge length extension in 50,8 mm (2.0 in), expressed in percent rounded to the nearest 0,5 % below 10 % and to the nearest unit percent for 10 % and larger;

f_{umn} is the specified minimum tensile strength, in MPa (psi);

k_{el} is the elongation constant, equal to 1 942,57 for SI units and 625 000 for USC units.

The equation for elongation was adopted at the June 1967 API Standardization Conference as reported in API Circular PS-1340.

13 Flattening tests

13.1 Flattening tests for casing and tubing

The distance between plates for flattening tests for welded casing and tubing is calculated from the equations shown in Table 10.

Table 10 — Casing and tubing flattening tests — Distance between plates

(1) Grade	(2) D/t ratio	(3) Maximum distance between plates in
H40	16 and over	$0{,}5D$
	less than 16	$D(0{,}830 - 0{,}020\ 6\ D/t)$
J55 and K55	16 and over	$0{,}65D$
	3,93 to 16	$D(0{,}980 - 0{,}020\ 6\ D/t)$
	less than 3,93	$D(1{,}104 - 0{,}051\ 8\ D/t)$
N80 [a]	9 to 28	$D(1{,}074 - 0{,}017\ 4\ D/t)$
L80	9 to 28	$D(1{,}074 - 0{,}019\ 4\ D/t)$
C95 [a]	9 to 28	$D(1{,}080 - 0{,}017\ 8\ D/t)$
Q125 [b]	All	$D(1{,}092 - 0{,}014\ 0\ D/t)$

[a] If the flattening test of C95 or N80 fails at 12 or 6 o'clock, the flattening should continue until the remaining portion of the specimen fails at the 3 or 9 o'clock position. Premature failure at the 12 or 6 o'clock position should not be considered basis for rejection.

[b] See ISO 11960 or API 5CT. Flattening should be a minimum of $0{,}85D$.

In Table 10,

D is the specified pipe outside diameter, in millimetres or inches;

t is the specified pipe wall thickness, in millimetres or inches.

The flattening test equation for Grade H40 was adopted at the May 1939 API Standardization Conference. The equations for Grades J55, K55, N80 and C95 were adopted at the June 1972 API Standardization Conference as reported in API Circular PS-1440. The equation for Grade L80 was adopted at the June 1974 API Standardization Conference as reported in API Circular PS-1487. The equation for Grade Q125 was adopted at the June 1984 API Standardization Conference as reported in API Circular PS-1736.

13.2 Flattening tests for line pipe

The maximum distance between plates for flattening tests for line pipe is calculated from the equations shown in Table 11.

Table 11 — Line pipe flattening tests — Distance between plates

(1) Grade	(3) Maximum distance between plates in
Less than X-52	$3{,}07t/(0{,}07+3t/D)$
X-52 and higher	$3{,}05t/(0{,}05+3t/D)$

In Table 11,

D is the specified pipe outside diameter, in millimetres or inches;

t is the specified pipe wall thickness, in millimetres or inches.

Flattening tests for line pipe are addressed in API 5L. The flattening test equations for line pipe were developed by the API Task Group on Welding and Weld Testing and adopted at the June 1970 API Standardization Conference as reported in API Circular PS-1398.

14 Hydrostatic test pressures

14.1 Hydrostatic test pressures for plain-end pipe, extreme-line casing and integral joint tubing

The hydrostatic test pressures for plain-end pipe, extreme-line casing, and integral-joint tubing are calculated according to the following equation, except for grade A25 line pipe, grades A and B line pipe in sizes less than Label 1: 2-3/8, and threaded and coupled line pipe in sizes Label 1: 6-5/8 and less, which were determined arbitrarily.

The hydrostatic test pressure, p_{ht}, expressed in kilopascals or pounds per square inch, is calculated as

$$p_{ht} = 2\sigma_f t/D \tag{146}$$

where

D is the specified pipe outside diameter, in millimetres or inches;

t is the specified pipe wall thickness, in millimetres or inches;

σ_f is the fibre stress corresponding to the percent of specified yield strength as given in Table 12, in kPa or psi.

Alternative test pressures should be used when specified on the purchase agreement and when agreed by the purchaser and manufacturer per ISO 11960 or API 5CT.

14.2 Hydrostatic test pressure for threaded and coupled pipe

The hydrostatic test pressure for threaded and coupled pipe is the same as for plain-end pipe, except where a lower pressure is required to avoid leakage due to insufficient internal yield pressure of the coupling or insufficient internal pressure leak resistance at the E_1 or E_7 plane as calculated in Clause 10.

The test pressure should be based on the lowest of the test pressure determined for plain-end pipe in 14.1, or 80 % of the internal coupling yield pressure result from Equation (66) in 10.2, or the internal pressure leak resistance result from Equation (69) in 10.3. The basis for this equation was adopted at the 1968 API Standardization Conference as shown in API Circular PS-1360.

Table 12 — Factors for test pressure equations

(1) Grade	(2) Label 1	Fibre stress as a percent of specified minimum yield strength		Maximum test pressure [a] kPa (psi)	
		(3) Standard test pressures	(4) Alternative test pressures	(5) Standard	(6) Alternative
A and B	2-3/8 – 3-1/2	60	75	17 240 (2 500)	17 240 (2 500)
A and B	Over 3-1/2	60	75	19 300 (2 800)	19 300 (2 800)
X Grades	4-1/2 and under	60	75	20 680 (3 000)	20 680 (3 000)
X Grades	5-9/16	75	[b]	20 680 (3 000)	[b]
X Grades	6-5/8 and 8-5/8	75	[b]	20 680 (3 000)	[b]
X Grades	10-3/4 – 18	85	[b]	20 680 (3 000)	[b]
X Grades	20 and larger	90	[b]	20 680 (3 000)	[b]
H40, J55 and K55	9-5/8 and under	80	80	20 680 (3 000)	68 950 (10 000)
H40, J55 and K55	10-3/4 and larger	60	80	20 680 (3 000)	68 950 (10 000)
M65	All sizes	60	80	20 680 (3 000)	68 950 (10 000)
L80 and N80	All sizes	80	[b]	68 950 [c] (10 000)	[b]
C90	All sizes	80	[b]	68 950 [c] (10 000)	[b]
C95	All sizes	80	[b]	68 950 [c] (10 000)	[b]
T95	All sizes	80	[b]	68 950 [c] (10 000)	[b]
P110	All sizes	80	80	68 950 [c] (10 000)	[d]
Q125	All sizes	80	80	68 950 [c] (10 000)	[d]

[a] Higher test pressures are permissible by agreement between purchaser and manufacturer.

[b] No alternative test pressure.

[c] Plain-end pipe is tested to 20 680 kPa (3 000 psi) maximum unless a higher pressure is agreed upon by the purchaser and manufacturer.

[d] No maximum test pressure, except that plain-end pipe is tested to 20 680 kPa (3 000 psi) unless a higher pressure is agreed upon by the purchaser and manufacturer.

15 Make-up torque for round thread casing and tubing

The values of optimum make-up torque listed in ISO 10405 or API RP 5C1 (in foot-pounds) were taken as 1 % of the calculated joint pull-out strength for round thread casing and tubing as determined from Equation (55).

In the study of make-up torque, the API Task Group on API RP 5C1 observed that the API round thread joint pull-out strength equation contains several of the variables believed to affect make-up torque. The task group investigated the possibility of using a modification of the joint strength equation for establishing torque values. They found that the torque values obtained by dividing the calculated pull-out value by 100 to be generally comparable to those values obtained by field make-up tests where the API modified thread compound was used.

This method for calculating make-up torque was adopted at the June 1970 API Standardization Conference as reported in API Circular PS-1398. Subsequently, optimum and maximum torques were dropped for large diameter (sizes Label 1: 16 to Label 1: 20) casing. Minimum torque was changed to 1 % of pull-out strength. This was adopted at the June 1980 API Standardization Conference as reported in API Circular PS-1637.

Action was taken by the API Committee on Standardization of Tubular Goods at the February 1991 meeting to eliminate minimum and maximum torque values (formerly 75 % and 125 % of the optimum make-up torque, respectively) and emphasize position on make-up.

16 Guided bend tests for submerged arc-welded line pipe

16.1 General

Dimensions for the jig for guided bend tests for submerged arc-welded line pipe are calculated from Equation (147) with reference to Figure 17.

The critical dimension on guided bend test jig, A_{gbtj}, denoted as dimension A in ISO 3183 or API 5L, is calculated as

$$A_{\text{gbtj}} = [1{,}15\ (D - 2t)]/[\varepsilon_{\text{eng}} D/t - 2\varepsilon_{\text{eng}} - 1] - t \qquad (147)$$

where

D is the specified pipe outside diameter;

t is the specified pipe wall thickness;

ε_{eng} is the engineering strain;

where the value of ε_{eng} depends on grade and additional dimensions (in units of inches) are defined by $R_{\text{A}} = A_{\text{gbtj}}/2$, $B = A_{\text{gbtj}} + 2t + 0.125$ in, $R_{\text{B}} = B/2$; see Table 13.

Dimensions in inches (millimetres)

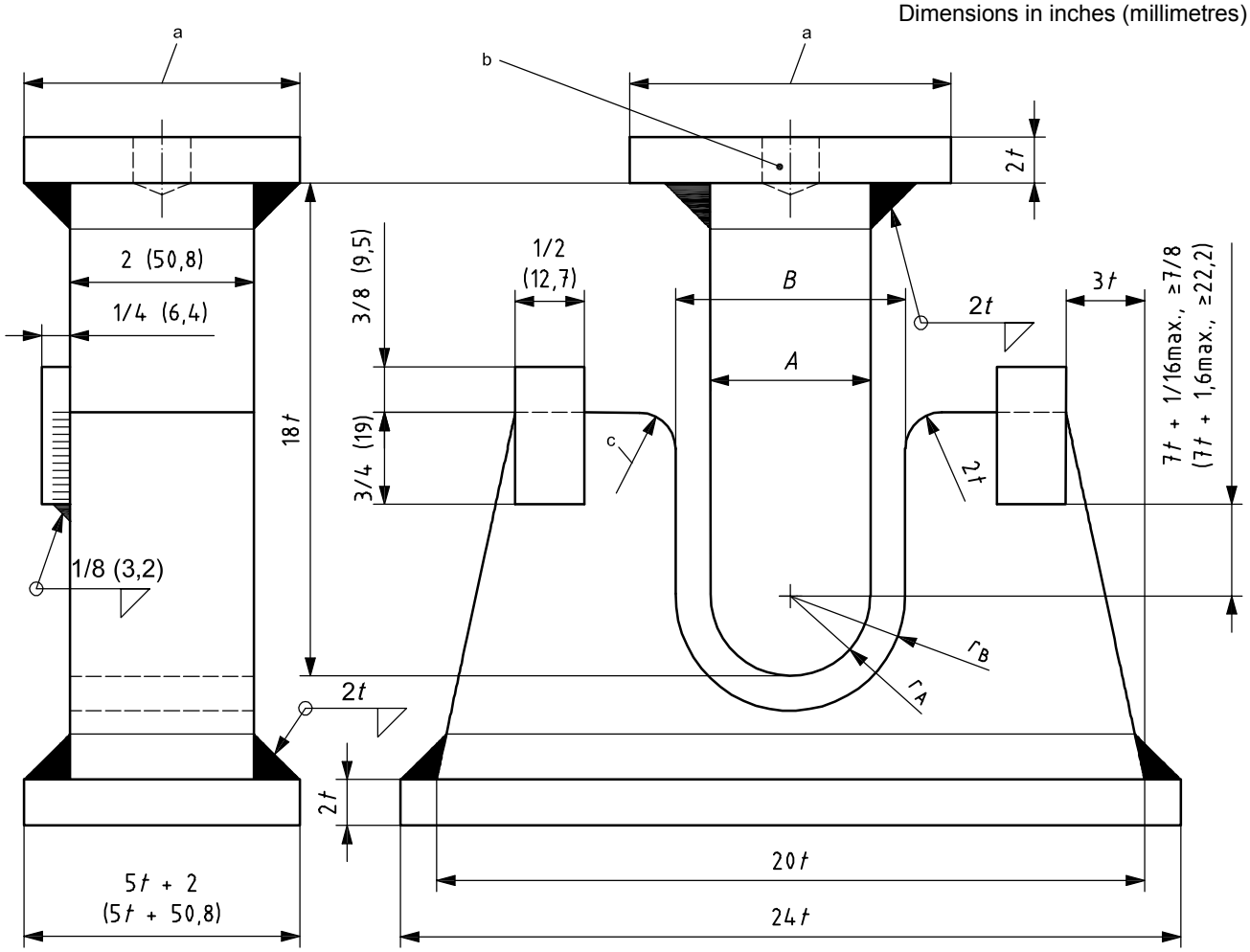

Key

$A = A_{gbtj}$ as defined in Equation (147)

$B = A_{gbtj} + 2t + 0.0125$ in

t specified pipe wall thickness ($t = 1$ in)

a As required.

b Tapped mounting hole.

c Shoulders hardened and greased hardened rollers may be substituted.

Figure 17 — Guided bend test jig

Table 13 — Values of strain for guided bend test

Grade	Strain ε_{eng}
A	0,167 5
B	0,137 5
X42	0,137 5
X46	0,132 5
X52	0,127 5
X56	0,120 0
X60	0,112 5
X65	0,110 0
X70	0,102 5
X80	0,090 0

16.2 Background

16.2.1 Values of ε_{eng}

Values for ε_{eng} are based on Equation (148) shown in Item 4a of API Circular PS-1340 reporting the actions of the 1967 Standardization Conference except for Grade X70, which were adopted at the June 1972 Standardization Conference and shown in API Circular PS-1440. The values calculated by means of Equation (148) are rounded to the nearest multiple of 0,002 5 with the exception of the values for Grades X52 and X56, which are rounded to the next higher multiple of 0,002 5.

The engineering strain, ε_{eng}, is calculated as

$$\varepsilon_{eng} = 3\,000\,(0.64)^{0.2}/f_{umnp}^{0.9} \tag{148}$$

where f_{umnp} is the specified minimum tensile strength of the pipe body, expressed in pounds per square inch.

16.2.2 Values of A_{gbtj}

The values of dimension A_{gbtj} in Annex E of ISO 3183:2007 or Appendix G of API 5L:2004 are calculated from Equation (147) and rounded as shown in Table 14.

Table 14 — Standard values for dimension A_{gbtj} in guided bend test

Unit	Dimension A										
mm	25,4	30,5	35,6	40,6	48,3	55,9	66,0	78,7	94,0	111,8	132,1
	157,5	188,0	223,5	266,7	320,0	383,5	459,7	551,2	660,4	792,5	
in	1.0	1.2	1.4	1.6	1.9	2.2	2.6	3.1	3.7	4.4	5.2
	6.2	7.4	8.8	10.5	12.6	15.1	18.1	21.7	26.0	31.2	

Derivation of the guided bend test equation is covered in Reference [7].

17 Determination of minimum impact specimen size for API couplings and pipe

17.1 Critical thickness

The Charpy V-Notch (CVN) absorbed energy requirements for API couplings are based on the coupling thickness at the critical thickness. The critical thickness for API couplings is defined as the thickness at the root of the thread at the middle of the coupling, based on the specified coupling diameter and the specified thread dimensions. The critical thickness for all API couplings is provided in Table 15 for various pipe; the critical thickness is the specified wall thickness.

Table 15 — Critical thickness of various API couplings

Pipe OD mm (in)	NU mm (in)	EU mm (in)	EU SC mm (in)	BC SC mm (in)	BC mm (in)	LC mm (in)	STC mm (in)
26,67 (1.050)	4,29 (0.169)	5,36 (0.211)					
33,40 (1.315)	5,36 (0.211)	6,55 (0.258)					
42,16 (1.660)	6,07 (0.239)	6,10 (0.240)					
48,26 (1.900)	4,98 (0.196)	6,38 (0.251)					
60,32 (2.375)	7,72 (0.304)	7,62 (0.300)	5,69 (0.224)				
73,02 (2.875)	9,65 (0.380)	9,09 (0.358)	6,45 (0.254)				
88,90 (3.500)	11,46 (0.451)	11,53 (0.454)	7,47 (0.294)				
101,60 (4.000)	11,53 (0.454)	11,63 (0.458)					
114,30 (4.500)	11,05 (0.435)	12,52 (0.493)		6,58 (0.259)	8,18 (0.322)	8,86 (0.349)	8,56 (0.337)
127,00 (5.000)				6,76 (0.266)	9,14 (0.360)	9,96 (0.392)	9,45 (0.372)
139,70 (5.500)				6,81 (0.268)	9,04 (0.356)	9,88 (0.389)	9,40 (0.370)
168,28 (6.625)				6,96 (0.274)	11,91 (0.469)	12,90 (0.508)	12,32 (0.485)
177,80 (7.000)				7,11 (0.280)	10,67 (0.420)	11,63 (0.458)	10,92 (0.430)
193,68 (7.625)				8,71 (0.343)	13,61 (0.536)	12,01 (0.473)	13,87 (0.546)
219,08 (8.625)				8,94 (0.352)	15,29 (0.602)	16,43 (0.647)	15,54 (0.612)
244,48 (9.625)				8,94 (0.352)	15,29 (0.602)	16,69 (0.657)	15,60 (0.614)
273,05 (10.750)				8,94 (0.352)	15,29 (0.602)		15,70 (0.618)
298,45 (11.750)					15,29 (0.602)		15,70 (0.618)
339,73 (13.375)					15,29 (0.602)		15,70 (0.618)
406,40 (16.000)					16,94 (0.667)		16,05 (0.632)
473,10 (18.625)					21,69 (0.854)		20,80 (0.819)
508,00 (20.000)					16,94 (0.667)	17,09 (0.673)	16,10 (0.634)

NOTE The coupling blank thickness is greater than indicated above, due to the thread height and manufacturing allowance to avoid black crested threads.

17.2 Calculated coupling blank thickness

The appropriate thread height is added to the critical thickness provided in Table 15, and the result is divided by 0,875 to determine the calculated thickness of the coupling blank. The coupling blank thicknesses calculated in this manner are provided in Table 16.

Table 16 — Calculated couplings blank thickness for API couplings

Pipe OD mm (in)	**NU** mm (in)	**EU** mm (in)	**EU SC** mm (in)	**BC SC** mm (in)	**BC** mm (in)	**LC** mm (in)	**STC** mm (in)
26,67 (1.050)	6,53 (0.257)	7,72 (0.304)					
33,40 (1.315)	7,72 (0.304)	9,09 (0.358)					
42,16 (1.660)	8,56 (0.337)	8,59 (0.338)					
48,26 (1.900)	7,32 (0.288)	8,92 (0.351)					
60,32 (2.375)	10,44 (0.411)	10,77 (0.424)	8,56 (0.337)				
73,02 (2.875)	12,65 (0.498)	12,47 (0.491)	9,45 (0.372)				
88,90 (3.500)	14,68 (0.578)	15,24 (0.600)	10,59 (0.417)				
101,60 (4.000)	15,24 (0.600)	15,37 (0.605)					
114,30 (4.500)	14,68 (0.578)	16,38 (0.645)		9,32 (0.367)	11,15 (0.439)	12,19 (0.480)	11,84 (0.466)
127,00 (5.000)				9,52 (0.375)	12,27 (0.483)	13,44 (0.529)	12,88 (0.507)
139,70 (5.500)				9,58 (0.377)	12,12 (0.477)	13,36 (0.526)	12,80 (0.504)
168,28 (6.625)				9,75 (0.384)	15,42 (0.607)	16,81 (0.662)	16,15 (0.636)
177,80 (7.000)				9,93 (0.391)	14,00 (0.551)	15,37 (0.605)	14,55 (0.573)
193,68 (7.625)				11,91 (0.469)	17,35 (0.683)	18,69 (0.736)	17,91 (0.705)
219,08 m (8.625)				12,01 (0.473)	19,28 (0.759)	20,85 (0.821)	19,84 (0.781)
244,48 (9.625)				12,01 (0.473)	19,28 (0.759)	21,13 (0.832)	19,89 (0.783)
273,05 (10.750)				12,01 (0.473)	19,28 (0.759)		20,02 (0.788)
298,45 (11.750)					19,28 (0.759)		20,02 (0.788)
339,73 (13.375)					19,28 (0.759)		20,02 (0.788)
406,40 (16.000)					21,16 (0.833)		20,40 (0.803)
473,10 (18.625)					26,59 (1.047)		25,86 (1.018)
508,00 (20.000)					21,16 (0.833)	21,59 (0.850)	20,47 (0.806)

17.3 Calculated wall thickness for transverse specimens

The calculated wall thickness necessary for full size, three-quarter size, and one-half size transverse impact test specimens for API couplings, including a 0.020-inch OD and a 0.020-inch ID machining allowance, is determined according to Equation (149) and provided in Table 17.

Table 17 — Transverse impact specimen size required for API couplings

(1)	(2)	(3)	(4)	(5)	(6)
Label 1	**Connection**	**Coupling outside diameter** mm (in)	**Calculated wall thickness required to machine transverse Charpy impact specimens** [a] mm (in)		
			Full size	**3/4 size**	**1/2 size**
3-1/2	NU	107,95 (4.250)	18,54 (0.730)	16,05 (0.632)	13,54 (0.533)
	EU	114,30 (4.500)	18,06 (0.711)	15,57 (0.613)	13,06 (0.514)
4	NU	120,65 (4.750)	17,65 (0.695)	15,14 (0.596)	12,65 (0.498)
	EU	127,00 (5.000)	17,27 (0.680)	14,78 (0.582)	12,27 (0.483)
4-1/2	NU	132,08 (5.200)	17,02 (0.670)	14,50 (0.571)	12,01 (0.473)
	EU	141,30 (5.563)	16,59 (0.653)	14,10 (0.555)	11,58 (0.456)
	STC/LC/BC	127,00 (5.000)	17,27 (0.680)	14,78 (0.582)	12,27 (0.483)
5	STC/LC/BC	141,30 (5.563)	16,59 (0.653)	14,10 (0.555)	11,58 (0.456)
5-1/2	STC/LC/BC	153,67 (6.050)	16,10 (0.634)	13,61 (0.536)	11,10 (0.437)
6-5/8	STC/LC/BC	187,71 (7.390)	15,14 (0.596)	12,62 (0.497)	10,13 (0.399)
7	STC/LC/BC	194,46 (7.656)	14,99 (0.590)	12,50 (0.492)	9,98 (0.393)
7-5/8	STC/LC/BC	215,90 (8.500)	14,58 (0.574)	12,07 (0.475)	9,58 (0.377)
8-5/8	STC/LC/BC	244,48 (9.625)	14,15 (0.557)	11,66 (0.459)	9,14 (0.360)
9-5/8	STC/LC/BC	269,88 (10.625)	13,84 (0.545)	11,35 (0.447)	8,84 (0.348)
10-3/4	STC/BC	298,45 (11.750)	13,56 (0.534)	11,07 (0.436)	8,56 (0.337)
11-3/4	STC/BC	323,85 (12.750)	13,36 (0.526)	10,87 (0.428)	8,36 (0.329)
13-3/8	STC/BC	365,13 (14.375)	13,11 (0.516)	10,59 (0.417)	8,10 (0.319)
16	STC/BC	431,80 (17.000)	12,78 (0.503)	10,29 (0.405)	7,77 (0.306)
18-5/8	STC/BC	508,00 (20.000)	12,50 (0.492)	10,01 (0.394)	7,52 (0.296)
20	STC/LC/BC	533,40 (21.000)	12,45 (0.490)	9,93 (0.391)	7,44 (0.293)

[a] Wall thicknesses provide a 0,51 mm (0.020 in) OD and 0,51 mm (0.020 in) ID machining allowance.

Minimum wall thickness (inches) = $(W/2) - [(W/2)^2 - 1.172\ 2]^{0.5} + 0.040$ in + k_i (0.393 7) (149)

where

k_i is the factor used to determine minimum wall thickness for transverse impact specimens
1,00 for full-size specimens
0,75 for three-quarter size specimens
0,50 for one-half size specimens;

W is the specified coupling outside diameter, in accordance with ISO 11960 or API 5CT.

17.4 Calculated wall thickness for longitudinal specimens

The calculated wall thickness necessary for full-size, three-quarter size, and one-half size longitudinal impact test specimens for API couplings, including a 0.020-in OD and a 0.020-in ID machining allowance, is determined according to Equation (150) and provided in Table 18.

Table 18 — Longitudinal impact specimen size required for API couplings

(1)	(2)	(3)	(4)	(5)	(6)
Label 1	**Connection**	**Coupling outside diameter** mm (in)	**Calculated wall thickness required to machine longitudinal Charpy impact specimens** [a] mm (in)		
			Full size	**3/4 size**	**1/2 size**
1.050	NU	33,35 (1.313)	11,79 (0.464)	9,27 (0.365)	6,78 (0.267)
	EU	42,16 (1.660)	11,61 (0.457)	9,12 (0.359)	6,63 (0.261)
1.315	NU	42,16 (1.660)	11,61 (0.457)	9,12 (0.359)	6,63 (0.261)
1.660	NU	52,17 (2.054)	11,51 (0.453)	8,99 (0.354)	6,50 (0.256)
	EU	55,88 (2.200)	11,46 (0.451)	8,97 (0.353)	6,48 (0.255)
1.900	NU	55,88 (2.200)	11,46 (0.451)	8,97 (0.353)	6,48 (0.255)
	EU	63,50 (2.500)	11,40 (0.449)	8,92 (0.351)	6,40 (0.252)
2-3/8	NU	73,02 (2.875)	11,35 (0.447)	8,86 (0.349)	6,35 (0.250)
	EU	77,80 (3.063)	11,33 (0.446)	8,84 (0.348)	6,35 (0.250)
2-7/8	NU	88,90 (3.500)	11,30 (0.445)	8,78 (0.346)	6,30 (0.248)
	EU	93,17 (3.668)	11,28 (0.444)	8,78 (0.346)	6,27 (0.247)
3-1/2	NU	107,95 (4.250)	11,25 (0.443)	8,74 (0.344)	6,25 (0.246)
	EU	114,30 (4.500)	11,23 (0.442)	8,74 (0.344)	6,22 (0.245)

Table 18 (*continued*)

(1)	(2)	(3)	(4)	(5)	(6)
Label 1	**Connection**	**Coupling outside diameter** mm (in)	**Calculated wall thickness required to machine longitudinal Charpy impact specimens** [a] mm (in)		
			Full size	**3/4 size**	**1/2 size**
4	NU	120,65 (4.750)	11,23 (0.442)	8,71 (0.343)	6,22 (0.245)
	EU	127,00 (5.000)	11,20 (0.441)	8,71 (0.343)	6,22 (0.245)
4-1/2	NU	132,08 (5.200)	11,20 (0.441)	8,71 (0.343)	6,20 (0.244)
	EU	141,30 (5.563)	11,20 (0.441)	8,69 (0.342)	6,20 (0.244)
	STC/LC/BC	127,00 (5.000)	11,20 (0.441)	8,71 (0.343)	6,22 (0.245)

[a] Wall thicknesses provide a 0,51 mm (0.020 in) OD and 0,51 mm (0.020 in) ID machining allowance.

$$\text{Minimum wall thickness (inches)} = (W/2) - [(W/2)^2 - 0.387\ 5]^{0.5} + 0.040\ \text{in} + k_i\ (0.393\ 7) \quad (150)$$

where

k_i is the factor used to determine minimum wall thickness for transverse impact specimens
1,00 for full-size specimens
0,75 for three-quarter size specimens
0,50 for one-half size specimens;

W is the specified coupling outside diameter, in accordance with ISO 11960 or API 5CT.

17.5 Minimum specimen size for API couplings

The calculated wall thickness of the coupling blank (see 17.2) is compared to the calculated wall thickness required for an impact test specimen (see Table 16 and Table 17). The minimum size impact test specimen that should be selected from Table 16 or Table 17 is the largest impact test specimen having a calculated wall thickness that is less than the calculated wall thickness of the coupling blank for the connection of interest. See Table 19 for the minimum acceptable size transverse specimens and Table 20 for the minimum acceptable size longitudinal specimens. Table 19 and Table 20 are used to determine the impact specimen orientation and size as required in ISO 11960 or API 5CT.

Table 19 — Minimum size transverse Charpy impact test specimens for various API couplings

(1)	(2)	(3)	(4)	(5)	(6)	(7)	(8)
Label 1	Minimum permissible size transverse Charpy impact test specimens [a]						
	NU	EU	EU	Special clearance [c] BC	BC	LC	STC
3-1/2	1/2	1/2	1/2	—	—	—	—
4	3/4	3/4	—	—	—	—	—
4-1/2	3/4	3/4	—	[b]	[b]	[b]	[b]
5	—	—	—	1/2	1/2	1/2	1/2
5-1/2	—	—	—	1/2	1/2	1/2	1/2
6-5/8	—	—	—	Full	Full	Full	Full
7	—	—	—	3/4	3/4	Full	3/4
7-5/8	—	—	—	Full	Full	Full	Full
8-5/8	—	—	—	Full	Full	Full	Full
9-5/8	—	—	—	Full	Full	Full	Full
10-3/4	—	—	—	Full	Full	—	Full
11-3/4	—	—	—	—	Full	—	Full
13-3/8	—	—	—	—	Full	—	Full
16	—	—	—	—	Full	—	Full
18-5/8	—	—	—	—	Full	—	Full
20	—	—	—	—	Full	Full	Full

NOTE Transverse specimens are not possible for couplings for pipe sizes smaller than 3.50 in.

[a] The size of the specimen is relative to a full-size specimen that is 10 mm × 10 mm.

[b] Should use longitudinal specimen.

[c] The Charpy impact specimen size assumes that special clearance couplings are machined from standard couplings.

Table 20 — Minimum size longitudinal Charpy impact test specimens for API couplings for all pipe less than Label 1: 3 1/2 outside diameter and for larger sizes where transverse test specimens one-half size or larger are not possible

(1)	(2)	(3)	(4)	(5)	(6)	(7)	(8)
Label 1	Minimum permissible size longitudinal Charpy impact test specimens [a]						
	NU	EU	EU	Special clearance [c] BC	BC	LC	STC
1.050	[b]	1/2	—	—	—	—	—
1.315	1/2	3/4	—	—	—	—	—
1.660	1/2	1/2	—	—	—	—	—
1.900	1/2	3/4	—	—	—	—	—
2-3/8	3/4	3/4	3/4	—	—	—	—
2-7/8	Full	Full	Full	—	—	—	—
3-1/2	N/A	N/A	N/A	—	—	—	—
4	N/A	N/A	—	—	—	—	—
4-1/2	N/A	N/A	—	3/4	3/4	Full	Full

NOTE N/A = Transverse impact test specimens should be used for all tubing connections for pipe Label 1: 3-1/2 OD and larger and for all casing Label 1: 5 OD and larger.

[a] The size of the specimen is relative to a full-size specimen that is 10 mm (0.39 in) × 10 mm (0.39 in).

[b] Pipe not thick enough to test based on calculations. However, if the coupling material is slightly thicker than calculated, it will be possible to machine a half-size longitudinal test specimen.

[c] The Charpy impact specimen size assumes that special clearance couplings are machined from standard couplings.

17.6 Impact specimen size for pipe

Procedures specified in 17.3 and 17.4 are used to determine the wall thickness necessary for impact test specimens for pipe except that the OD term is the specified pipe OD. Tables specifying the calculated wall thickness necessary to machine full-size, three-quarter-size, and one-half size transverse and longitudinal impact test specimens are provided in Clause 4 and SR16 of ISO 11960 or API 5CT.

17.7 Larger size specimens

In some cases it can be possible to machine larger impact test specimens if

a) the coupling blank is thicker than that calculated in 17.2,

b) the full 0.020-in-OD and 0.020-in-ID machining allowances are not utilized, or

c) the impact test specimens are partially rounded due to the OD curvature of the original tubular product (see ISO 11960 or API 5CT).

17.8 Reference information

For a discussion of fracture mechanics and the equations used in ISO 11960 or API 5CT to determine the absorbed energy requirements, see Reference [6]. The transverse requirement is based on this reference. The longitudinal requirement is based on the transverse requirements, and a longitudinal-to-transverse ratio of 1,33 for Grades J55 and K55 and 2,0 for higher strength grades. See Reference [5] for the correlation of K_c to CVN for high strength steel.

The requirement for pipe in SR16 of ISO 11960 or API 5CT is based on the minimum specified yield strength rather than the maximum specified yield strength used for couplings. This choice is made since the stress level of the pipe is typically expected to be less than the stress level of the couplings.

Annex A
(informative)

Discussion of equations for triaxial yield of pipe body

A.1 Triaxial yield of pipe body

A.1.1 General

The criterion for triaxial pipe body yield is that proposed by von Mises. The elastic state leading to incipient yield consists of the superposition of

a) radial and circumferential stress as determined by the Lamé Equations for a thick cylinder,

b) uniform axial stress due to all sources except bending,

c) axial bending stress for a Timoshenko beam,

d) torsional shear stress due to a moment aligned with the axis of the pipe.

A.1.2 Equations for elastic pipe stresses

A.1.2.1 General

Yield, as defined in this subclause, assumes a material for which the elastic limit, the proportional limit and the yield stress coincide. Further, yield of the material marks the boundary between elastic and inelastic behaviour. This boundary has no relation to standardized definitions of minimum yield strength. Standard definitions, such as the minimum yield strength as specified in ISO 11960 or API 5CT, are more appropriately discussed in conjunction with the design equation.

The limit state for pipe body yield addresses the stress state at which yield is about to occur. That is, the pipe body is still entirely elastic, with one or more locations just reaching yield. Therefore, the stresses defining the yield limit state in the pipe body can be defined with equations based on linear elastic behaviour.

A.1.2.2 Lamé Equations

Given a tube exposed to internal and external pressure, the radial stress, σ_r, and the circumferential (or hoop) normal stress, σ_h, in the tube are given by:

$$\sigma_r = [(p_i d^2 - p_o D^2) - (p_i - p_o) d^2 D^2/(4r^2)]/(D^2 - d^2) \quad \text{(A.1)}$$

$$\sigma_h = [(p_i d^2 - p_o D^2) + (p_i - p_o) d^2 D^2/(4r^2)]/(D^2 - d^2) \quad \text{(A.2)}$$

where

D is the specified pipe outside diameter;

d is the pipe inside diameter, $d = D - 2t$;

p_i is the internal pressure;

p_o is the external pressure;

r is the radial coordinate, $(d/2) \leqslant r \leqslant (D/2)$;

t is the specified pipe wall thickness.

The elastic radial and hoop stresses do not depend on the axial load.

A.1.2.3 Uniform axial stress

The gravitational force field, along with other environmental loads (e.g. hydrostatic pressure on shoulders, changes in temperature and pressure, landing practice) give rise to an axial force, F_a. The resulting axial stress, σ_a, i.e. the component of axial stress not due to bending, assumed uniform across any cross section, is

$$\sigma_a = F_a/A_p \tag{A.3}$$

where

A_p is the area of the pipe cross section, $A_p = \pi/4\ (D^2 - d^2)$;

D is the specified pipe outside diameter;

d is the pipe inside diameter, $d = D - 2t$;

t is the specified pipe wall thickness;

F_a is the axial force.

In some cases, F_a is known and the axial stress is determined from Equation (A.3). In other instances, the axial stress is known, and F_a is determined from the axial stress. For example, if the pipe is cemented in a well, then stretching and contracting in the axial direction are not allowed. The axial stress, and hence the axial force, is then partially a function of changes in pressure and temperature. That is, the axial stress and axial force are secondary, rather than primary variables. The relation in Equation (A.3) still applies.

A.1.2.4 Bending stress

The axial stress component due solely to bending is given by

$$\sigma_b = \pm M_b r/I = \pm Ecr \tag{A.4}$$

where

c is the tube curvature, the inverse of the radius of curvature to the centreline of the pipe;

D is the specified pipe outside diameter;

d is the pipe inside diameter, $d = D - 2t$;

E is Young's modulus;

I is the moment of inertia of the pipe cross section; $I = \pi/64\ (D^4 - d^4)$;

M_b is the bending moment;

r is the radial coordinate, $(d/2) \leqslant r \leqslant (D/2)$;

t is the specified pipe wall thickness.

The ± sign indicates that the component of axial stress due to bending can be positive (tension) or negative (compression), depending on the location of the point in the cross section. Points in the pipe cross section closer to the centre of tube curvature than the centreline of the pipe experience compressive bending stress. Points in the pipe cross section farther from the centre of tube curvature than the centreline of the pipe experience tensile bending stress.

The variable c has units radian/length, which are not the norm for the petroleum industry. The more common measure of c in the industry is °/30 m. If, therefore, the required units for c are radians per metre, and c is expressed in °/30 m, the right hand side of Equation (A.4) should be multiplied by the constant $\pi/(180 \times 30) = 5{,}817\ 8 \times 10^{-4}$.

A.1.2.5 Torsional stress

The torsional shear stress, τ_{ha}, acting in the circumferential direction on the pipe cross section is

$$\tau_{ha} = Tr/J_p \tag{A.5}$$

where

D is the specified pipe outside diameter;

d is the pipe inside diameter; $d = D - 2t$;

J_p is the polar moment of inertia of the pipe cross section; $J_p = \pi/32\ (D^4 - d^4)$;

r is the radial coordinate, $(d/2) \leqslant r \leqslant (D/2)$;

T is the applied torque;

t is the specified pipe wall thickness.

A.1.3 Triaxial yield limit state equation

A.1.3.1 General

Given the internal and external pressures, axial force, and bending and torsional moments, the equivalent stress, σ_e, is defined as

$$\sigma_e = [\sigma_r^2 + \sigma_h^2 + (\sigma_a + \sigma_b)^2 - \sigma_r\sigma_h - \sigma_r(\sigma_a + \sigma_b) - \sigma_h(\sigma_a + \sigma_b) + 3\,\tau_{ha}^2]^{1/2} \tag{A.6}$$

where

σ_r is the radial stress, and σ_h, the circumferential or hoop stress, given by Equations (A.1) and (A.2) respectively;

σ_a is the component of axial stress not due to bending, given by Equation (A.3);

σ_b is the component of axial stress due to bending, given by Equation (A.4);

τ_{ha} is the torsional (shear) stress, given by Equation (A.5).

The onset of yield is defined as

$$\sigma_e = f_y \tag{A.7}$$

where $\sigma_e < f_y$ corresponds to elastic behaviour, and

σ_e is the equivalent stress;

f_y is the yield strength of a representative tensile specimen.

In the absence of bending and torsion, the highest value of equivalent stress always occurs at the inner radius of the pipe body. In the presence of bending ($\sigma_b \neq 0$), Equation (A.7) should be checked four times, i.e. once at the inner diameter and once at the outer diameter, for each of the possible positive and negative values of σ_b.

A.1.3.2 Special cases of the yield criterion

A.1.3.2.1 Pipe exposed to axial stress alone

In the absence of internal and external pressure, bending and torsion, Equation (A.6) reduces to

$$\sigma_e^2 = \sigma_a^2 \tag{A.8}$$

where

σ_a is the component of axial stress not due to bending;

σ_e is the equivalent stress.

Yield of the pipe occurs when the axial stress equals $\pm f_y$, where f_y is the yield strength of a representative tensile specimen.

A.1.3.2.2 Pipe exposed to internal and external pressure and axial stress

In the absence of bending and torsion, Equation (A.6) reduces to

$$\sigma_e = [\sigma_r^2 + \sigma_h^2 + \sigma_a^2 - \sigma_r\sigma_h - \sigma_r\sigma_a - \sigma_h\sigma_a]^{1/2} \tag{A.9}$$

where

σ_e is the equivalent stress;

σ_a is the component of axial stress not due to bending;

σ_h is the circumferential or hoop stress;

σ_r is the radial stress.

Substituting Equations (A.1) and (A.2) into (A.9), and using the yield criterion in Equation (A.7), at the inner radius of the pipe body,

$$f_y^2 = [(p_i d^2 - p_o D^2)/(D^2 - d^2)]^2 + 3(p_i - p_o)^2 D^4/(D^2 - d^2)^2 + \sigma_a^2 - 2[(p_i d^2 - p_o D^2)/(D^2 - d^2)]\sigma \tag{A.10}$$

or

$$f_y^2 = [\sigma_a - (p_i d^2 - p_o D^2)/(D^2 - d^2)]^2 + 3\,[(p_i - p_o)\, D^2/(D^2 - d^2)]^2 \tag{A.11}$$

where

D is the specified pipe outside diameter;

d is the pipe inside diameter; $d = D - 2t$;

f_y is the yield strength of a representative tensile specimen;

p_i is the internal pressure;

p_o is the external pressure;

t is the specified pipe wall thickness;

σ_a is the component of axial stress not due to bending;

which is the equation of an ellipse with its major and minor axes bisecting the coordinate axes, as illustrated in Figure A.1 .

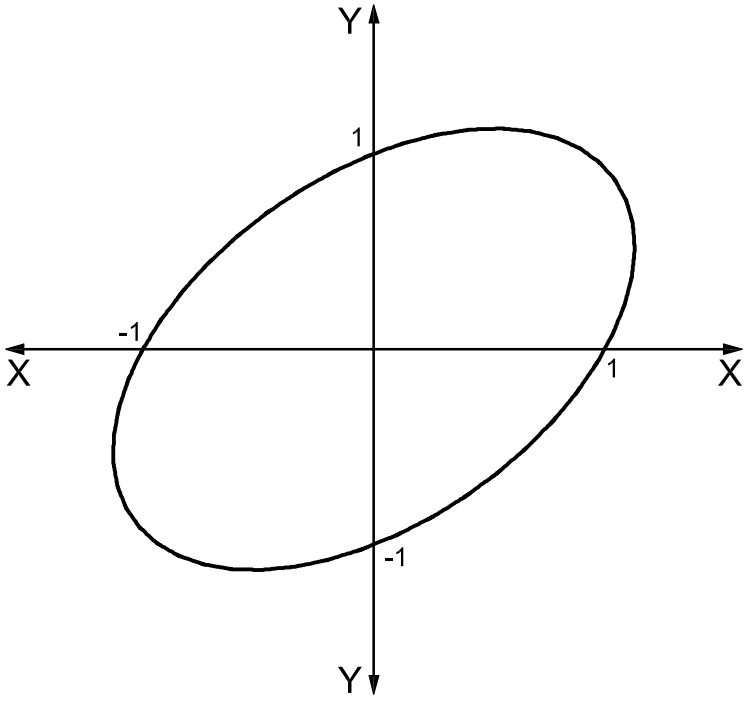

Key

X $(\sigma_a + p_i)/f_y$

Y $1/2\ [(D/t)^2/(D/t - 1)][(p_i - p_o)/f_y]$

Figure A.1 — von Mises yield criterion for a tube loaded by internal and external pressures and axial stress

A.1.3.2.3 Alternative representation of yield surface

A consequence of the expression of the yield criterion in terms of internal and external pressures and axial stress is that the pressure and axial stress terms cannot be explicitly separated. One solution, employed in ISO 13679 and API RP 5C5, is to divide the expression of yield into two special cases representing only external pressure or only internal pressure in combination with axial load. Further, the geometric factor appearing on the abscissa in Figure A.1 is incorporated in the yield surface by simplifying the abscissa to p_i (upper two quadrants) and p_o (lower two quadrants). The resulting pictorial representation (see Figure A.2) of yield is similar to that of Figure A.1 , with the exception that the yield criterion is not smooth at $p_i = p_o = 0$.

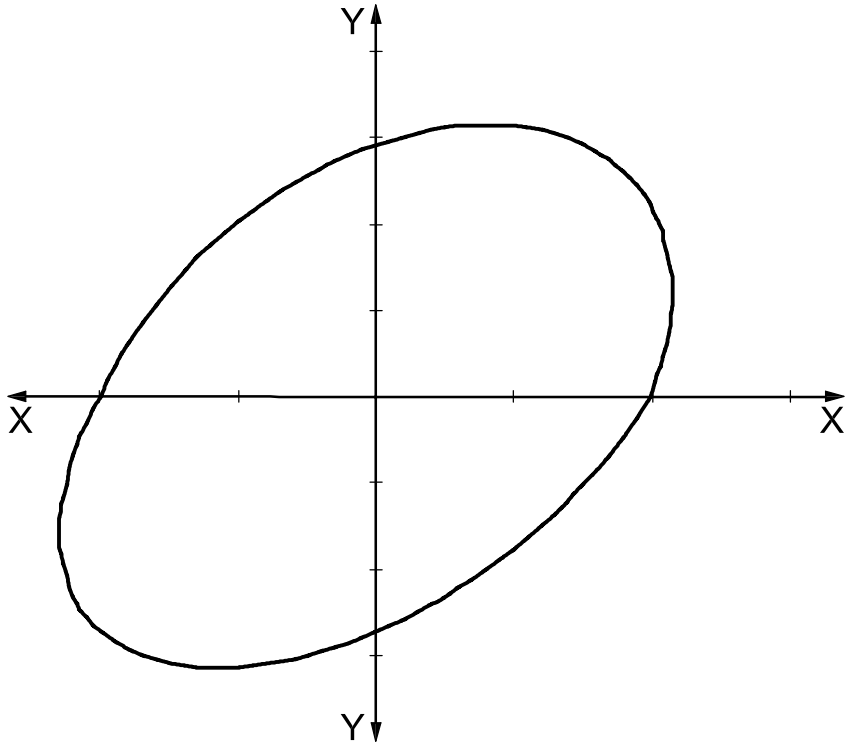

Key
X axial load, kN
Y pressure, MPa

Figure A.2 — von Mises yield criterion for a tube loaded by internal and external pressure and axial stress, ISO 13679 or API RP 5C5 representation

The equation for the upper two quadrants ($p_o = 0$) is

$$p_i = (-k_B \pm [k_B^2 - 4k_A k_C]^{1/2})/(2k_A) \quad \text{(A.12)}$$

where

$$k_A = k_{pi}^2 + k_{pi} + 1 \quad \text{(A.13)}$$

$$k_B = (1 - k_{pi})\ \sigma_a \quad \text{(A.14)}$$

$$k_C = \sigma_a^2 - f_y^2 \quad \text{(A.15)}$$

$$k_{pi} = (D^2 + d^2)/(D^2 - d^2) \quad \text{(A.16)}$$

The equation for the lower two quadrants ($p_i = 0$) is

$$p_o = (-k_B \pm [k_B^2 - 4k_A k_C]^{1/2})/(2k_A) \quad \text{(A.17)}$$

where

$$k_A = k_{po}^2 \quad \text{(A.18)}$$

$$k_B = k_{po}\ \sigma_a \quad \text{(A.19)}$$

$$k_C = \sigma_a^2 - f_y^2 \quad \text{(A.20)}$$

$$k_{po} = 2D^2/(D^2 - d^2) \quad \text{(A.21)}$$

In both instances,

D is the specified pipe outside diameter;

d is the pipe inside diameter; $d = D - 2t$;

f_y is the yield strength of a representative tensile specimen;

p_i is the internal pressure;

p_o is the external pressure;

t is the specified pipe wall thickness;

σ_a is the component of axial stress not due to bending.

A.1.3.2.4 Effective stress representation of yield surface

It is sometimes convenient to express pipe equations in terms of the effective stress, σ_{eff}, which is defined as

$$\sigma_{eff} = \sigma_a - (p_i d^2 - p_o D^2)/(D^2 - d^2) \quad \text{(A.22)}$$

where

D is the specified pipe outside diameter;

d is the pipe inside diameter; $d = D - 2t$;

p_i is the internal pressure;

p_o is the external pressure;

t is the specified pipe wall thickness;

σ_a is the component of axial stress not due to bending.

In this case, the equivalent of Equation (A.11) is

$$f_y^2 = \sigma_{eff}^2 + 3(p_i - p_o)^2 D^4/(D^2 - d^2)^2 \quad \text{(A.23)}$$

where f_y is the yield strength of a representative tensile specimen, for which the graphical representation is a circle (see Figure A.3).

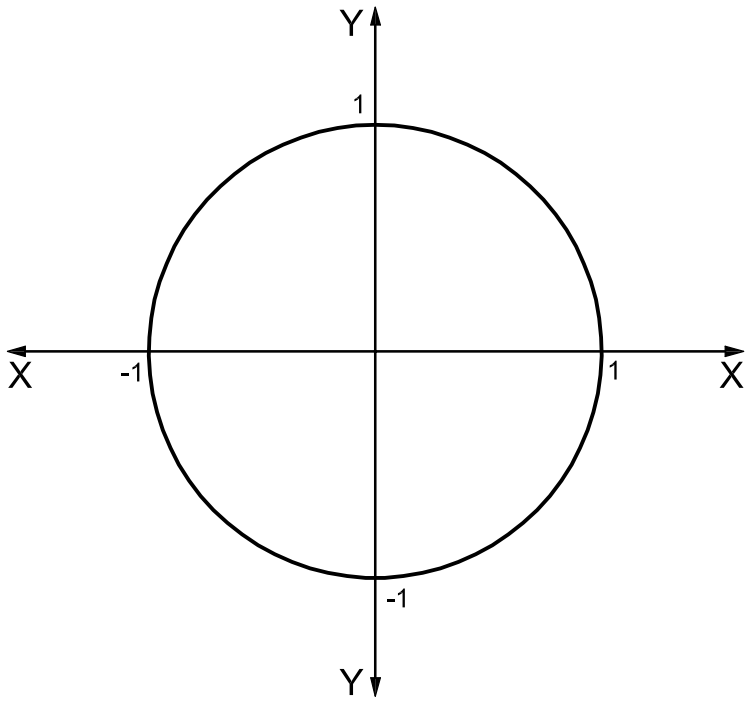

Key

X σ_{eff}/f_y

Y $\sqrt{3}\,[D^2/(D^2 - d^2)][(p_i - p_o)/f_y]$

Figure A.3 — von Mises yield criterion expressed in terms of internal and external pressure and effective stress

A.1.3.3 Assumptions and limitations

A.1.3.3.1 General

Equations (A.6) and (A.7) are based on the assumptions given in A.1.3.3.1.1 to A.1.3.3.1.4.

A.1.3.3.1.1 Concentric, circular cross-sectional geometry

The equations for radial stress, circumferential or hoop stress, bending and torsion presume the pipe cross section to consist of inner and outer surfaces that are circular and concentric.

A.1.3.3.1.2 Isotropic yield

The yield strength of the material of which the pipe is composed is assumed to be independent of direction. An axial sample and a circumferential sample are assumed to possess identical elastic moduli and yield stresses in both tension and compression.

A.1.3.3.1.3 No residual stress

For determination of the onset of yield, residual stresses due to manufacturing processes are assumed to be negligible, and are ignored.

A.1.3.3.1.4 Cross-sectional instability (collapse) and axial instability (column buckling)

Particularly in instances where $p_o > p_i$, it is possible for the pipe cross section to collapse due to instability prior to yield. For external pressure greater than internal pressure, see Clause 8 on collapse. Similarly, if $\sigma_{eff} < 0$, it is possible for the pipe to buckle as a column prior to yield, and the bending stress due to buckling should be included in the yield check.

A.1.3.3.2 Elongation under load at which the yield strength is determined

The values for the elongation under load at which the yield strength is determined in ISO 11960 or API 5CT, ISO 11961 or API 5D and ISO 3183 or API 5L for pipe with specified minimum yield strengths of 655 MPa (95 000 psi) or less have been arbitrarily established at 0,5 %.

The values for the elongation under load at which the yield strength is determined in ISO 11960 or API 5CT, ISO 11961 or API 5D and ISO 3183 or API 5L for pipe with specified minimum yield strengths greater than 655 MPa (95 000 psi) are determined with Equation (A.24), where ε_{ymn} is the strain at which specified minimum yield strength is determined.

$$\varepsilon_{ymn} = (f_{ymn}/E) + 0{,}002 \tag{A.24}$$

where

f_{ymn} is the specified minimum yield strength;

E is Young's modulus, taken to be 193×10^3 MPa (28×10^6 psi).

The calculated values of ε_{ymn} are rounded to the nearest 0,005.

A.1.4 Triaxial yield design equation

In all of the general and simplified forms of Equation (A.7), a design equation is formulated with the following substitutions:

a) replace t with $k_{wall}\ t$ in Equations (A.1) and (A.2) for the radial and circumferential or hoop stresses, respectively, but not in Equations (A.3) to (A.5) for the axial and torsional stresses;

b) replace f_y with f_{ymn}.

The purpose of the design equation is to determine the stress state which results in the onset of pipe yield when the properties of the pipe are at their worst-case, minimum allowable values. The wall thickness of the pipe at all times accounts for the extreme allowable thin-wall eccentricity which comes about naturally as part of the pipe manufacturing process.

A.2 Initial yield of pipe body, Lamé Equation for pipe when external pressure, bending and torsion are zero

A.2.1 General

The Lamé Equations for the radial and hoop stresses of the pipe are based on the three-dimensional equations of equilibrium for a linear elastic cross section. As such these equations are triaxial equations and provide the most accurate calculation of pipe stresses. Two equations are provided: open-end with zero axial stress, and closed-end with axial stress due to internal pressure acting on the end cap.

A.2.2 Yield limit state equation, special case for capped-end conditions

Initial yield of a capped-end thick tube is a special case of Equations (A.6) and (A.7) when external pressure, bending and torsion are zero. The axial stress is generated solely by the action of internal pressure on the ends of the sample (e.g. the capped-end condition). In this case, the effective stress is zero [see Equation (A.22)].

The internal pressure at yield for a capped-end thick tube, p_{iYLc}, is calculated as

$$p_{iYLc} = f_y\,(D^2 - d^2)/(\sqrt{3}\,D^2) \tag{A.25}$$

where

D is the specified pipe outside diameter;

d is the pipe inside diameter; $d = D - 2t$;

f_y is the yield strength of a representative tensile specimen;

t is the specified pipe wall thickness.

This equation is subject to the same assumptions and limitations as the more general expressions from which it is derived (see A.1.3.3).

There is no adjustment to Equation (A.25) for axial tension, as all axial tension is generated by the action of internal pressure on the (closed) ends of the pipe. The more general case, where axial stress is generated by other than the action of internal pressure on the ends of the pipe, is addressed by the triaxial yield criterion, Equations (A.6) and (A.7).

A.2.3 Yield design equation, special case for capped-end conditions

A design equation for initial yield of the pipe body with capped-end conditions and using the Lamé Equations for the radial and hoop stresses should be formulated from Equation (A.9) with the following substitutions:

a) replace t with $k_{wall}\,t$ in Equations (A.1) and (A.2) for the radial and circumferential or hoop stresses, respectively, but not in Equation (A.3) for the axial stress;

b) replace f_y with f_{ymn}.

The resulting design equation for p_{iYLc}, internal pressure at yield for a capped-end thick tube, is

$$p_{iYLc} = f_{ymn}/\{(3\,D^4 + d_{wall}{}^4)/(D^2 - d_{wall}{}^2)^2 + d^4/(D^2 - d^2)^2 - 2d^2d_{wall}{}^2/[(D^2 - d^2)\,(D^2 - d_{wall}{}^2)]\}^{1/2} \tag{A.26}$$

where

D is the specified pipe outside diameter;

d is the pipe inside diameter; $d = D - 2t$;

d_{wall} is the inside diameter based on $k_{wall}\,t$; $d_{wall} = D - 2k_{wall}\,t$;

f_{ymn} is the specified minimum yield strength;

k_{wall} is the factor to account for the specified manufacturing tolerance of the pipe wall. For example, for a tolerance of −12,5 %; $k_{wall} = 0{,}875$;

t is the specified pipe wall thickness.

Note that the use of different wall thicknesses in the radial/circumferential and axial stresses precludes deriving this design equation directly from Equation (A.25).

A.2.4 Yield limit state equation, special case for open-end conditions with zero external pressure and axial load

Initial yield of an open-ended thick tube is a special case of Equations (A.6) and (A.7) when the uniform axial stress, external pressure, bending and torsion are zero. In this case, the internal pressure at yield for an open-ended thick tube, p_{iYLo}, is

$$p_{iYLo} = f_y\,(D^2 - d^2)/(3\,D^4 + d^4)^{1/2} \tag{A.27}$$

where

D is the specified pipe outside diameter;

d is the pipe inside diameter; $d = D - 2t$;

f_y is the yield strength of a representative tensile specimen;

t is the specified pipe wall thickness.

This equation is subject to the same assumptions and limitations as the more general expressions from which it is derived (see A.1.3.3).

The more general case where axial stress is non-zero is addressed by the triaxial yield criterion, Equations (A.6) and (A.7).

A.2.5 Yield design equation, special case for open-end conditions with zero external pressure and axial load

A design equation for initial yield of the pipe body with open-end conditions and using the Lamé Equations for the radial and hoop stresses should be formulated from Equation (A.9) with the following substitutions:

a) replace t with $k_{wall}\,t$ in Equations (A.1) and (A.2) for the radial and circumferential or hoop stresses, respectively;

b) replace f_y with f_{ymn}.

The resulting design equation for internal pressure at yield for an open-end thick tube, p_{iYLo}, is

$$p_{iYLo} = f_{ymn}(D^2 - d_{wall}^2)/(3\,D^4 + d_{wall}^4)^{1/2} \tag{A.28}$$

where

D is the specified pipe outside diameter;

d is the pipe inside diameter; $d = D - 2t$;

d_{wall} is the inside diameter based on $k_{wall}\,t$; $d_{wall} = D - 2k_{wall}\,t$;

f_{ymn} is the specified minimum yield strength;

k_{wall} is the factor to account for the specified manufacturing tolerance of the pipe wall. For example, for a tolerance of −12,5 %; $k_{wall} = 0{,}875$;

t is the specified pipe wall thickness.

Since axial stress is absent in this expression, the design equation can be derived directly from Equation (A.27).

A.3 Initial yield pressure of pipe body, historical API equation

A.3.1 General

The Barlow Equation for pipe yield, which is the historical API equation, is based on a one-dimensional (not triaxial), approximate formulation of the von Mises yield condition, combined with an approximate expression for the hoop stress in the pipe. In essence, the Barlow Equation approximates the hoop stress and then equates this approximation to the yield strength. This approximation is less accurate than the Lamé Equation of yield discussed in A.1. Because the Barlow Equation neglects axial stress, there is no distinction between pipe with capped ends, pipe with open ends or pipe with tension end load.

A.3.2 Historical, one-dimensional yield pressure limit state equation

Historically, the API design equation for internal yield pressure is presented without reference to a limit state equation.

A.3.3 Historical, one-dimensional yield pressure design equation

Initial yield of a thin tube is defined by the following expression, where p_{iYAPI} is the internal pressure at yield for a thin tube:

$$p_{\text{iYAPI}} = 2 f_{\text{ymn}} k_{\text{wall}}\, t/D \tag{A.29}$$

where

D is the specified pipe outside diameter;

f_{ymn} is the specified minimum yield strength;

k_{wall} is the factor to account for the specified manufacturing tolerance of the pipe wall. For example, for a tolerance of −12,5 %; $k_{\text{wall}} = 0{,}875$;

t is the specified pipe wall thickness.

This equation is subject to the same assumptions and limitations as the more general expressions from which it can be derived (by methods other than that used by Barlow) (see A.1.3.3).

A.3.4 Comparison of historical, one-dimensional yield pressure design equation with open-end Lamé Equation for internal pressure with zero axial load

Equations (A.28) and (A.29) are compared in Figure A.4 by plotting the difference between the Lamé and API historical equations as a percentage of the Barlow Equation, e.g. $[(p_i/f_y)_{\text{Lamé}}/(p_i/f_y)_{\text{Barlow}} - 1] \times 100$ %, for the range of diameter:thickness ratio values typical of oil field tubulars.

Two significant conclusions are:

a) for stated yield stress and cross-sectional dimensions, the Barlow design equation predicts a higher internal pressure resistance than the Lamé Equation for open-ended pipe;

b) the difference between the limit pressures predicted by the two equations is less than 8 % for the range of diameter:thickness ratios typical of oil field tubulars ($D/t > 4{,}9$).

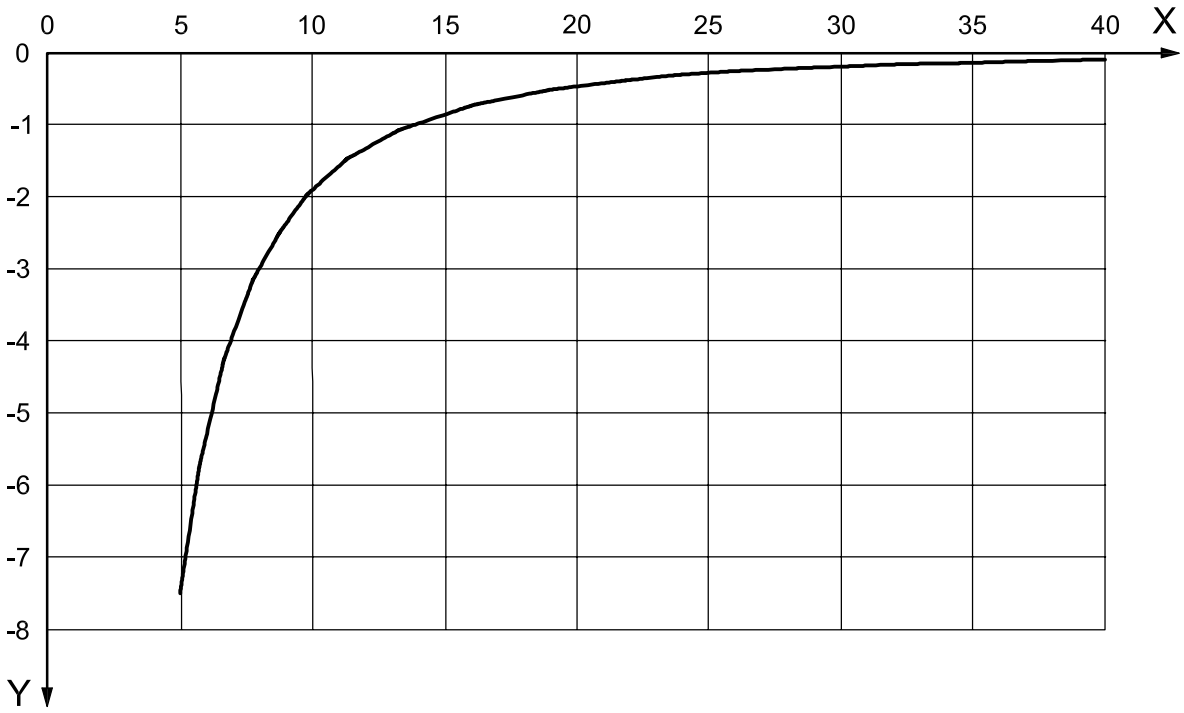

Key

X D/t

Y difference in p/σ_y, (Lamé/Barlow-1) $\times$ 100 %

Figure A.4 — Comparison of API historical and Lamé/von Mises predictions of yield pressure with zero axial load as a function of pipe body cross-sectional geometry, k_{wall} = 0,875

Annex B
(informative)

Discussion of equations for ductile rupture

B.1 Introduction

Internal pressure resistance equations differentiate between yield (Annex A) and rupture of the pipe body, and for rupture, between ductile and brittle material response. Table B.1 outlines the treatment of internal pressure resistance in the subclauses to follow.

Table B.1 — Equations for rating a pipe body for internal pressure resistance

Limit state	Definition	Pertinent annex
Ductile rupture	Failure of a tube in the plastic deformation range, which is characteristic of pipe with adequate and lasting toughness for the environment in which it is used.	B
Fracture	Failure of a tube due to propagation of a crack.	D

B.2 Ductile rupture of pipe body

B.2.1 General

The equations for ductile rupture pertain to the actual failure of the pipe body due to internal pressure. While the yield equations of Annex A are intended to describe the onset of permanent plastic deformation and not loss of pressure integrity, the rupture equations are intended to describe the ultimate pressure capacity of the pipe at a pressure which fails the pipe body with loss of internal pressure integrity.

These equations are applicable only when the pipe material in its environment has sufficient toughness to meet a minimum criterion such that the deformation of the pipe in its environment, through to rupture, is ductile and not brittle, even in the presence of small imperfections.

The equations for ductile rupture depend on the minimum physical wall thickness and the pipe outer diameter, the maximum depth of imperfections which have a reasonable probability of passing through the inspection process undetected, the fracture toughness of the material, the work hardening of the material and the ultimate tensile strength of the pipe. Yield strength has no direct impact on the ductile rupture pressure, except through the correlation of the work-hardening parameter n.

The ductile rupture equations can be derived from the mechanics of pipe equilibrium combined with a model of pipe plasticity and a model of the effect of imperfections. These derivations are outside the scope of this Technical Report (see References [25] and [32]).

The ductile rupture limit state and design equations consist of three interlinked concepts:

a) an equation for equilibrium-plasticity-based rupture of a pipe with known physical wall thickness and diameter;

b) subtraction of a penalty for wall loss in proportion to depths of imperfections which may not be detected by the manufacturing and inspection system;

c) a criterion for minimum toughness at which ductile rupture applies.

These equations are applicable to direct pressure and axial loading, but do not describe the capacity of the pipe under fatigue loading. The subtraction to the pipe wall for the presence of imperfections and the interrelated role of pipe toughness are based on a fracture mechanics approach relating J_{Ic} toughness measurements of sample pipes to numerically calculated crack-tip intensities (J-Integrals) as a function of imperfection depth. This is explained in detail later in this annex.

Further information can be found in References [24] and [35].

B.2.2 Capped-end ductile rupture limit state equation

B.2.2.1 General

Ductile rupture of a capped-end tube under internal pressure alone is given by the following expression, in which p_{iR} is the internal pressure at rupture:

$$p_{iR} = 2k_{dr}t_{dr}f_u/(D - t_{dr}) \tag{B.1}$$

where

$$t_{dr} = t_{min} - k_a a \tag{B.2}$$

and

- a is, for a limit state equation, the actual maximum depth of a crack-like imperfection; for a design equation, the maximum depth of a crack-like imperfection that could likely pass the manufacturer's inspection system;
- D is the specified pipe outside diameter;
- f_u is the tensile strength of a representative tensile specimen;
- k_a is the burst strength factor, having the numerical value 1,0 for quenched and tempered (martensitic structure) or 13Cr products and 2,0 for as-rolled and normalized products based on available test data; and the default value set to 2,0 where the value has not been measured. The value of k_a can be established for a specific pipe material based on testing;
- k_{dr} is the correction factor based on pipe deformation and material strain hardening, having the numerical value $[(1/2)^{n+1} + (1/\sqrt{3})^{n+1})]$;
- n is the dimensionless hardening index used to obtain a curve fit (see B.2.3.3) of the true stress-strain curve derived from the uniaxial tensile test;
- t_{min} is the actual minimum pipe wall thickness disregarding crack-like imperfections.

The value selected for k_{dr} renders p_{iR} the average of rupture pressures predicted using Tresca's yield condition and von Mises' yield condition for the case of an end-capped pipe. It accounts for the material hardening and the pipe deformation up to rupture.

B.2.2.2 Origin of the limit state equation

The limit state Equation (B.1) is based on the mechanics of equilibrium for capped-end pipe subjected to internal pressure, combined with hardening plasticity. This limit state equation was selected from a review of six candidate equations. The limit state equations were compared with full-scale pipe rupture data for a wide assortment of pipe grades and pipe diameter-to-wall (D/t) ratios. The candidate equations and the data used to evaluate the equations are listed in B.3. For each combination of model and source set of data, the results of the comparisons are expressed in terms of the mean and the standard deviation (coefficient of variation) of the ratio of actual and predicted test pressures. The limit state Equation (B.1) provided the best accuracy across the different data sets. When all the data are combined, Equation (B.1) has a mean of 1,004 and a coefficient of variation of 4,7 % for the ratio of actual to predicted rupture pressure.

So far as can be determined, the test data used to calibrate the rupture equation did not have naturally occurring, sharp-bottomed imperfections present. This is understandable considering the frequency of occurrence of sharp-bottomed imperfections for pipe which have been inspected. Likewise, the fundamental mechanics equation for the limit state starts without a penalty for imperfections. However, the equation for the limit state was then generalized to account for external pressure and axial compression or tension different from capped-end conditions, and furthermore to account for the presence of sharp-bottomed imperfections which can just pass undetected through the inspection system. The basis for the imperfection penalty is explained in B.7.

The limit state Equation (B.1) includes the penalty for the maximum actual imperfection in the pipe. Furthermore, pipe can be and occasionally actually is manufactured with imperfections coincident with minimum wall geometry. If the limit state equation is used to make a deterministic calculation of the rupture pressure, the limit state equation should assume that a sharp-bottomed imperfection is present 100 % of the time, and that the depth of the imperfection is equal to the inspection threshold.

However, if Equation (B.1) is used to make a probabilistic calculation of the rupture pressure, then the calculation can account for the frequency at which the sharp imperfection occurs and the distribution of wall thickness. Analysis in B.7 makes the case that the low frequency imperfection with depth equal to the inspection threshold has more impact on the rupture pressure than the high frequency imperfection of more shallow depth. Because of this, the probabilistic rupture calculation is dominated by the large imperfection (with depth equal to the inspection threshold) that rarely occurs.

Hence, the limit state Equation (B.1) for rupture should always include the correction for imperfection depth, and the probabilistic limit state equation should account for the frequency at which the sharp-bottomed imperfection is likely to occur. For the deterministic calculation of the rupture pressure, the limit state analysis should assume that the imperfection frequency is 100 %, and that the imperfection depth will equal the inspection threshold. For the probabilistic calculation of the rupture pressure, the imperfection frequency should be based on inspection data for pipe which already has been subjected to the inspection system.

B.2.3 Assumptions and limitations

B.2.3.1 General

Equation (B.1) is based on the assumptions explained in B.2.3.2 and B.2.3.3.

B.2.3.2 Material with adequate toughness

In order for Equation (B.1) to be valid, the pipe material should have minimum toughness equal to or exceeding that embodied in ISO 11960 or API 5CT and its supplement SR16.

Although the fundamental derivation leading to Equation (B.1) does not depend on the shape of the stress-strain curve, the final form of the equation assumes the true stress-strain curve can be adequately fitted for larger strains of, say, between 2 % and the strain at maximum load by the relation for true (Cauchy) stress, σ_c:

$$\sigma_c = C\varepsilon_{ln}^{n} \tag{B.3}$$

where

$$C = (2{,}718/n)^n f_u \tag{B.4}$$

and

f_u is the tensile strength of a representative tensile specimen;

n is the dimensionless hardening index used to obtain a curve fit (see B.2.3.3) of the true stress-strain curve derived from the uniaxial tensile test;

ε_{ln} is the logarithmic strain.

B.2.3.3 Determination of the hardening index

A specimen from material with true stress-strain relation of the form given in Equation (B.3) would reach a maximum load in a uniaxial tensile test at a logarithmic strain of n. The best method is to derive n from fitting the actual true stress-strain curve with Equation (B.3) in the relevant strain range of % to the strain at maximum load. Although less accurate, one could alternatively approximate n equal to the actual logarithmic strain at the maximum load point of the tensile test. If the engineering strain at the maximum load is given, the logarithmic strain, $\varepsilon_{\ln}$, is

$$\varepsilon_{\ln} = \ln(1 + \varepsilon_{\text{eng}}) \tag{B.5}$$

where ε_{eng} is the engineering strain.

The relatively flat nature of the stress-strain curve in the plastic region of most OCTG grades makes determination of n through this last method often rather difficult. As a third alternative, in the absence of stress-strain information, the following values of n are suggested.

Table B.2 — Suggested values for hardening index in ductile rupture equation

Grade	n
H40	0,14
J55	0,12
K55	0,12
M65	0,12
N80	0,10
L80 Type 1	0,10
L80 Chrome	0,10
C90	0,10
C95	0,09
T95	0,09
P110	0,08
Q125	0,07

If the grade of the material is unknown but is not high hardening, the hardening index can alternatively be determined from the correlation given in Figure B.1. The effort expended to determine n should be weighed against the fact that the equation for ductile rupture is relatively insensitive to this quantity for commonly used OCTG. However, if a high-hardening material such as duplex steel is used, it is important to determine n to avoid a non-conservative rupture strength prediction. Values of n for these materials can be as high as 0,30.

The parameter n has relatively small effect on the value of p_{iR}, but should not be ignored. At $n = 0{,}12$ a 14 % change in n is necessary to produce a 1 % change in predicted rupture pressure. Two materials may have the same tensile strength, but if one material has $n = 0{,}12$ it will have a 4 % lower rupture strength than a material with $n = 0{,}06$. When selecting a value of n for OCTG grades in the absence of experimental data, estimating n using specified minimum yield strength, f_{ymn}, is conservative.

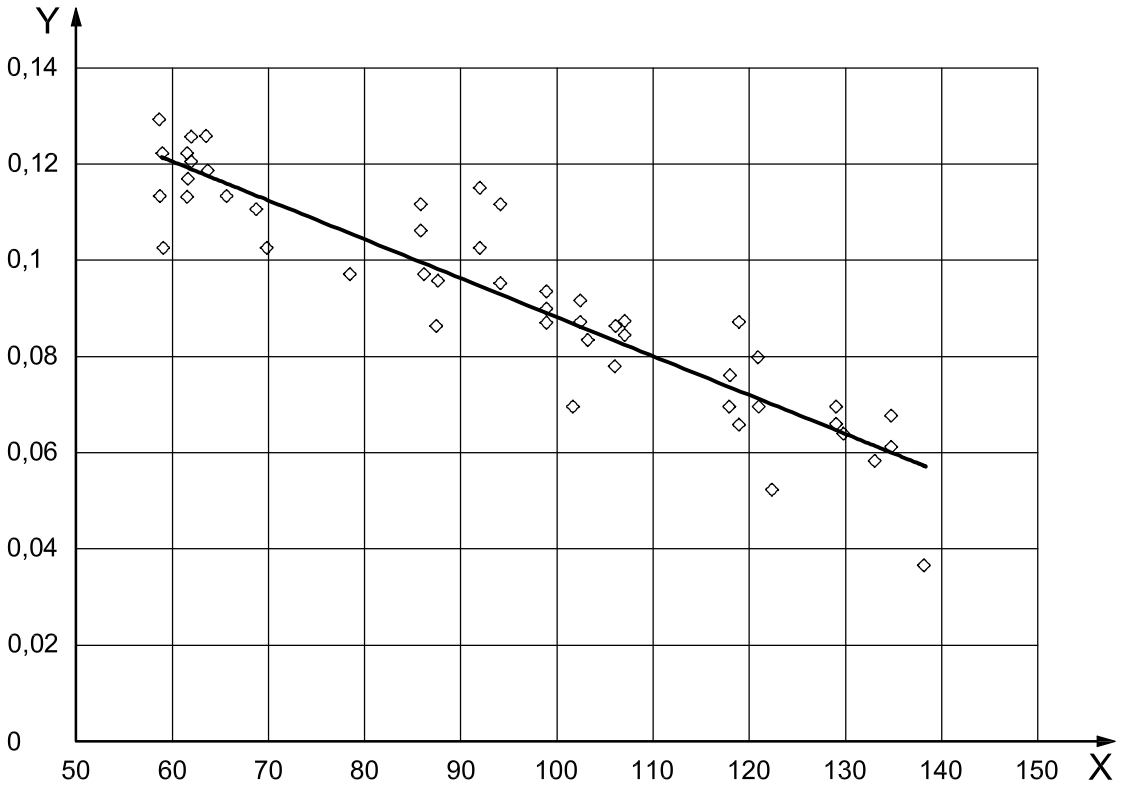

Key

X measured yield strength, ksi

Y n

NOTE Least squares fit of data results in $n = 0{,}169\ 3 - 0{,}000\ 812 \times$ measured yield strength; coefficient of variance = 0,10.

Figure B.1 — Correlations for hardening index from typical experimental data for steel grades listed in Table B.2

B.2.4 Adjustment for the effect of axial tension and external pressure

B.2.4.1 General

The ductile rupture strength Equation (B.1) was developed for the situation of an end-capped pipe, where the axial tension is determined by the internal pressure acting on the closed inner pipe surface area. This is a special case of a more general situation where a pipe can reach a maximum internal pressure load, that is a rupture load, under the simultaneous action of arbitrary external pressure and arbitrary axial tension or compression. The combined loads together determine when the pipe is going to yield and how it will plastically deform towards the point of rupture. A fundamental criterion when this rupture load is attained can still be expressed, but this will now be a more involved equation governed by the equation of the von Mises or Tresca yield surface in terms of axial stress, radial stress and hoop stress.

Moreover, rupture is only the prevailing failure mechanism if the axial tension is not too large. For large axial tension and smaller internal over-pressure, a maximum axial load (a precursor to necking and axial splitting of the pipe) is reached before the maximum pressure phenomenon occurs.

Below, equations for both rupture and necking under combined loads are described, together with a criterion to identify which phenomenon occurs first. The equation is given in terms of “effective axial tension” associated with “effective axial stress” defined in A.1.3.2.4. For effective axial tension, these approximate equations are very accurate when compared to the exact theoretical Equation (24); performance against combined loading test data is given in B.6.2.

For negative values of effective axial tension, i.e. effective axial compression, the pipe may buckle as a column, depending on the quality of lateral support. If buckling is adequately suppressed, the equation for rupture under combined loads is valid also for effective axial compression. However, for higher values of effective axial compression, it is the phenomenon of local buckling of the pipe wall ("wrinkling") that presents the governing failure mechanism. Therefore, there exists a value of effective axial compression that limits the validity of the exact combined loading rupture equation.

B.2.4.2 Ductile rupture under combined loads

In the presence of external pressure and axial tension or compression different from capped-end conditions, the general equation for ductile rupture is

$$p_{iRa} = p_o + \min[1/2(p_M + p_{ref\,T}), p_M] \tag{B.6}$$

with

$$p_M = p_{ref\,M}\,[1 - k_R\,(F_{eff}/F_{uts})^2]^{1/2} \tag{B.7}$$

where

$$F_a = \pi\, t\,(D - t)\,\sigma_a \tag{B.8}$$

$$F_{eff} = F_a + p_o\,\pi\, t\,(D - t) - p_M\, t\,(D - t)/[t_{dr}\,(D - t_{dr})]\;\pi/4\;(D - 2\,t_{dr})^2 \tag{B.9}$$

$$F_{uts} = \pi\, t\,(D - t)\, f_u \tag{B.10}$$

$$p_{uts} = 2\,t_{dr} f_u/(D - t_{dr}) \tag{B.11}$$

$$p_{ref} = 1/2\;(p_{ref\,M} + p_{ref\,T}), \text{ used in Figure B.2} \tag{B.12}$$

$$p_{ref\,M} = (2/\sqrt{3})^{1+n}\,(1/2)^n\, p_{uts} \tag{B.13}$$

$$p_{ref\,T} = (1/2)^n\, p_{uts} \tag{B.14}$$

$$k_R = (4^{1-n} - 1)/3^{1-n} \tag{B.15}$$

$$t_{dr} = t_{min} - k_a a \tag{B.16}$$

and

- a is, for a limit state equation, the actual maximum depth of a crack-like imperfection; for a design equation, the maximum depth of a crack-like imperfection that could likely pass the manufacturer's inspection system;
- D is the specified pipe outside diameter;
- F_a is the axial force;
- F_{eff} is the effective axial load, i.e. for a perfect pipe the axial load additional to the end-cap forces induced by internal and external pressures;
- f_u is the tensile strength of a representative tensile specimen;
- k_a is the burst strength factor, having the numerical value 1,0 for quenched and tempered (martensitic structure) or 13Cr products and 2,0 for as rolled and normalized products based on available test data; and the default value set to 2,0 where the value has not been measured. The value of k_a can be established for a specific pipe material based on testing;

n is the dimensionless hardening index used to obtain a curve fit (see B.2.3.3) of the true stress-strain curve derived from the uniaxial tensile test;

p_{iR} is the internal pressure at ductile rupture of an end-capped pipe;

p_{iRa} is the p_{iR} adjusted for axial load and external pressure;

p_o is the external pressure;

t is the average pipe wall thickness;

t_{min} is the minimum pipe wall thickness disregarding crack-like imperfections.

Equation (B.6) is illustrated in Figure B.2, together with the exact equation.

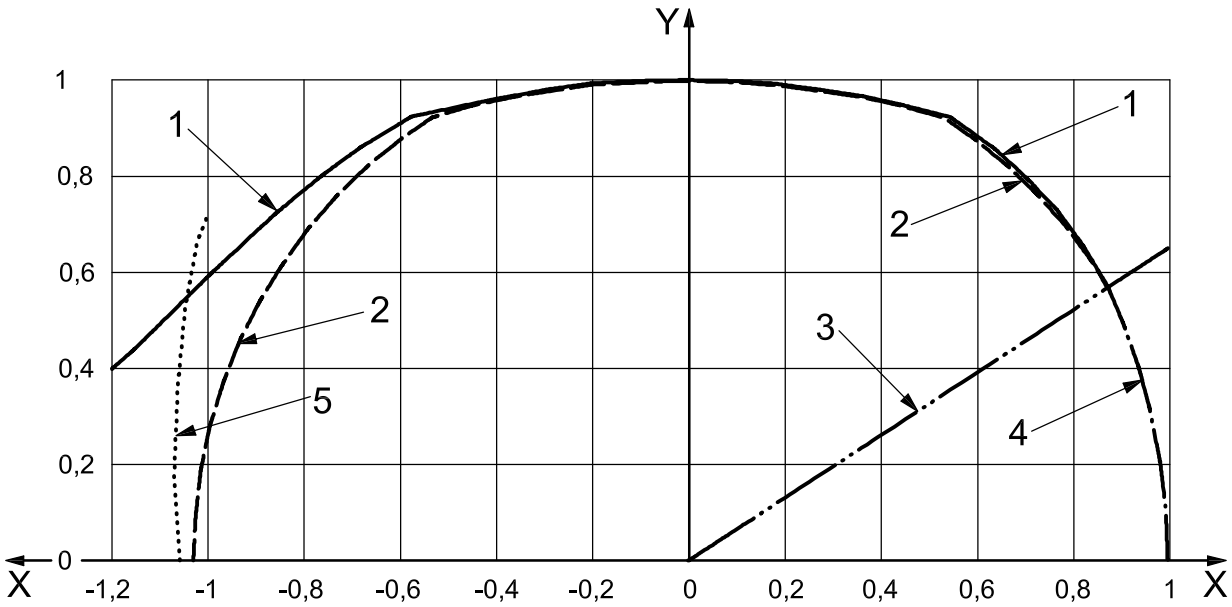

Key

X effective axial tension (F_{eff}/F_{uts})

Y pressure differential $(p_i - p_o)/p_{ref}$

1 rupture (exact)

2 rupture [Equation (B.6)]

3 transition

4 necking [Equation (B.18)]

5 wrinkling

Figure B.2 — Illustration of the effect of effective axial tension and external pressure on ductile rupture

Under capped-end conditions, the effective axial load is zero and Equation (B.6) reduces to Equation (B.1).

The rupture equation is valid, i.e. rupture occurs before necking, when

$$F_{eff}/F_{uts} \leqslant (\sqrt{3}/2)^{1-n} \tag{B.17}$$

B.2.4.3 Ductile necking under combined loads

In the presence of internal and external pressure the general equation for ductile necking is

$$F_{eff} = F_{uts}\,[1 - k_N\,[(p_i - p_o)/p_{ref\,M}]^2]^{1/2} \tag{B.18}$$

where

$$F_a = \pi\, t\,(D - t)\,\sigma_a \tag{B.19}$$

$$F_{eff} = F_a + p_o\,\pi\, t\,(D - t) - p_M\, t\,(D - t)/[t_{dr}\,(D - t_{dr})]\,\pi/4\,(D - 2\,t_{dr})^2 \tag{B.20}$$

$$F_{uts} = \pi\, t\,(D - t)\, f_u \tag{B.21}$$

$$p_{uts} = 2\,t_{dr} f_u/(D - t_{dr}) \tag{B.22}$$

$$p_{ref\,M} = (2/\sqrt{3})^{1+n}.(1/2)^n\, p_{uts} \tag{B.23}$$

$$k_N = 4^{(1-n)} - 3^{(1-n)} \tag{B.24}$$

Under zero pressure conditions, the effective axial load equals the true axial load, and Equation (B.18) for the maximum axial load reverts to the ultimate tensile strength.

The necking equation is valid, i.e. necking occurs before rupture, when

$$(p_i - p_o)/p_{ref\,M} \leqslant (1/2)^{1-n} \tag{B.25}$$

B.2.4.4 Boundary between rupture and necking

Comparing Equations (B.6) and (B.18) reveals that the necking criterion is reached earlier than the rupture criterion when

$$F_{eff}/F_{uts} \geqslant (3/2)\,(p_i - p_o)/p_{uts} \tag{B.26}$$

and this criterion (also shown in Figure B.2) describes the boundary between rupture and necking.

B.2.4.5 Axisymmetric wrinkling under combined loads

Figure B.2 shows that, in the axial compression range, i.e. for negative values of the effective axial load, Equation (B.6) is conservative when compared to both the exact rupture equation and the local pipe wall buckling limit, called wrinkling. Although it would be easy to construct an equation such as (B.7) with a different factor k_R that would better fit the exact rupture curve in the effective axial compression range, it is perceived such a separate equation would not have great practical impact.

B.2.5 Ductile rupture and necking design equations

Minimum ductile rupture and necking of a tube is defined by replacing t_{dr} with $k_{wall}\,t - k_a\,a_N$ and f_u with f_{umn} in the limit state Equations (B.1), (B.9) to (B.11), and (B.20) to (B.22):

$$p_{iR} = 2k_{dr} f_{umn}(k_{wall}\,t - k_a a_N)/[D - (k_{wall}\,t - k_a a_N)] \tag{B.27}$$

where

a_N is the imperfection depth associated with a specified inspection threshold, i.e. the maximum depth of a crack-like imperfection that could reasonably be missed by the pipe inspection system. For example, for a 5 % imperfection threshold inspection in a 12,7 mm (0.500 in) wall thickness pipe, a_N = 0,635 mm (0.025 in);

D is the specified pipe outside diameter;

f_{umn} is the specified minimum tensile strength;

k_a is the burst strength factor, having the numerical value 1,0 for quenched and tempered (martensitic structure) or 13Cr products and 2,0 for as-rolled and normalized products based on available test data; and the default value set to 2,0 where the value has not been measured. The value of k_a can be established for a specific pipe material based on testing;

k_{wall} is the factor to account for the specified manufacturing tolerance of the pipe wall. For example, for a tolerance of −12,5 %, k_{wall} = 0,875;

p_{iR} is the internal pressure at ductile rupture of an end-capped pipe;

t is the specified pipe wall thickness.

The factor k_{wall} addresses minimum pipe body wall thickness without considering imperfections. This value may be adjusted if minimum wall is guaranteed by a particular process or purchasing agreement.

Crack-like imperfections are accounted for by a_N. The term $k_a a_N$ represents a further reduction in minimum wall thickness associated with crack-like imperfections which are outside the sensitivity setting of the inspection equipment and assumed coincident with the location of minimum wall thickness. This stacking of minimum wall thickness and a crack-like imperfection depends on the frequency of occurrence of thin wall and the frequency of occurrence of sharp-bottomed imperfections approaching the depth of the inspection threshold.

For the deterministic calculation of rupture pressure, it is necessary to calculate a conservative ductile rupture design pressure. In this case, the frequency of occurrence of the imperfection is set to 100 % and the imperfection depth equals the inspection threshold.

For the probabilistic calculation of rupture pressure, the depth of the imperfection still equals the depth of the inspection threshold, but the calculation takes account of the actual frequency of occurrence of thin wall and the actual frequency of occurrence of sharp-bottomed imperfections with depth comparable to the inspection threshold.

B.3 Selection of a ductile rupture model

B.3.1 General

Six closed-form, analytical models were evaluated as candidates for the ductile rupture model. In the absence of a sharp-bottomed imperfection, the closed form candidates were:

— ad-hoc Barlow Equation

$$p_{iR} = 2 f_u t / D \tag{B.28}$$

— ad-hoc von Mises Equation

$$p_{iR} = f_u (D^2 - d^2)/(\sqrt{3} D^2) \tag{B.29}$$

— Klever-Stewart Equation (see References [25] and [32])

$$p_{iR} = 2 k_{dr} f_u t_{min}/(D - t_{min}) \tag{B.30}$$

— ad-hoc Paslay Equation (see Reference [29])

$$p_{iR} = 2f_u t_{min}/(D - t_{min}) \quad \text{(B.31)}$$

— ad-hoc Moore Equation

$$p_{iR} = f_u(D^2 - d^2)/(D^2 + d^2) \quad \text{(B.32)}$$

— Nadai Equation

$$p_{iR} = 2f_u \ln[D/(D - 2t)]/\sqrt{3} \quad \text{(B.33)}$$

where, in the above equations,

D is the specified pipe outside diameter;

d is the pipe inside diameter; $d = D - 2t$;

f_u is the tensile strength of a representative tensile specimen;

k_{dr} is the correction factor based on pipe deformation and material strain hardening, having the numerical value $[(1/2)^{n+1} + (1/\sqrt{3})^{n+1}]$;

n is the dimensionless hardening index used to obtain a curve fit (see B.2.3.3) of the true stress-strain curve derived from the uniaxial tensile test;

p_{iR} is the internal pressure at ductile rupture of an end-capped pipe;

t is the specified pipe wall thickness;

t_{min} is the actual minimum pipe wall thickness, disregarding crack-like imperfections.

For the Klever-Stewart model, the value selected for k_{dr} renders p_{iR} the average of rupture pressures predicted using Tresca's yield condition and von Mises' yield condition for end-capped pipes. It accounts for the material hardening and the pipe deformation up to rupture.

Of the many alternative rupture models existing in the published literature, the above list provides sufficient diversity to ensure an accurate final selection. The names corresponding to the models indicate either the developer of the model or the advocate for considering the model. The term "ad-hoc" is used for the first two models because they are generalizations of the Barlow and Mises yield equations, where yield strength has been replaced by tensile strength. There is no fundamental mechanistic justification or derivation for the ad-hoc models; only an appeal to their generalization from the yield equations. Likewise, the fourth and fifth candidates are ad-hoc models. Alternatively, the Klever-Stewart and Nadai Equations can be derived from fundamental physical principles, specifically different levels of approximation of the equations of equilibrium. Through their fundamental derivations, the Nadai and Klever-Stewart Equations depend on the pipe tensile strength. The Paslay Equation can be shown to be a special case of the Klever-Stewart model.

In the forms shown here, these equations address internal pressure without external pressure. All equations are for capped-end pipe, and therefore include axial tension acting on end caps of the pipe model, e.g. tension equal to the internal pressure times the bore area of the pipe.

The candidate models were compared with capped-end burst test data from full sized casing and tubing. On the basis of that accuracy, a single rupture equation was recommended. The recommended model was then generalized to account for external pressure and axial load other than that from pressure on end caps; and to account for the influence of a sharp-bottomed imperfection (ductile rupture).

B.3.2 Values of n used to evaluate the Klever-Stewart model

The Klever-Stewart model requires a stress-strain parameter, n, obtained by fitting the true stress-strain curve in the range of 2 % to the uniform strain (the strain at maximum load in a tensile test). Alternatively, n may be approximated as the true (logarithmic) strain at which a tensile stress-strain coupon experiences maximum load (maximum engineering stress). Whenever available, actually measured values for n were used in evaluating the model against rupture test data. Otherwise, the value of n used in the model is based on a regression fit of both round and strip stress-strain coupons. See Table B.3.

Table B.3 — Values of n used to evaluate the Klever-Stewart model

API grade	Yield strength psi	n
H40	40 000	0,137
J55	55 000	0,125
K55	55 000	0,125
M65	65 000	0,117
N80	80 000	0,104
L80	80 000	0,104
C90	90 000	0,096
C95	95 000	0,092
T95	95 000	0,092
P110	110 000	0,080
Q125	125 000	0,068

B.4 Pipe rupture data sets used to validate the rupture models

One hundred six data points from full-scale pipe rupture tests under capped-end conditions were donated from three industry sources in seven different data sets as listed below. Five of the data sets contain pipe failures with measured wall thickness, while two of the data sets contain pipe failures with specified wall thickness. In general, the evaluations of model accuracy were not sensitive to the manner in which wall thickness was reported. All tests reported the specified pipe outside diameter and the measured tensile strength. The list below indicates the source company and data set:

Capped-end rupture data sets with measured pipe wall thickness:

— Shell Btest1

— Hydril Measured Wall

— Grant Prideco

— Shell Super Duplex

— Shell Not-Worn

Capped-end rupture data sets with specified pipe wall thickness:

— Shell Pipeline

— Hydril Nominal

All tubes are believed to have been tested in ductile condition and without the presence of sharp, crack-like imperfections. The absence of sharp imperfections is understandable, as the pipes were well inspected, and the frequency of occurrence of small (below inspection threshold) sharp-bottomed imperfections is very low.

B.5 Comparison between the different rupture models and pipe rupture data under capped-end conditions

Table B.4 compares the rupture models with the donated pipe rupture data. For each data point used in the comparison, the ratio of the actual rupture test pressure to the prediction of the model evaluated at the thinnest reported section of pipe wall thickness is reported. All calculations use the specified pipe diameters, since only the specified diameters were reported. All calculations use the measured tensile strengths of the samples. For each set of comparisons, the mean and the standard deviation are also reported.

Table B.4 — Comparison of rupture predictions for candidate models

Data source			(1) Ad-hoc Barlow Actual/ predicted	(2) Ad-hoc Mises Actual/ predicted	(3) Klever Stewart Actual/ predicted	(4) Paslay Actual/ predicted	(5) Moore Actual/ predicted	(6) Nadai Actual/ predicted
Shell-Pipeline Nominal Wall	28 data	Mean	1,071	1,021	0,991	0,973	0,984	1,172
		Stdev	0,059	0,085	0,036	0,035	0,038	0,117
		COV, %	5,5	8,4	3,6	3,6	3,9	10,0
Hydril Data Nominal Wall	11 data	Mean	1,092	1,023	0,997	1,010	1,017	0,978
		Stdev	0,052	0,052	0,060	0,061	0,058	0,079
		COV, %	4,8	5,0	6,0	6,0	5,7	8,0
Shell Btest1 Measured Wall	18 data	Mean	1,125	1,052	1,014	1,042	1,050	1,043
		Stdev	0,051	0,080	0,029	0,030	0,032	0,102
		COV, %	4,5	7,6	2,9	2,9	3,0	9,8
Hydril Data Measured Wall	5 data	Mean	1,150	1,052	1,046	1,086	1,090	1,086
		Stdev	0,013	0,012	0,013	0,013	0,013	0,067
		COV, %	1,1	1,1	1,2	1,2	1,2	6,2
Not-Worn Pipe Data Set	2 data	Mean	1,075	Model eliminated	0,979	1,021	Model eliminated	1,003
		Stdev	0,025		0,010	0,007		0,006
		COV, %	2,3		1,0	0,7		0,6
Super Duplex Data Set	4 data	Mean	0,990		0,982	0,940		1,044
		Stdev	0,008		0,009	0,008		0,049
		COV, %	0,8		0,9	0,9		4,7
Grant Prideco Measured Wall	38 data	Mean			1,026	1,062		
		Stdev			0,041	0,043		
		COV, %			4,0	4,0		
Average mean			1,09	1,03	1,01	1,03	1,02	1,09
Average COV, %			4,4	7,0	3,6	3,6	3,7	8,8

Table B.4 also reports the average of all the means and the average of all the coefficients of variance (COVs). In some cases, the comparison between equation and test data was stopped when progress was obtained with a more accurate and fundamental model.

Table B.5 shows the average of the means from the above comparisons (weighted according to the amount of data in each population) and the corresponding standard deviation between means. This was calculated to provide a measure of the scatter in the predictive ability of each equation to represent the mean rupture pressure of the population.

Table B.5 — Illustration of equation performance over population

Parameter	(1)	(2)	(3)	(4)	(5)	(6)
	Ad-hoc Barlow	Ad-hoc Mises	Klever Stewart	Paslay	Moore	Nadai
	Actual/ predicted	Actual/ predicted	Actual/ predicted	Actual/ predicted	Actual/ predicted	Actual/ predicted
Mean of means	1,08	1,04	1,00	1,02	1,04	1,05
Stdev of means	0,050	0,015	0,023	0,047	0,039	0,063
COV of means	4,6 %	1,5 %	2,3 %	4,6 %	3,8 %	5,9 %

Based on the results in Tables B.4 and B.5, the Klever-Stewart Equation was selected to predict ductile rupture.

B.6 Comparison between the recommended rupture model and pipe rupture data under capped-end conditions

B.6.1 General

Table B.6 compares the measured and predicted rupture pressure from the Klever-Stewart model when all the capped-end test data from the sets listed in B.4 are combined into a single data set. The mean ratio of actual to predicted is 1,004, the standard deviation is 0,047, and the coefficient of variation is 4,7 %.

Table B.6 — Statistical evaluation of Klever-Stewart rupture model for all data

Test number	Measured yield strength psi	Measured ultimate tensile strength psi	n value	Measured outer diameter in	Measured minimum wall thickness in	D/t ratio	Measured rupture pressure psi	Calculated rupture pressure psi	Actual burst/ predicted burst	Data set
1	97 150	120 350	0.18 [a]	10.709	0.535	20.00	12 050	12 217	0.986	super duplex
2	97 150	121 945	0.21 [a]	10.709	0.539	19.85	12 108	12 246	0.989	super duplex
3	79 750	109 765	0.20 [a]	10.709	0.539	19.85	10 919	11 091	0.984	super duplex
4	97 150	122 670	0.18 [a]	10.709	0.539	19.85	12 166	12 549	0.969	super duplex
5	121 800	142 100	0.05 [a]	13.465	0.524	25.71	11 687	12 021	0.972	not worn set
6	134 850	155 150	0.06 [a]	9.922	0.606	16.36	20 735	20 996	0.988	not worn set
7	67 600	107 000	0.11	7.064	0.352	20.07	11 270	11 268	1.000	shell btest1
8	100 900	109 400	0.09	3.530	0.254	13.90	17 300	17 319	0.999	shell btest1
9	131 400	144 200	0.06	7.805	0.575	13.57	25 210	23 776	1.060	shell btest1
10	120 700	131 000	0.07	7.068	0.524	13.49	22 090	21 631	1.021	shell btest1
11	88 600	105 000	0.10	7.076	0.408	17.34	13 370	13 038	1.025	shell btest1
12	122 600	133 200	0.07	7.076	0.407	17.39	17 190	16 779	1.024	shell btest1
13	92 900	104 000	0.09	9.724	0.388	25.06	8 860	8 790	1.008	shell btest1
14	88 000	102 000	0.10	9.929	0.531	18.70	11 830	11 692	1.012	shell btest1
15	87 500	106 200	0.10	3.502	0.567	6.18	42 740	41 611	1.027	shell btest1
16	100 300	121 200	0.09	2.649	0.154	17.20	16 440	15 270	1.077	shell btest1
17	112 600	130 000	0.08	7.070	0.473	14.95	19 740	19 143	1.031	shell btest1
18	131 400	144 200	0.06	7.805	0.577	13.53	24 900	23 865	1.043	shell btest1
19	131 400	144 200	0.06	7.089	0.585	12.12	25 900	26 889	0.963	shell btest1
20	84 900	102 000	0.10	11.134	0.560	19.88	11 140	10 942	1.018	shell btest1
21	97 600	116 000	0.09	2.776	0.333	8.34	33 540	32 232	1.041	shell btest1
22	72 300	80 700	0.11	2.382	0.124	19.21	9 140	8 920	1.025	shell btest1
23	127 000	147 000	0.07	3.524	0.282	12.50	25 980	26 451	0.982	shell btest1

Table B.6 (*continued*)

Test number	Measured yield strength psi	Measured ultimate tensile strength psi	n value	Measured outer diameter in	Measured minimum wall thickness in	D/t ratio	Measured rupture pressure psi	Calculated rupture pressure psi	Actual burst/ predicted burst	Data set
24	145 000	149 000	0.05	3.514	0.287	12.24	26 800	27 661	0.969	shell btest1
25	128 700	140 000	0.06	9.625	0.538	17.89	17 770	17 161	1.035	hydril M-wall
26	128 700	140 000	0.06	9.625	0.531	18.13	17 720	16 925	1.047	hydril M-wall
27	119 000	143 000	0.07	16.000	0.857	18.67	17 700	16 675	1.061	hydril M-wall
28	119 000	143 000	0.07	16.000	0.870	18.39	17 700	16 942	1.045	hydril M-wall
29	119 000	143 000	0.07	16.000	0.870	18.39	18 160	16 942	1.072	hydril M-wall
30	120 670	134 130	0.07	7.056	0.511	13.81	23 080	21 595	1.069	grant prideco
31	120 670	134 130	0.07	7.063	0.533	13.25	22 600	22 576	1.001	grant prideco
32	120 670	134 130	0.07	7.054	0.528	13.36	21 870	22 378	0.977	grant prideco
33	120 670	134 130	0.07	7.049	0.527	13.38	21 960	22 349	0.983	grant prideco
34	120 670	134 130	0.07	7.060	0.543	13.00	21 030	23 046	0.913	grant prideco
35	120 670	134 130	0.07	7.048	0.524	13.45	22 080	22 215	0.994	grant prideco
36	129 800	142 700	0.06	7.695	0.490	15.70	20 190	20 104	1.004	grant prideco
37	129 800	142 700	0.06	7.691	0.491	15.66	20 060	20 159	0.995	grant prideco
38	129 800	142 700	0.06	7.700	0.496	15.52	20 195	20 353	0.992	grant prideco
39	129 800	142 700	0.06	7.694	0.468	16.44	19 900	19 145	1.039	grant prideco
40	129 800	142 700	0.06	7.694	0.476	16.16	20 055	19 494	1.029	grant prideco
41	129 800	142 700	0.06	7.698	0.502	15.33	20 230	20 622	0.981	grant prideco
42	124 000	132 700	0.07	7.663	0.472	16.24	19 208	17 991	1.068	grant prideco
43	124 000	132 700	0.07	7.679	0.474	16.20	19 338	18 032	1.072	grant prideco
44	128 700	144 800	0.06	9.746	0.539	18.08	17 985	17 551	1.025	grant prideco
45	128 700	144 800	0.06	9.729	0.533	18.25	17 975	17 376	1.034	grant prideco
46	128 700	144 800	0.06	9.730	0.535	18.19	18 025	17 443	1.033	grant prideco

Table B.6 (*continued*)

Test number	Measured yield strength psi	Measured ultimate tensile strength psi	n value	Measured outer diameter in	Measured minimum wall thickness in	D/t ratio	Measured rupture pressure psi	Calculated rupture pressure psi	Actual burst/ predicted burst	Data set
47	128 700	144 800	0.06	9.724	0.536	18.14	18 080	17 489	1.034	grant prideco
48	128 700	144 800	0.06	9.722	0.525	18.52	17 835	17 113	1.042	grant prideco
49	128 700	144 800	0.06	9.738	0.542	17.97	18 005	17 669	1.019	grant prideco
50	105 900	125 350	0.08	9.660	0.542	17.82	16 500	15 252	1.082	grant prideco
51	133 900	144 810	0.06	9.953	0.620	16.05	20 853	19 969	1.044	grant prideco
52	133 900	144 810	0.06	9.931	0.620	16.02	20 631	20 016	1.031	grant prideco
53	124 355	138 976	0.07	11.831	0.509	23.24	13 300	12 908	1.030	grant prideco
54	124 355	138 976	0.07	11.837	0.497	23.82	12 900	12 583	1.025	grant prideco
55	124 355	138 976	0.07	11.840	0.482	24.56	12 950	12 184	1.063	grant prideco
56	124 355	138 976	0.07	11.823	0.527	22.43	13 550	13 395	1.012	grant prideco
57	127 150	136 000	0.07	13.456	0.497	27.07	11 523	10 791	1.068	grant prideco
58	127 150	136 000	0.07	13.473	0.509	26.47	11 740	11 047	1.063	grant prideco
59	127 150	136 000	0.07	13.443	0.495	27.16	11 447	10 756	1.064	grant prideco
60	127 150	136 000	0.07	13.465	0.489	27.54	11 840	10 603	1.117	grant prideco
61	127 150	136 000	0.07	13.451	0.505	26.64	11 414	10 975	1.040	grant prideco
62	127 150	136 000	0.07	13.459	0.504	26.70	11 914	10 946	1.088	grant prideco
63	93 450	107 400	0.09	13.682	0.626	21.86	11 226	10 475	1.072	grant prideco
64	94 450	107 400	0.09	13.673	0.617	22.16	9 744	10 330	0.943	grant prideco
65	95 450	107 400	0.09	13.669	0.612	22.33	10 312	10 251	1.006	grant prideco
66	96 450	170 400	0.09	13.670	0.621	22.01	10 750	10 413	1.032	grant prideco
67	96 258	113 072	0.09	16.080	0.474	33.92	7 330	6 996	1.048	grant prideco
68	62 700	86 400	0.12	5.562	0.750	7.42	25 460	26 976	0.944	shell pipeline
69	62 700	86 400	0.12	5.562	0.750	7.42	25 800	26 976	0.956	shell pipeline

Table B.6 (*continued*)

Test number	Measured yield strength psi	Measured ultimate tensile strength psi	n value	Measured outer diameter in	Measured minimum wall thickness in	D/t ratio	Measured rupture pressure psi	Calculated rupture pressure psi	Actual burst/ predicted burst	Data set
70	62 700	86 400	0.12	5.562	0.750	7.42	25 980	26 976	0.963	shell pipeline
71	62 700	86 400	0.12	5.562	0.750	7.42	26 320	26 976	0.976	shell pipeline
72	62 700	86 400	0.12	5.562	0.750	7.42	26 090	26 976	0.967	shell pipeline
73	61 600	76 100	0.12	5.562	0.750	7.42	24 930	23 747	1.050	shell pipeline
74	65 700	86 200	0.12	6.625	0.562	11.79	15 900	16 030	0.992	shell pipeline
75	65 700	86 200	0.12	6.625	0.562	11.79	15 870	16 030	0.990	shell pipeline
76	47 800	72 800	0.13	6.625	0.562	11.79	13 170	13 418	0.982	shell pipeline
77	47 800	72 800	0.13	6.625	0.562	11.79	13 270	13 418	0.989	shell pipeline
78	47 700	73 100	0.13	6.625	0.562	11.79	12 900	13 472	0.958	shell pipeline
79	47 700	73 100	0.13	6.625	0.562	11.79	12 940	13 472	0.960	shell pipeline
80	51 160	77 540	0.13	4.500	0.345	13.04	12 810	12 823	0.999	shell pipeline
81	51 160	77 540	0.13	4.500	0.345	13.04	12 800	12 823	0.998	shell pipeline
82	51 160	77 540	0.13	4.500	0.345	13.04	12 800	12 823	0.998	shell pipeline
83	74 500	90 500	0.11	12.750	0.750	17.00	11 370	11 398	0.998	shell pipeline
84	74 500	90 500	0.11	12.750	0.750	17.00	11 140	11 398	0.977	shell pipeline
85	74 500	90 500	0.11	12.750	0.750	17.00	11 250	11 398	0.987	shell pipeline
86	57 660	78 680	0.12	8.625	0.495	17.42	8 710	9 572	0.910	shell pipeline
87	57 660	78 680	0.12	8.625	0.495	17.42	8 550	9 572	0.893	shell pipeline
88	57 660	78 680	0.12	8.625	0.495	17.42	8 640	9 572	0.903	shell pipeline
89	43 990	73 740	0.13	8.625	0.507	17.01	8 760	9 140	0.958	shell pipeline
90	43 990	73 740	0.13	8.625	0.507	17.01	8 770	9 140	0.960	shell pipeline
91	43 990	73 740	0.13	8.625	0.507	17.01	8 830	9 140	0.966	shell pipeline
92	78 920	95 010	0.11	8.625	0.875	9.86	21 720	21 663	1.003	shell pipeline

Table B.6 (*continued*)

Test number	Measured yield strength psi	Measured ultimate tensile strength psi	n value	Measured outer diameter in	Measured minimum wall thickness in	D/t ratio	Measured rupture pressure psi	Calculated rupture pressure psi	Actual burst/ predicted burst	Data set
93	78 920	95 010	0.11	8.625	0.875	9.86	21 930	21 663	1.012	shell pipeline
94	71 540	91 560	0.11	8.625	1.000	8.63	23 560	24 161	0.975	shell pipeline
95	71 540	91 560	0.11	8.625	1.000	8.63	23 690	24 161	0.981	shell pipeline
96	121 000	132 800	0.07	2.875	0.308	9.33	30 410	32 863	0.925	hydril n-wall
97	120 700	131 500	0.07	2.875	0.308	9.33	29 710	32 536	0.913	hydril n-wall
98	116 000	126 200	0.08	2.875	0.308	9.33	29 800	31 152	0.957	hydril n-wall
99	115 400	124 200	0.08	2.875	0.308	9.33	28 750	30 649	0.938	hydril n-wall
100	116 400	131 300	0.07	13.625	0.625	21.80	12 460	12 989	0.959	hydril n-wall
101	100 700	111 000	0.09	3.500	0.254	13.78	17 960	17 733	1.013	hydril n-wall
102	145 700	166 000	0.05	5.500	0.304	18.09	21 600	20 280	1.065	hydril n-wall
103	142 000	162 400	0.05	5.500	0.304	18.09	20 830	19 803	1.052	hydril n-wall
104	145 400	170 200	0.05	5.500	0.304	18.09	20 700	20 790	0.996	hydril n-wall
105	90 500	130 700	0.10	7.625	0.430	17.73	11 680	12 589	0.928	hydril n-wall
106	85 100	97 400	0.10	9.625	0.545	17.66	12 320	11 843	1.040	hydril n-wall
								Mean	1.006	
								Stdev	0.045	
								COV	0.045	

[a] These n-values denote the measure for the pipe tested to rupture. All other n-values are based on regression fit of OCTG stress-strain data. n OCTG = 0.169 3-0.000 812 × Yield (ksi) with Yield being actual measured yield, ksi.

Figure B.3 summarizes the same data in graphical form.

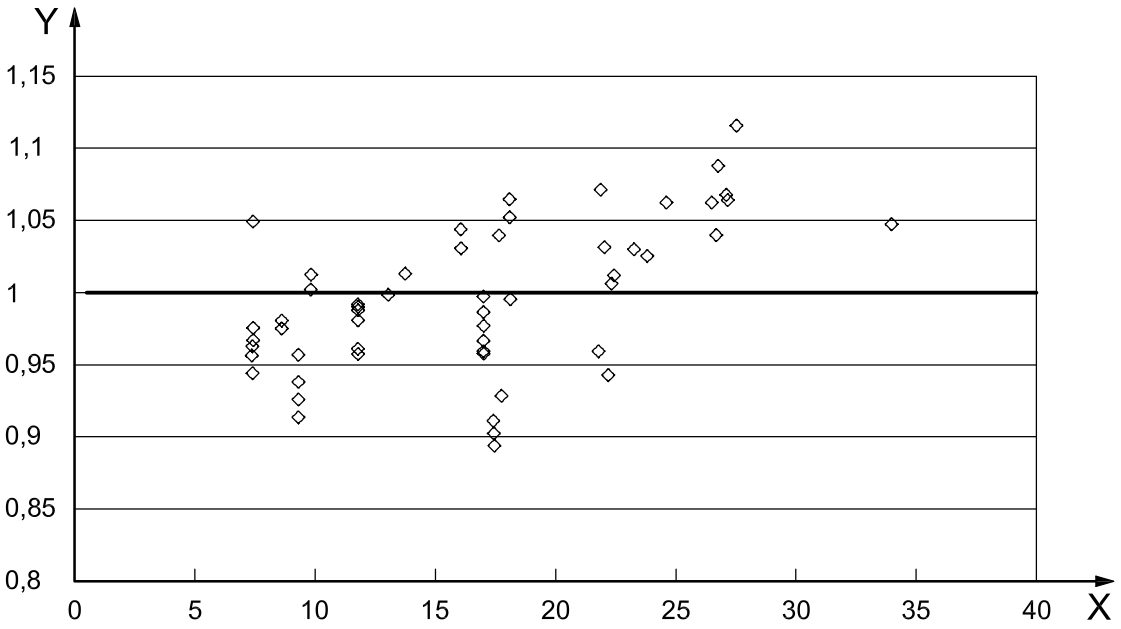

Key

X D/t ratio

Y ratio of actual to predicted

NOTE Mean = 1,006; COV = 4,5 %.

Figure B.3 — Ratio of actual to predicted rupture pressures for Klever-Stewart model

B.6.2 Additional pipe rupture data under combined pressure and axial tension

Only a small amount of data were available reporting measured pipe rupture pressure at axial load different from the capped-end load. These data are summarized in Table B.7 and compared with the predictions of the Klever-Stewart Equation generalized to include the influence of axial tension or compression. Overall, the equation becomes more conservative at increasing axial tension. No data were available to evaluate the model at compressive axial load.

Table B.7 — Comparison of rupture Equation (B.6) and necking Equation (B.18) with Shell mini-pipe [12] test data at axial tension exceeding the capped-end load (italic numbers are considered given)

Test number	Outside diameter in	Wall thickness in	Test		Check Equation (B.22)	Model		
			F_{eff}/F_{uts}	p_i/p_{uts}		F_{eff}/F_{uts}	p_i/p_{uts}	Actual/ predicted
1	0,90	0,106 5	1,029	*0,000*	N	1,000	*0,000*	1,029
2	0,90	0,106 5	0,922	*0,500*	N	0,910	*0,500*	1,012
3	0,90	0,106 5	0,000	*0,922*	R	0,000	*1,027*	0,966
4	0,90	0,106 5	0,395	*0,983*	R	0,395	*0,985*	0,998
5	0,90	0,106 5	0,468	*0,965*	R	0,468	*0,967*	0,998
6	0,90	0,106 5	0,774	*0,765*	R	0,774	*0,731*	1,046
							Mean	1,008
							COV	0,025

In Table B.7, the effective axial tension is the amount of tension in excess of the load from pressure acting on the end caps of the pipe.

Table B.8 offers additional validation of the Klever-Stewart Equation with rupture data for the special case of zero axial tension. The tests in this instance were conducted on ring specimens rather than tubes.

Table B.8 — Comparison of rupture equation and test data at zero axial tension, ring tests

Number	f_u MPa	n	D mm	t_{min} mm	D/t_{min}	p_{iR} MPa		Actual/ predicted
						Test	Model	
1	563	0,13	914,2	22,20	41,18	26,30	25,99	1,012
2	563	0,13	914,2	22,20	41,18	26,40	25,99	1,016
3	563	0,13	914,2	15,54	58,83	18,70	19,27	0,971
4	563	0,13	914,2	15,76	58,00	19,50	19,55	0,997
5	563	0,13	914,2	11,54	79,19	14,80	14,24	1,040
6	563	0,13	914,2	10,43	87,62	13,00	12,85	1,012
7	563	0,13	914,2	6,88	132,84	8,56	8,43	1,015
8	563	0,13	914,2	6,66	137,27	8,08	8,16	0,990
9	563	0,13	914,2	6,88	132,84	8,22	8,43	0,975
							Mean	1,003
							COV	0,022

B.7 The role of imperfections in the ductile rupture equation

B.7.1 General

The ductile rupture equation is recommended only with pipe small wall eccentricity and inspection-threshold sized imperfection depth included in the equation. The equation should not be used without accounting for these imperfections. In the deterministic equation of rupture, thin wall eccentricity is accounted for through the minimum possible physical wall thickness. In the probabilistic equation of rupture, thin wall eccentricity is accounted for through the mean and standard deviation of the minimum wall thickness on a per length basis.

In a deterministic formulation of rupture, sharp-bottomed imperfections are accounted for through the maximum size imperfection which is able to pass undetected through the inspection threshold; that is, an imperfection with depth equal to the inspection threshold. It is assumed that each length of pipe has an imperfection of this depth. This conservative equation uses the worst-case possible frequency for the imperfection.

In a probabilistic formulation of rupture, the depth of the sharp-bottom imperfection is still set equal to the inspection threshold; but the occurrence of the imperfection is based on statistical observations. In this case, the penalty for the presence of the imperfection accounts for the mean and the standard deviation of the frequency of occurrence of sharp-bottomed imperfections in pipe that has been inspected. A typical frequency of occurrence of imperfections of all kinds during secondary inspection is 2 % to 5 %. But for sharp-bottomed imperfections, the frequency can be much less, for example 0,5 % to 0,05 %. This frequency can have significant impact on the probability of rupture at a particular pressure.

Figure B.4 is a conceptual illustration of the role that the sharp-bottomed imperfection plays in decreasing the rupture strength of the pipe.

Figure B.5 is a more in-depth illustration of the role of the imperfection penalty for 9-5/8 inch OD, 53,5 lb/ft, P110 casing.

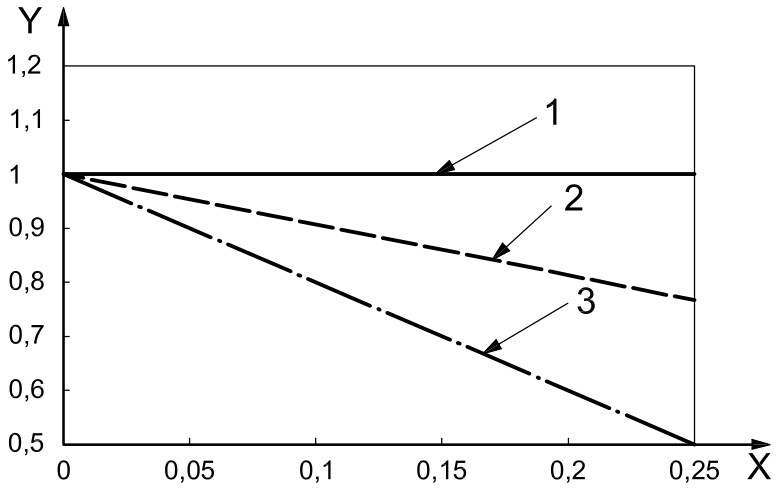

Key

X crack depth, a/t

Y p_{crit}/p_{ref}

1 no cracks 2 crack, high toughness 3 crack, low toughness

Figure B.4 — Rupture de-rating for cracks (crack assumed on minimum wall)

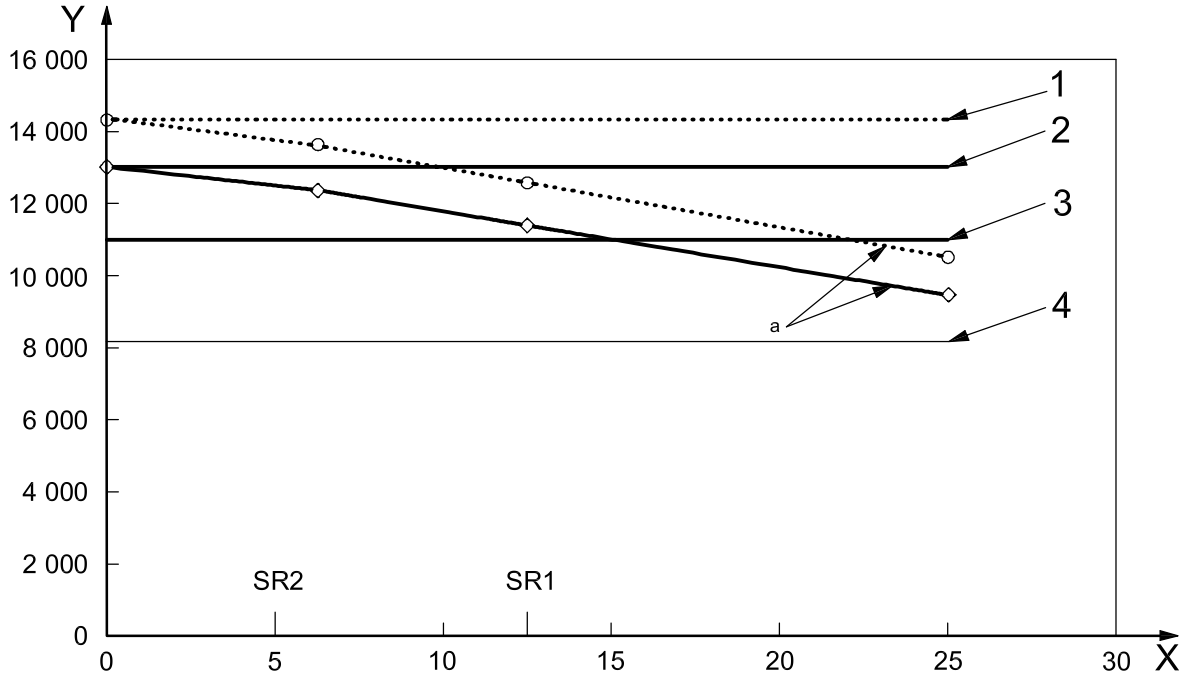

Key

X crack depth as a fraction of wall thickness, %

Y internal pressure, psi

SR1, SR2 Supplemental Requirements as defined in Annex A, ISO 11960:2004

1 mean rupture without a flaw 3 rating based on minimum yield

2 minimum rupture without a flaw 4 historical design on yield divided by a design factor

[a] Influence of crack-like imperfections in pipe with good toughness.

Figure B.5 — Influence of the imperfection penalty for 9-5/8 in, 53,5 lb/ft, P110 casing

In order to have a conservative deterministic calculation of the rupture pressure, the penalty for sharp imperfections should be applied on top of the physical thin-wall geometry. This is because this case does occur in pipe manufacturing, and the deterministic model should capture the minimum pressure that is possible for pipe that is produced in compliance with manufacturing specifications. If one seeks to address how rare this combination of imperfections is, then a probabilistic rupture equation should be applied.

B.7.2 The fracture mechanics basis for the burst strength factor in the ductile rupture equation

The burst strength factor, k_a, in the ductile rupture equation is an ad-hoc generalization of the Klever-Stewart ductile rupture equation. The burst strength factor is based on the fracture mechanics concept of crack growth as measured by the material property J_{1C} and the J-Integral. To determine k_a, first J_{1C} values were measured for representative samples of pipe and coupling material. Table B.9 is an example of such data.

Table B.9 — Typical J_{1C} values

Grade	Test	Grade	Test
J55	900	13Cr95	1 200
J55	925	13Cr95	1 225
K55	501	C100	1 100
K55	612	C100	1 200
K55	640	CYP110	836
K55	875	P110	340
K55	1 000	P110	360
L80	710	P110	360
L80	720	P110	402
L80	743	P110	418
L80	750	P110	450
L80	780	P110	455
L80	780	P110	490
L80	810	P110	520
L80	863	P110	550
L80	925	P110	580
L80	925	P110	585
L80	940	P110	585
L80	950	P110	640
L80	1 020	P110	660
L80	1 025	P110	660
N80	850	P110	675
N80	1 025	P110	700
C90	610	P110	752
C90	682	P110	800
C95	472	P110	848
C95	485	P110	921

Next, for several pipes, the value of the J-Integral was calculated using the finite element method. The calculation of the J-Integral is based on the crack depth, the internal pressure acting on the pipe, and the measured stress-strain curve of the same pipe material that supplied the sample for J_{1C} measurement. Figures B.6 and B.7 show typical curves of the J-Integral. The figures also show an overlay of the measured J_{1C} value. Theoretically, the point where the J-Integral equals J_{1C} represents the failure pressure of the pipe; and the decrease of the failure pressure with depth of the crack indicates the increasing influence of the crack depth.

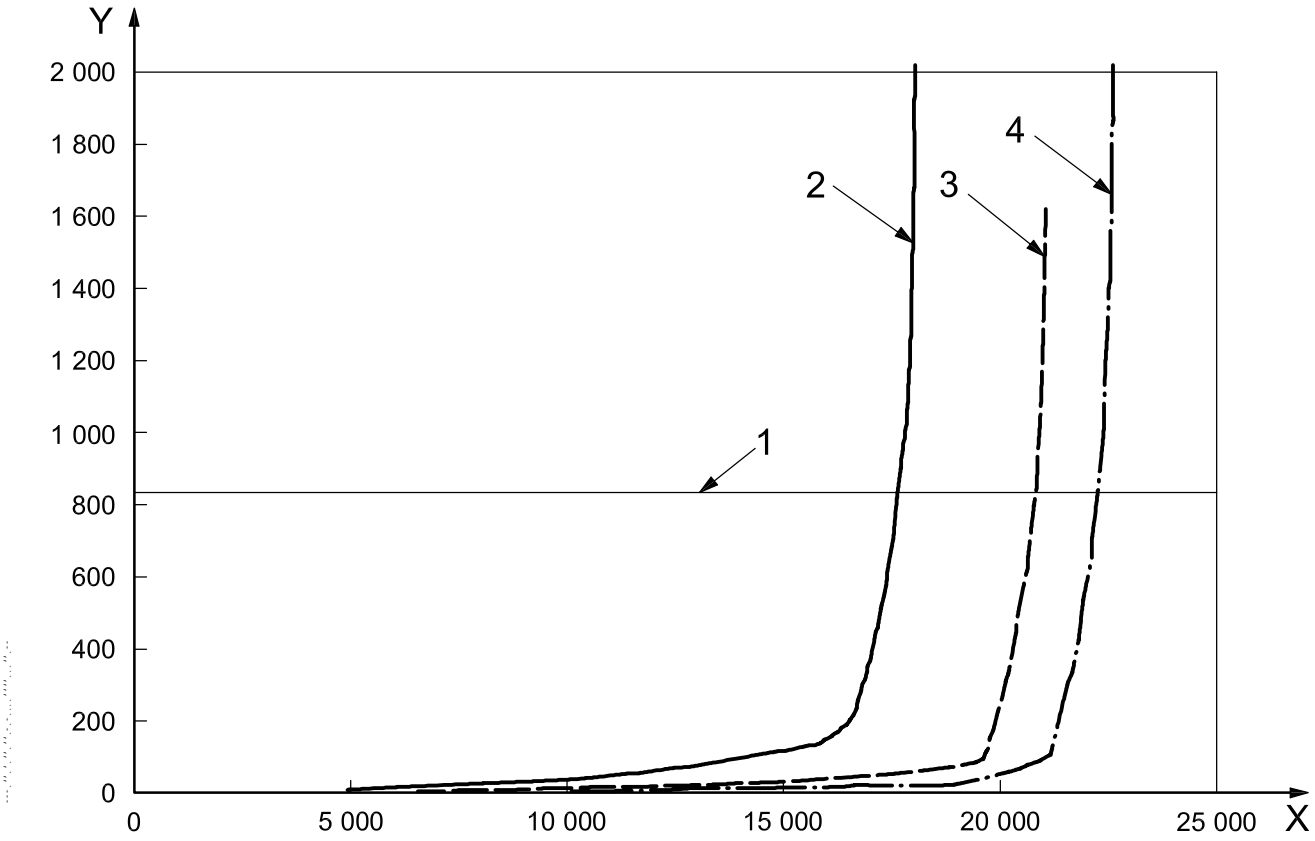

Key

X internal burst pressure, psi

Y J integral, psi·in

1 J_{1c}

2 1/4 wall

3 1/8 wall

4 1/16 wall

Figure B.6 — J-Integral and J_{1C} for a P110 pipe

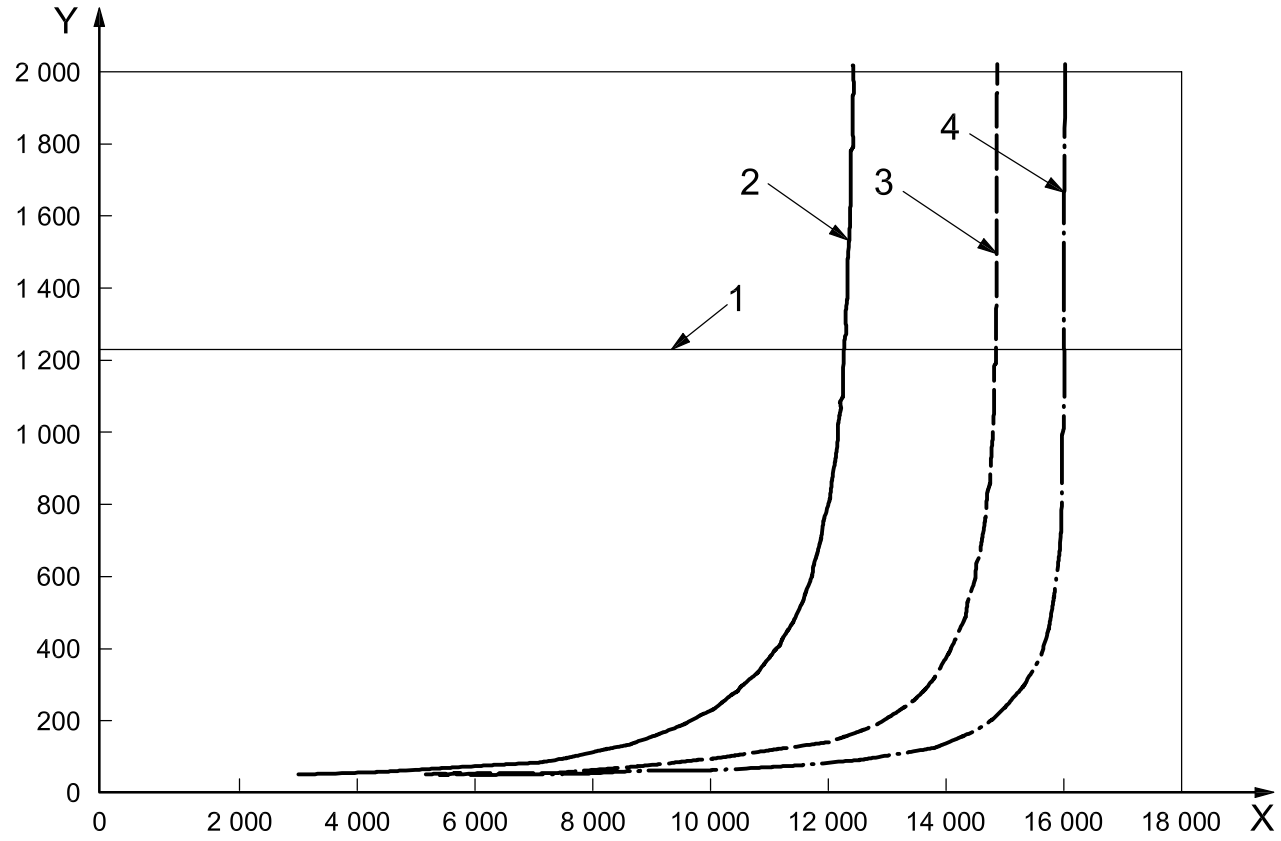

Key

X internal burst pressure, psi

Y J integral, psi·in

1 J_{1c}

2 1/4 wall

3 1/8 wall

4 1/16 wall

Figure B.7 — J-Integral and J_{1C} for a 13-Cr-95 pipe

Based on the change of the intersection between J_{1C} and the J-Integral with internal pressure for several calculations and measurements, Figure B.8 shows the predicted ratio of rupture pressure with an imperfection divided by rupture pressure without an imperfection, for different imperfection depths and grades of pipe. Figure B.8 shows that in general for the quenched and tempered pipes, the influence of the sharp imperfection is about equal to the imperfection depth. This is the origin of the burst strength parameter $k_a = 1$ for quenched and tempered pipes in the rupture equation. However, Figure B.8 also shows that for some pipes, such as J55 and K55, the influence of the sharp imperfection is approximately equal to twice the imperfection depth. For this reason, when the toughness behaviour of the pipe is unknown, the burst strength parameter $k_a = 2$ is used in the ductile rupture equation.

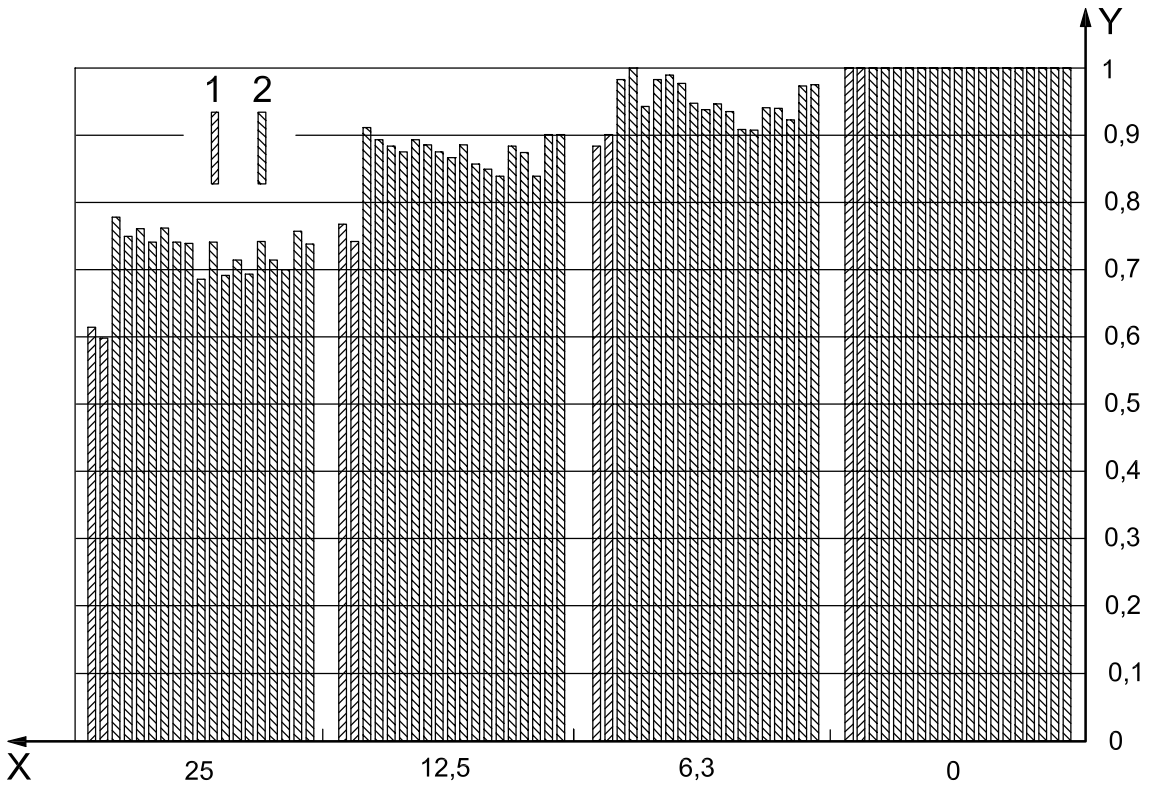

Key

X flaw depth/nominal wall thickness, %

Y burst pressure with flaw/burst pressure without flaw

1 non-Q&T (Grade K)

2 Q&T (various grades)

Figure B.8 — Influence of crack depth on ductile rupture

B.8 Template for probabilistic calculation of ductile rupture strength

B.8.1 General

The actual ductile rupture pressure for a given pipe is uncertain because many of the factors affecting it are random. A deterministic calculation of the rupture pressure assumes that all of the factors are known with absolute certainty and the equations used to calculate the strength are exact. The calculation assumes that if the pressure exceeds the calculated strength, it ruptures. In this case, a given set of input parameters corresponds to a single, deterministic predicted pressure. In order to ensure that the prediction is conservative and errs on the safe side, the deterministic calculation should use the worst-case allowable set of input parameters for a pipe in compliance with its product specifications. Of course, this is not reality. The actual ductile rupture pressure could be above or below the predicted value. In a design situation, a set of worst-case input parameters are used to calculate a lower bound pressure.

In contrast to the deterministic equation, a probabilistic estimate of the strength accounts for the uncertainties in the input parameters and results in a relation between the applied pressure and the rupture probability. In this manner, the calculation provides the likely ductile rupture pressure instead of the worst possible ductile rupture pressure.

Why use a probabilistic model for pipe ductile rupture strength? A simple universal design factor can result in inconsistent failure probabilities or inconsistent risks. A probabilistic strength calculation can be used to justify a low cost design when the failure cost is low and a higher failure probability can be tolerated. In contrast, it

can be used to produce a highly reliable design when the costs and safety consequences of failure are large. The goal of a probabilistic model of ductile rupture can be to determine the failure probability, either with deterministic loads or in conjunction with a randomized load model.

The following paragraphs briefly summarize the steps needed to develop a simple probabilistic model for ductile rupture. These steps follow the generalized procedure:

a) determine the failure mode (in this case ductile rupture);

b) determine the physics of failure and express failure mathematically as a limit state function, $g(\vec{x})$, where the component fails whenever $g(\vec{x}) < 0$;

c) determine uncertainty models for the variables, $\vec{x}$ in the limit state, where possible basing these models on statistical analysis of these parameters;

d) finally, estimate the failure probability as the probability that $g(\vec{x}) < 0$. In the case summarized, this can be estimated using Monte Carlo simulation, or first and second order reliability methods (FORM/SORM). (In the steps below, FORM is demonstrated.)

In the pipe ductile rupture case, a possible limit state could be $g(\vec{x}) = R(\vec{x}) - p_{\mathrm{a}}(\vec{x})$, where $R(\vec{x})$ is the equation used to calculate the rupture pressure from size and strength parameters, and $p_{\mathrm{a}}(\vec{x})$ is the applied pressure. The limit state function, $g(\vec{x})$, depends on a vector consisting of all the significant random parameters affecting failure. These random variables could include material properties such as yield and tensile strength, geometric properties such as metal thickness and loads such as the lifetime maximum applied pressure, or the uncertainty in model idealization. The limit state divides the space of all possibilities into two sets: the safe set, where failure does not occur, and the set where failure occurs.

The limit state input parameters, $\vec{x}$, are modelled as random variables. In the case where all the parameters are mutually independent, each parameter is assigned an appropriate probability distribution function. These distribution functions should be based on a statistical analysis of the measurements of the parameters. Input parameters used to model the idealization uncertainties should be based where possible on measurements of actual and predicted loads or strengths.

With the limit state and the probabilistic models for each of the input parameters, the probability of failure, P_{f} is determined as:

$$P_{\mathrm{f}} = \int_{g(x)<0} f(\vec{x})\,\mathrm{d}\vec{x} \tag{B.34}$$

where

$f(\vec{x})$ is the joint probability density function of the variables in $\vec{x}$;

$g(\vec{x})$ is the limit state function;

$\vec{x}$ is a vector of random variables.

In order to calculate the probability of ductile rupture at a particular pressure, a closed-form solution of the probability integral usually is not possible. In practice, methods other than the direct integration are used to estimate the failure probability. The most familiar method is Monte Carlo simulation, which is not usually recommended for rare events ($P < 10^{-3}$) such as pipe ductile rupture because of the large number of individual calculations that are required to estimate a small failure probability. In cases where the probability is small, there are other methods such as FORM/SORM. The Gaussian central moment method, summarized below, demonstrates one such method to estimate rupture probability. This method is not too accurate; however it can be used to approximate failure probabilities and can be used to investigate the sensitivity of a given design to various input parameters. Furthermore, unlike FORM/SORM or simulation, the Gaussian central moment method depends only on the mean and the standard deviation of the various input variables, and as a result, it is easy to apply.

The probabilistic rupture pressure is based on the deterministic model for rupture pressure, p_{iR}, including the effect of sharp imperfections, where p_{iR} is the internal pressure at ductile rupture of an end-capped pipe:

$$p_{iR} = 2k_{dr}f_u(t_{min} - k_a a_N)/[D - (t_{min} - k_a a_N)] \quad \text{(B.35)}$$

where

a_N is the imperfection depth associated with a specified inspection threshold, i.e. the maximum depth of a crack-like imperfection that could reasonably be missed by the pipe inspection system. For example, for a 5 % imperfection threshold inspection in a 12,7 mm (0.500 in) wall thickness pipe, a_N = 0,635 mm (0.025 in);

D is the specified pipe outside diameter;

f_u is the tensile strength of a representative tensile specimen;

k_a is the burst strength factor, having the numerical value 1,0 for quenched and tempered (martensitic structure) or 13Cr products and 2,0 for as-rolled and normalized products based on available test data; and the default value set to 2,0 where the value has not been measured. The value of k_a can be established for a specific pipe material based on testing;

k_{dr} is the correction factor based on pipe deformation and material strain hardening, having the numerical value $[(1/2)^{n+1} + (1/\sqrt{3})^{n+1})]$;

n is the dimensionless hardening index used to obtain a curve fit (see B.2.3.3) of the true stress-strain curve derived from the uniaxial tensile test;

t_{min} is the actual minimum pipe wall thickness disregarding crack-like imperfections.

The rupture pressure, p_{iR} is used with the applied pressure, p_i, to form the limit state function:

$$g = C_{iR}p_{iR}(f_u, n, t, D) - p_i \quad \text{(B.36)}$$

where C_{iR} is the random variable that represents model uncertainty.

This function is less than zero when the applied pressure, p_i, exceeds the ductile rupture resistance, $C_{iR}p_{iR}(f_u, n, t, D)$.

Using this limit state, the ductile rupture probability can be estimated using closed-form equations from mean value FORM:

$$\overline{g} = \overline{p}_i - \overline{C}_{iR}\overline{p}_{iR}\left(\overline{f}_u, \overline{n}, \overline{t}, \overline{D}\right) \quad \text{(B.37)}$$

$$s_g^2 = s_p^2\left(\frac{dg}{dp_i}\right)^2_{\vec{x}=\vec{X}} + s_u^2\left(\frac{dg}{df_u}\right)^2_{\vec{x}=\vec{X}} + \ldots + s_D^2\left(\frac{dg}{dD}\right)^2_{\vec{x}=\vec{X}} \quad \text{(B.38)}$$

$$\beta = \frac{\overline{g}}{s_g} \quad \text{(B.39)}$$

$$p_{crude} = \Phi(-\beta) \quad \text{(B.40)}$$

where

— the “barred” variables are the means;

— the s_x^2 are the estimated variances (squared standard deviations) of the random variables;

— the derivatives $\mathrm{d}g/\mathrm{d}x$ are evaluated at the mean values for f_u, n, t,…, etc.;

— β is the crude, first-order reliability index;

— and $\Phi(-\beta)$ is the cumulative probability function (CPF) of a standard unit normal random variable (mean = 0 and standard deviation = 1) evaluated at $-\beta$.

This estimated probability corresponds to a length of pipe that has a significant defect. The ductile rupture equation includes the effect of a defect with a depth equal to the inspection notch depth, a_N. This is the largest defect that should be expected in an inspected length of pipe, depending on the quality of the inspection. Larger defects are possible, because inspection could miss a significant defect. However, in general not every length has a defect as deep or as sharp-bottomed as assumed by this equation. Consequentially, when using this formulation, it is important to consider the effect of imperfection frequency; for example, a low imperfection frequency expected in a run of pipe where a high quality inspection was used. In this case, almost all lengths of pipe with defects greater than the threshold are culled, and only a few lengths will have any significant defect.

B.8.2 Approach to random variables in the probabilistic rupture equation

In the probabilistic formulation of rupture pressure, there are four variables that are treated as random, such that the mean and the standard deviation (or coefficient of variation) of these variables impact the probability of rupture at a particular pressure:

— the pipe ultimate tensile strength,

— the pipe diameter,

— the pipe physical (no imperfection) minimum wall thickness,

— the frequency at which sharp-bottomed imperfections occur in pipe which has received primary inspection.

At the same time, there are three variables that are treated as fixed (deterministic) in the probabilistic formulation:

— the stress-strain curve parameter n,

— the material toughness parameter m,

— and the maximum imperfection depth, set equal to the inspection threshold setting a_N.

It is appropriate that care be used to select the frequency of sharp-bottomed imperfections in the probabilistic treatment of the rupture equation. First, this frequency should be set to the reject rate of sharp-bottomed imperfections and not to the reject rate including round-bottom imperfections. Second, the value of this frequency can depend on the equipment and methods used for the combination of primary and secondary inspection.

— If pipe is first inspected (by the mill) to SR2 (5 %) depth and then re-inspected to SR1 (12,5 %), the imperfection depth should be set equal to the inspection threshold used for the SR1 inspection, but the frequency in this case is less than in the case where SR2 depth is used for the second inspection.

— Alternatively, if SR2 also is used for the second inspection, then the mean and standard deviation of the imperfection frequency should be based on the frequency observed at the second inspection, and the imperfection depth used in the probabilistic rupture equations should be set equal to the inspection threshold used in the second SR2 inspection.

— When the type of inspection equipment is changed for either the first or second inspection, this will usually result in a different mean and standard deviation of imperfection frequency in the probabilistic rupture calculations.

The imperfection frequency is an important parameter in the probabilistic ductile rupture calculation. For the deterministic ductile rupture calculation, the frequency of occurrence of the imperfection is 100 %, and the penalty for the imperfection is severe and conservative. For the probabilistic calculation, the penalty for the imperfection only occurs a small part of the time.

B.8.3 Approach to probable imperfection depth and frequency

The inspection threshold allows passage of imperfections equal or smaller in size than the setting of the inspection threshold. The threshold setting usually is slightly smaller than the imperfection depth of the inspection, but this depends on the setting and line speed of individual inspection equipment. Even with perfect imperfection detection, it is important to recognize that the threshold setting allows pipe imperfections to pass when the imperfection depths are equal or smaller than the depth of the threshold setting.

There are two potential limits to the way that imperfections smaller than the inspection threshold impact the rupture strength of the pipe. At one extreme, rarely occurring, large imperfections equal in size to the threshold setting impose the largest penalty against rupture strength. At the other extreme, frequently occurring imperfections much smaller than the inspection threshold setting do impact the rupture strength, not due to their depth but due to their frequency.

This clause provides a comparison of the likely impact of imperfection depth compared with imperfection frequency. It is found that the rare deep imperfection (equal in depth to the inspection threshold) tends to have more dominant impact compared with the smaller more frequent imperfections. On the strength of this premise, the probabilistic equation for ductile pipe rupture has based the rupture strength of the pipe on the probable wall thickness combined with a penalty for the probable imperfection with depth set equal to the inspection threshold setting (to be conservative) and with frequency set equal to the frequency at which sharp crack-like or seam lap imperfections are detected and proven during secondary inspection.

What effect does the shape of the imperfection frequency distribution below the inspection limit have on the probability of failure? As a first stage of the answer to this question, the distribution of the maximum defect size was investigated to determine how the shape of the imperfection size distribution below the inspection threshold affects the largest expected imperfection size in a string.

The following assumptions were made:

— after the inspection, the distribution of defects is truncated at the threshold. In this case, the numerical study assumes this is 5 %;

— the imperfection frequency of defects greater than 5 % is 3 %. There is a 3 % probability that the deepest imperfection in an un-inspected length of casing is deeper than 5 % of the specified wall;

— the distribution of imperfections is modelled by a Weibull distribution. This distribution is chosen only for convenience, because its shape can be easily modified using the distribution's slope parameter.

The following charts compare the shape of the distribution of imperfection shape with the distribution of the deepest extreme imperfection in 50 lengths. These four charts parameterize the shape of the distribution of imperfection size in an arbitrary length by the b-parameter of the Weibull distribution used to model each. This distribution is truncated at a depth of 5 % specified. As b increases from 0,5 to 4, the coefficient of variation of the distribution decreases from 224 % to 28 %. The probability density functions for these are shown by the solid line in the Figures B.9 through B.12.

The dashed lines in the charts are the probability densities for the deepest defect in 50 lengths. It is related to the probability density and cumulative probability functions of the underlying distribution of the deepest imperfection in an arbitrary length. This distribution is also truncated at a depth of 5 % of specified. These extreme-value probability density functions show that the majority of the probability weight is towards the upper limit of 5 %. In fact, because the underlying distribution of imperfection size is truncated at the imperfection threshold, the most likely depth imperfection depth is equal to the imperfection threshold (5 %). This effect becomes more pronounced as the b parameter in the underlying distribution increases.

Even when the probability distribution is biased toward 0 % ($b = 0{,}5$), the most likely deepest defect is 5 % of specified. In this case, the distribution is evenly spread over the interval between 3,5 % to 5 %.

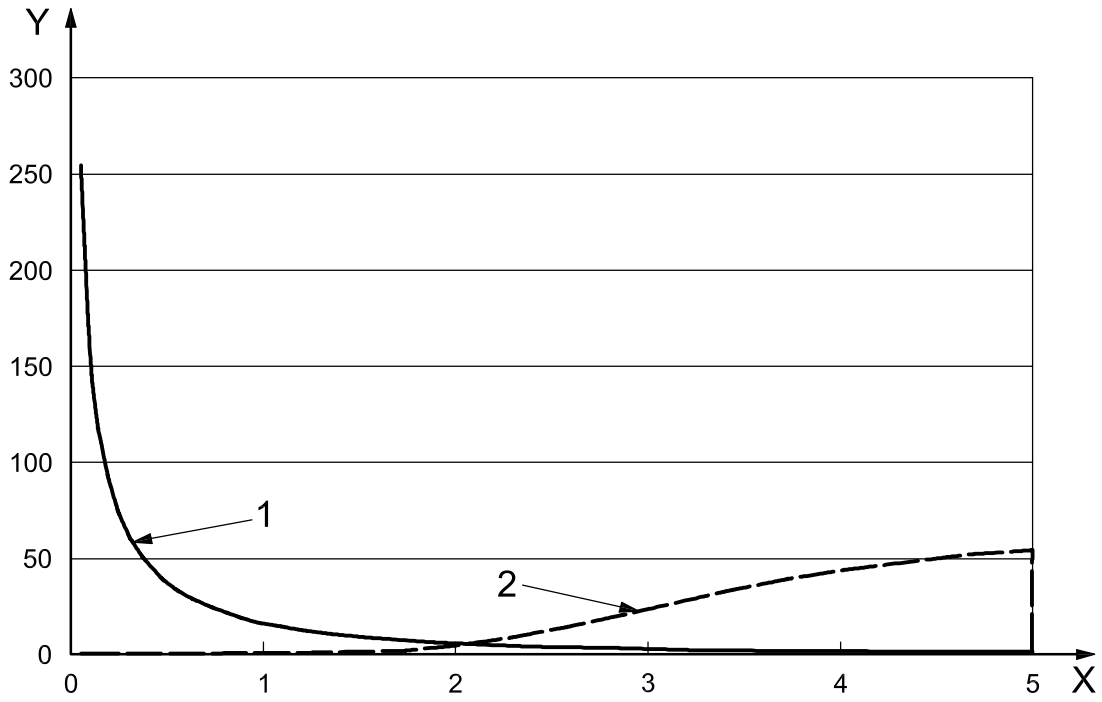

Key

X defect, % of nominal 1 single joint
Y PDF (probability density function) 2 maximum of 50 joints

NOTE $b = 0{,}5$; mean = 0,81 %; standard deviation = 1,82 %.

Figure B.9 — Distribution bias to very small defects — Very high COV

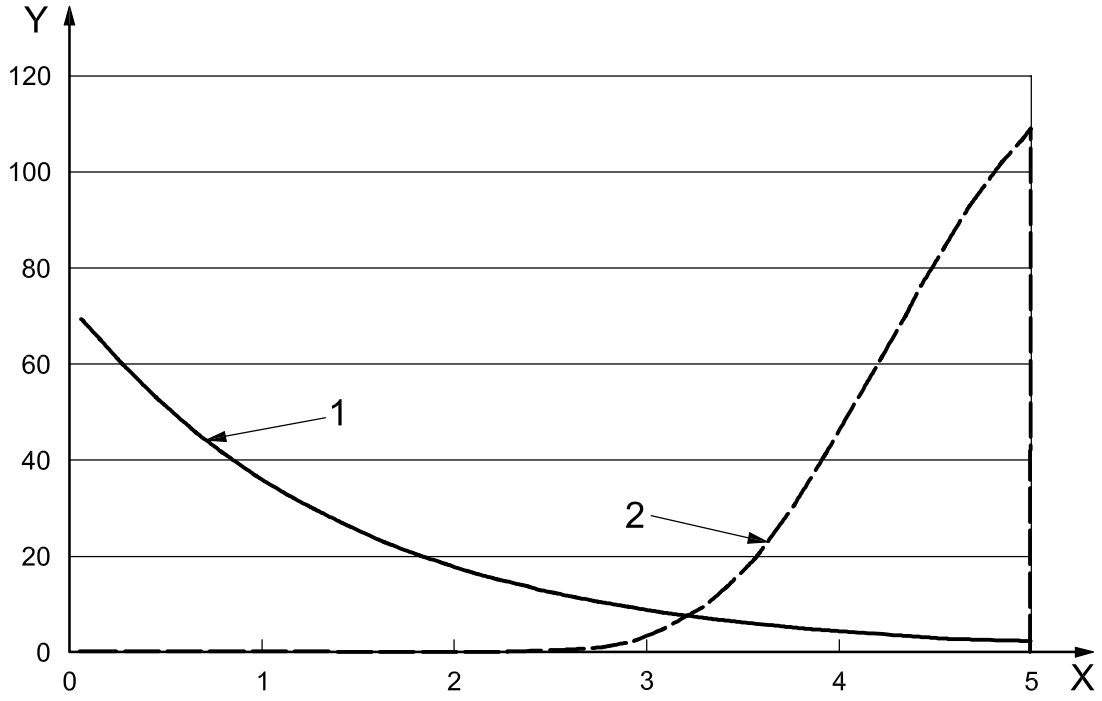

Key

X defect, % of nominal 1 single joint
Y PDF (probability density function) 2 maximum of 50 joints

NOTE $b = 1{,}0$; mean = 1,43 %; standard deviation = 1,43 %.

Figure B.10 — Exponential distribution of defect sizes — Large COV

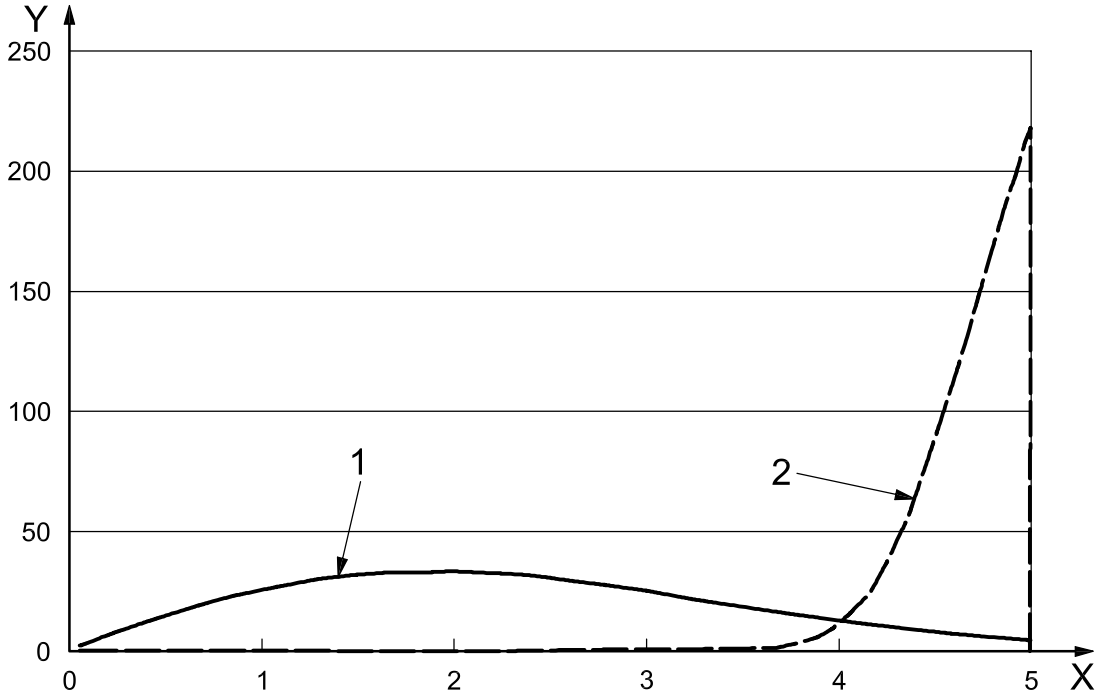

Key

X defect, % of nominal

Y PDF (probability density function)

1 single joint

2 maximum of 50 joints

NOTE $b = 2{,}0$; mean = 2,37 %; standard deviation = 1,24 %.

Figure B.11 — Distribution of defects more evenly dispersed in interval — COV ~50 %

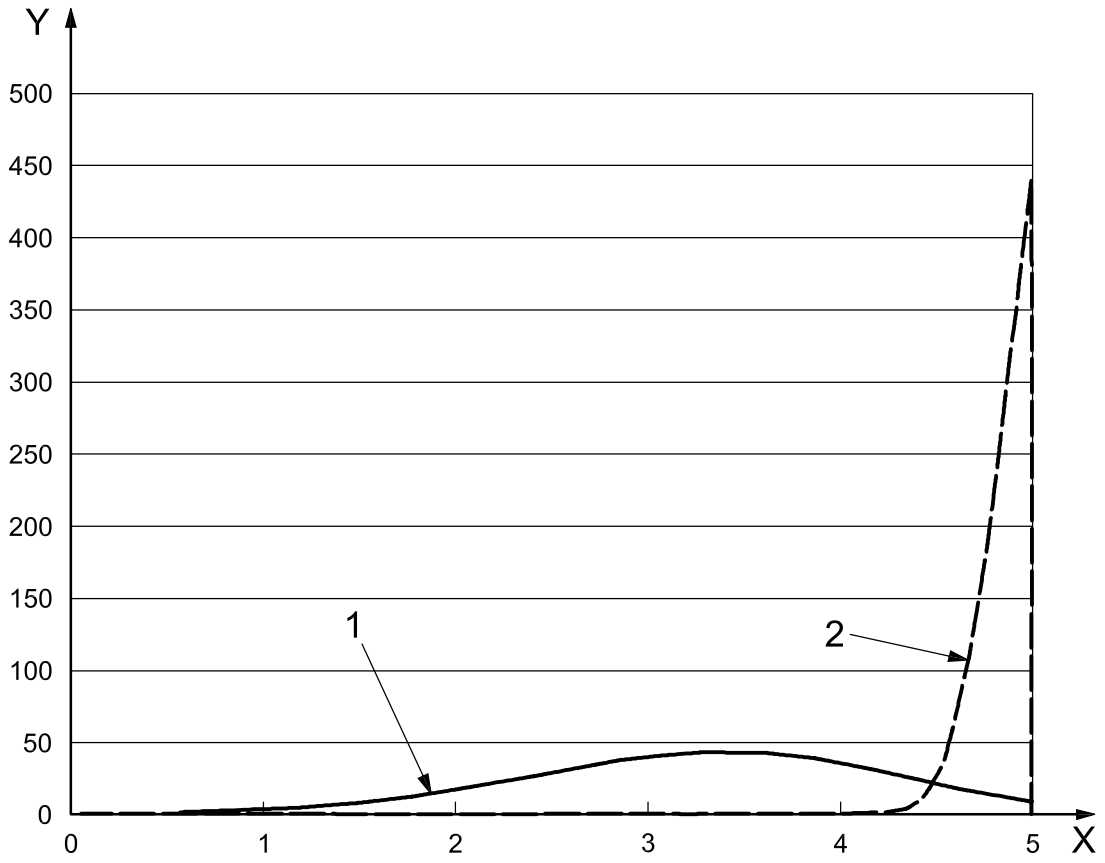

Key

X defect, % of nominal

Y PDF (probability density function)

1 single joint

2 maximum of 50 joints

NOTE $b = 4{,}0$; mean = 3,31 %; standard deviation = 0,93 %.

Figure B.12 — Distribution bias to larger but undetected sizes — COV ~ 30 %

This $\beta = 0{,}5$ distribution is probably a good match for the actual defect distribution, when only defect depth is analysed exclusive of the possibility of stacking. A rough analysis of defect sizes deeper than 5 % of specified wall thickness was made. Here, it was assumed that the probability of exceeding 5 % depth is about 5 % per length of pipe. This analysis finds that the upper tail of defect depths corresponds to a b-parameter value of about 0,55 (see Figure B.13).

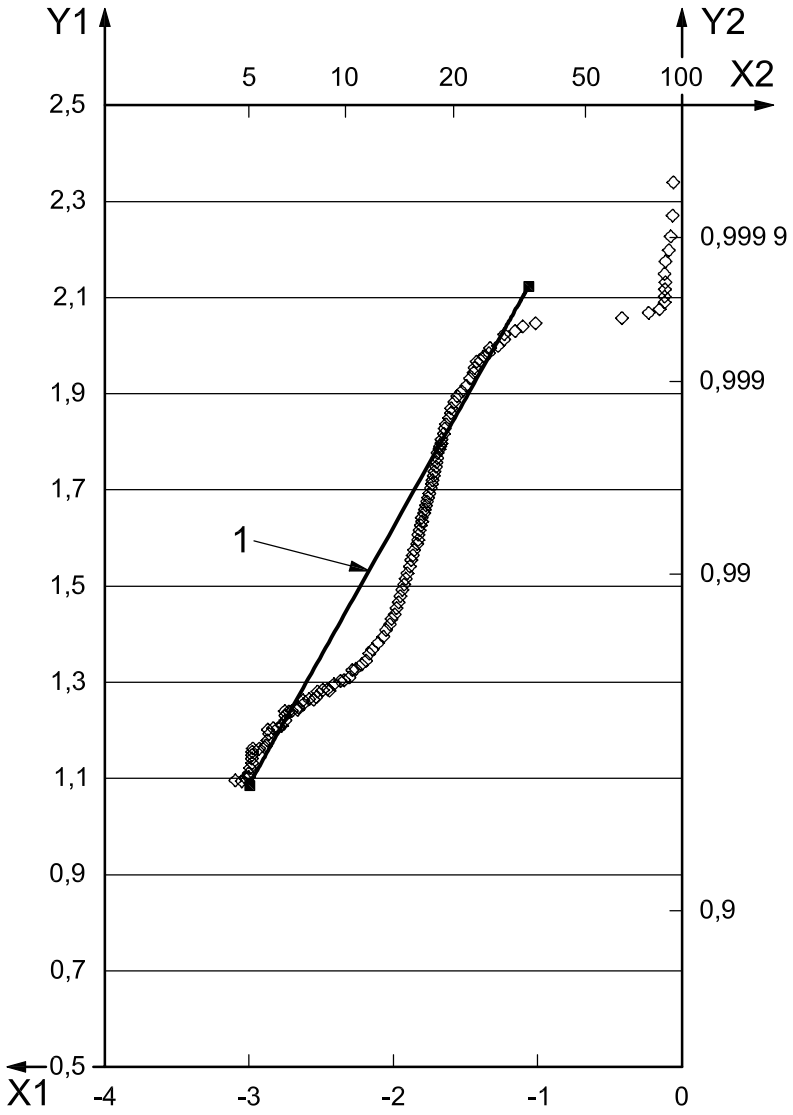

Key

X_1 ln (% of depth)

X_2 % of nominal

Y_1 ln [–ln(1–probability)]

Y_2 CDF (cumulative distribution function)

1 Weibull fit with b-parameter = 0,55

Figure B.13 — Upper tail of seam lap defect depths plotted on a Weibull probability scale

The four charts in Figure B.14 show how the probability distribution for pipe ductile rupture varies based on the different below-the-threshold distribution shapes. These are based on the following assumptions:

— the ratio of the pressure capacity to the applied pressure, p_{cap}/p_{app}, is normal;

— the mean factor of safety is 1,3 and 1,5. The mean factor of safety is the ratio of the mean ductile rupture pressure to the applied pressure. For example, if a simple hoop stress equals tensile strength defines failure, then this factor of safety SF is equal to the mean of the ratio between the pressure capacity and the applied pressure;

— the coefficient of variability of this safety factor is 5 %;

— the normalized strength p_{cap}/p_{app} of an imperfect length is simply $(1 - d_i)' p_{cap}/p_{app}$, where d_i is the imperfection depth as a percent or fraction of specified wall;

— the distribution for defects is a truncated Weibull distribution, where the defect depth is truncated at the threshold depth (5 %). The shape of this distribution is varied using the b-parameter, where $b = 0{,}5$ is most variable but the majority of defects are near 0 % in depth and $b = 4$ indicates a low variability but deeper mean depth.

These charts show that the shape of the distribution below the threshold does not significantly change the distribution of the ratio p_{cap}/p_{app}. The failure probabilities can be read off these charts by noting the probabilities associated with $p_{cap}/p_{app} = 1$. The bar charts in Figures B.15 and B.16 compare the probability of failure for the length with the deepest imperfection in a string of 50 lengths with the probability of failure for a single arbitrary imperfect length.

This case study suggests that the rare large imperfection has more impact on the failure probability than the cumulative effect of frequently occurring “below-the-threshold” small imperfections. This has been used to develop part of the framework for the probabilistic calculation of pipe ductile rupture strength. The rupture probability for a length is a function of the probability distributions for material ultimate strength, wall thickness, and the uncertainty of idealization; but the presence of an imperfection is modelled deterministically. In the probabilistic ductile rupture equation, the depth of the imperfection is set equal to the maximum allowed, i.e. the depth of the inspection threshold. The effect of the imperfection on the probability of failure is accounted for by using the frequency of occurrence for threshold-deep imperfections. In the recommended model, this is set equal to the frequency of occurrence of sharp imperfections as measured during secondary inspection.

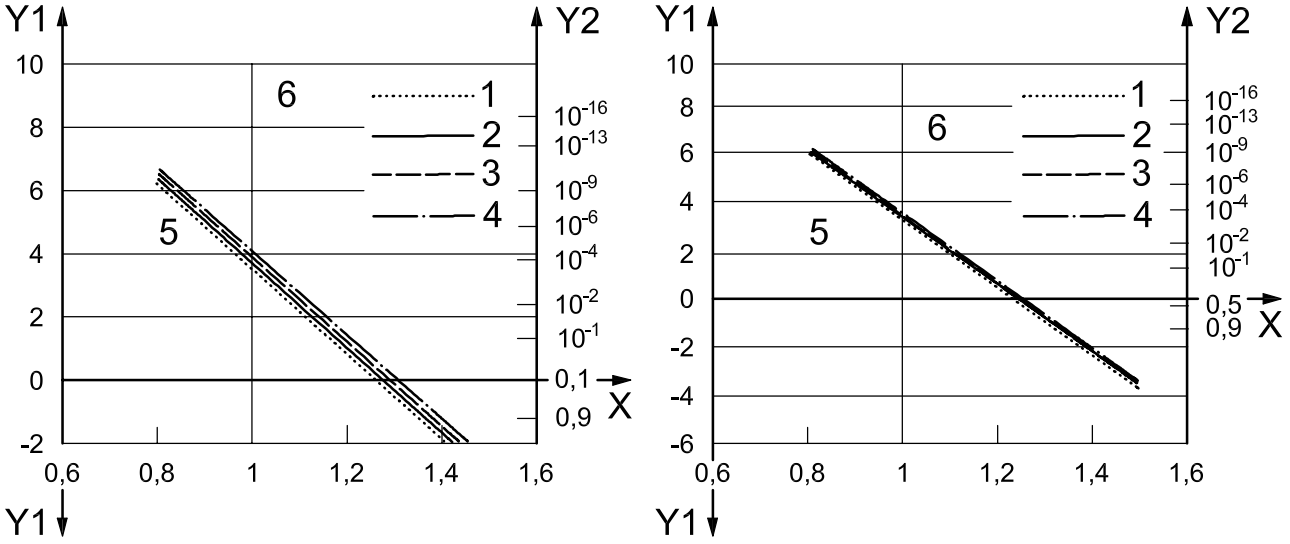

a) Single joint — Mean factor of safety of 1,3

b) Deepest defect in 50 joints — Mean factor of safety of 1,3

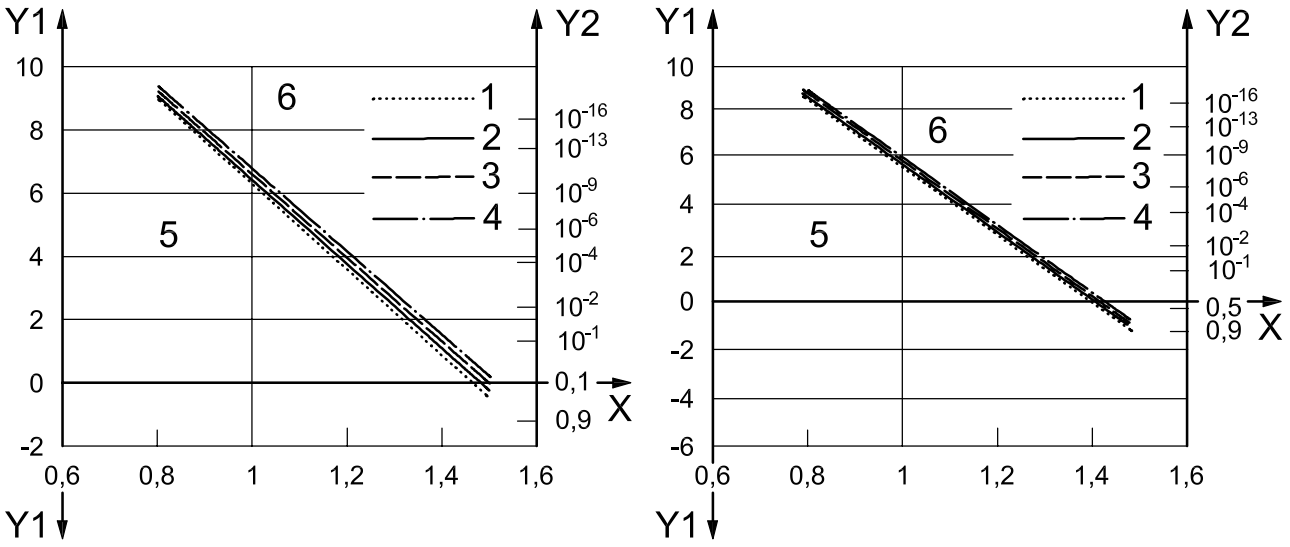

c) Single joint — Mean factor of safety of 1,5

d) Deepest defect in 50 joints — Mean factor of safety of 1,5

Key

X p_{cap}/p_{app}
Y reliability index

1 $b = 4{,}0$
2 $b = 2{,}0$
3 $b = 1{,}0$
4 $b = 0{,}5$
5 fail
6 safe

Figure B.14 — Effect of "below-the-threshold" imperfection distribution on the probability distribution for ductile rupture strength

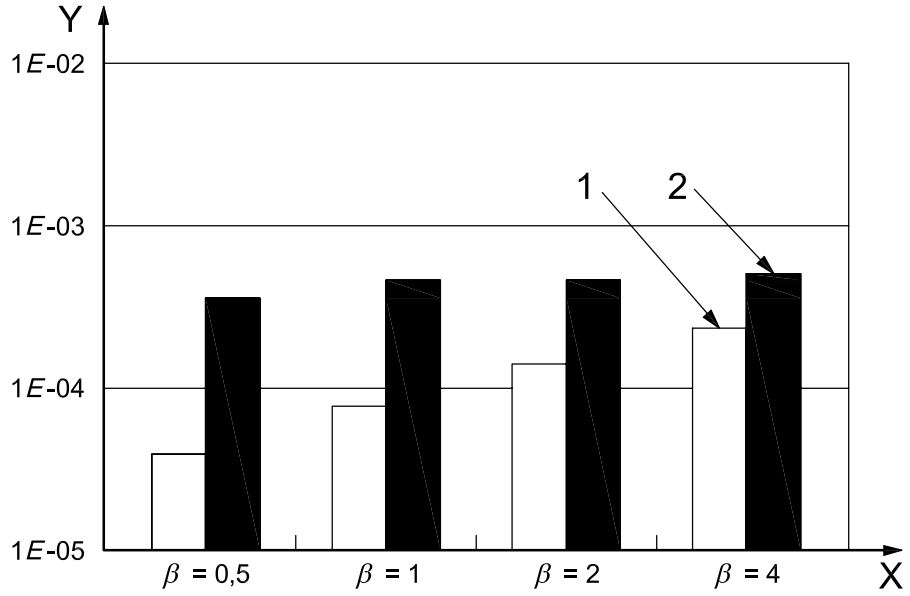

Key

X Weibull shape factor, b

Y probability of failure

1 single joint

2 string of 50 joints

Figure B.15 — Comparison of shape factor effect on the probability of failure of a single length and a string (mean safety factor of 1,3)

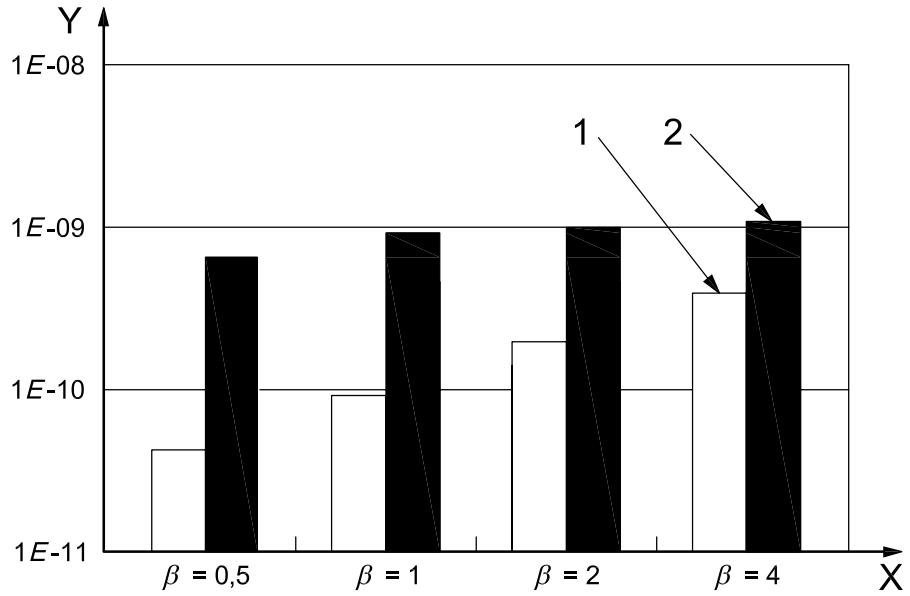

Key

X Weibull shape factor, b

Y probability of failure

1 single joint

2 string of 50 joints

Figure B.16 — Comparison of shape factor effect on the probability of failure of a single length and a string (mean safety factor of 1,5)

Annex C
(informative)

Rupture test procedure

C.1 Specimen ends

Pipe rupture tests should be performed with the pipe ends capped by either welded, slip-in plugs (most common) or threaded end caps (API or premium connections). While other test setups are possible, such as end plugs that are self-restraining via a centre bar, they are rarely used and produce a different stress state and test results. Plug ends that are self-restraining via a centre bar are not acceptable. The capped-end test condition produces an axial stress on the pipe via the internal fluid pressure acting on the end caps. The axial stress is about equal to one-half the average hoop membrane stress and is the load condition that, according to the von Mises theory of yield, produces the maximum possible internal pressure.

C.2 Minimum specimen length

C.2.1 Background

In the mid 1980s, an API workgroup was formed that produced API RP 5C5 for performance testing of tubing and casing connections. One of the workgroup tasks was to establish the required length of specimens. In 1986, the API workgroup addressed information concerning the end effect of a rigid, radial restraint on the end of a cylinder. Analysis from Timoshenko's Theory of Plates & Shells was considered, in addition to results from a simple FEA model. End-effect calculations were made for several pipe sizes and both light and heavy pipe walls. This resulted in a recommendation of a minimum pipe (pup) length of at least $8{,}4(R/t)^{1/2}$, which was later changed to $L_p + D + 6(Dt)^{1/2}$, which is given in Figure 1 of API RP 5C5:1996.

This length provides the following:

— distance of $3(Dt)^{1/2}$ from the specimen end cap required to remove end effects from the end cap;

— distance of D (one pipe diameter) of pipe that is removed from any end effects and behaves as an infinitely long cylinder (full length of pipe);

— distance of $3(Dt)^{1/2}$ from the specimen coupling or connection required to remove end effects from the coupling/connection.

ISO 13679 and API RP 5C5 have also adopted this minimum length for specimen pup length.

C.2.2 Specification of minimum length

In order to follow this rupture test procedure, adopt the minimum length from ISO 13679 or API RP 5C5 as shown in Figure C.1.

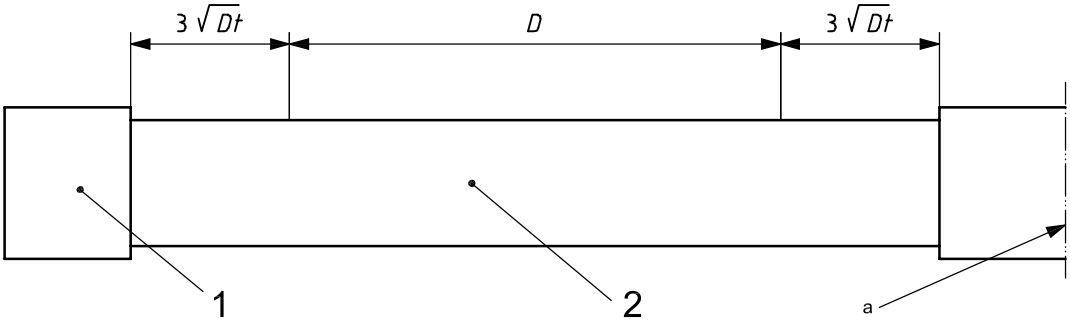

Key

D specified pipe outside diameter

t specified pipe wall thickness

1 end cap

2 pipe (pup)

a Coupling centreline.

Figure C.1 — Illustration of minimum specimen length for a pipe rupture test

C.3 Application of pressure

Pipe rupture tests are to be performed using water and an internal filler bar. The filler bar is used to reduce the volume of water and therefore minimize the stored energy for safety purposes. This also reduces the size of the rupture in the pipe, which has not been of any consequence. In both ISO 13679 and API RP 5C5, the pressure application rate is limited to 34,474 MPa/min (5 000 psi/min). When pressuring to rupture, ductile pipe will begin to yield and, for typical lab-type pumps, the pressure rate becomes much less as the pipe swells. When a pressure above the yield pressure is reached and shut-in (valve closed), the pipe briefly continues to swell and the pressure drops accordingly. For this reason, the pressure should be continuously applied at a low rate of 6,895 MPa/min (1 000 psi/min) or less.

A pressure transducer should be used to measure/record the fluid pressure. A transducer located at the opposite end of the specimen from the pressure line removes spikes in the observed pressure that are related to stroking of the pump. A digital data acquisition system is preferred, with a recording rate of at least every 5 s. This rate will capture the maximum pressure reached, and the final rupture pressure that is typically a few percent less than the maximum pressure obtained.

Annex D
(informative)

Discussion of equations for fracture

D.1 Material-induced fracture of the pipe body

This annex provides equations which may be used to calculate the pressure at which a pipe will fail due to propagation of a pre-existing sharp crack or due to initiation and growth of a new sharp crack. These elastic-plastic equations apply to pipe that is ductile, brittle or anywhere between the two extremes. These equations represent an extension of other established fracture mechanics standards to the full range of oil and gas environments. Use of the equations and their related material test data can require substantial expertise, and it is not always straightforward to generate the needed property data. The equations can be used provided the fracture toughness (K_{Imat}) of the material can be determined experimentally for the particular environment of interest. For some pipes, the wall thickness is too thin to enable a conclusive test to determine K_{Imat}. Currently, there is no proposed framework for the case for which K_{Imat} cannot be measured. It may be possible to determine K_{Imat} from empirically based calculations using other K_{Imat} data.

There are two types of fracture failure phenomena: failure due to unstable propagation of a pre-existing crack, and failure due to initiation and stable growth of a crack where there previously was no detectable crack. The first failure phenomenon (addressed in D.2) occurs due to stress-intensity overloading of the crack tip, and failure is determined as a function of the applied stress, the crack size and the fracture toughness of the material in a particular environment. This failure phenomenon addresses a crack of given size and the conditions under which the crack either propagates or arrests.

The second failure phenomenon (addressed in D.3) is environmental cracking, which occurs due to a combination of stress, material and environment without requiring any pre-existing imperfection. This failure phenomenon addresses conditions which produce stable growth of a crack which may not have initially existed. Once created, the crack grows in a stable way until it becomes large enough to satisfy the fracture mechanics condition for unstable propagation to failure. Environmental cracking can occur independently of fracture propagation, so both the equations in D.2 and the threshold stress criterion in D.3 need to be satisfied to prevent failure through fracture. This means that there are two limit states that need to be satisfied to prevent fracture, and both limit states depend on the stress and the material fracture toughness in its environment.

D.2 The crack propagation model

D.2.1 General

The approach to fracture here is similar to that used in determining performance of pressure vessels, and is extensively utilized to predict the fitness-for-service of these structures. Integrity of cracked structures has been successfully safeguarded using fracture mechanics standards such as the British PD 6493, now revised and re-issued as BS 7910, and API RP 579.

A pipe performance calculation based on tensile strength, yield strength and other material and dimensional properties does not address failure due to propagation of crack-like imperfections where failure is determined by the stress intensity around the crack. When the applied stress intensity factor, K, reaches a critical value referred to as K_{Imat}, the crack propagates and pipe rupture is imminent. The value of K_{Imat} is a function of both the environment and the material. The units of K_{Imat} are MPa-m$^{1/2}$ (ksi-in$^{1/2}$).

Under H_2S environments, the value of K_{Imat} will be smaller than in non-H_2S environments, and the fracture mode can control the failure pressure of the pipe. The value of K_{Imat} changes based on environmental exposure (H_2S, temperature, pH, etc.). Once this value is determined in laboratory testing for a specific material in a unique environment, it can be used to evaluate the integrity of a pipe with imperfections for that environment. K_{Imat} can be considered to be the amount of fracture toughness necessary to prevent or stop further crack propagation in the environment. In order to preserve the integrity of the pipe, K_{Imat} needs to be sufficiently high to prevent the propagation of a crack in the service environment.

A failure assessment diagram (FAD) can be utilized to assess the integrity of the pipe over the whole range of brittle and ductile fractures. The FAD is a plot of the stress intensity ratio (K_r or J_r) on the ordinate versus the load ratio (L_r) on the abscissa, where K_r is the ratio of applied K to K_{mat}, and L_r is a ratio of applied load to limit load. The limit load in this case commonly represents an approximation of the load where the cracked pipe yields without crack growth. For further understanding of FAD concepts, see the fracture mechanics standards in Reference [13]. The FAD corresponding to the fracture propagation Equations (D.1) and (D.3) covers both the elastic and combined elastic-plastic behaviours of the material. For materials which are ductile in a particular environment, the value of K_{Imat} will be high and the fracture pressure will correspond to the elastic-plastic part of the FAD curve. For materials which are brittle in a particular environment, the value of K_{Imat} will be low and the fracture pressure will correspond to the elastic part of the FAD curve.

A variety of fracture mechanics test samples have been used to develop K_{Imat} data. The double cantilever beam (DCB) specimen has been extensively utilized to develop K_{Imat} data (also known as K_{Imat} for the SSC mechanism) for oil field materials. This specimen is described in ANSI-NACE TM0177-96 as Method D. The DCB is notched or pre-cracked and then the arms of the DCB are held open at a constant displacement by loading with a wedge. The DCB is loaded such that the applied K level is above the K_{Imat} for the material. The loaded specimen is exposed to the test environment (e.g. H_2S aqueous). With initiation, the crack grows and the load drops (displacement is approximately constant) and the applied K drops until it reaches K_{Imat}, halting crack propagation. After an appropriate period when the crack growth stops, the measured force to remove the wedge from the DCB specimen and the measured crack length are used to calculate the applied K at the end of the test. At this point, K_{Imat} is equal to the applied K.

A “fit-for-purpose” (FFP) assessment of pipe performance can be made by using K_{Imat} corresponding to a specific environment of interest. The evaluation of fracture pressure of casing and tubing in a specific environment requires the measurement of K_{Imat} in that environment and comparison to the maximum applied K within the component. The applied K depends on the pipe geometry, the imperfection geometry and the applied load. Within any one chemistry, increasing the yield strength generally results in a lower value of K_{Imat}. However, K_{Imat} can increase or decrease with increasing yield strength due to changes of chemistry and heat treatment and manufacturing process. Temperature, pH and concentration of sulfide ions all affect the environmental fracture toughness. As temperature and pH increase, the environmental fracture toughness of the material also increases. Microstructure also can cause variation in the environmental fracture toughness. Materials with higher transformation products, such as bainite and pearlite, have lower environmental fracture toughness when compared to martensitic materials. Increasing the partial pressure of H_2S decreases the environmental fracture toughness. Partial pressure of H_2S is calculated by multiplying the absolute pressure by the mole fraction of H_2S in the gas.

D.2.2 Assumptions and limitations

The following are assumptions relative to the FAD approach:

— only Mode I failure is considered. This is crack propagation perpendicular to the applied load, i.e. a deepening of the crack, as opposed to Mode II, sliding, and Mode III, tearing;

— elastic-plastic fracture mechanics starting from the “J-Integral” is used as the general basis for the FAD curve. The applied K is the linear elastic solution for a crack in the pipe wall. The intersection of K_r and the FAD curve determines the fracture pressure. The depth of the crack-like imperfection should be set equal to the depth of the inspection gate setting;

— the pipe is infinitely long, with an infinitely long longitudinal crack-like imperfection;

— the longitudinal crack is on the inner surface of the pipe. A longitudinal crack on the inner surface of the pipe is slightly more conservative than an identical crack on the outer surface of the pipe;

— pressure acts on the faces of the crack;

— the ductile rupture limit state with influence of axial load (p_{iRa}, see 7.5) represents the ultimate ductile failure mode.

D.2.3 Fracture limit state equation

The fracture limit pressure of a tube is defined by Equation (D.1), and it cannot be explicitly solved for p_{iF}, the internal pressure at which fracture will occur, but must be solved in an iterative manner by numerical coding or graphically. Equation (D.1) is based on fracture mechanics, and is an equation for failure due to propagation of a pre-existing crack. Equation (D.1) is not an equation for environmentally induced failure of a material which does not have a large crack.

$$(1 - 0{,}14L_r^2)\,(0{,}3 + 0{,}7\exp[-0{,}65L_r^6]) = [p_{iF}\,(D/2)^2\,(\pi a)^{1/2}]/[((D/2)^2 - (D/2 - t)^2)\,K_{Imat}] \times \{2G_0 - 2G_1[a/(D/2 - t)] + 3G_2[a/(D/2 - t)]^2 - 4G_3[a/(D/2 - t)]^3 + 5G_4[a/(D/2 - t)]^4\} \quad \text{(D.1)}$$

or $p_{iF} = p_{iRa}$, if p_{iRa} is less than the solution from Equation (D.1)

where

$$L_r = \sqrt{3}/2\,(p_{iF}/f_y)\,[(d/2 + a)/(t - a)] \quad \text{(D.2)}$$

and

a is, for a limit state equation, the maximum actual depth of a crack-like imperfection; for a design equation, the maximum depth of a crack-like imperfection that could likely pass the manufacturer's inspection system;

d is the pipe inside diameter; $d = D - 2t$;

D is the specified pipe outside diameter;

f_y is the yield strength of a representative tensile specimen;

K_{Imat} is the fracture toughness of the material in a particular environment;

L_r is the load ratio;

p_{iF} is the internal pressure at fracture;

p_{iR} is the internal pressure at ductile rupture of an end-capped pipe;

p_{iRa} is p_{iR} adjusted for axial load and external pressure;

t is the specified pipe wall thickness.

The left side of Equation (D.1) is the FAD curve. The right side of Equation (D.1) is the stress intensity ratio K_r.

Table D.1 of G-influence coefficients used in the equation is for a longitudinal crack located on the inside of the pipe. This is slightly more conservative than a crack on the outside of the pipe.

Table C.9 in API RP 579, January 2000, is the source for the G-influence coefficients shown in Table D.1 and allows interpolation for intermediate values of d/t or d_{wall}/t and a/t.

Table D.1 — Values of G_0 to G_4 for FAD curve

d/t or d_{wall}/t	a/t	G_0	G_1	G_2	G_3	G_4
4	0,0	1,120 000	0,682 000	0,524 500	0,440 400	0,379 075
4	0,2	1,242 640	0,729 765	0,551 698	0,458 464	0,392 759
4	0,4	1,564 166	0,853 231	0,620 581	0,503 412	0,427 226
10	0,0	1,120 000	0,682 000	0,524 500	0,440 400	0,379 075
10	0,2	1,307 452	0,753 466	0,564 298	0,466 913	0,398 757
10	0,4	1,833 200	0,954 938	0,676 408	0,539 874	0,454 785
20	0,0	1,120 000	0,682 000	0,524 500	0,440 400	0,379 075
20	0,2	1,332 691	0,763 153	0,569 758	0,470 495	0,401 459
20	0,4	1,957 764	1,002 123	0,702 473	0,556 857	0,467 621
40	0,0	1,120 000	0,682 000	0,524 500	0,440 400	0,379 075
40	0,2	1,345 621	0,768 292	0,572 560	0,472 331	0,402 984
40	0,4	2,028 188	1,028 989	0,717 256	0,566 433	0,475 028
80	0,0	1,120 000	0,682 000	0,524 500	0,440 400	0,379 075
80	0,2	1,351 845	0,770 679	0,573 795	0,473 108	0,403 649
80	0,4	2,064 088	1,042 414	0,724 534	0,571 046	0,478 588
NOTE The parameters G_0 to G_4 are obtained exactly following the methodology in API RP 579.						

D.2.4 Design equation for fracture of the pipe body due to the presence of crack-like imperfections

The fracture design equation is:

$$(1 - 0{,}14L_r^2)\,(0{,}3 + 0{,}7\exp[-0{,}65L_r^6]) = [p_{iF}\,(D/2)^2\,(\pi a)^{1/2}]/[((D/2)^2 - (D/2 - k_{wall}t)^2)\,K_{Imat}] \times \{2G_0 - 2G_1[a/(D/2 - k_{wall}t)] + 3G_2[a/(D/2 - k_{wall}t)]^2 - 4G_3[a/(D/2 - k_{wall}t)]^3 + 5G_4[a/(D/2 - k_{wall}t)]^4\} \quad \text{(D.3)}$$

or $p_{iF} = p_{iRa}$, if p_{iRa} is less than the solution from Equation (D.3)

where

$$L_r = \sqrt{3}/2\,(p_{iF}/f_{ymn})\,[(d_{wall}/2 + a)/(k_{wall}t - a)] \quad \text{(D.4)}$$

and

a is, for a limit state equation, the maximum actual depth of a crack-like imperfection; for a design equation, the maximum depth of a crack-like imperfection that could likely pass the manufacturer's inspection system;

d_{wall} is the inside diameter based on $k_{wall}\,t$; $d_{wall} = D - 2k_{wall}\,t$;

D is the specified pipe outside diameter;

f_{ymn} is the specified minimum yield strength;

K_{Imat} is the fracture toughness of the material in a particular environment;

k_{wall} is the factor to account for the specified manufacturing tolerance of the pipe wall. For example, for a tolerance of −12,5 %, k_{wall} = 0,875;

L_r is the load ratio;

p_{iF} is the internal pressure at fracture;

p_{iR} is the internal pressure at ductile rupture of an end-capped pipe;

p_{iRa} is p_{iR} adjusted for axial load and external pressure;

t is the specified pipe wall thickness.

In Equation (D.3) the G-influence coefficients are the same as listed in Table D.1. For calculation of the fracture design pressure, d_{wall} in Table D.1 is the specified inner diameter of the pipe.

The left side of Equation (D.3) is the FAD curve. The right side of Equation (D.3) is the stress intensity ratio K_r. Equation D.3 is an equation for failure due to propagation of a pre-existing crack. Equation (D.3) is not an equation for environmentally induced failure of a material which does not have a large crack.

Figure D.1 shows an example of the predicted fracture pressure based on Equations (D.3) and (D.4) for a 7.0 in diameter, 0.730 in wall, C90 casing as a function of the fracture toughness K_{Imat}, assuming 5 % imperfection (inspection gate) combined with k_{wall} = 0.875.

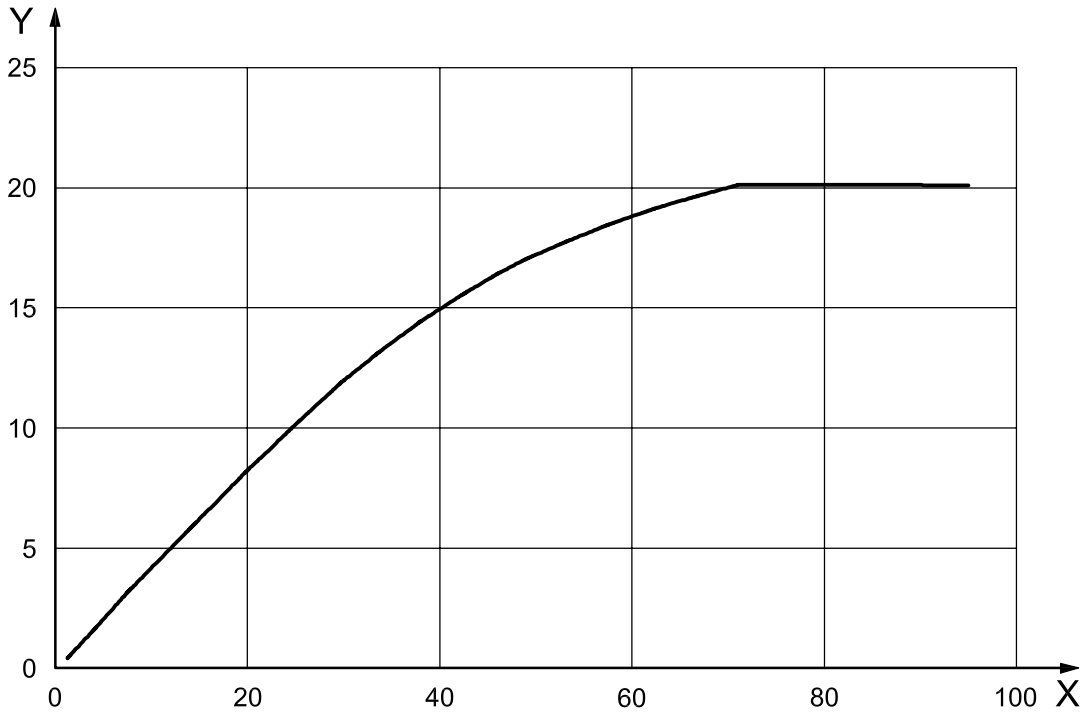

Key

X K_{Imat}, ksi·in^{0,5}

Y predicted fracture pressure, ksi

Figure D.1 — Influence of K_{Imat} on fracture propagation pressure (7 in diameter, 0.730 in wall, C90 with 5 % imperfection, 0.875 wall factor)

D.3 Fracture due to environmental crack initiation

D.3.1 General

For a material in a particular environment, environmental crack initiation can occur and result in fracture (failure) when there was no pre-existing crack in the material. This is due to a combination of crack initiation and stable environmental crack growth to failure. For this reason, both the fracture propagation equations in D.2 and the environmental crack initiation criterion in D.3 need to be satisfied to prevent failure through fracture. Environmental crack initiation is said to occur when the von Mises equivalent stress exceeds what is called the threshold stress (σ_{th}) of the material. The fracture pressure for environmental crack initiation is the pressure which causes the von Mises equivalent stress to equal the threshold stress, i.e.:

$$\sigma_e = \sigma_{th} \tag{D.5}$$

where

σ_e is the equivalent stress;

σ_{th} is the threshold stress.

The threshold stress can vary with the particular material and environment. See ANSI-NACE TM0177-96 for an explanation of threshold stress. The threshold stress usually is determined by a series of NACE Method-A tensile tests in a specific environment. Above the threshold stress, the tensile specimen fails during the NACE Method-A tensile test; below the threshold stress, the tensile specimen passes the NACE Method-A tensile test. In an H_2S environment, the threshold stress usually is less than the yield strength of the material.

Environmental crack initiation can typically start at the bottom of a corrosion pit, and depends on the combination of the environment (CO_2, pH, H_2S), temperature, material microstructure and mechanical stress. Below a “threshold” combination of these factors, crack initiation does not occur and beyond the threshold, stress crack initiation does occur. For most applications, the mechanical loads on the pipe are constant and the crack, once initiated, will grow to failure. The situation thus deteriorates until the crack reaches the size where unstable crack propagation leads to final fracture. The time between crack initiation and unstable fracture is uncertain, and therefore it is prudent to avoid crack initiation altogether by keeping the von Mises equivalent stress sufficiently low compared with the threshold stress.

The fracture initiation limit pressure is the pressure for which the von Mises equivalent stress equals the threshold stress [Equation (D.5)], where the von Mises equivalent stress is calculated using measured pipe dimensions. The fracture initiation design pressure is the pressure for which the von Mises equivalent stress equals the threshold stress, where the von Mises equivalent stress is calculated using specified pipe dimensions and the pipe wall thickness tolerance factor k_{wall}. A margin between applied (service) equivalent stress and the apparent threshold stress should be maintained to account for scatter on the estimation of the threshold stress.

Just as with the yield equation, the von Mises equivalent stress is used to combine the individual, three-dimensional stresses into a single parameter to compare with the threshold stress. The equivalent stress is used because, based on data in Reference [13], it appears to provide the most accurate combination of stresses which brings about crack initiation failure of pipe in an H_2S environment. Equation (D.5) is applicable only when the internal pressure exceeds the external pressure. Test data in axial compression suggest that the equation can cease to apply, i.e. that crack initiation failure might not occur, when the mean hydrostatic stress becomes compressive. That is, in the absence of torsion, the equation can cease to apply when the sum of the axial stress, radial stress and hoop stress added together becomes negative.

D.3.2 Example calculation

Calculate the design crack initiation failure pressure for a 244,48 mm (9-5/8 in), 13,84 mm (0.545 in) wall thickness, C90 grade [f_{ymn} = 621 MPa (90 000 psi)] casing subjected to internal pressure with capped end conditions, if the threshold stress is 90 % of the yield strength of the pipe material and the k_{wall} = 0,875.

First the von Mises equivalent stress is set equal to the threshold stress, which is 90 % of the yield stress [Equation (D.5)]. For the loading combination where the pipe has capped-end conditions and there are no torsional and bending stresses, then Equation (D.5) reduces to the following, similar in form to the equation for p_{iYLc}, Equation (8) of 6.6.1.1:

$$p_{iF} = 0{,}9\, f_{ymn}/\{(3\, D^4 + d_{wall}{}^4)/(D^2 - d_{wall}{}^2)^2 + d^4/(D^2 - d^2)^2 - 2d^2 d_{wall}{}^2/[(D^2 - d^2)\,(D^2 - d_{wall}{}^2)]\}^{1/2} \qquad \text{(D.6)}$$

where

D is the specified pipe outside diameter;

d is the pipe inside diameter; $d = D - 2t$;

d_{wall} is the inside diameter based on $k_{wall}\, t$; $d_{wall} = D - 2k_{wall}\, t$;

f_{ymn} is the specified minimum yield strength;

k_{wall} is the factor to account for the specified manufacturing tolerance of the pipe wall. For example, for a tolerance of −12,5 %, k_{wall} = 0,875;

p_{iYLc} is the internal pressure at yield for a capped-end thick tube;

t is the specified pipe wall thickness.

Then the crack initiation fracture pressure for the example pipe is 60,6 MPa (8 788 psi).

Annex E
(informative)

Discussion of historical API collapse equations

E.1 Collapse pressure equations

E.1.1 General

The minimum collapse pressures given in Annex K are calculated by means of Equations (E.1), (E.3), (E.5) and (E.7), adopted at the 1968 API Standardization Conference and reported in API Circular PS-1360 dated September 1968.

Equations (E.2), (E.4) and (E.6) for the intersections between the four collapse pressure equations have been determined algebraically, and used for calculating the applicable D/t range for each collapse pressure equation. Factors A_c, B_c, C_c, F_c and G_c have been calculated using Equations (E.21), (E.22), (E.23), (E.26) and (E.27). When determining the appropriate equation to be used for calculating collapse resistance for a particular D/t ratio and minimum yield strength, the D/t ranges determined by Equations (E.2), (E.4) and (E.6) govern, rather than the collapse equation that gives the lowest collapse pressure. The D/t ranges are given in Tables E.1, E.2, E.3 and E.4.

Theoretical studies of the effect of ovality on tubular collapse resistance consistently indicate that an ovality of 1 % to 2 % can effect a reduction in collapse resistance on the order of 25 %. However, experimental/empirical investigations indicate a much smaller effect. Test data indicate that ovality is only one of many pipe parameters that influence collapse (including residual stress, isotropy, shape of stress-strain curve/microstructure, and yield strength). Thorough review of industry collapse data indicates that the influence of ovality does not warrant singling out the ovality as a dominant parameter. A workgroup on collapse resistance concluded the effect of ovality on tubular collapse has been handled during the adjustment of average collapse predictions to minimum performance values and that ovality should not be awarded the status of an independent variable in an API equation for collapse performance.

The collapse equations presented here were originally developed in USC units, and should only be used in these units.

E.1.2 Yield strength collapse pressure equation

The yield strength collapse pressure is not a true collapse pressure, but rather the external pressure, p_{Yp}, that generates minimum yield stress, f_{ymn}, on the inside wall of a tube as calculated by Equation (E.1).

$$p_{Yp} = 2 f_{ymn} [(D/t) - 1]/[(D/t)^2] \quad \text{(E.1)}$$

where

D is the specified pipe outside diameter;

f_{ymn} is the specified minimum yield strength;

t is the specified pipe wall thickness.

Equation (E.1) for yield strength collapse pressure is applicable for D/t values up to the value of D/t corresponding to the intersection with the plastic collapse [Equation (E.3)]. This intersection, $(D/t)_{yp}$, is calculated by Equation (E.2) as follows:

$$(D/t)_{yp} = \{[(A_c - 2)^2 + 8(B_c + C_c/f_{ymn})]^{1/2} + (A_c - 2)\}/[2(B_c + C_c/f_{ymn})] \quad \text{(E.2)}$$

where

A_c is the empirical constant in historical API collapse equation;

B_c is the empirical constant in historical API collapse equation;

C_c is the empirical constant in historical API collapse equation;

f_{ymn} is the specified minimum yield strength.

The parameters used to calculate collapse pressures depend on the pipe yield strength and on the axial load, as explained in later subclauses.

The applicable D/t ratios for yield strength collapse are shown in Table E.1.

Table E.1 — Yield collapse pressure equation range

Grade [a]	D/t **range** [b]
H40	16,40 and less
–50	15,24 and less
J55, K55	14,81 and less
–60	14,44 and less
–70	13,85 and less
C75, E75	13,60 and less
L-N-80	13,38 and less
C90	13,01 and less
C95, T95, X95	12,85 and less
–100	12,70 and less
P105, G105	12,57 and less
P110	12,44 and less
–120	12,21 and less
Q125	12,11 and less
–130	12,02 and less
S135	11,92 and less
–140	11,84 and less
–150	11,67 and less
–155	11,59 and less
–160	11,52 and less
–170	11,37 and less
–180	11,23 and less

[a] Grades indicated without letter designation are not API grades but are grades in use or grades being considered for use and are shown for information purposes.

[b] The D/t range values were calculated from Equations (E.2), (E.21), (E.22) and (E.23).

E.1.3 Plastic collapse pressure equation

The minimum collapse pressure for the plastic range of collapse, p_P, is calculated by Equation (E.3):

$$p_P = f_{ymn}\,[A_c/(D/t) - B_c] - C_c \qquad \text{(E.3)}$$

where

A_c is the empirical constant in historical API collapse equation;

B_c is the empirical constant in historical API collapse equation;

C_c is the empirical constant in historical API collapse equation;

D is the specified pipe outside diameter;

f_{ymn} is the specified minimum yield strength;

t is the specified pipe wall thickness.

The equation for minimum plastic collapse pressure is applicable for D/t values ranging from $(D/t)_{yp}$, Equation (E.2) for yield strength collapse pressure, to the intersection with Equation (E.5) for transition collapse pressure $(D/t)_{pt}$. Values for $(D/t)_{pt}$ are calculated by means of Equation (E.4):

$$(D/t)_{pt} = [f_{ymn}\,(A_c - F_c)]/[C_c + f_{ymn}\,(B_c - G_c)] \qquad \text{(E.4)}$$

where

A_c is the empirical constant in historical API collapse equation;

B_c is the empirical constant in historical API collapse equation;

C_c is the empirical constant in historical API collapse equation;

F_c is the empirical constant in historical API collapse equation;

f_{ymn} is the specified minimum yield strength;

G_c is the empirical constant in historical API collapse equation.

The factors and applicable D/t ranges for the plastic collapse equation are shown in Table E.2.

Table E.2 — Equation factors and D/t range for plastic collapse

Grade [a]	A_c	B_c	C_c **MPa** (psi)	D/t **range** [b]
H40	2,950	0,046 5	5,20 (754)	16,40 to 27,01
–50	2,976	0,051 5	7,281 (1 056)	15,24 to 25,63
J55, K55	2,991	0,054 1	8,315 (1 206)	14,81 to 25,01
–60	3,005	0,056 6	9,349 (1 356)	14,44 to 24,42
–70	3,037	0,061 7	11,42 (1 656)	13,85 to 23,38
C75, E75	3,054	0,064 2	12,45 (1 806)	13,60 to 22,91
L-N-80	3,071	0,066 7	13,48 (1 955)	13,38 to 22,47
C90	3,106	0,071 8	15,54 (2 254)	13,01 to 21,69
C95, T95, X95	3,124	0,074 3	16,57 (2 404)	12,85 to 21,33
–100	3,143	0,076 8	17,60 (2 553)	12,70 to 21,00
P105, G105	3,162	0,079 4	18,63 (2 702)	12,57 to 20,70
P110	3,181	0,081 9	19,66 (2 852)	12,44 to 20,41
–120	3,219	0,087 0	21,73 (3 151)	12,21 to 19,88
Q125	3,239	0,089 5	22,76 (3 301)	12,11 to 19,63
–130	3,258	0,092 0	23,79 (3 451)	12,02 to 19,40
S135	3,278	0,094 6	24,83 (3 601)	11,92 to 19,18
–140	3,297	0,097 1	25,86 (3 751)	11,84 to 18,97
–150	3,336	0,102 1	27,94 (4 053)	11,67 to 18,57
–155	3,356	0,104 7	28,99 (4 204)	11,59 to 18,37
–160	3,375	0,107 2	30,03 (4 356)	11,52 to 18,19
–170	3,412	0,112 3	32,13 (4 660)	11,37 to 17,82
–180	3,449	0,117 3	34,24 (4 966)	11,21 to 17,47

[a] Grades indicated without letter designation are not API grades but are grades in use or grades being considered for use and are shown for information purposes.

[b] The D/t range values and equation factors were calculated from Equations (E.2), (E.4), (E.21), (E.22), (E.23), (E.26) and (E.27).

E.1.4 Transition collapse pressure equation

The minimum collapse pressure for the plastic to elastic transition zone, p_T, is calculated by Equation (E.5):

$$p_T = f_{ymn} [F_c/(D/t) - G_c] \quad \text{(E.5)}$$

where

D is the specified pipe outside diameter;

F_c is the empirical constant in historical API collapse equation;

f_{ymn} is the specified minimum yield strength;

G_c is the empirical constant in historical API collapse equation;

p_T is the pressure for transition collapse;

t is the specified pipe wall thickness.

The equation for p_T is applicable for D/t values from $(D/t)_{pt}$, Equation (E.4) for plastic collapse pressure, to the intersection $(D/t)_{te}$ with Equation (E.7) for elastic collapse. Values for $(D/t)_{te}$ are calculated by Equation (E.6):

$$(D/t)_{te} = [2 + B_c/A_c]/[3(B_c/A_c)] \quad \text{(E.6)}$$

where

A_c is the empirical constant in historical API collapse equation;

B_c is the empirical constant in historical API collapse equation.

The factors and applicable D/t ranges for the transition collapse pressure equation are shown in Table E.3.

Table E.3 — Equation factors and D/t range for transition collapse

Grade [a]	F_C	G_C	D/t range [b]
H40	2,063	0,032 5	27,01 to 42,64
–50	2,003	0,034 7	25,63 to 38,83
J55, K55	1,989	0,036 0	25,01 to 37,21
–60	1,983	0,037 3	24,42 to 35,73
–70	1,984	0,040 3	23,38 to 33,17
C75, E75	1,990	0,041 8	22,91 to 32,05
L-N-80	1,998	0,043 4	22,47 to 31,02
C90	2,017	0,046 6	21,69 to 29,18
C95, T95, X95	2,029	0,048 2	21,33 to 28,36
–100	2,040	0,049 9	21,00 to 27,60
P105, G105	2,053	0,051 5	20,70 to 26,89
P110	2,066	0,053 2	20,41 to 26,22
–120	2,092	0,056 5	19,88 to 25,01
Q125	2,106	0,058 2	19,63 to 24,46
–130	2,119	0,059 9	19,40 to 23,94
S135	2,133	0,061 5	19,18 to 23,44
–140	2,146	0,063 2	18,97 to 22,98
–150	2,174	0,066 6	18,57 to 22,11
–155	2,188	0,068 3	18,37 to 21,70
–160	2,202	0,070 0	18,19 to 21,32
–170	2,231	0,073 4	17,82 to 20,60
–180	2,261	0,076 9	17,47 to 19,93

[a] Grades indicated without letter designation are not API grades but are grades in use or grades being considered for use and are shown for information purposes.

[b] The D/t range values and equation factors were calculated from Equations (E.2), (E.4), (E.21), (E.22), (E.23), (E.26) and (E.27).

E.1.5 Elastic collapse pressure equation

The minimum collapse pressure for the elastic range of collapse, p_E, is calculated by Equation (E.7):

$$p_E = 46{,}95 \times 10^6/[(D/t)\,(D/t - 1)^2] \tag{E.7}$$

where

D is the specified pipe outside diameter;

t is the specified pipe wall thickness.

The applicable D/t range for elastic collapse is shown in Table E.4.

Table E.4 — D/t range for elastic collapse

Grade [a]	D/t range [b]
H40	42,64 and greater
–50	38,83 and greater
J55, K55	37,21 and greater
–60	35,73 and greater
–70	33,17 and greater
C75, E75	32,05 and greater
L-N-80	31,02 and greater
C90	29,18 and greater
C95, T95, X95	28,36 and greater
–100	27,60 and greater
P105, G105	26,89 and greater
P110	26,22 and greater
–120	25,01 and greater
Q125	24,46 and greater
–130	23,94 and greater
S135	23,44 and greater
–140	22,98 and greater
–150	22,11 and greater
–155	21,70 and greater
–160	21,32 and greater
–170	20,60 and greater
–180	19,93 and greater

[a] Grades indicated without letter designation are not API grades but are grades in use or grades being considered for use and are shown for information purposes.

[b] The D/t range values were calculated from Equations (E.6), (E.21) and (E.22).

E.1.6 Collapse pressure under axial tension stress

The collapse resistance of casing in the presence of an axial stress is calculated by modifying the yield stress to an axial stress equivalent grade according to Equation (E.8):

$$f_{yax} = \{[1–0.75(\sigma_a/f_{ymn})^2]^{1/2} – 0.5\ \sigma_a/f_{ymn}\}\, f_{ymn} \quad \text{(E.8)}$$

where

f_{yax} is the equivalent yield strength in the presence of axial stress;

f_{ymn} is the specified minimum yield strength;

σ_a is the component of axial stress not due to bending.

Collapse resistance equation factors and D/t ranges for the axial stress equivalent grade are then calculated by means of Equations (E.2), (E.4), (E.6), (E.21), (E.22), (E.23), (E.26) and (E.27). Using equation factors for the axial stress equivalent grade, collapse resistance under axial stress is calculated by means of Equations (E.1), (E.3), (E.5) and (E.7).

API collapse resistance equations are not valid for the yield strength of axial stress equivalent grade (f_{yax}) less than 24 000 psi.

Equation (E.8) is based on the Hencky-von Mises maximum strain energy of distortion theory of yielding.

E.1.7 Effect of internal pressure on collapse

The external pressure equivalent of external pressure and internal pressure is determined by means of Equation (E.9), where p_{ci} is the collapse pressure in the presence of internal pressure.

The equation is based on the internal pressure acting on the inside diameter and the external pressure acting on the outside diameter.

$$p_{ci} = p_c + (1 - 2\,t/D)\,p_i \tag{E.9}$$

where

D is the specified pipe outside diameter;

p_c is the collapse pressure;

p_i is the internal pressure;

t is the specified pipe wall thickness.

The value p_c is the collapse resistance calculated neglecting internal pressure, but accounting for any axial load as described in E.1.6. Equation (E.9) was taken from Reference [56].

E.2 Derivation of collapse pressure equations

E.2.1 General

Of the four equations used for collapse pressure, those for yield strength collapse and elastic collapse were derived on a theoretical basis, the plastic equation was derived empirically from 2 488 collapse tests for grades K55, N80 and P110, while the plastic/elastic transition collapse pressure equation was determined on an arbitrary basis. The plastic and transition collapse equations and the modification of the elastic collapse equation constant were developed by G. Hebard [117].

E.2.2 Yield strength collapse pressure equation derivation

For heavy wall pipe, the use of plastic collapse Equation (E.3) or p_P could result in compression stresses equalling or exceeding the yield strength. While there was experimental evidence that the collapse pressure could exceed the external pressure causing yielding, it was thought unsafe to use a collapse pressure value causing yielding. Therefore, the yield strength collapse is based on the pressure that generates minimum yield stress on the inside wall of the tube, calculated by means of the Lamé Equation. The derivation of the Lamé Equation can be found in books covering theoretical elastic stress analysis.

E.2.3 Plastic collapse pressure equation derivation

Equation (E.3) for plastic collapse pressure, p_P, and factors A_c, B_c and C_c were derived by statistical regression analysis from 402 collapse tests on K55, 1 440 collapse tests on N80, and 646 collapse tests on P110 seamless casing. The data used are reported in Reference [55] (available upon request from the API Dallas office). The data were gathered to represent the D/t ranges typically involved in plastic collapse for the particular grades. The regression analysis resulted in the equations of the Stewart type shown in Table E.5 originally developed by Professor Reid Stewart of Western University, Allegheny, Pennsylvania, (predecessor of the present University of Pittsburgh) and published as an American Society of Mechanical Engineers (ASME) paper in May 1906. These regression equations [(E.10), (E.11)] for average collapse pressure are substantially the same as those on which the collapse values given in the eleventh edition (1969) of API Bulletin 5C2 were based. The difference in the new equations from the old arises from the method of determining minimum values from the average values. The new minimum values were determined by subtracting a constant pressure determined for the particular grade from the average, while the old minimum values were determined by reducing the average values by 25 %.

Table E.5 — Average plastic collapse pressure regression equations

Grade	Average plastic collapse regression equation	Coefficient of det. R^2	Standard error Sp	Equation number
K55	$p_P = 164\,450/(D/t) - 2\,976$	0,647 8	435	(E.10)
N80	$p_P = 245\,600/(D/t) - 5\,336$	0,862 7	719	(E.11)
P110	$p_P = 349\,800/(D/t) - 9\,020$	0,772 0	1 048	(E.12)

Statistical minimum values for the regression equations are based on one-sided tolerance limits developed following methods that can be found in Reference [118]. Equations (E.13), (E.14), (E.15) and (E.16) for one-sided tolerance limits are developed by such methods. These tolerance limits are subtracted from the average collapse pressure equations to obtain minimum collapse pressure equations.

$$C_c = t_p(\theta_p)\, Z_p\, S_p \tag{E.13}$$

$$t_p(\theta_p) \cong \{u_{1-\theta} + u_p\,[(1 - u_p^2/2f)/N_t + u_{1-\theta}^2/2f]^{1/2}\}/(1 - u_p^2/2f) \tag{E.14}$$

$$t_{0,95}(0{,}005) = \{2{,}570 + 1{,}645\,[(1 - 1{,}353\,0/(N_t - 1))/N_t + 3{,}302\,45/(N_t - 1)]^{1/2}\}/[1 - 1{,}353\,0/(N_t - 1)] \tag{E.15}$$

$$Z_p = [1 + 1/N_t + (t/D - a_{t/D})^2/(N_t\, s_{t/D})]^{1/2} \tag{E.16}$$

where

$a_{t/D}$ is the average value of t/D ratios used in the regression;

C_c empirical constant in historical API collapse equation;

D specified pipe outside diameter;

f degrees of freedom = $N_t - 1$;

N_t number of tests;

S_p standard error of estimate of the regression equation;

$s_{t/D}$ standard deviation of t/D ratios used in the regression;

t specified pipe wall thickness;

t_p tolerance interval corresponding to a confidence level of p that the proportion of the population not included does not exceed;

u_p fractile corresponding to confidence level p;

$u_{1-\theta}$ fractile, the deviation from the mean of a standardized normal cumulative distribution that includes the fraction $1 - \theta_p$ of the population;

Z_p correction factor for variation in t/D from average;

θ_p the proportion of the population not included.

Equation (E.14) was taken directly from Reference [118]. Equation (E.16) provides a correction for variation from average t/D used in the regression, and is based on information taken from Reference [119].

The quantity C_c is to be regarded as a tolerance limit to be subtracted from the average collapse pressure Equation to obtain the minimum collapse pressure equation. Regarding the term $(t/D - a_{t/D})$, the maximum absolute value of this quantity occurring in the test data is to be used in Equation (E.16) for calculating Z_p.

Equation (E.15) was obtained from Equation (E.14) by taking the confidence level to be 0,95 and $\theta_p = 0{,}005$ and substituting the corresponding values of $u_p = u_{0,95} = 1{,}645$ and $u_{1-\theta} = u_{0,995} = 2{,}574$ obtained from a table of probability integrals.

Values for the tolerance limit C_c were calculated using Equations (E.13) through (E.16) and are shown in Table E.9.

Subtracting the tolerance limit C_c values from the average collapse pressure Equations (E.10), (E.11) and (E.12), the following Equations (E.17), (E.18) and (E.19) presented in Table E.6 for minimum collapse pressures, p_P, are obtained:

Table E.6 — Minimum plastic collapse equations for grades K, N and P

Grade	Average plastic collapse regression equation	Equation number
K55	$p_P = 164\,450/(D/t) - 418\,1$	(E.17)
N80	$p_P = 245\,600/(D/t) - 729\,1$	(E.18)
P110	$p_P = 349\,800/(D/t) - 118\,75$	(E.19)

These equations for minimum plastic collapse pressure are based on the conception that there is a 95 % probability or confidence level that the collapse pressure will exceed the minimum stated with no more than 0,5 % failures.

While Equations (E.17), (E.18) and (E.19) could be used in the form shown, they have been converted to the following standard form, primarily to facilitate extrapolation and interpolation to obtain collapse equations for other grades for which adequate collapse test data are not available from which to obtain equations direct:

$$p_P = f_{ymn}\,[A_c/(D/t) - B_c] - C_c \qquad \text{(E.20)}$$

where

A_c is the empirical constant in historical API collapse equation;

B_c is the empirical constant in historical API collapse equation;

C_c is the empirical constant in historical API collapse equation;

D is the specified pipe outside diameter;

f_{ymn} is the specified minimum yield strength;

p_P is the pressure for plastic collapse;

t is the specified pipe wall thickness.

The following factors A_c, B_c and C_c for grades K55, N80 and P110, given in Table E.7, were curve-fit to provide equations for determining these factors for other grades by extrapolation and interpolation:

Table E.7 — Plastic collapse equation factors for grades K, N and P

Grade	A_c	B_c	C_c
K55	2,990	0,054 1	1 205
N80	3,070	0,066 7	1 955
P110	3,180	0,082 0	2 855

$$A_c = 2{,}876\ 2 + 0{,}106\ 79 \times 10^{-5} f_{ymn} + 0{,}213\ 01 \times 10^{-10} f_{ymn}^2 - 0{,}531\ 32 \times 10^{-16} f_{ymn}^3 \quad \text{(E.21)}$$

$$B_c = 0{,}026\ 233 + 0{,}506\ 09 \times 10^{-6} f_{ymn} \quad \text{(E.22)}$$

$$C_c = -465{,}93 + 0{,}030\ 867 f_{ymn} - 0{,}104\ 83 \times 10^{-7} f_{ymn}^2 + 0{,}369\ 89 \times 10^{-13} f_{ymn}^3 \quad \text{(E.23)}$$

where

A_c is the empirical constant in historical API collapse equation;

B_c is the empirical constant in historical API collapse equation;

C_c is the empirical constant in historical API collapse equation;

f_{ymn} is the specified minimum yield strength.

Factors for grades K55, N80 and P110 calculated using Equations (E.21), (E.22) and (E.23) are given in Table E.8.

Table E.8 — Plastic collapse equation factors for grades K, N and P as calculated

Grade	A_c	B_c	C_c
K55	2,991	0,054 10	1 206
N80	3,071	0,066 70	1 955
P110	3,181	0,081 92	2 852

The maximum deviation of the factors determined by the equations from those determined by regression analysis is 0,122 %.

The tolerance limit for Grades K55, N80 and P110 to be subtracted from average collapse equations to convert to a minimum base are shown in Table E.9.

Table E.9 — Tolerance limit C_c to be subtracted from average collapse equations to convert to a minimum base

Grade	C_c
K55	1 205
N80	1 955
P110	2 855

As additional data become available, these equations can be verified or modified where necessary. Analysis of collapse test data should conform to the principles followed in developing the present equations.

E.2.4 Transition collapse pressure equation derivation

When the curves of the equations for average plastic collapse pressures are extended to higher D/t values, they intersect the average elastic collapse pressure curve. However, as the curves for minimum plastic collapse pressures are extended to higher D/t values, they fall below the minimum elastic collapse pressure curve without intersecting it. In order to overcome this anomaly, a plastic/elastic transition collapse pressure equation has been developed that intersects the D/t value where the average plastic collapse pressure equation gives a collapse pressure of zero and is tangent to the minimum elastic collapse pressure Equation (E.7). This equation is used to determine minimum collapse pressures between its tangency to the elastic collapse pressure curve and its intersection with the plastic collapse pressure curve. This is shown in Figure E.1 for grade N80 casing.

The equation for plastic/elastic transition collapse pressure, p_T, is of the Stewart form as follows:

$$p_T = f_{ymn}\,[F_c/(D/t) - G_c] \tag{E.24}$$

where

D is the specified pipe outside diameter;

F_c is the empirical constant in historical API collapse equation;

f_{ymn} is the specified minimum yield strength;

G_c is the empirical constant in historical API collapse equation;

t is the specified pipe wall thickness.

The two conditions mentioned,

a) intersection with the average collapse pressure curve p_P (average) $= f_{ymn}\,[A_c/(D/t) - B_c]$, where p_P (average) $= 0$, and

b) tangent to the elastic curve,

$$p_E = 46{,}95 \times 10^6/[(D/t)\,(D/t - 1)^2] \tag{E.25}$$

where

D is the specified pipe outside diameter;

p_E is the pressure for elastic collapse;

t is the specified pipe wall thickness;

permit evaluation of A_c and B_c according to Equations (E.26) and (E.27) as follows:

$$F_c = 46{,}95 \times 10^6 \, [(3 \, B_c/A_c)/(2 + B_c/A_c)]^3/\{f_{ymn} \, [(3 \, B_c/A_c)/(2 + B_c/A_c) - B_c/A_c][1 - (3 \, B_c/A_c)/(2 + B_c/A_c)]^2\} \quad \text{(E.26)}$$

$$G_c = F_c \, B_c/A_c \quad \text{(E.27)}$$

where

A_c is the empirical constant in historical API collapse equation;

B_c is the empirical constant in historical API collapse equation;

C_c is the empirical constant in historical API collapse equation;

F_c is the empirical constant in historical API collapse equation;

f_{ymn} is the specified minimum yield strength;

G_c is the empirical constant in historical API collapse equation.

E.2.5 Elastic collapse pressure equation derivation

The minimum elastic collapse pressure equation was derived from the theoretical elastic collapse pressure equation developed by Clinedinst [54], where p_E is the pressure for elastic collapse:

$$p_E = 2E/(1 - \nu^2)/[(D/t) \, (D/t - 1)^2] \quad \text{(E.28)}$$

where

D is the specified pipe outside diameter;

E is Young's modulus;

t is the specified pipe wall thickness;

ν is Poisson's ratio.

The curve plotted from the equation for theoretical elastic collapse, assuming $E = 30 \times 10^6$ and $\nu = 0.3$, was found to be an adequate upper boundary for collapse pressure as determined by test.

The average collapse resistance equation adopted by API in 1939 was taken as 95 % of the theoretical equation for elastic collapse resistance, rounded to two decimals. The minimum elastic collapse resistance equation adopted in 1968 was taken as 75 % of the average elastic collapse resistance equation, rounded to three decimals:

$$p_E = 46{,}95 \times 10^6/[(D/t) \, (D/t - 1)^2] \quad \text{(E.29)}$$

where

D is the specified pipe outside diameter;

p_E is the pressure for elastic collapse;

t is the specified pipe wall thickness.

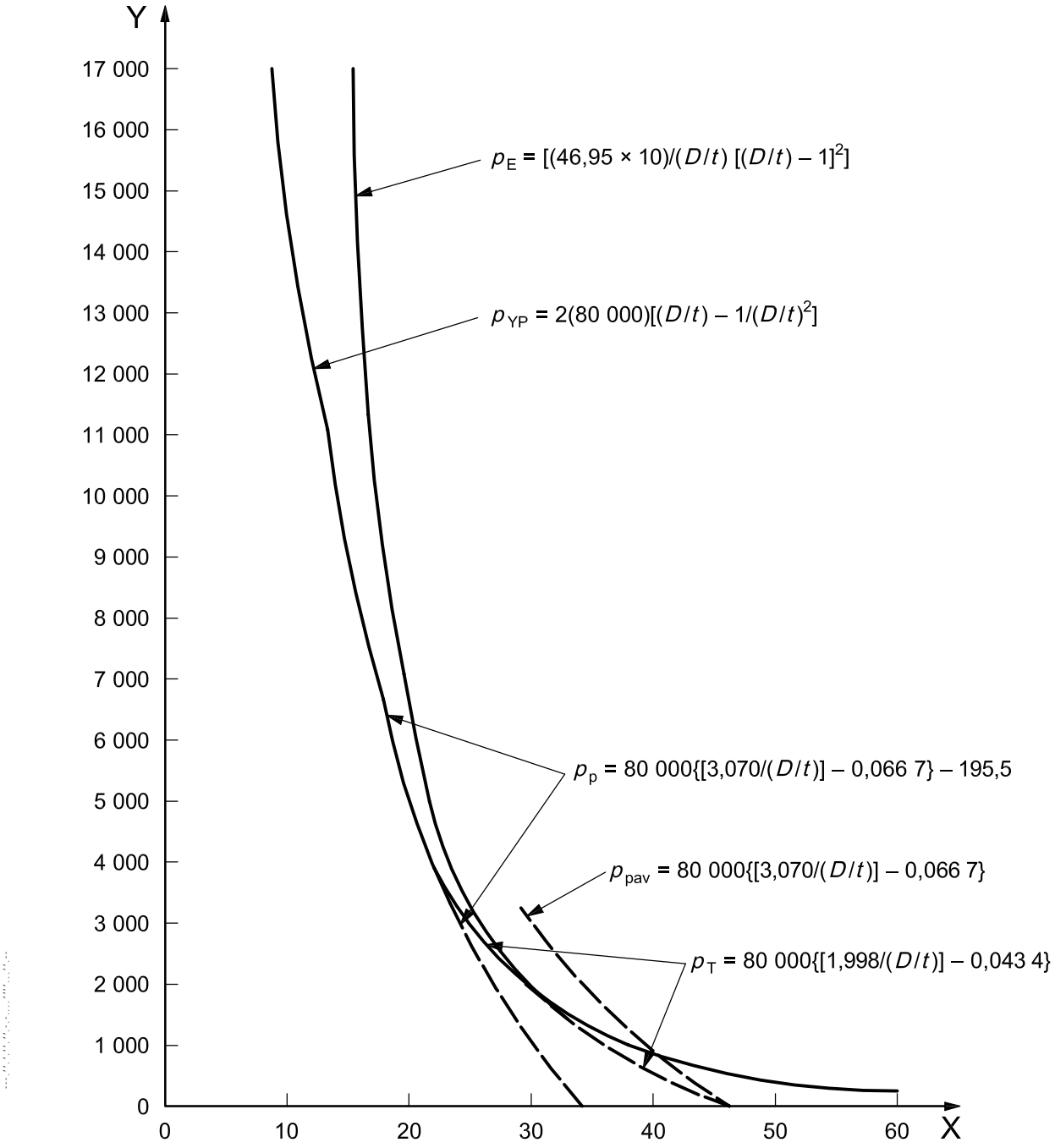

Key

X D/t

Y collapse pressure, psi

D is the specified pipe outside diameter

t is the specified pipe wall thickness

p_E pressure for elastic collapse

p_{YP} pressure for yield strength collapse

p_P pressure for plastic collapse

p_{Pav} pressure for average plastic collapse

p_T pressure for transition collapse

Figure E.1 — Grade N80 transition collapse equation derivation

Annex F
(informative)

Development of probabilistic collapse performance properties

F.1 Introduction

F.1.1 Limitations of previous approach

The technical basis of the API Bulletin 5C3[2] collapse strength equations was developed in the early 1960s. Various limitations have been identified since their first publication, as follows.

a) Some of the collapse tests[55] were for short specimens ($L/D = 2$), which are now known to overestimate the collapse strength of real pipe [65], [66], [98], [99].

b) The collapse strength equations resulted in a widely varying margin between the ultimate and design collapse strengths over the D/t range for well tubulars[75], and thus also in predicted failure probability[41], [70].

c) The mean value equations were relatively poor predictors of ultimate collapse strength, and modern formulations have been shown to be much more accurate (Table F.2) [48].

d) The same equations were used for both quenched and tempered (Q&T) and non-Q&T pipe. However, recent work [44] has shown that the two classes have different collapse behaviour, and therefore need individual strength equations.

e) The collapse test specimens were manufactured using a wide range of production methods (e.g., seamless and welded, cold and hot rotary straightening), and no attempt was made to determine the various effects on collapse strength. Subsequent work[44] has demonstrated that both straightening and heat treatment have a significant effect on collapse strength, and thus should be included explicitly in any modern treatment.

f) The formulation for plastic collapse strength was implicitly based on the assumption that collapse strength is proportional to the specified minimum, rather than the actual, yield stress. This is acceptable as long as the ratio of actual to specified minimum yield stress is constant for all grades. However, analysis of production quality data[48] has shown that this ratio varies considerably by grade, and thus that the previous treatment can and should be improved.

g) Finally, the previous approach could not accommodate non-API grades, such as high-collapse (HC) pipe.

Given that this is the case, it can be asked why the new probabilistic treatment is given here, as an informative annex, with the old (1963) method retained in Clause 8. There was a broad consensus in the workgroup that the new collapse strength equations (Clauses F.2 and F.4) are more accurate than the old; that the statistical data for a given production case (Subclauses F.3.1 to F.3.3) can be reliably determined; and that the probabilistic method (Clause F.5) gives the correct results in such cases.

However, at present there is no consensus on how pipe data for all API/ISO production should be characterized for calculation of design ratings. The text of Subclause F.3.4 represents the workgroup's best efforts in this regard. Some members felt that the ratings thus calculated (Clause F.6) are already an improvement on the old, and therefore should now replace the old Clause 8. Others, however, believed that the industry needs more time to consider the new method, and in particular the question of characterization of probabilistic data for worldwide production.

The new work has therefore been kept as informative at this stage. It is hoped that as the industry becomes more familiar with the method, the question of data characterization can be fully resolved. In this event, the document will be reissued with the new guidance (Clause F.6) replacing the existing Clause 8.

F.1.2 Choice of method

Design collapse strength can be determined either directly, from collapse test results (Annex G), or indirectly using production quality statistics (that is, the statistics of parameters such as yield stress, outside diameter, and wall thickness), and probabilistic analysis with a predictive equation for ultimate collapse strength (Annex H).

The direct method requires collapse test data for every pipe case (outside diameter, weight and grade), for a representative range of mills. As these data were not available, it was necessary to use the second approach. The advantage of the indirect method is that production quality data is more readily available than collapse data, and in larger quantities. Collapse data is only necessary in order to choose the ultimate strength equation, and determine any empirical adjustment(s).

The accuracy of performance properties obtained using the indirect approach depends on the accuracy of both the calculation method, and the probabilistic data. Comparison for individual pipe sizes (Table F.1) shows that, in general, the direct and indirect calculation methods give very similar results for both the large and small dataset analyses[87].

The probabilistic data were a combination of measurement data contributed by participating mills, and potentially governing design cases chosen by the workgroup, based on production experience. While any such choices will be arbitrary to some extent, comparison with ensemble collapse test data (Figures F.12, F.13) shows that the desired target reliability level is being achieved.

Moreover, the new performance properties give a near-uniform predicted safety level (Figure F.10), and therefore correct the primary limitation of the old collapse strength equations (Annex E).

The application of the method is described in the following subclauses. Limited space precludes more than an overview of analysis details, and the reader is referred to the literature[52], [81], [103] for a fuller treatment.

Table F.1 — Comparison of design collapse strengths

	Rotary straight-ening	Samples	Collapse test		Large dataset ratings ksi			Direct/ correl. indirect	Small dataset ratings ksi			Direct/ correl. indirect
			Mean ksi	COV	Direct (collapse test)	Indirect (synthesis) Indep-endent	Indirect (synthesis) Correl-ated		Direct (collapse test)	Indirect (synthesis) Indep-endent	Indirect (synthesis) Correl-ated	
Nippon 1977-2000												
7 in 23.0 lb/ft HC95	None	68	6.609	0.050 2	5.755	5.510	5.787	0.994 5	5.594	5.374	5.649	0.990 3
7 in 26.0 lb/ft HC95	None	76	9.459	0.056 0	8.094	7.905	8.178	0.989 7	7.855	7.740	8.019	0.979 5
7 in 29.0 lb/ft HC95	None	56	11.81	0.035 3	10.74	10.00	10.73	1.000 9	10.51	9.769	10.53	0.998 1
7 5/8 in 26.4 lb/ft HC95	None	42	5.518	0.059 2	4.677	4.519	4.709	0.993 2	4.465	4.366	4.572	0.976 6
7-5/8 in 29.7 lb/ft HC95	None	84	8.261	0.052 9	7.136	6.791	7.178	0.994 1	6.949	6.636	7.031	0.988 3
7-5/8 in 33.7 lb/ft HC95	None	49	10.96	0.058 3	9.318	8.951	9.377	0.993 7	8.938	8.670	9.131	0.978 9
9-5/8 in 43.5 lb/ft HC95	None	36	6.625	0.053 3	5.715	5.663	5.751	0.993 7	5.464	5.502	5.595	0.976 6
9-5/8 in 47.0 lb/ft HC95	None	116	8.357	0.054 8	7.177	7.079	7.209	0.995 6	7.015	6.966	7.097	0.988 4
9-5/8 in 53.5 lb/ft HC95	None	129	11.03	0.070 8	9.022	8.836	9.060	0.995 8	8.757	8.677	8.916	0.982 2
	Total	656					Mean	0.994 6			Mean	0.984 3
Tenaris 2004												
4-1/2 in 11.6 lb/ft P110	Cold	70	9.397	0.080 6	7.445	7.409	7.538	0.987 7	7.086	7.153	7.282	0.973 1
4-1/2 in 11.6 lb/ft P110	Hot	99	10.38	0.070 9	8.482	8.403	8.539	0.993 3	8.198	8.189	8.323	0.985 0
5-1/2 in 17.0 lb/ft P110 [a]	Cold	21	8.896	0.080 2	7.057	7.608	7.139	0.988 5	6.333	7.363	6.896	0.918 4
5-1/2 in 17.0 lb/ft P110	Hot	60	10.47	0.063 4	8.757	8.859	8.840	0.990 6	8.414	8.658	8.643	0.973 5
	Total	250					Mean	0.990 0			Mean	0.962 5

[a] Collapse strength distribution not Gaussian.

Table F.2 — Predictive accuracies (Q&T only)

Dataset	Axial force	Position(s) for geometry measurements	Tests	Actual collapse strength/predicted collapse strength																	
				Abbassian and Parfitt 1995-9a		API Bulletin 5C3 (average)		API Bull. 5C3 / Clinedinst 1985		Haagsma and Schaap 1981		Jianzeng and Taihe 2001		Klever-Tamano		Tamano *et al.* 1983		Tamano modified 4	
				Mean	COV	Mean	COV	Mean	COV	Mean	COV	Mean	COV	Mean	COV	Mean	COV	Mean	COV
API product																			
Mannesmann 1983	No	Multiple	89	**0,983**	0,069			1,035	**0,049**	0,955	0,067	0,930	0,069	0,956	0,055	0,968	0,064	0,964	0,064
API 1985	No	Not known	106	1,023	0,046	0,978	0,083	1,016	0,048	0,925	0,082	0,973	0,060	0,989	0,044	1,004	0,051	**0,996**	**0,042**
Nippon 1977-87	No	Pipe centre	433	0,996	0,072	1,088	0,136	1,054	0,080	0,944	0,100	0,978	0,077	0,992	**0,057**	**1,003**	0,069	0,981	0,060
Nippon 1988-2000	No	Pipe centre	95	1,020	0,104	1,026	0,107	1,060	0,097	0,947	0,115	0,994	0,110	**1,004**	**0,093**	1,019	0,104	0,996	0,095
Manufacturer FD00	No	Pipe end	129	1,019	**0,077**	1,019	0,085	1,055	0,093	0,956	0,107	0,988	0,095	**1,000**	0,078	1,017	0,087	0,997	0,077
DEA-130	No	Pipe centre	52	1,019	0,066	1,017	0,097	1,065	0,071	0,966	0,083	0,974	0,082	0,993	**0,063**	**1,006**	0,073	0,987	0,066
API 1981	Yes	Collapse point	96	1,040	0,108	1,037	0,136	1,062	0,099	0,965	0,106	**1,004**	**0,080**	1,030	0,102	1,035	0,085	1,019	0,098
Mannesmann 1983	Yes	Multiple	63	1,030	0,098	1,114	0,168	1,052	**0,082**	1,009	0,084	0,976	0,087	**1,003**	0,084	1,021	0,084	1,016	0,090
Dataset average				1,016	0,080	1,040	0,116	1,050	0,077	0,958	0,093	0,977	0,083	**0,996**	**0,072**	1,009	0,077	0,994	0,074
Ensemble average [a]			1 138	1,012	0,080			1,049	0,081	0,952	0,097	0,981	0,083	**0,997**	**0,071**	1,010	0,077	0,992	0,072
Dataspace average [a]				1,026	0,024					0,975	0,044			0,993	**0,011**	1,021	0,032	**1,000**	0,015
HC product																			
API 1982	No	Pipe end	141	0,977	0,125	0,961	0,111	**1,013**	0,114	0,949	**0,109**	0,950	0,118	0,944	0,115	0,979	0,118	0,949	0,122
API 1987	No	Pipe end	107	1,093	0,076	1,158	0,066	1,132	**0,054**	**1,054**	0,075	1,073	0,085	1,073	0,065	1,101	0,078	1,069	0,070
Nippon 1977-87	No	Pipe centre	794	1,016	0,052	1,124	0,072	1,135	0,063	1,030	0,073	1,016	0,073	1,005	**0,050**	1,039	0,063	**1,000**	0,052
Vallourec 1987-98	No	Collapse point	304	1,019	0,054	1,082	0,050	1,135	0,057	1,027	0,064	1,007	0,079	1,009	**0,046**	1,037	0,066	**1,006**	0,052
Japanese RR 1987	No	Not known	54	1,005	0,056	1,107	0,057	1,077	0,048	0,988	0,065	0,990	0,079	**1,000**	**0,053**	1,017	0,069	0,988	0,055
Nippon 1988-2000	No	Pipe centre	291	1,012	**0,058**	1,127	0,076	1,124	0,059	1,030	0,063	**1,003**	0,079	0,995	0,059	1,028	0,069	0,992	0,060
Manufacturer FD00	No	Pipe end	75	0,960	0,058	1,126	0,069	1,034	0,061	0,901	0,063	0,919	0,055	**0,968**	**0,054**	0,952	0,056	0,946	0,057
DEA-130	No	Pipe centre	26	1,019	0,090	1,037	0,087	1,074	**0,062**	0,985	0,088	1,008	0,088	**1,001**	0,072	1,029	0,082	0,997	0,082
API 1981	Yes	Collapse point	56	0,986	0,049	1,218	0,148	1,089	0,059	1,014	**0,048**	0,967	0,062	0,973	0,056	**0,997**	0,052	0,968	0,051
Dataset average				1,010	0,069	1,104	0,082	1,090	0,064	**0,998**	0,072	0,993	0,080	0,996	**0,063**	1,020	0,073	0,991	0,067
Ensemble average			1 848	1,014	0,068	1,108	0,088	1,115	0,073	1,017	0,080	1,005	0,084	**1,001**	**0,064**	1,031	0,076	0,996	0,067
Dataspace average				1,026	0,021					1,032	0,046			1,007	**0,013**	1,039	0,047	**1,007**	0,023

NOTE 1 Of the datasets above, those used for calibration of empirical coefficients were as follows:

- Klever-Tamano: all
- Tamano modified 4: all except manufacturer FD00, Nippon 1988-2000, and DEA-130
- Abbassian and Parfitt 1995-9a: all except Japanese RR 1987, manufacturer FD00, Nippon 1988-2000, and DEA-130
- API Bulletin 5C3/Clinedinst 1985: API 1985.

NOTE 2 Bold type denotes the best fit for each dataset.

[a] Includes one line from Grant Prideco 2000.

F.2 Selection of ultimate limit state equation

F.2.1 Collapse test data

Table F.2 lists the collapse test datasets [57], [66], [88], [96], [97], [100], 109], [110], [111], [112], [113], [114], [115], [116] made available to the workgroup. All the data is in the public domain, and the manufacturer of each sample is identified in all but five datasets. The anonymous datasets were provided in confidence as part of the 1982, 1985 and 1987 API collapse test programmes, the 1999-2000 API data survey, and Drilling Engineering Association project DEA-130.

The collapse test ensemble contained 3 171 tests, broken down as follows:

— Q&T pipe: 2 986 tests (1 138 for API grades, 1 848 for HC);

— non-Q&T pipe: 185 tests, all for API grades.

All tests were for long specimens ($L/D \geqslant 7$), and in each case the relevant strength and geometry properties (yield stress, average outside diameter, average wall thickness, eccentricity, ovality, and residual stress) were accurately measured prior to collapse testing. All datasets were QA checked, duplicate and suspect lines rejected, and approved by unanimous consensus of the workgroup.

F.2.2 Candidate ULS equations

Eleven sets of predictive equations were evaluated against the Q&T collapse test results, namely:

— Abbassian and Parfitt 1999a[44];

— API Bulletin 5C3 (for mean strength, i.e. with the down-rating factors for design collapse strength removed)[2];

— API Bulletin 5C3 mean strength (yield, elastic)/Clinedinst 1985 (plastic)[56];

— Haagsma and Schaap 1981[62];

— Issa and Crawford 1993[67];

— Jianzeng and Taihe 2001[68];

— Ju *et al.* 1998[71];

— Klever-Tamano[74];

— Tamano *et al.* 1983[101];

— Tamano modified 4[48];

— Tokimasa and Tanaka 1986[105].

The equations of most of these are discussed in the referenced papers, with three exceptions. Abbassian and Parfitt 1999a is an extension of Abbassian and Parfitt 1995[39]; the additions are empirically derived down-rating factors for eccentricity and residual stress, and an empirical adjustment to the elastic collapse strength term to avoid overprediction.

NOTE 1 Elastic collapse occurs at high D/t, for which failure occurs via buckling. Yield collapse occurs at low D/t, for which failure occurs via yielding.

Tamano modified 4 is a modification of Tamano *et al*. 1983. It involved recalibration of the empirical coefficients on the ovality, eccentricity and residual stress terms, and addition of an empirical adjustment to the elastic collapse strength term, to give a flat actual/predicted strength response over the input and output dataspaces (Adams 2000a,b[45], [48]).

NOTE 2 The dataspace is the range of values which physical pipe can assume. The input dataspace is thus the ranges of the strength and geometry variables (yield stress, average outside diameter, average wall thickness, etc.) (Figure F.2); and the output dataspace is the collapse strength range (Figure F.1).

Klever-Tamano (KT) is a new model inspired by Tamano *et al*. 1983. A global adjustment was made to obtain the correct limit behaviour, and separate factors applied to the elastic and yield terms, allowing each to be individually calibrated. The yield and elastic equations were rederived, and suggestions made on improvements to the old API equations. The various empirical coefficients were calibrated by Adams[50] to give a flat actual/predicted strength response over the input and output dataspaces (Figure F.2).

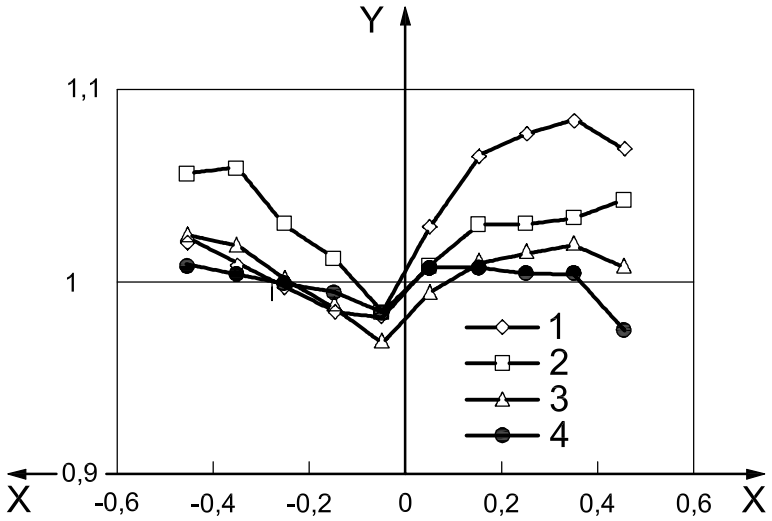

Key

X log (yield/elastic strength)
Y mean of actual/predicted collapse strength
1 Tamano *et al*. 1983
2 Abbassian and Parfitt 1999a
3 Tamano modified 4
4 Klever-Tamano

Figure F.1 — Predictive accuracy (mean) vs. dataspace position

F.2.3 Predictive accuracy

F.2.3.1 Mean

Table F.2 summarizes predictive accuracy for mean collapse strength by the ULS equation and dataset, as well as for the API and high-collapse (HC) ensembles. In each case, the tabular results show the mean and coefficient of variance (COV) of actual collapse strength/ predicted collapse strength; thus, the most accurate predictive equation is the one with the mean nearest unity and the COV nearest zero. Only the eight best-performing equations are shown.

NOTE Coefficient of variance (COV) is a dimensionless measure of the spread of a random variable, given by standard deviation/mean.

Table F.2 shows that the Klever-Tamano (KT) equations have the best combination of a near-unity mean and a low COV, for both the API and HC ensembles. Moreover, they give by far the flattest actual/predicted collapse strength response over the dataspace (Figure F.1). Accordingly, the KT equations were taken forward to the next step of the validation process, namely determination of predictive accuracy for collapse strength dispersion.

F.2.3.2 Dispersion

Figure F.3 shows predictive accuracy for collapse strength dispersion. The points represent the largest pipe cases (that is, given combinations of OD, weight and grade) in the combined Nippon 1977-2000 and Tenaris 2004 collapse test datasets (Table F.1). Only pipe cases exceeding 30 tests were used, to ensure statistical significance, and all cases were checked for homogeneity of production quality variables (see F.3). The agreement is very good, with all the points in the range 0,97 to 1,00.

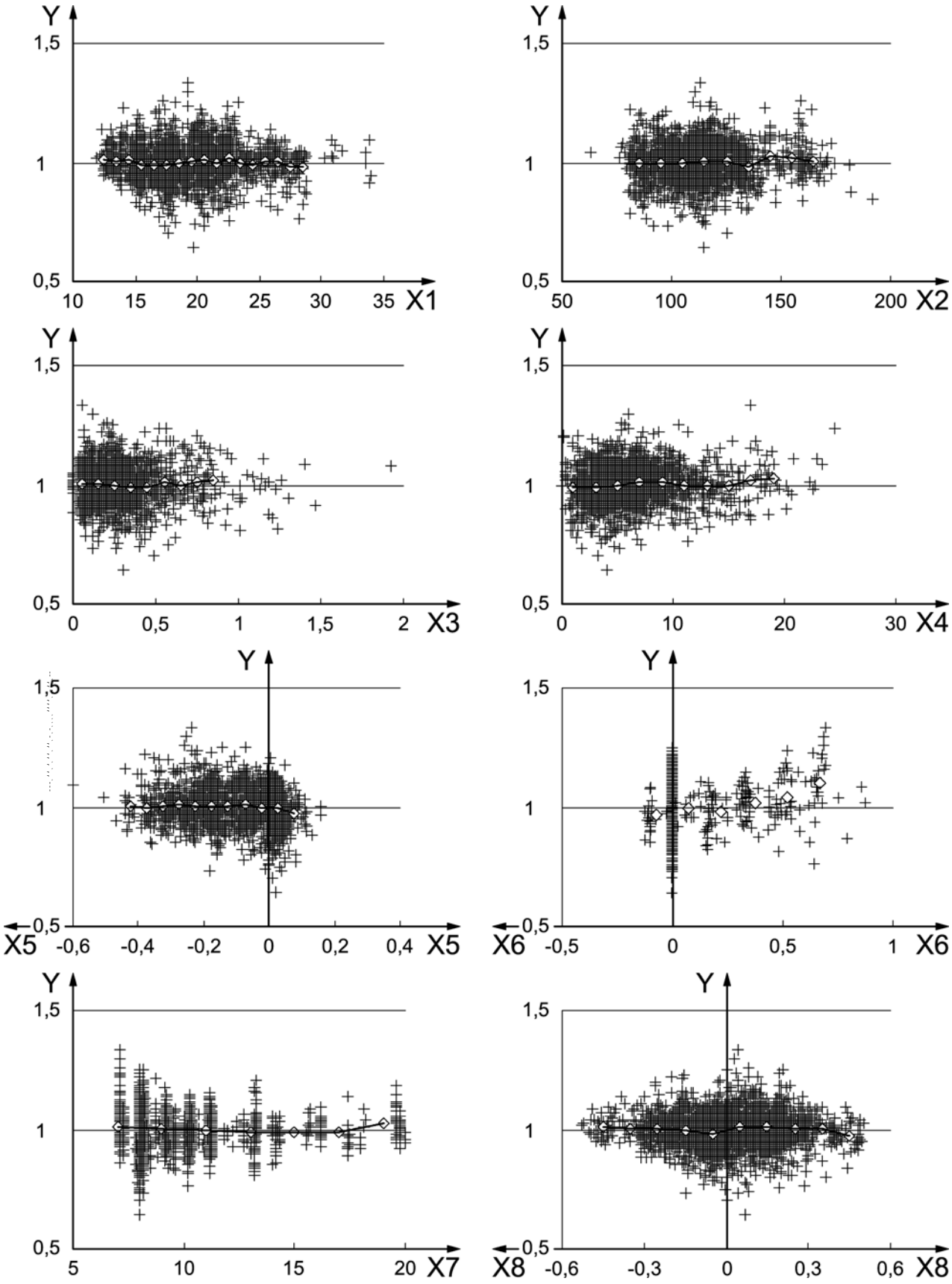

Figure F.2 (*continued*)

Key

X1 average outside diameter/average wall thickness
X2 actual API yield stress, ksi
X3 ovality, %
X4 eccentricity, %
X5 residual/actual API yield stress
X6 axial/actual API yield stress
X7 sample length/outside diameter
X8 log (yield/elastic strength)
Y actual/predicted strength

+ collapse tests
◊ mean of collapse tests for each data band

Figure F.2 — Actual/Klever-Tamano predicted strength vs. dataspace position

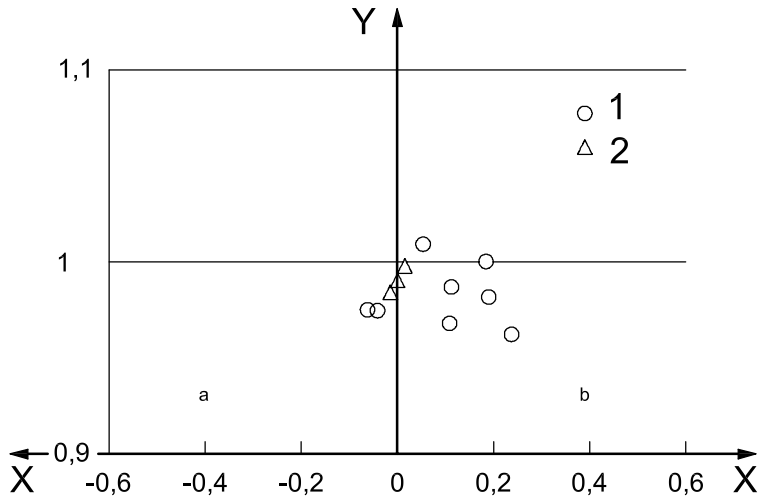

Key

X log (yield/elastic strength)
Y actual/predicted coefficient of variance

1 Nippon 1977-2000
2 Tenaris 2004

a Yield.
b Elastic.

Figure F.3 — Klever-Tamano predictive accuracy (dispersion) vs. dataspace position

NOTE The COVs were calculated including cross-correlation between input variables[84]. This improves predictive accuracy, but can be conservatively omitted for calculation of ratings, see F.3.3.

On the basis of their excellent predictive accuracy for both mean and dispersion, the Klever-Tamano equations were chosen for calculation of collapse ratings.

F.2.3.3 Model uncertainty

The model uncertainty[60] is the statistical variation due to errors and/or limitations in the ULS model; that is, the remaining variability once the effect of variation of the other input parameters has been removed. It is therefore equal to the variation of actual/predicted strength, calculated with the other input variables accurately measured; and this is given in the COV columns of Table F.2.

The model uncertainty is included in the probabilistic analysis (see F.5.1.1). This requires knowledge of its probability distribution and PDF parameters. For the KT equations and the Q&T ensemble (2 986 collapse tests, Table F.2), mean = 0,999 1, COV = 0,067 0, with a Gaussian distribution.

F.3 Input variable data

F.3.1 Analysis methods

F.3.1.1 Distribution type

The production quality data were taken from the collapse test datasets (Table F.2) and the API 1999 data survey[48]. The distribution types for the input variables were determined by plotting the data frequency distributions onto probability scales[52] [103]. They were[49]:

— average OD, average WT, yield stress, residual stress, and model uncertainty: Gaussian;

— ovality and eccentricity: two-parameter Weibull.

The PDF parameters were evaluated directly from the moments of the observed datasets[58].

Extreme outliers were removed where necessary[79]. This is because outliers are generally not from the parent process, but are departures from it, typically due to typos in data recording or to production errors. Leaving them in the dataset would therefore lead to unrepresentative PDFs. The proportion of outliers was well below 1 % throughout.

Censoring is best done by the mills, when the data and its correlation to manufacturing process is fresh to hand. If done later, censoring can be performed using the probability scales plot, on which outliers will appear as strong deviations from the best-fit line.

F.3.1.2 Ensemble PDFs

The ensemble PDF for each input variable was obtained by sampling the individual dataset PDFs (Tables F.3, F.4), using Monte Carlo analysis[47]. This ensures that each dataset has equal weight.

F.3.2 Results (individual datasets)

Tables F.3 and F.4 give production quality statistics for each input variable, and Figure F.4 presents the same data in graphical form. Several trends can be identified, as follows:

— yield stress bias varies with grade;

— mean yield stress varies with batch[43];

— yield stress dispersion varies with mean yield;

— yield stress dispersion varies with straightening method (cold/hot);

— ovality and eccentricity vary with forming process (seamless/EW);

— residual stress varies with straightening method (cold/hot/none).

Table F.3 — Production quality data (API survey only) — API yield stress

Manufact. reference	Quantity	Grade																									
		H40		J55		K55		L80		L80 9Cr		L80 13Cr		N80		C90		C95		T95		P110		Q125	
AE04	Mean					1,292	NO	1,119	NO					1,243	NO							1,147	QT	1,109	QT
	COV					0,046 6	CX	0,038 7	CX					0,048 3	CX							0,037 3	CS	0,022 6	CS
	Samples					191	WE	151	WE					83	WE							133	WE	121	WE
AP00	Mean					1,300	AR	1,087	QT					1,214	QT							1,145	QT	1,120	QT
	COV					0,033 3	CX	0,023 9	HR					0,034 2	HR							0,025 7	HR	0,027 2	HR
	Samples					220	SS	150	SS					196	SS							220	SS	210	SM
CG37	Mean													1,231	QT							1,117	QT		
	COV													0,033 1	CX							0,046 3	CX		
	Samples													473	WE							33	WE		
FD00	Mean							1,099	QT					1,205	QT							1,160	QT		
	COV							0,036 6	HR					0,043 7	HR							0,035 4	HR		
	Samples							30	SR					53	SR							46	SR		
FF12	Mean					1,091	AR	1,089	QT													1,087	QT	1,067	QT
	COV					0,032 6	HR	0,039 8	HR													0,026 7	HR	0,013 3	HR
	Samples					240	SR	390	SR													300	SR	28	SR
HH02	Mean							1,100	QT					1,233	QT					1,112	QT	1,162	QT	1,117	QT
	COV							0,034 4	HR					0,032 7	HR					0,023 5	HR	0,029 1	HR	0,029 2	HR
	Samples							166	SR					48	SR					36	SR	427	SR	298	SR
JP01	Mean			1,198	AR	1,219	AR	1,122	QT					1,216	QT							1,084	QT	1,101	QT
	COV			0,049 1	CX	0,043 4	CX	0,040 1	HR					0,049 7	HR							0,025 6	HR	0,032 2	HR
	Samples			33	SR	49	SR	185	SR					62	SR							335	SR	227	SR
RH29	Mean	1,364	AR	1,169	AR																				
	COV	0,041 7	CX	0,048 1	CX																				
	Samples	90	WE	684	WE																				
SS22	Mean															1,062	QT	1,058	QT	1,066	QT				
	COV															0,032 5	HR	0,017 6	HR	0,031 5	HR				
	Samples															42	SS	63	SS	426	SS				
VT01	Mean			1,199	QT	1,132	AR	1,086	QT					1,187	QT							1,116	QT		
	COV			0,052 4	?	0,054 0	?	0,047 2	?					0,063 3	?							0,049 5	?		
	Samples			21	SR	39	SR	55	SR					33	SR							26	SR		
YF01	Mean	1,603	AR	1,318	AR	1,301	NO	1,098	QT					1,220	QT										
	COV	0,053 1	CX	0,065 5	CX	0,052 1	CX	0,037 2	CX					0,056 3	CX										
	Samples	98	WE	1 094	WE	28	WE	223	WE					594	WE										
1	Mean											1,126													
	COV											0,021 8													
	Samples											65													
2	Mean											1,064													
	COV											0,026 2													
	Samples											33													
3	Mean											1,069													
	COV											0,023 9													
	Samples											250													
CRS ensemble	Mean [a]	1,35		1,23		1,23		1,10		1,07		1,07		1,21		1,08		1,08		1,08		1,10		1,10	
	COV	0,059 5		0,071 9		0,071 9		0,052 9		0,053 3		0,053 3		0,051 1		0,051 1		0,050 0		0,050 0		0,046 4		0,043 2	
HRS ensemble	Mean [a]							1,10		1,07		1,07		1,21		1,08		1,08		1,08		1,10		1,10	
	COV							0,042 2		0,042 6		0,042 6		0,040 5		0,040 4		0,039 4		0,039 4		0,036 0		0,032 9	

Table F.3 (*continued*)

NOTE 1 Type of heat treatment/cold working

- AR = as rolled; CR = control rolled; NO = normalized; NT = normalized and tempered; QT = quenched and tempered
- CP = cold worked, pilgered; CD = cold worked, drawn

NOTE 2 Type of straightening

- NS = not straightened; CG = cold gag straightened; CX = cold cross rolled straightened; CS = cold straightened and stress relieved; HR = hot rotary straightened

NOTE 3 Process of manufacture

- SP = seamless, pilger mill; SM = seamless, plug mill; SR = seamless, retained or floating mandrel mill; SS = seamless, stretch reduced; SE = seamless, hot expanded
- WE = welded, electric weld; WL = welded, laser weld; WS = welded, submerged arc weld

NOTE 4 Mean and COV are of actual yield/nominal yield.

NOTE 5 The mean mill COVs were calculated from:

CRS:COV = -0,000 158 1 fy + 0,056 64

HRS:COV = -0,000 151 7 fy + 0,047 43

where fy is adopted API yield stress in ksi. These equations were obtained as the best least squares fit to the mill yield stress vs. COV data (Figure F.4).

NOTE 6 The ensemble COVs were calculated by factoring the mean mill COVs by the ratio mean (ensemble COV/mean mill COV), where this ratio was developed from the five largest datasets for a given grade and straightening type, as follows:

Dataset	Ensemble COV	Mean mill COV	Ensemble/ mean mill
K55 CRS	0,051 8	0,045 5	1,138
L80 HRS	0,037 2	0,034 1	1,092
N80 HRS	0,041 4	0,032 7	1,264
P110 HRS	0,042 3	0,029 1	1,455
Q125 HRS	0,032 8	0,026 6	1,235
		Mean	1,237

NOTE 7 Where applicable, datasets were censored by removal of outliers considered not to belong to the parent process, e.g. data entry typos and production errors.

NOTE 8 The ensemble COV for J/K55 CRS is from Monte Carlo simulation, not the regression line.

[a] Adopted values for Q&T grades.

Table F.4 — Production quality data (all datasets) — Other variables

Dataset	Quantity	Average OD		Average WT		Ovality		Eccentricity		Residual stress [a]		
		SL	EW	SL	EW	SL	EW	SL	EW	Cold str.	Hot str.	Not str.
API 1981	Mean	1,004 8		1,005 4		0,197		5,471		–0,209		0,028 3
	COV	0,001 18		0,019 4		0,613		0,566		0,195		0,377
	Samples	140		140		140		140		84		56
API 1982	Mean	1,007 7	1,009 8	1,009 9	1,001 1	0,525	0,492	8,828	5,114			
	COV	0,001 84	0,002 33	0,030 7	0,028 5	0,558	0,556	0,463	0,605			
	Samples	64	77	64	77	64	77	64	77			
API 1985	Mean					0,298	0,603	7,927	4,534	–0,243		
	COV					0,573	0,395	0,482	0,706	0,278		
	Samples					321	38	321	38	261		
API 1987	Mean	1,005 8		1,005 8		0,345		5,769			–0,123	
	COV	0,001 25		0,026 4		0,588		0,479			0,632	
	Samples	91		91		91		91			75	
Japanese RR 1987	Mean	1,004 8		1,017 6		0,239		5,204				
	COV	0,001 20		0,022 5		0,433		0,291				
	Samples	54		54		54		54				
Mannesmann 1983	Mean	1,001 7		1,035 0		0,424		11,43				
	COV	0,002 76		0,028 9		0,550		0,374				
	Samples	169		169		169		169				
Nippon 1977-87	Mean	1,003 5		0,995 7		0,166		4,883		–0,269		0,019 6
	COV	0,002 06		0,023 1		0,675		0,447		0,288		0,793
	Samples	1 247		1 247		1 247		1 247		235		710
Vallourec 1987-98	Mean	1,005 5		1,011 0		0,198		6,496				
	COV	0,001 49		0,024 0		0,593		0,411				
	Samples	295		304		303		299				
Nippon 1988-2000	Mean	1,003 5		0,999 7		0,184		4,928		–0,239		0,019 2
	COV	0,001 75		0,024 4		0,727		0,428		0,440		0,705
	Samples	583		577		575		578		121		426
Manufacturer AE04	Mean		1,005 8		1,012 5		0,182		3,342			
	COV		0,001 95		0,013 7		0,658		0,501			
	Samples		999		997		997		1 000			
Manufacturer CG37	Mean		1,009 0		1,027 6		0,534		1,857			
	COV		0,002 41		0,013 3		0,425		0,485			
	Samples		62		62		62		62			
Manufacturer DA01	Mean	1,006 5		1,008 2		0,313		1,390				
	COV	0,001 32		0,032 0		0,394		0,556				
	Samples	203		208		201		208				
Manufacturer FD00	Mean	1,007 1		1,006 8		0,241		5,170		–0,211	–0,142	
	COV	0,001 89		0,021 7		0,338		0,317		0,383	0,189	
	Samples	203		132 [b]		204		194		84	54	

Table F.4 (*continued*)

Dataset	Quantity	Average OD		Average WT		Ovality		Eccentricity		Residual stress [a]		
		SL	EW	SL	EW	SL	EW	SL	EW	Cold str.	Hot str.	Not str.
Manufacturer FF12	Mean	1,005 6		1,001 0		0,122		3,493				
	COV	0,001 02		0,018 2		0,555		0,478				
	Samples	1 012		1 012		1 009		1 008				
Manufacturer HH02	Mean	1,006 2		1,011 4		0,269		1,276				
	COV	0,001 10		0,035 7		0,389		0,592				
	Samples	957		991		956		987				
Manufacturer JP01	Mean	1,006 4				0,181						
	COV	0,001 34				0,410						
	Samples	655				648						
Manufacturer HM03	Mean										−0,149	
	COV										0,652	
	Samples										32	
Tenaris 2002	Mean										−0,185	
	COV										0,247	
	Samples										74	
DEA-130	Mean	1,006 4	1,007 4	1,010 4	0,990 3	0,227	0,328	4,699	1,484	−0,206		
	COV	0,001 80	0,001 92	0,017 1	0,013 6	0,460	0,539	0,495	0,477	0,297		
	Samples	96	44	94	43	94	44	95	43	65		
Manufacturer FD00	Mean									−0,282	−0,091	
	COV									0,232	0,398	
	Samples									93	235	
Ensemble [c, d]	Mean	1,005 9		1,006 9		0,217		3,924		−0,237	−0,138	0,022 4
	COV	0,001 81		0,025 9		0,541		0,661		0,332	0,507	0,628

NOTE 1 SL = seamless, EW = welded

NOTE 2 The quantities measured were as follows:

Variable	Quantity	Units	Distribution
Yield stress	Actual API yield/nominal yield	None	Gaussian
Average OD	Average OD/nominal OD	one	Gaussian
Average WT	Average WT/nominal WT	None	Gaussian
Ovality	(Maximum OD − minimum OD)/average OD	%	Two-parameter Weibull
Eccentricity	(Maximum WT − minimum WT)/average WT	%	Two-parameter Weibull
Residual stress	Residual stress/actual API yield stress	None	Gaussian

NOTE 3 The measurement basis for the geometry variables was:

– local, single-point: API 1982, API 1987, Nippon 1977-87, Vallourec 1987-98, Nippon 1988-2000;

– local, multiple-point average: API 1981, Mannesmann 1983;

– not known: API 1985, Japanese RR 1985-87.

[a] Sign convention: stress at ID face, tension positive.

[b] The HC dataset (75 lines) had a much higher bias, and is therefore not representative of API pipe.

[c] With each dataset normalized to the same number of samples.

[d] For the geometric properties, the ensemble values were calculated from the post-1987 data only.

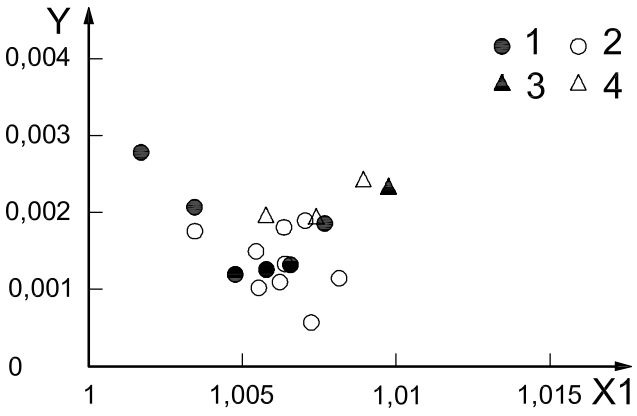

a) Average outside diameter

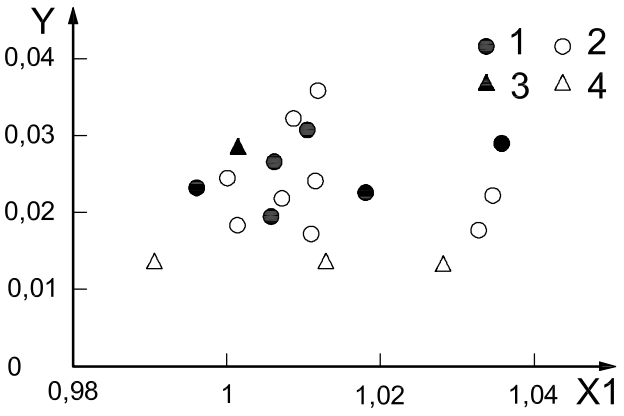

b) Average wall thickness

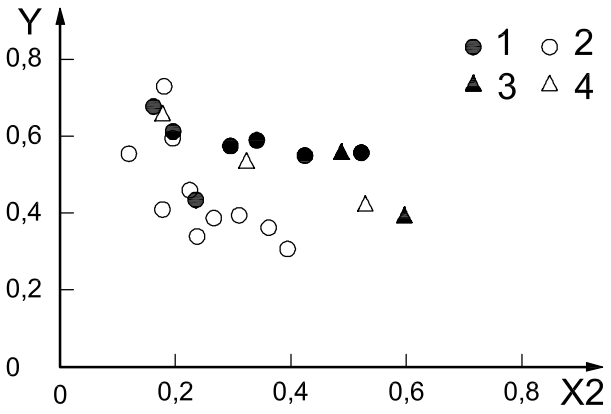

c) Ovality

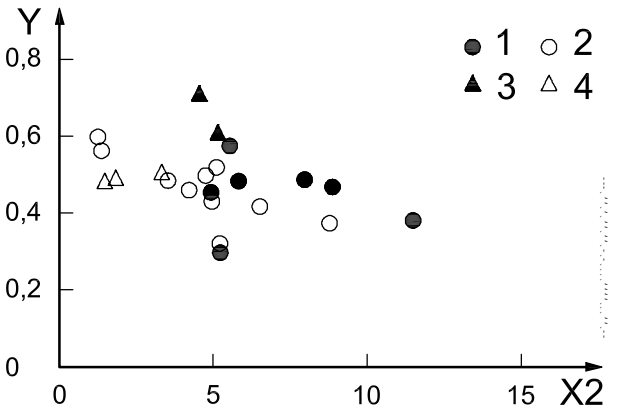

d) Eccentricity

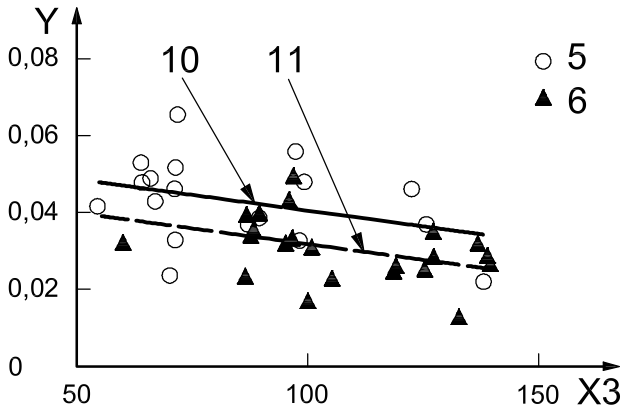

e) Yield stress (API survey only)

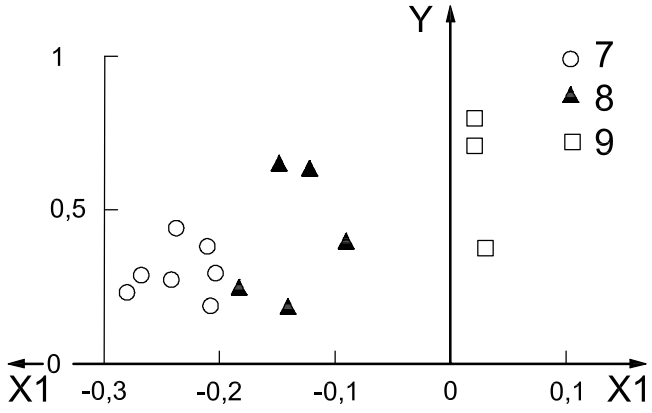

f) Residual stress

Figure F.4 (*continued*)

Key

X_1 mean
X_2 mean, %
X_3 mean, ksi
Y coefficient of variance

1 seamless - pre-1987 data
2 seamless - post-1987 data
3 EW - pre-1987 data
4 EW - post-1987 data
5 API, cold rotary straightened - post-1987 data
6 API, hot rotary straightened - pre-1987 data
7 cold rotary straightened - post-1987 data
8 hot rotary straightened - pre-1987 data
9 not rotary straightened - post-1987 data
10 trend line for cold rotary straightened product
11 trend line for hot rotary straightened product

NOTE 1 The quantities measured were as follows:

Variable	Quantity	Basis	Units
Average outside diameter	Average outside diameter/nominal outside diameter	Local	
Average wall thickness	Average wall thickness/nominal wall thickness	Local	
Ovality	(Maximum outside diameter – minimum OD)/average OD	Local	%
Eccentricity	(Maximum WT – minimum WT)/average WT	Local	%
Residual stress	Residual stress/actual API yield stress	Local	

Figure F.4 — Pipe dimension and stress data

It is therefore necessary to prepare separate collapse ratings for cold and hot rotary straightened product. In principle, it is also necessary to prepare separate ratings for seamless and EW pipe; however, the EW production data are currently insufficient to permit this. Present results suggest that strengths calculated for seamless pipe are generally conservative for welded pipe from the higher-performing mills[42].

F.3.3 Input variable correlation

Statistical analysis[84] shows that, in general, the input variables have a slight negative cross-correlation. Figure F.5 shows the effect of including cross-correlation. The predicted failure probabilities ϕ_f were calculated using the production quality statistics for each of the larger collapse test datasets, for the down-rating factors obtained from independent variable analysis (F.5.4.1). ϕ_f for correlated variables is lower than for independent variables (compare Figure F.5 with Figure F.10, for which the same down-rating factors give ϕ_f very close to the TRL). It is therefore conservative to omit the effect, and treat the input variables as independent.

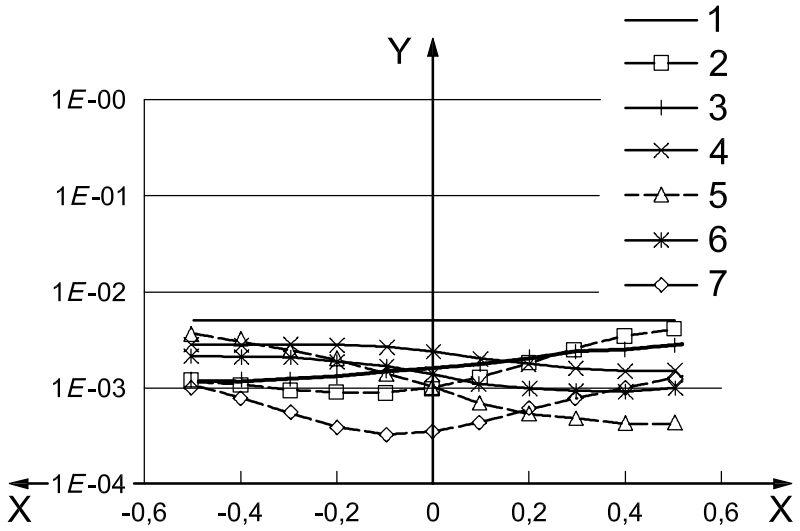

Key

X log (yield/elastic strength)
Y predicted failure probability
1 TRL
2 API 1982 (141 tests)
3 Nippon 1988 HC (291 tests)
4 Nippon 1977 API (433 tests)
5 Manufacturer FD00 API (129 tests)
6 Nippon 1977 HC (794 tests)
7 API 1987 (107 tests)

NOTE L80 seamless CRS, $k_e = 0{,}83$, $k_y = 0{,}855$.

Figure F.5 — Effect of input variable cross-correlation

F.3.4 Choice of data for calculation of ratings

The ensemble data in F.3.2 represents the historical range of aim points for yield stress, wall thickness, etc. Ensemble PDFs may govern, and must be considered when developing collapse ratings.

The other potentially governing case is that of a single lot or batch. Production aim points may be placed anywhere within the ranges specified by ISO 11960 or API 5CT, commensurate only with an economic reject rate. The in-lot dispersion is much lower than the ensemble dispersion[102], and therefore a potentially governing case is the in-lot PDF placed adjacent to the relevant tolerance limit. Figure F.6 illustrates possible PDFs for calculating collapse performance properties, developed as given in Table F.5.

Table F.5 — Development of PDFs for potentially governing cases

Parameter	0,5 % exceedence value located at	PDF dispersion given by
Yield stress	minimum yield	15 000 psi between 0,5 % exceedence limits
Average WT	0,982 5 specified WT	COV
Ovality	1 %	COV
Eccentricity	20 %	COV
Residual stress (CRS)	residual/yield = –0,4	COV
Residual stress (HRS)	residual/yield = –0,3	COV

For collapse, either the ensemble or the governing case PDF can govern, and hence both possibilities should be considered.

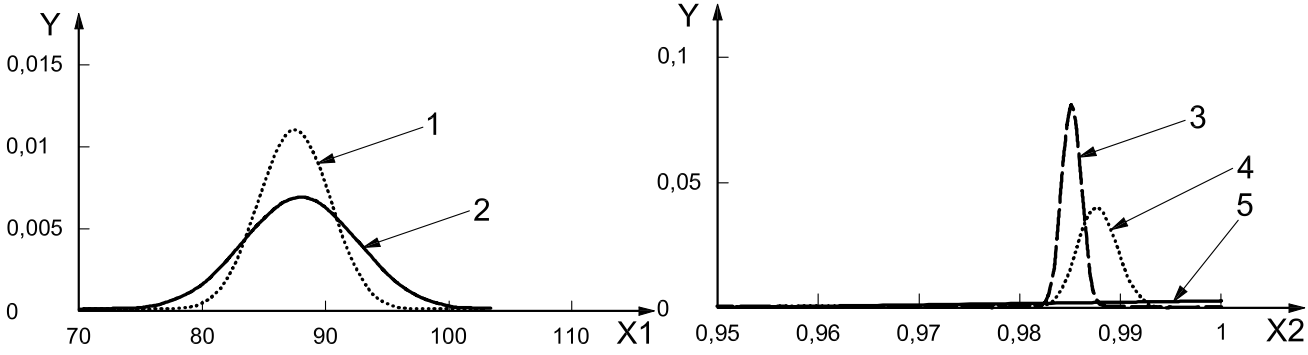

a) Yield stress (L80 CRS) **b) Average wall thickness**

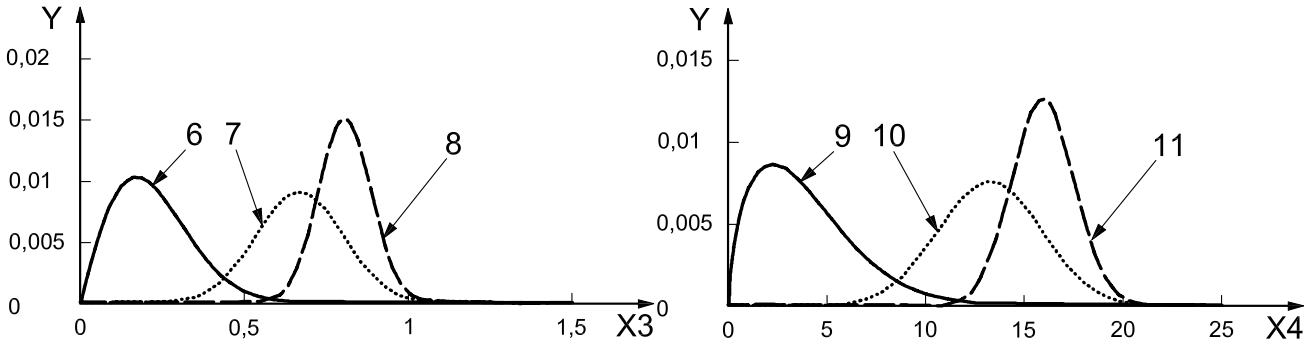

c) Ovality **d) Eccentricity**

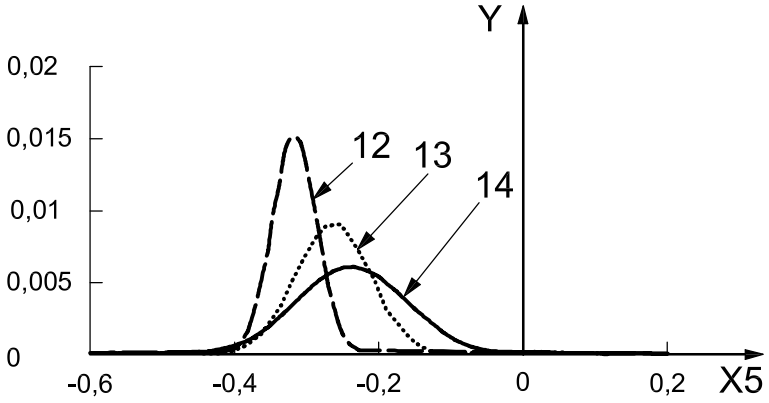

e) Residual stress (CRS)

Figure F.6 (*continued*)

Key

X1 yield stress, ksi
X2 average/nominal wall thickness
X3 ovality, %
X4 eccentricity, %
X5 residual/yield stress
Y probability

1 governing case, mean = 87,5; coefficient of variance = 0,033 3
2 dataset ensemble (mean = 88,0; coefficient of variance = 0,052 9)
3 governing case, mean = 0,985 0; coefficient of variance = 0,001
4 governing case, mean = 0,987 6; coefficient of variance = 0,002
5 dataset ensemble (mean = 1,006 9; coefficient of variance = 0,025 9)
6 dataset ensemble (mean = 0,217; coefficient of variance = 0,054 1)
7 governing case, mean = 0,660; coefficient of variance = 0,2
8 governing case, mean = 0,795; coefficient of variance = 0,1
9 dataset ensemble (mean = 3,924; coefficient of variance = 0,661)
10 governing case, mean = 13,2; coefficient of variance = 0,2
11 governing case, mean = 15,9; coefficient of variance = 0,1
12 dataset ensemble (mean = –0,237; coefficient of variance = 0,332)
13 governing case, mean = –0,264; coefficient of variance = 0,2
14 governing case, mean = –0,318; coefficient of variance = 0,1

Figure F.6 — Possible PDFs for calculation of design collapse strengths

F.4 Selection of design equation

F.4.1 Ultimate limit state equation

Klever and Tamano 2004[74] describes the development of the KT equations. A slightly simplified version was used, as below, to calculate the ultimate collapse pressure, p_{ult}.

$$p_{ult} = \{(p_{e\,ult} + p_{y\,ult}) - [(p_{e\,ult} - p_{y\,ult})^2 + 4p_{e\,ult}\,p_{y\,ult}\,Ht_{ult}]^{1/2}\}/[2\,(1 - Ht_{ult})] \quad \text{(F.1)}$$

where

$$p_{e\,ult} = k_{e\,uls}\,2E/[(1 - \nu^2)\,(D_{ave}/t_{c\,ave})\,(D_{ave}/t_{c\,ave} - 1)^2] \quad \text{(F.2)}$$

$$p_{y\,ult} = k_{y\,uls}\,2f_y\,(t_{c\,ave}/D_{ave})\,[1 + t_{c\,ave}/(2D_{ave})] \quad \text{(F.3)}$$

$$Ht_{ult} = 0{,}127\,ov + 0{,}003\,9\,ec - 0{,}440\,(rs/f_y) + h_n, \text{ with the limitation } H_{ult} \geqslant 0 \quad \text{(F.4)}$$

and

D_{ave} is the average actual outside diameter;

D_{max} is the maximum actual outside diameter;

D_{min} is the minimum actual outside diameter;

E is Young's modulus;

ec is the eccentricity, in percent; $ec = 100\,(t_{c\,max} - t_{c\,min})/t_{c\,ave}$;

f_y is the actual yield strength of a representative tensile specimen;

h_n is the stress-strain curve shape factor;

Ht_{ult} is a decrement factor;

$k_{e\ uls}$ is the calibration factor for ultimate elastic collapse: 1,089;

$k_{y\ uls}$ is the calibration factor for ultimate yield collapse: 0,991 1;

ov is the ovality, in percent; $ov = 100\ (D_{max} - D_{min})/D_{ave}$;

$p_{e\ ult}$ is the ultimate elastic collapse term;

$p_{y\ ult}$ is the ultimate yield collapse term;

rs is the residual stress (negative for compression at ID face, positive for tension at ID face);

$t_{c\ ave}$ is the average actual wall thickness;

$t_{c\ max}$ is the maximum actual wall thickness;

$t_{c\ min}$ is the minimum actual wall thickness;

ν is Poisson's ratio.

The quantity h_n was obtained empirically from collapse test data. The great majority of Q&T product has sharp-kneed stress-strain curves (SSCs), for which no correction is necessary ($h_n = 0$, Figure F.12). However, collapse test results suggest that a small minority of Q&T pipe has rounded-kneed SSCs, which reduce collapse strength, and in this event $h_n = 0{,}017$ is required to give the desired TRL (Figure F.13; the average for the four grades was taken).

The calibration factors $k_{e\ uls}$ and $k_{y\ uls}$ were also obtained empirically, to give the flattest possible actual/predicted collapse strength response in each of the input variables, for the 2 986 Q&T collapse tests (Figure F.2). The calibration process did not aim to set mean actual/predicted strength to 1,0 or to minimize its dispersion; nevertheless, it was found that both quantities were very accurately predicted, with mean = 0,999 1 and COV = 0,067 0.

Collapse test results[51] suggest that Equation (F.1) does not apply to very thin wall pipe [$\log_{10}(p_y/p_e) > 0{,}4$] with very high compressive residual stress ($rs/f_y < -0{,}5$).

F.4.2 Design equation (ensemble PDFs)

F.4.2.1 External pressure only

Equations (F.1) to (F.4) are for ultimate collapse strength; that is, they predict when the casing actually fails. For design, down-rated strengths are used, which contain a safety margin appropriate to the desired target reliability level. In this case, the margin was obtained by applying multiplicative down-rating factors $k_{y\ des}$ and $k_{e\ des}$ to the yield and elastic strengths respectively, as below.

$$p_{des} = \{(k_{e\ des}\ p_e + k_{y\ des}\ p_y) - [(k_{e\ des}\ p_e - k_{y\ des}\ p_y)^2 + 4\ k_{e\ des}\ p_e\ k_{y\ des}\ p_y\ Ht_{des}]^{1/2}\}/[2\ (1 - Ht_{des})] \qquad (F.5)$$

where

$$p_e = 2E/[(1 - \nu^2)\ (D/t)\ ((D/t) - 1)^2] \qquad (F.6)$$

$$p_y = 2f_{ymn}\,(t/D)\,[1 + t/(2D)] \quad \text{(F.7)}$$

and

D is the specified outside diameter;

E is Young's modulus: $206{,}9 \times 10^9$ N/m^2 (30×10^6 psi);

f_{ymn} is specified minimum yield strength;

Ht_{des} is a decrement factor;

$k_{e\ des}$ is the down-rating factor for design elastic collapse;

$k_{y\ des}$ is the down-rating factor for design yield collapse;

p_{des} is the design collapse pressure;

p_e is the elastic collapse term;

p_y is the yield collapse term;

t is the specified wall thickness;

ν is Poisson's ratio: 0,28.

Note that p_e and p_y are calculated using the specified dimensions and the specified minimum yield stress, rather than the actual values as for the ultimate strength.

For calculation of case-specific collapse strengths, the decrement factor Ht_{des} was obtained from the means of the relevant production variables, to give uniform scaling between the ULS and design strengths. For pipe with sharp-kneed stress-strain curves, and the ensemble means (Table F.4):

CRS $Ht_{des} = (0{,}127 \times 0{,}217) + (0{,}003\,9 \times 3{,}924) - [0{,}440 \times (-0{,}237)] + 0 = 0{,}147\,1$ (F.8)

HRS $Ht_{des} = (0{,}127 \times 0{,}217) + (0{,}003\,9 \times 3{,}924) - [0{,}440 \times (-0{,}138)] + 0 = 0{,}103\,6$ (F.9)

Similarly, for pipe with rounded-kneed stress-strain curves:

CRS $Ht_{des} = (0{,}127 \times 0{,}217) + (0{,}003\,9 \times 3{,}924) - [0{,}440 \times (-0{,}237)] + 0{,}017 = 0{,}164\,1$ (F.10)

HRS $Ht_{des} = (0{,}127 \times 0{,}217) + (0{,}003\,9 \times 3{,}924) - [0{,}440 \times (-0{,}138)] + 0{,}017 = 0{,}120\,6$ (F.11)

The working in Equations (F.8) to (F.11) is given purely as an example of its later use in Annex H on case-specific collapse strengths. For the probabilistic ratings in Clause F.6, Ht_{des} was calculated from the governing case PDFs, resulting in 0,22 for CRS and 0,20 for HRS (F.5.3.3).

F.4.2.2 Combined loads

Axial tension reduces collapse strength, and internal pressure increases it. This subclause gives a method for calculating collapse strength under one or both combined loads, based on Klever and Tamano 2004[74].

Elastic collapse pressure is unaffected by axial tension, so Δp_e is obtained from Equation (F.6) as before:

$$\Delta p_{e\ des} = k_{e\ des}\ 2E/[(1 - \nu^2)\,(D/t)\,(D/t - 1)^2] \quad \text{(F.12)}$$

where Δp_e is interpreted as a pressure difference $p_o - p_i$. The Tresca design yield pressure $\Delta p_{y\ T\ des}$ is calculated as

$$\Delta p_{y\ T\ des} = k_{y\ des}\ 2 f_{ymn}\ t/(D - t) \tag{F.13}$$

The von Mises design yield pressure $\Delta p_{y\ vme\ des}$ is obtained as

$$\Delta p_{y\ vme\ des} = (4/3^{1/2})\ k_{y\ des} f_{ymn}\ [t/(D - t)]\ [1 - (F_{eff}/F_{y\ des})^2]^{1/2} = p_o - p_i \tag{F.14}$$

where

$$F_{eff} = F_a - p_i\ A_i + p_o\ A_o \tag{F.15}$$

$$F_{y\ des} = k_{y\ des} f_{ymn}\ A_s \tag{F.16}$$

and

A_i is the area to ID $= \pi\ (D - 2t)^2/4$;

A_o is the area to OD $= \pi\ D^2/4$;

A_s is the cross-sectional area $= A_o - A_i$;

F_a is the component of axial force not due to bending, tension positive;

p_i is the internal pressure;

p_o is the external pressure.

F_{eff} is itself a function of p_o [Equation (F.15)]; thus, Equation (F.14) is solved either by iteration, or by using the root-finding function in a mathematical spreadsheet (see example, F.6.3.2).

The actual yield collapse pressure is taken as either the von Mises yield pressure or the average of the von Mises (vme) and Tresca (T) yield pressures, depending on the position on the VME ellipse. Thus:

$$\Delta p_{y\ des} = (\Delta p_{y\ T\ des} + \Delta p_{y\ vme\ des})/2 \qquad \text{if } \Delta p_{y\ vme\ des} > \Delta p_{y\ T\ des} \tag{F.17}$$

$$\Delta p_{y\ des} = \Delta p_{y\ vme\ des} \qquad \text{if } \Delta p_{y\ vme\ des} < \Delta p_{y\ T\ des} \tag{F.18}$$

Δp_{des} is then calculated as in Equation F.5, but with Δp_e and Δp_y in place of p_e and p_y:

$$\Delta p_{des} = \{(\Delta p_{e\ des} + \Delta p_{y\ des}) - [(\Delta p_{e\ des} - \Delta p_{y\ des})^2 + 4 \Delta p_{e\ des}\ \Delta p_{y\ des}\ Ht_{des}]^{1/2}\}/[2\ (1 - Ht_{des})] \tag{F.19}$$

Finally, the external design pressure $p_{o\ des}$ is calculated as

$$p_{o\ des} = \Delta p_{des} + p_i \tag{F.20}$$

F.5 Risk-calibrated collapse ratings

F.5.1 Analysis methods

F.5.1.1 Model uncertainty

For probabilistic analysis, Equation (F.1) is multiplied by the model uncertainty[60] giving:

$$p_{ult} = mu\ \{(p_{e\ ult} + p_{y\ ult}) - [(p_{e\ ult} - p_{y\ ult})^2 + 4 p_{e\ ult}\ p_{y\ ult}\ Ht_{ult}]^{1/2}\}/[2(1 - Ht_{ult})] \tag{F.21}$$

where

mu is the model uncertainty;

$p_{\text{e ult}}$ is the ultimate elastic collapse term, Equation (F.2);

$p_{\text{y ult}}$ is the ultimate yield collapse term, Equation (F.3);

and mu is a random variable.

F.5.1.2 Calculation of failure probabilities

Predicted failure probabilities were calculated using FORM (First Order Reliability Method). For independent input variables, a Rackwitz 1976[92] search routine was employed, with the normal tail approximation[52], [81] for non-Gaussian variables. For correlated variables, the correlated non-Gaussian variable set was mapped to a correlated Gaussian set using the Nataf transformation[83], with transformed correlations as given by Liu and der Kiureghian 1986[78], and mapped again to an independent non-standard Gaussian set with the orthogonal transformation[81]. Positions in the independent standard Gaussian space were mapped back into the original variable space via the Jacobian matrix[81]. A Hohenbichler and Rackwitz 1981[63] search routine was adopted. Both methods were implemented as computer spreadsheets, and validated against SORM (Second Order Reliability Method), Monte Carlo, and textbook examples [46], [47], [84].

F.5.1.3 Downrating factors

The required values of $k_{\text{e des}}$ and $k_{\text{y des}}$ were calculated by iteration, to give the flattest possible response over the dataspace for a given target reliability level (TRL).

F.5.2 Target reliability level

In design code calibration, the target reliability level (TRL) is often taken as the average predicted failure probability for the previous version of the code. This was obtained by:

— calculating design collapse strength, using API Bulletin 5C3[2];

— setting the external pressure equal to the design strength;

— running the probabilistic analysis with the ensemble input PDFs (Tables F.3, F.4), and ultimate collapse strength calculated using Equation (F.21).

Figure F.7 shows typical results[47], [86]. Predicted failure probability varies by five orders of magnitude, from 0,096 6 at the yield-plastic boundary for CRS pipe, to $5{,}11 \times 10^{-7}$ at the plastic-transition boundary for NS pipe. This is far too great a variation to be acceptable; moreover, the average values (Table F.6) are very different, and also vary with grade. It was therefore concluded that this approach was not suitable, and it was decided to adopt TRL = 0,5 % as specified (but not achieved) by the previous version.

Table F.6 — Average predicted failure probability for API Bulletin 5C3 [2] (seamless L80)

Straightening	TRL
Cold	$1{,}26 \times 10^{-2}$
Hot	$6{,}41 \times 10^{-3}$
None	$2{,}48 \times 10^{-3}$

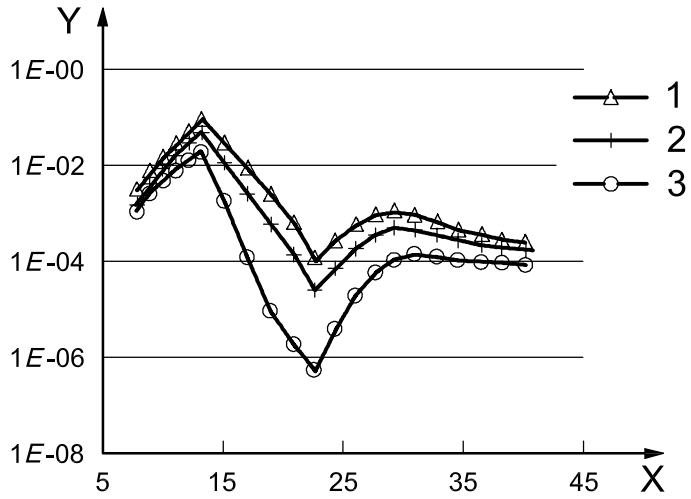

Key

X specified outside diameter/specified wall thickness

Y predicted failure probability

1 cold rotary straightened

2 hot rotary straightened

3 not straightened

NOTE L80 seamless.

Figure F.7 — Predicted failure probabilities for API Bulletin 5C3 [2]

F.5.3 Selection of input data

F.5.3.1 Yield stress

The more onerous of the ensemble and potential governing case PDFs was taken for each grade. In general, the ensemble PDF is more onerous for grades with narrow permissible yield stress ranges (e.g. T95), and the governing case PDF more onerous for grades with wide ranges (e.g. N80).

F.5.3.2 Average wall thickness

The ensemble condition governs, and was used throughout.

F.5.3.3 Eccentricity, ovality, and residual stress

These parameters appear in the decrement term Ht_{des} of Equation (F.5) for design collapse strength. For ensemble data, the mean values of each parameter (Table F.4) were used in calculating Ht_{des}, see Equations (F.8) to (F.11). This gives a flat reliability response, Figure F.10. For governing case data, using the respective governing case means in Equations (F.8) to (F.11) instead of the ensemble means also gives nearly uniform reliability (Figure F.8)[85].

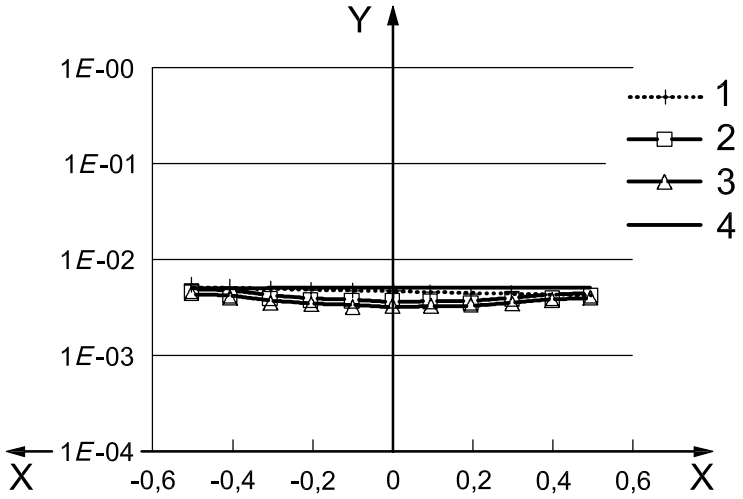

Key

X log (yield/elastic strength)

Y predicted failure probability

1 ensemble data

2 governing case data, coefficients of variance = 0,2

3 governing case data, coefficients of variance = 0,1

4 target reliability level

NOTE L80 seamless CRS ($k_e = 0{,}825$, $k_y = 0{,}855$).

Figure F.8 — Predicted failure probabilities with potential governing case means in Ht_{des}

This shows that the effect of Ht_{des} is almost independent of the down-rating factors $k_{e\,des}$ and $k_{y\,des}$. Therefore, the value of Ht_{des} can be set for some desired governing case combination of eccentricity, ovality and residual stress, and this value will (to a good approximation) apply for all grades, sizes, and weights.

Figure F.9 shows the effect of Ht_{des} on pipe mass[85]. Using the ensemble PDFs gives an average mass increase of 1,2 % over all pipe sizes, weights and grades. Using potential governing case PDFs gives mass increases of 1,0 % to 5,6 %, depending on the number of cases taken, and the PDF dispersion assumed for each case (Figure F.6). For calculation of collapse ratings, it was decided to use $Ht_{des} = 0{,}2$; this allows for one moderately severe governing case, or two mild governing cases.

This allowance is additional to that for stress-strain curve shape (F.4.1). The total value of Ht_{des} is therefore 0,22 ($\cong 0{,}20 + 0{,}017$) for cold rotary straightened pipe, and 0,20 for HRS.

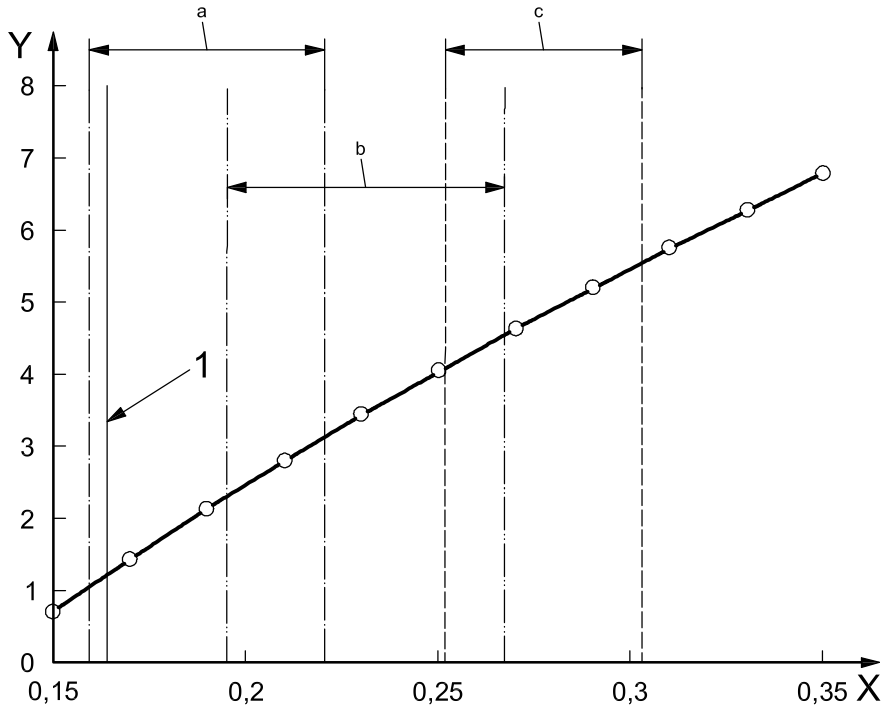

Key

X Ht_{des}

Y mass change, %, with respect to API Bulletin 5C3[2]

1 ensemble PDFs

a One of ovality, eccentricity, residual stress governing case.

b Two of ovality, eccentricity, residual stress governing case.

c Ovality, eccentricity, residual stress all governing case.

Figure F.9 — Effect of Ht_{des} on pipe mass

Table F.7 summarizes the input data used for calculation of design collapse ratings.

Table F.7 — Summary of probabilistic data

Parameter	Type	Distribution	Ensemble data		Potential governing case data	
			Mean	COV	0,5 % exceedence value located at	PDF dispersion given by
Yield stress [a]	ensemble	Gaussian	Table F.3	Table F.3	n/a	n/a
	potential governing case	Gaussian	n/a	n/a	minimum yield	15 ksi between 0,5 % exceedence limits
Average WT [b]	ensemble	Gaussian	1,006 9	0,025 9	n/a	n/a
Average OD [c, d]	ensemble	Gaussian	1,005 9	0,001 81	n/a	n/a
Ovality Eccentricity Residual stress	potential governing case [e, f]	Gaussian	n/a	n/a	see footnotes	see footnotes
Model uncertainty [g]	ensemble	Gaussian	0,999 1	0,067 0	n/a	n/a

[a] Design strength calculated for both cases, and the lower values taken.

[b] Normalized by specified wall thickness.

[c] Normalized by specified outside diameter.

[d] Low sensitivity factor (Figure F.15).

[e] Ht_{des} = 0,2 allows for one severe or two mild governing cases.

[f] Ensemble PDFs used for calculation of $k_{e\ des}$ and $k_{y\ des}$.

[g] Q&T pipe dataset.

F.5.4 Results

F.5.4.1 Down-rating factors

Down-rating factors (Table F.8) were calculated[84] for seamless pipe, for cold and hot rotary straightening, for a TRL of 0,5 %.

Table F.8 — Down-rating factors

Grade	Cold rotary straightened		Hot rotary straightened	
	$k_{e\ des}$	$k_{y\ des}$	$k_{e\ des}$	$k_{y\ des}$
H40	0,830	0,910	n/a	n/a
J/K55	0,830	0,890	n/a	n/a
M65	0,830	0,880	n/a	n/a
L80	0,825	0,855	0,825	0,865
L80 9Cr	0,825	0,830	0,825	0,840
L80 13Cr	0,825	0,830	0,825	0,840
N80 type 1	0,825	0,870	n/a	n/a
N80 Q&T	0,825	0,870	0,825	0,870
C90	n/a	n/a	0,825	0,850
C95	0,825	0,840	0,825	0,855
T95	n/a	n/a	0,825	0,855
P110	0,825	0,855	0,825	0,855
Q125	n/a	n/a	0,825	0,850

For the sake of simplicity, $k_{e\ des} = 0{,}825$ was adopted for all grades. Figure F.10 shows predicted failure probability for the new design equations[84]. It is nearly constant, in contrast to the highly variable reliability for the previous equations (Figure F.7). Moreover, it is likewise nearly constant for all grades and straightening methods.

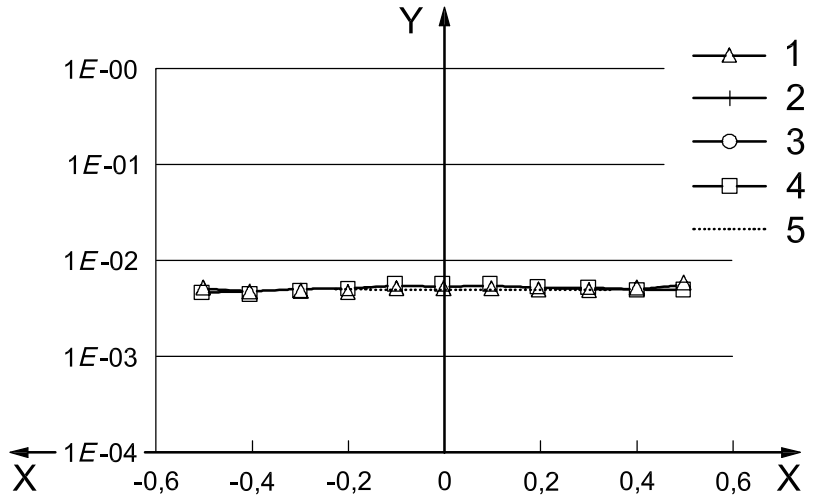

Key

X	log (yield/elastic strength)	3	P110
Y	predicted failure probability	4	Q125
1	J/K55	5	TRL
2	L80		

NOTE Seamless CRS, TRL = 0,005.

Figure F.10 — Predicted failure probabilities for probabilistic method

Figure F.11 shows design margin, as predicted ULS strength/design strength, for both the old and new design equations. The new equations give a much more uniform margin across the dataspace, and it is this which is giving the more uniform predicted failure probabilities.

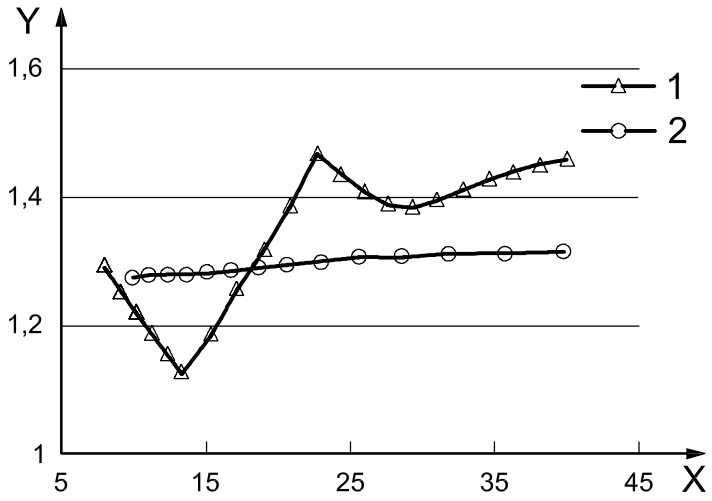

Key

X specified outside diameter/specified wall thickness

Y margin

1 API Bulletin 5C3[2]

2 probabilistic method (this annex)

NOTE L80 seamless CRS.

Figure F.11 — Comparison of design margin

F.5.4.2 Comparison with collapse test data

Figures F.12 and F.13 compare the proposed design collapse strengths against collapse test data (Table F.2). The smaller datasets are not statistically significant, and do not support firm conclusions. However, the larger datasets show that the required TRL is being achieved.

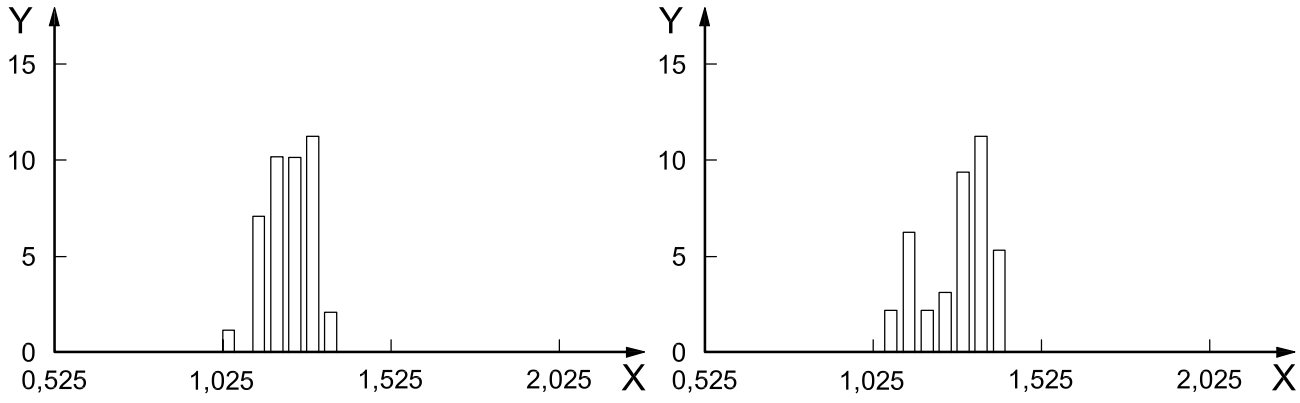

a) L80 HRS (41 tests) **b) P110 CRS (38 tests)**

Figure F.12 (*continued*)

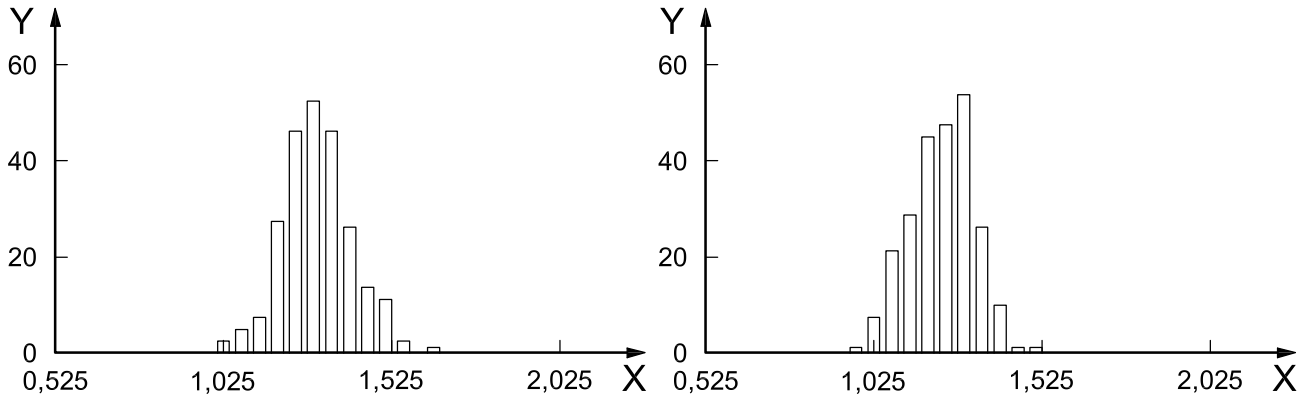

c) P110 HRS (234 tests) **d) Mfr FD00 P110 HRS (235 tests)**

Key

X actual/design collapse strength

Y occurrences

Figure F.12 — Comparison of design collapse strengths with collapse test data (sharp-kneed SSCs), $h_n = 0$

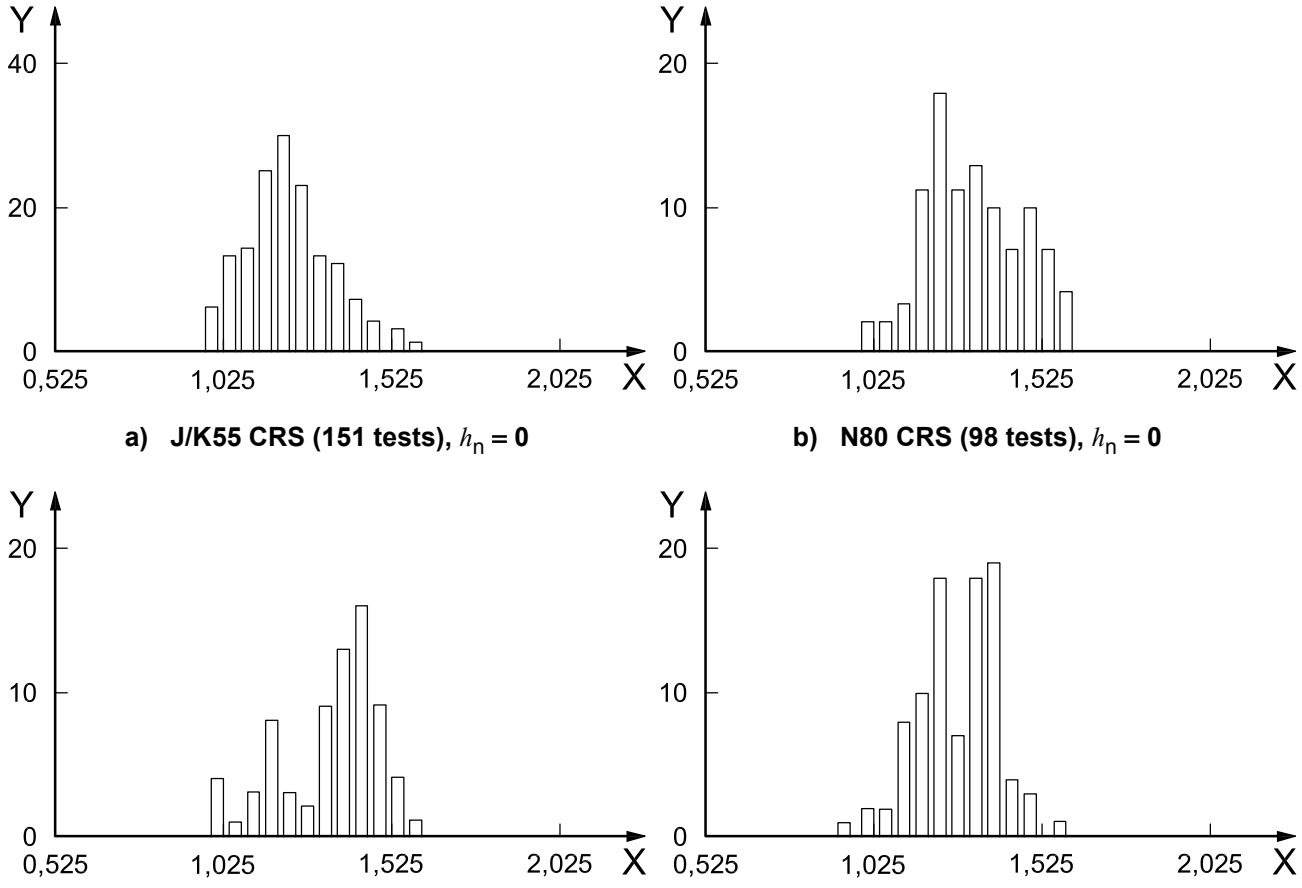

a) J/K55 CRS (151 tests), h_n = 0 **b) N80 CRS (98 tests), h_n = 0**

c) N80 HRS (73 tests), h_n = 0,014 **d) Mfr FD00 P110 CRS (93 tests), h_n = 0,053**

Key

X actual/design collapse strength

Y occurrences

Figure F.13 — Calibration of h_n via design strength (rounded-kneed SSCs)

It was, however, found necessary to omit six tests for 10 3/4 in 40.5 lb/ft N80 with high residual stresses from the test data catalogue, as all six tests gave low outliers (0,73 < actual/design strength < 1,01)[51]. It is therefore suggested that Equation (F.1) does not apply to very thin wall pipe [$\log_{10}(p_y/p_e) > 0{,}4$] with very high compressive residual stress ($rs/f_y < -0{,}5$).

F.5.4.3 Comparison with API Bulletin 5C3 [2]

Figure F.14 shows the change in design collapse strength with respect to the API Bulletin 5C3 [2] values, for seamless pipe and a TRL of 0,005[86]. A positive value denotes an increase in strength with respect to Reference [2], and a negative value a reduction in strength.

For Q&T CRS product, the new design strengths are 13 % to 17 % lower than the old values at the high-risk peak (D/t = 12 to 13), and 2 % to 7 % greater at the low-risk trough (D/t = 20 to 23). For Q&T HRS, the new strengths are also 13 % to 17 % lower at the high-risk peak, and 3 % to 8 % greater at the low-risk trough.

For non-Q&T product, the new strengths are 9 % to 17 % less than the old values at the high-risk peak (D/t = 13 to 16), and 5 % to 11 % greater at the low-risk trough (D/t = 23 to 28).

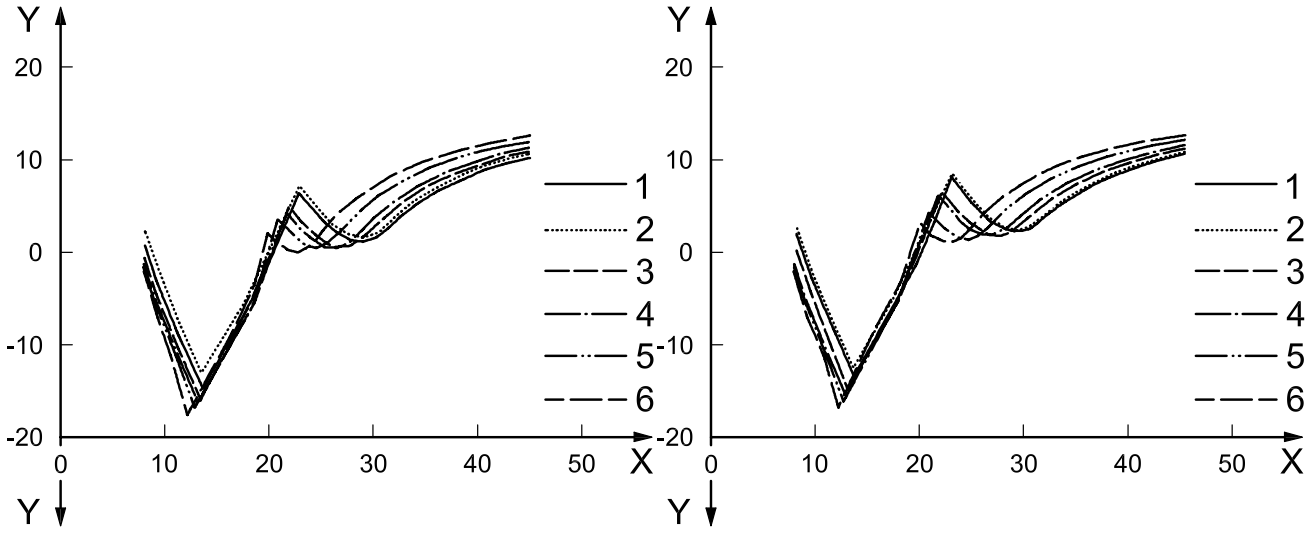

a) CRS (Ht_{des} = 0,22) **b) HRS** (Ht_{des} = 0,20)

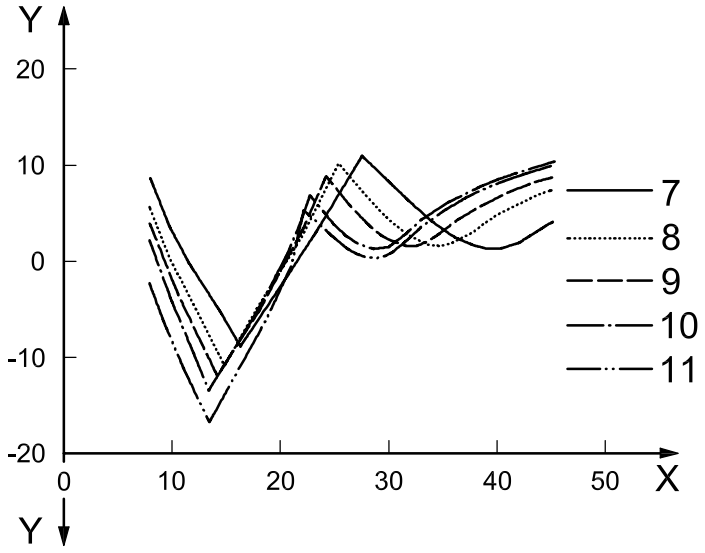

c) CRS (Ht_{des} = 0,22)

Figure F.14 (*continued*)

Key

X	specified outside diameter/specified wall thickness	6	Q125
Y	strength difference, %, with respect to API Bulletin 5C3[2]	7	H40
1	L80	8	J/K55
2	N80 Q&T	9	M65
3	C90	10	L80 9Cr and 13Cr
4	C95, T95	11	N80 type 1
5	P110		

Figure F.14 — Comparison of previous and revised design strengths

F.5.4.4 Sensitivity factors

Figure F.15 shows sensitivity factors (also called alpha values) versus dataspace position, for a TRL of 0,005[86]. They are a measure of the sensitivity of failure probability to each input variable[52], [81], [103], and may therefore be employed by manufacturers and users to gauge the effect of changes in production quality on safety. The values given are for L80 seamless CRS and the ensemble production quality statistics (Tables F.3, F.4).

NOTE In the ULS equation, eccentricity, ovality and residual stress have empirically derived coefficients. The accuracy of their sensitivity factors is therefore likely to be rather lower than for the other variables, which have a stronger theoretical basis.

Model uncertainty is the dominant variable over most of the dataspace, with $\alpha = 0{,}76$ to 0,69; this means that the remaining limitations of the collapse strength equations have a rather greater effect than all the other input variables put together. At the left-hand (yield) end of the dataspace, yield stress has the next largest effect, with $\alpha = 0{,}54$: this is expected, given the form of the yield collapse equation and the various COVs (Table F.4). As one goes rightwards across the dataspace, the contribution (and alpha) of each variable changes. At the right-hand (elastic) end of the dataspace, wall thickness has narrowly the greatest effect, with $\alpha = 0{,}71$, and variables other than model uncertainty having negligible influence.

Comparison analyses[46] have shown that sensitivity factors vary significantly by manufacturer and product. Mills are therefore encouraged to develop their own values, using the methods described in Annex H.

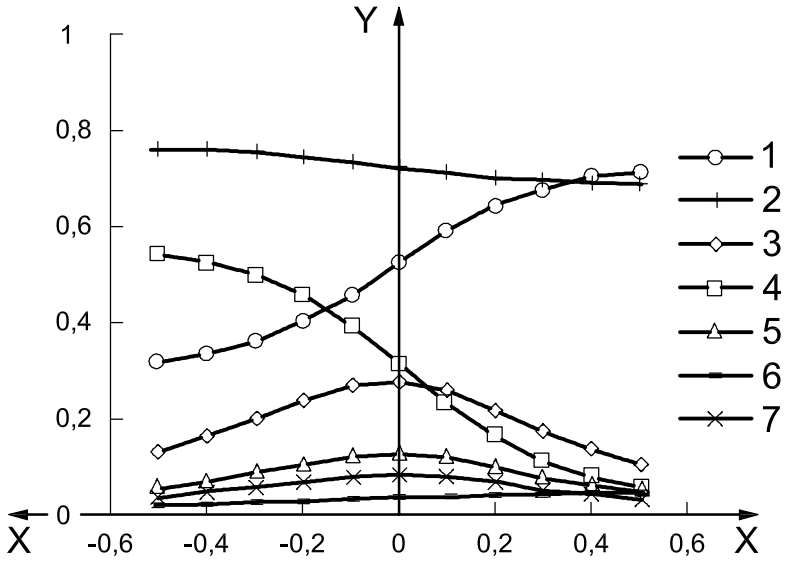

Key

X	log (yield/elastic strength)	4	yield stress
Y	sensitivity factor	5	ovality
1	average wall thickness	6	average outside diameter
2	model uncertainty	7	eccentricity
3	residual stress		

Figure F.15 — Sensitivity factors

F.6 Summary

F.6.1 Design equation (governing case PDFs)

The minimum (or design) collapse strength for pipe under external pressure only is given by Equation (F.22). For pipe under external pressure and axial force and/or internal pressure, see F.4.2.2.

$$p_{\text{des}} = \{(p_{\text{e des}} + p_{\text{y des}}) - [(p_{\text{e des}} - p_{\text{y des}})^2 + 4p_{\text{e des}}\, p_{\text{y des}}\, Ht_{\text{des}}]^{1/2}\}/[2\,(1 - Ht_{\text{des}})] \quad \text{(F.22)}$$

where

$$p_{\text{e des}} = 0{,}825 \times 2E/[(1 - \nu^2)\,(D/t)\,((D/t) - 1)^2] \quad \text{(F.23)}$$

$$p_{\text{y des}} = k_{\text{y des}} \times 2f_{\text{ymn}}\,(t/D)\,[1 + t/(2D)] \quad \text{(F.24)}$$

and

D is the specified outside diameter;

E is Young's modulus, 30×10^6 psi $= 206{,}9 \times 10^9$ N/m^2;

f_{ymn} is the specified minimum yield strength;

Ht_{des} is a decrement factor: 0,22 for CRS product and 0,20 for HRS;

$k_{\text{y des}}$ is the down-rating factor for design yield collapse, Table F.9;

p_{des} is the design collapse pressure;

$p_{\text{e des}}$ is the design elastic collapse term;

$p_{\text{y des}}$ is the design yield collapse term;

t is the specified wall thickness;

ν is Poisson's ratio, 0,28.

Table F.9 — Values of Ht_{des} and $k_{y\,des}$

Grade [a]	Cold rotary straightened		Hot rotary straightened	
	Ht_{des} [b]	k_{ydes} [b]	Ht_{des} [b]	k_{ydes} [b]
H-40	0,22	0,910	Not applicable [c]	
J-55	0,22	0,890	Not applicable [c]	
K-55	0,22	0,890	Not applicable [c]	
M-65	0,22	0,880	Not applicable [c]	
L-80	0,22	0,855	0,20	0,865
L-80 9Cr	0,22	0,830	0,20	0,840
L-80 13Cr	0,22	0,830	0,20	0,840
N-80 type 1	0,22	0,870	Not applicable [c]	
N-80 Q&T	0,22	0,870	0,20	0,870
C-90	Not applicable [d]		0,20	0,850
C-95	0,22	0,840	0,20	0,855
T-95	Not applicable [d]		0,20	0,855
P-110	0,22	0,855	0,20	0,855
Q-125	Not applicable [d]		0,20	0,850

[a] The data for the specified grade should be used; do not interpolate for actual yield stress.

[b] Ht_{des} and $k_{y\,des}$ are dimensionless, and can be used with any consistent units system.

[c] Hot rotary straightening not normally used for this grade.

[d] ISO 11960 or API 5CT does not allow cold rotary straightening.

F.6.2 Assumptions and limitations

Equation (F.22) is based on an ultimate limit state (ULS) equation, pipe dimension and stress statistics (that is, the statistical variation of measured pipe OD, wall thickness, yield stress, etc.), and a target reliability level (TRL).

The ULS equation predicts the pipe failure pressure; that is, it does not include a safety factor. It was chosen to give the best fit to collapse test results for 2 986 samples of Q&T pipe, manufactured between 1977 and 2000. All tests were conducted at room temperature; therefore, the collapse design factor should allow for any use at elevated temperatures.

Equation (F.22) (the design equation) was developed from the ULS equation using pipe dimension and stress statistics from at least 14 API mills, mostly for modern pipe, to satisfy a TRL of 0,005 for moderate production worst cases. This is broadly consistent with the TRL specified for plastic collapse in API Bulletin 5C3[2].

The production quality statistics were based on worldwide API production, and thus the predicted reliability level for any individual mill and product can differ from 0,005. Annexes G and H give procedures for the calculation of case-specific design collapse strengths from collapse test data and pipe dimension and stress statistics respectively.

The design strengths assume rounded-kneed stress-strain curves (SSCs) for cold rotary straightened product, and sharp-kneed SSCs for hot rotary straightened product. Therefore, the CRS design strengths are slightly conservative for pipe with sharp-kneed SSCs, and the HRS design strengths are slightly unconservative for pipe with rounded-kneed SSCs.

Equation (F.22) does not directly check the onset of yield, and therefore does not cover sour service. If required, yield onset should be checked separately using the von Mises equations in 6.4.

F.6.3 Example

F.6.3.1 Design collapse strength

Calculate the design collapse strength for 9-5/8 in 53,5 lb/ft L80 cold rotary straightened product. For 9-5/8 in 53.5 lb/ft, $t = 0.545$ in, and for L80 CRS, $k_{y\ des} = 0.855$ and $Ht_{des} = 0.22$ (Table F.9), so, in USC units:

$$p_{e\ des} = 0.825 \times 2 \times 30 \times 10^6/[(1 - 0.28^2)\ (9.625/0.545)\ ((9.625/0.545) - 1)^2] = 10\ 957 \text{ psi} \quad \text{(F.25)}$$

$$p_{y\ des} = 0.855 \times 2 \times 80\ 000\ (0.545/9.625)\ \{[1 + [0.545/(2 \times 9.625)]\} = 7\ 965 \text{ psi} \quad \text{(F.26)}$$

$$p_{des} = \{(10\ 957 + 7\ 965) - [(10\ 957 - 7\ 965)^2 + (4 \times 10\ 957 \times 7\ 965 \times 0.22)]^{1/2}\}/[2\ (1 - 0.22)] = 6\ 194 \text{ psi} \quad \text{(F.27)}$$

F.6.3.2 Design collapse strength under combined loads

Repeat the example in F.6.3.1 for an internal pressure of 5 000 psi, applied together with a tensile axial stress of 20 000 psi. From F.4.2.2:

$$\Delta p_{y\ T\ des} = 2 \times 0.855 \times 80\ 000 \times 0.060\ 02 = 8\ 211 \text{ psi} \quad \text{(F.28)}$$

$$A_o = \pi \times 9.625^2/4 = 72.76 \text{ in}^2 \quad \text{(F.29)}$$

$$A_i = \pi \times 8.535^2/4 = 57.21 \text{ in}^2 \quad \text{(F.30)}$$

$$A_s = 72.76 - 57.21 = 15.55 \text{ in}^2 \quad \text{(F.31)}$$

$$F_{y\ des} = 0.855 \times 80\ 000 \times 15.55 = 1\ 063 \text{ kip} \quad \text{(F.32)}$$

$$F_{ax} = 20\ 000 \times 15.55 = 310.9 \text{ kip} \quad \text{(F.33)}$$

If a root-finding routine is available, p_o can be obtained as the root of [see Equation (F.14)]:

$$f(p_o) = \Delta p_{y\ vme\ des}(p_o) - p_o + p_i = 0 \quad \text{(F.34)}$$

Otherwise, iteration can be started by assuming $p_o \cong \Delta p_{y\ T\ des} + p_i = 8\ 211 + 5\ 000 = 13\ 211$ psi. Then, from Equation (F.15):

$$F_{eff} = 310\ 900 - (5\ 000 \times 57.21) + (13\ 211 \times 72.76) = 986.1 \text{ kip} \quad \text{(F.35)}$$

In Equation (F.14):

$$\Delta p_{y\ vme\ des} = (4/3^{1/2})\ 0.855 \times 80\ 000\ [0.545/(9.625 - 0.545)]\ [1 - (986.1/1\ 063)^2]^{1/2} = 3\ 549 \text{ psi} \quad \text{(F.36)}$$

The starting value for the next iteration is obtained as:

$$p_{o\ new} = 0.5\ (p_o + \Delta p_{y\ vme\ des} + p_i) = 0.5\ (13\ 211 + 3\ 549 + 5\ 000) = 10\ 880 \text{ psi} \quad \text{(F.37)}$$

The remainder of the iterations are given in Table F.10 below. Other iterative methods (e.g. Newton-Raphson) can be used if desired.

Table F.10 — Iteration for p_o

p_o psi	F_{eff} kip	$\Delta p_{y\ vme\ des}$ psi	$p_{o\ new}$ psi
13 211	986.1	3 549	10 880
10 880	816.5	6 074	10 977
10 977	823.6	5 998	10 988
10 988	824.3	5 990	10 989
10 989	824.4	5 989	10 989

$\Delta p_{y\ vme\ des} < \Delta p_{y\ T\ des}$, hence $\Delta p_{y\ des} = \Delta p_{y\ vme\ des} = 5\ 989$ psi, and:

$$\Delta p_{des} = \{(10\ 957 + 5\ 989) - [(10\ 957 - 5\ 989)^2 + (4 \times 10\ 957 \times 5\ 989 \times 0.22)]^{1/2}\}/[2\ (1 - 0.22)] = 5\ 043 \text{ psi} \quad \text{(F.38)}$$

$$p_{o\ des} = 5\ 043 + 5\ 000 = 10\ 043 \text{ psi} \quad \text{(F.39)}$$

Annex G
(informative)

Calculation of design collapse strength from collapse test data

G.1 Introduction

The design collapse strengths in Annex F were calculated for API pipe only, and do not apply to non-API cases such as high-collapse pipe or special sour service grades (e.g. C110). This annex describes the calculation procedure used to obtain design collapse strengths for non-API product, using collapse test data. Manufacturers may also, if desired, develop design collapse strengths for API pipe. All case-specific collapse strengths should be substantiated by provision, upon request, of collapse test datasets.

Design collapse strength calculated from test data is subject to statistical uncertainty. The uncertainty increases as dataset size n reduces. For very large datasets ($n \geqslant 1\,000$), its effect is negligible, and design collapse strength may be calculated as in G.3. For smaller datasets ($n < 1\,000$), the effect is significant, and design collapse strength should be calculated as in G.4. In both cases, it is assumed that the collapse test data are homogeneous; that is, the mean and dispersion are constant during production.

G.2 Collapse test data

All collapse test data should be for the size/weight/grade combination and manufacturing process for which design collapse strengths are to be calculated. The manufacturing process is deemed to include forming process, heat treatment, and rotary straightening. The minimum length of the test specimen should be:

— eight times the specified diameter for specified diameters of 9-5/8 and below;

— seven times the specified diameter for specified diameters of 10-3/4 and above.

G.3 Large datasets

The design collapse strength should be calculated from Equation (G.1):

$$p_{\text{des}} = \mu_{\text{s}} - 2{,}576\ \sigma_{\text{s}} \qquad \text{(G.1)}$$

where

p_{des} is the design collapse strength, for a target reliability level (TRL) of 0,5 %;

μ_{s} is the mean of collapse test dataset;

σ_{s} is the standard deviation of collapse test dataset $= [\Sigma_{i=1}^{n} (p_{\text{ult i}} - \mu_{\text{s}})^2/(n-1)]^{1/2}$.

This method should not be used for $n < 1\,000$.

G.4 Small datasets

G.4.1 Calculation method

The design collapse strength should be calculated from Equation (G.2):

$$p_{\text{des }0,95} = \mu_s - F\,\sigma_s \tag{G.2}$$

where

$p_{\text{des }0,95}$ is the 95 % confidence design collapse strength, for a target reliability level (TRL) of 0,5 %;

μ_s is the mean of collapse test dataset;

σ_s is the standard deviation of collapse test dataset = $[\Sigma_{i\,=\,1}^{n}\,(p_{\text{ult i}} - \mu_s)^2/(n-1)]^{1/2}$;

n is the number of collapse tests;

F is a correction factor for dataset size, Table G.1[85]. Values not tabulated may be obtained as[85]:

$$F = 24{,}327\,20 - 57{,}455\,45\ \log_{10}n + 72{,}102\,44\ (\log_{10}n)^2 - 52{,}727\,79\ (\log_{10}n)^3 + 23{,}641\,13\ (\log_{10}n)^4 - 6{,}416\,48\ (\log_{10}n)^5 + 0{,}969\,53\ (\log_{10}n)^6 - 0{,}062\,67\ (\log_{10}n)^7 \tag{G.3}$$

$p_{\text{des }0,95}$ has a 95 % probability of being lower than the large-dataset value ($n = \infty$). Equation (G.3) is valid for $10 \leqslant n \leqslant 1\,000$. It should not be used for $n < 10$.

Table G.1 — Dataset size factor F (TRL = 0,5 %)

n	F	n	F	n	F	n	F
3	11,628	16	3,812	70	3,051	300	2,786
4	7,748	18	3,710	80	3,016	400	2,756
5	6,313	20	3,628	90	2,987	500	2,736
6	5,566	25	3,478	100	2,963	600	2,722
7	5,103	30	3,376	110	2,942	700	2,710
8	4,787	35	3,300	120	2,925	800	2,701
9	4,556	40	3,242	130	2,910	900	2,694
10	4,378	45	3,195	140	2,896	1 000	2,688
12	4,122	50	3,157	150	2,884	∞	2,576
14	3,944	60	3,096	200	2,837		

Figure G.1 shows how reduction in design strength varies with n and dataset coefficient of variance (COV = σ_s/μ_s). Note the analysis does not imply that mean collapse strength reduces with n; rather, the decrease in design strength allows for sampling uncertainty as n reduces. In particular, small datasets usually underestimate standard deviation[85].

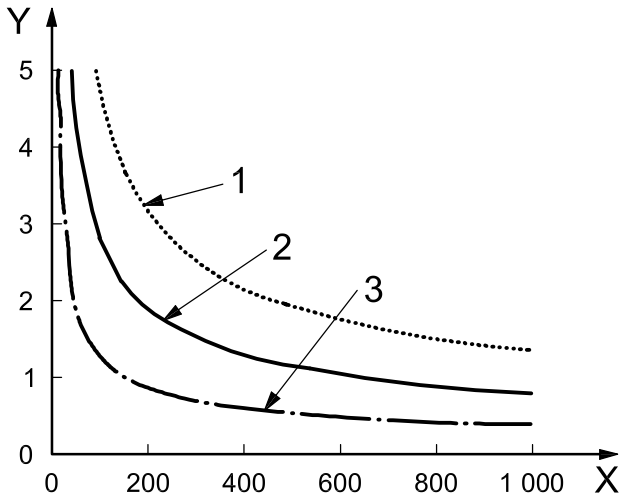

Key

X dataset size

Y reduction with respect to large dataset limit, %

1 coefficient of variance = 0,09

2 coefficient of variance = 0,06

3 coefficient of variance = 0,03

Figure G.1 — Reduction in design strength vs. dataset size

G.4.2 Derivation

As dataset size reduces, the uncertainty in sample mean and standard deviation (SD) increases, and it becomes necessary to treat them as random variables. For a Gaussian population, sample mean is Gaussian-distributed, and sample variance is chi-squared[72]; therefore, the minimum value is distributed as non-central Student's t [77], [69], [89]. The values in Table G.1 were calculated[85] using Lenth's algorithm for the non-central t CDF[76], and checked via numerical integration of the PDF expressions of Rinne[93] and Wolfram[107] for $n \leqslant 150$, and using the Gaussian approximation of Eisenhart *et al*. [61] for $n \geqslant 200$.

G.4.3 Example

Sixty-eight collapse tests were performed for a production run of 7 in 23.0 lb/ft HC95 HRS. The aim points and process conditions were held steady during production. The sample mean and standard deviation were 6,609 and 0.331 8 ksi respectively. Calculate the design collapse strength.

From Equation (G.3):

$$F = 24.327\,20 - 57.455\,45 \log_{10}68 + 72.102\,44 (\log_{10}68)^2 - 52.727\,79 (\log_{10}68)^3 + 23.641\,13 (\log_{10}68)^4 - 6.416\,48 (\log_{10}68)^5 + 0.969\,53 (\log_{10}68)^6 - 0.062\,67 (\log_{10}68)^7 = 3.059 \quad \text{(G.4)}$$

From Equation (G.2):

$$p_{\text{des } 0.95} = 6.609 - 3.059 \times 0.331\,8 = 5.594 \text{ ksi} \quad \text{(G.5)}$$

This compares with 5.754 ksi (a 2.9 % increase) had the design strength been calculated without the correction.

Annex H
(informative)

Calculation of design collapse strengths from production quality data

H.1 Introduction

The design collapse strengths in Annex F were calculated for API pipe only, and do not apply to non-API cases such as high-collapse pipe or special sour service grades (e.g. C110). This Annex describes the calculation procedure used to obtain design collapse strengths for non-API product, using production quality data. Manufacturers may also, if desired, develop design collapse strengths for API pipe. All case-specific collapse strengths should be substantiated by provision, upon request, of current production quality statistics and model uncertainty data.

Design collapse strength calculated from measurement data is subject to statistical uncertainty. The uncertainty increases as dataset size n reduces. For very large datasets ($n \geqslant 1\,000$), its effect is negligible, and design collapse strength may be calculated as in H.3.2 and H.3.4.1. For smaller datasets ($n < 1\,000$), the effect is significant, and design collapse strength should be calculated as in H.3.3 and H.3.4.2. In both cases, it is assumed that the production quality data are homogeneous; that is, the means and dispersions are constant during production.

The calculation procedure is in two main parts, namely:

— measurement and statistical characterization of the parameters determining collapse strength (average outside diameter, average wall thickness, eccentricity, ovality, yield stress, residual stress, and model uncertainty);

— probabilistic analysis, to determine the down-rating factors which satisfy the required safety level.

These are described in turn below.

H.2 Production quality data

H.2.1 Representativeness

Data representativeness should be as specified in Table H.1 below. Measurement of each parameter should be in accordance with Annex I.

Table H.1 — Data representativeness

Parameter	Data should be for the applicable
Average outside diameter	forming process [a]
Average wall thickness	forming process [a]
Eccentricity	forming process [a]
Ovality	forming process [a]
Yield stress	grade, heat treatment, and rotary straightening type
Residual stress	rotary straightening type
Collapse pressure	[b]

[a] Pipe geometry data are not required for the sizes and weights for which design collapse strengths are to be calculated, but the range of sizes and weights chosen should be representative of the product.

[b] Collapse strengths are only used to develop model uncertainty data, and therefore the collapse tests need not be for the manufacturing process (forming process, heat treatment, and rotary straightening) for which design collapse strengths are to be calculated. However, the dataset used should be representative of the product.

H.2.2 Data analysis

H.2.2.1 Pipe dimensions and stresses

Average outside diameter, average wall thickness, yield stress and residual stress are then generalized via the use of bias factors, as follows:

— average outside diameter: actual value/specified outside diameter;

— average wall thickness: actual value/specified wall thickness;

— yield stress: actual value/specified minimum yield stress;

— residual stress: actual value/actual yield stress.

The mean and coefficient of variance (COV, standard deviation/mean) of each bias factor is then calculated. Eccentricity and ovality are already in bias form, hence the mean and COV are obtained directly from the measured values.

H.2.2.2 Model uncertainty

Model uncertainty is obtained by calculating:

— the predicted collapse pressure for each collapse test sample, using the Klever-Tamano ULS equation [Equation (F.1)] with the measured pipe dimensions and stresses;

— actual/predicted collapse pressure for each sample;

— the mean and COV of actual/predicted collapse pressure for the collapse test dataset.

H.3 Probabilistic analysis

H.3.1 Analysis method

H.3.1.1 Probabilistic analysis

A recognized technique (e.g. FORM, SORM, Monte Carlo) should be used.

H.3.1.2 Ultimate collapse strength equation

The ultimate collapse strength should be calculated from Equation (F.21). More general forms of the Klever-Tamano Equation[74] may be used if desired, but values of additional factors should be properly substantiated by calibration against a statistically significant amount of collapse test data.

H.3.1.3 Design collapse strength equation

The design collapse strength should be calculated from Equation (F.5), with the decrement factor Ht_{des} obtained using

$$Ht_{\text{des}} = 0{,}127\mu_{\text{ov}} + 0{,}003\,9\mu_{\text{ec}} - 0{,}440\,(\mu_{\text{rs}}/\mu_{\text{fy}}) + h_{\text{n}} \tag{H.1}$$

where

h_{n} is the stress-strain curve shape coefficient;

μ_{ec} is the mean eccentricity, in percent, $ec = 100\,(t_{\text{c max}} - t_{\text{c min}})/t_{\text{c ave}}$;

μ_{fy} is the mean actual yield strength;

μ_{ov} is the mean ovality, in percent, $ov = 100\,(D_{\text{max}} - D_{\text{min}})/D_{\text{ave}}$;

μ_{rs} is the mean residual stress (compression at ID face is negative);

and $h_{\text{n}} = 0{,}017$ for cold rotary straightened (CRS) product, and $h_{\text{n}} = 0$ for hot rotary straightened (HRS) product.

H.3.1.4 Target reliability level

The target reliability level (TRL) should be 0,005.

H.3.2 Data — Large datasets

Input variable data should be as specified in Table H.2 below.

Potential governing case data may be used instead of ensemble data if required (see F.3.4 and F.5.3). In this event, the probability distribution and PDF parameters should generally be for an individual lot or batch. The distribution chosen should be justified by plotting the data frequency distribution onto probability scales[52], [103].

Table H.2 — Probability data — Large datasets

Parameter	Probability distribution	PDF parameters
Average outside diameter	Gaussian	deterministic, μ, σ = as calculated in H.2.2.1
Average wall thickness	Gaussian	deterministic, μ, σ = as calculated in H.2.2.1
Eccentricity	two-parameter Weibull [a]	deterministic, B, C = as calculated in Equations (H.2) and (H.3)
Ovality	two-parameter Weibull [a]	deterministic, B, C = as calculated in Equations (H.2) and (H.3)
Yield stress	Gaussian	deterministic, μ, σ = as calculated in H.2.2.1
Residual stress	Gaussian	deterministic, μ, σ = as calculated in H.2.2.1
Model uncertainty	Gaussian	deterministic, μ, σ = as calculated in H.2.2.2

[a] For worst case PDF data with COV < 0.2, the Gaussian distribution is generally applicable.

For two-parameter Weibull distributions, the PDF parameters should be calculated from:

Shape parameter C obtained as solution of $\{\Gamma[1 + (2/C)]\}/\{\Gamma[1 + (1/C)]\}^2 - 1 - (\sigma/\mu)^2 = 0$ (H.2)

Scale parameter $B = \mu/\Gamma\,[1 + (1/C)]$ (H.3)

where

μ is the mean;

σ is the standard deviation;

Γ denotes the gamma function[40].

Equation (H.2) can be solved by iteration, or by using the root-finding function in a mathematical spreadsheet.

H.3.3 Data — Small datasets

Input variable data should be as specified in Table H.3 below[72]. Large-dataset PDFs (Table H.2) may be used for any variables with $n \geqslant 1\,000$.

Potential governing case data can be used instead of ensemble data if required (see F.3.4 and F.5.3). In this event, the probability distribution and PDF parameters should generally be for an individual lot or batch. The distribution chosen should be justified by plotting the data frequency distribution onto probability scales[52], [103].

Table H.3 — Probability data —Small datasets

Parameter	Probability distribution	PDF parameters
Average OD	Gaussian	random
Average OD: mean	Gaussian	$\mu = \mu_S$ (as calculated in H.2.2.1), $\sigma = \sigma_S/n^{0,5}$
Average OD: SD	Gaussian [a]	$\mu = \sigma_S$ (as calculated in H.2.2.1), $\sigma = \sigma_S/(2n)^{0,5}$
Average WT	Gaussian	random
Average WT: mean	Gaussian	$\mu = \mu_S$ (as calculated in H.2.2.1), $\sigma = \sigma_S/n^{0,5}$
Average WT: SD	Gaussian [a]	$\mu = \sigma_S$ (as calculated in H.2.2.1), $\sigma = \sigma_S/(2n)^{0,5}$
Eccentricity	two-parameter Weibull [b]	random
Eccentricity: scale parameter	Gaussian [c]	$\mu_B = B$ from Equations (H.4) and (H.5), σB from Equations (H.6) to (H.9)
Eccentricity: shape parameter	log-normal [c]	$\mu_C = C$ from Equation (H.4), σC from Equations (H.5) to (H.10)
Ovality	two-parameter Weibull [b]	random
Ovality: scale parameter	Gaussian [c]	$\mu_B = B$ from Equations (H.4) and (H.5), σB from Equations (H.6) to (H.9)
Ovality: shape parameter	log-normal [c]	$\mu_C = C$ from Equation (H.4), σC from Equations (H.5) to (H.10)
Yield stress	Gaussian	random
Yield stress: mean	Gaussian	$\mu = \mu_S$ (as calculated in H.2.2.1), $\sigma = \sigma_S/n^{0,5}$
Yield stress: SD	Gaussian [a]	$\mu = \sigma_S$ (as calculated in H.2.2.1), $\sigma = \sigma_S/(2n)^{0,5}$
Residual stress	Gaussian	random
Residual stress: mean	Gaussian	$\mu = \mu_S$ (as calculated in H.2.2.1), $\sigma = \sigma_S/n^{0,5}$
Residual stress: SD	Gaussian [a]	$\mu = \sigma_S$ (as calculated in H.2.2.1), $\sigma = \sigma_S/(2n)^{0,5}$
Model uncertainty	Gaussian	random
Model uncertainty: mean	Gaussian	$\mu = \mu_S$ (as calculated in H.2.2.2), $\sigma = \sigma_S/n^{0,5}$
Model uncertainty: SD	Gaussian [a]	$\mu = \sigma_S$ (as calculated in H.2.2.2), $\sigma = \sigma_S/(2n)^{0,5}$

[a] Strictly, $n\sigma_S^2/\sigma^2$ is chi-square distributed, where σ_S = sample SD, σ = process SD; but as σ is unknown, this does not enable PDF calculation. In practice, a Gaussian PDF can be used for $n \geqslant 20$, as the chi-square PDF tends to the Gaussian PDF for large n.

[b] For worst case PDF data with COV < 0,2, the Gaussian distribution is generally applicable.

[c] See Reference [86].

The sampling uncertainties for two-parameter Weibull variables can be calculated as below[79], [86]. C is obtained as the solution of Equation (H.4):

$$(1/C) + (1/n)\,[\Sigma_{i=1}^{n} \ln(x_i)] - [\Sigma_{i=1}^{n} x_i^{\,C} \ln(x_i)]\,[\Sigma_{i=1}^{n} x_i^{C}]^{-1} = 0 \qquad \text{(H.4)}$$

where

n is the dataset size;

x_i is the measurements;

and $\Sigma_{i=1}^{n}$ denotes a sum taken over the terms $i = 1, 2, \ldots, n$.

Equation (H.4) can be solved by iteration or by using the root-finding function in a mathematical spreadsheet.

$$B = [(\Sigma_{i=1}^{n} x_i^C)/n]^{1/C} \quad \text{(H.5)}$$

$$\partial^2 \ln L/\partial B^2 = CB^{-2}\,[n - (C+1)\,B^{-C}\,\Sigma_{i=1}^{n} x_i^C] \quad \text{(H.6)}$$

$$\partial^2 \ln L/\partial C^2 = -nC^{-2} - B^{-C}\,\{\Sigma_{i=1}^{n} x_i^C\,[\ln(x_i)]^2 + \ln(B)\,[2\,\Sigma_{i=1}^{n} x_i^C \ln(x_i) - \Sigma_{i=1}^{n} x_i^C]\} \quad \text{(H.7)}$$

$$\partial^2 \ln L/\partial B\partial C = -nB^{-1} + B^{-(C+1)}\,\{C\,\Sigma_{i=1}^{n} x_i^C \ln(x_i) + [1 - C\ln(B)]\,\Sigma_{i=1}^{n} x_i^C\} \quad \text{(H.8)}$$

$$\sigma B = \{\text{abs}[\partial^2 \ln L/\partial C^2\,(\partial^2 \ln L/\partial B^2\,\partial^2 \ln L/\partial C^2 - (\partial^2 \ln L/\partial B\partial C)^2)^{-1}]\}^{0,5} \quad \text{(H.9)}$$

$$\sigma C = \{\text{abs}[\partial^2 \ln L/\partial B^2\,(\partial^2 \ln L/\partial B^2\,\partial^2 \ln L/\partial C^2 - (\partial^2 \ln L/\partial B\partial C)^2)^{-1}]\}^{0,5} \quad \text{(H.10)}$$

H.3.4 Analysis procedure

H.3.4.1 Large datasets

To calculate design strengths for a range of pipe sizes, the method should be as follows.

a) Calculate the PDF parameters for each input variable, for measurements as specified in H.2.

b) For a given grade, heat treatment, and rotary straightening type, calculate the D/t implied by dataspace positions $\log_{10}(p_y/p_e)$ of −0,5 to +0,5 by intervals of 0,2, with p_e and p_y from Equations (F.6) and (F.7) respectively.

c) Calculate the design collapse strength for each dataspace position, using Equation (F.5) with the specified values of the input variables, and assumed values of $k_{e\,des}$ and $k_{y\,des}$. The decrement factor Ht_{des} is obtained from Equation (H.1).

d) Calculate the predicted failure probability (ϕ_f) for each dataspace position, for a deterministic load L_{nom} given by the design collapse strength in each case. Either correlated or independent variable analysis may be used; the former is more accurate but more complicated, whereas the latter is simpler but slightly conservative[87]. ϕ_f is the probability of collapse strength being less than the design strength. Plot ϕ_f against dataspace position.

e) Iterate over steps c) and d), adjusting $k_{e\,des}$ and $k_{y\,des}$ so as to obtain the flattest possible reliability response over the data space, and an average ϕ_f within ±10 % of the TRL.

f) Use the final values of $k_{e\,des}$ and $k_{y\,des}$ in Equation (F.5), with Ht_{des} as calculated in step c), to obtain design collapse strengths for the desired pipe sizes and masses.

If only a single pipe size is of interest, the design strength can be calculated by setting D and t to the appropriate values, and calculating ϕ_f for a range of deterministic loads L_{nom}. The design strength is the value of L_{nom} to give ϕ_f equal to the TRL.

H.3.4.2 Small datasets

This approach should be used whenever the smallest dataset contains fewer than 1 000 samples. For simplicity, the method for a single pipe case is described.

a) Calculate the PDF parameters for each input variable sample, for measurements as specified in H.2, and the relevant values of D and t.

b) For the input variables with fewer than 1 000 samples, determine the sampling uncertainties of each PDF parameter, as described in H.3.3. For input variables with $n > 1\,000$, the PDF parameters can be taken as deterministic, with the values calculated in a) above.

c) Use the sampling uncertainties to develop a minimum of 10 000 random realizations for each PDF parameter. This can be done by the inverse transform method[52], [81], [103], or by using the random-variates generation facility in a mathematical spreadsheet.

d) Calculate the predicted failure probability (ϕ_f) for a given deterministic load L_{nom}, for each realization of PDF parameters. Either correlated or independent variable analysis can be used; the former is more accurate but more complicated, whereas the latter is simpler but slightly conservative[87]. The sample correlation coefficients can be used as an approximation to the correlations for each realization; this gives reasonable results in practice[87].

e) Plot the frequency of occurrence of ϕ_f; that is, its probability distribution.

f) Interpolate the cumulative probability distribution for the 95 % confidence value.

g) Repeat steps d) to f) for a range of load levels L_{nom}, chosen so as to make the 95 % confidence ϕ_f bracket the TRL.

h) The design strength is the value of L_{nom} to give a 95 % confidence ϕ_f equal to the TRL. This can be obtained by interpolation.

H.4 Example

H.4.1 Large datasets

H.4.1.1 Introduction

This example uses the P110 hot rotary straightened (HRS) data for mill FD00 of Annex F. The calculation steps are as in H.3.4. First, all the measurement datasets will be assumed to contain more than 1 000 samples, such that calculation of sampling uncertainty is not required.

H.4.1.2 Single pipe size

Determine the design collapse strength for 9-5/8 in 47 lb/ft P110 HRS from mill FD00.

a) First, we determine the input variable PDF parameters. These are given in Tables F.2, F.3 and F.4 and are reproduced in Table H.4 below.

Table H.4 — Input variable PDFs (bias and COV format)

Variable	Mean	COV	Distribution	Units
Average OD	1.007 1	0.001 89	Gaussian	—
Average WT	1.006 8	0.021 7	Gaussian	—
Yield stress	1.160	0.035 4	Gaussian	—
Ovality	0.241	0.338	two-parameter Weibull	%
Eccentricity	5.170	0.317	two-parameter Weibull	%
Residual/yield	−0.142	0.189	Gaussian	—
Model uncertainty	0.968 1	0.054 3	Gaussian	—

b) Some of the PDF parameters are in dimensionless (generalized) format, and must be converted to means and standard deviations (SDs) for the pipe size of interest. The dimensional means are obtained as specified value × bias, that is:

— mean average outside diameter = 9.625 × 1.007 1 = 9.693 in;

— mean average wall thickness = 0.472 × 1.006 8 = 0.475 2 in;

— mean yield stress = 110 × 1.160 = 127.6 ksi;

— the residual stress data are normalized by yield, and need to be converted to a stress proper, as follows:

$$\mu_{rs} \cong \mu_{rs/fy} \times \mu_{fy} = \mu_{rs/fy} \times (\mu_{fy}/f_{ymn}) \times f_{ymn} = -0.142 \times 1.160 \times 110 = -18.12 \text{ ksi} \quad \text{(H.11)}$$

$$COV_{rs} \cong (COV_{rs/fy}^2 - COV_{fy}^2)^{0.5} \text{ (assuming SRSS)} = (0.189^2 - 0.035\,4^2)^{0.5} = 0.186 \quad \text{(H.12)}$$

The SDs are obtained as dimensional mean × COV. Table H.5 summarizes the various values.

Table H.5 — Input variable PDFs (mean and SD format, 9-5/8 in 47 lb/ft P110 HRS)

Variable	Mean	SD	Distribution	Units
Average OD	9.693	0.018 32	Gaussian	in
Average WT	0.475 2	0.010 31	Gaussian	in
Yield stress	127.6	4.517	Gaussian	ksi
Ovality	0.240 7	0.081 46	two-parameter Weibull	%
Eccentricity	5.170	1.639	two-parameter Weibull	%
Residual stress	−18.12	3.364	Gaussian	ksi
Model uncertainty	0.968 1	0.052 57	Gaussian	—

c) Next, calculate predicted failure probability ϕ_f for the Table H.5 PDF data and a given deterministic load L_{nom}. Taking L_{nom} = 6 100 psi gives $\phi_f = 4.51 \times 10^{-3}$, calculated using FORM. This is too low, so L_{nom} is increased until ϕ_f brackets the TRL, as shown in Table H.6 below.

Table H.6 — Case-specific calibration for mill FD00 (9-5/8 in 47 lb/ft P110 HRS) — Large datasets

L_{nom} psi	ϕ_f
6 100	4.511×10^{-3}
6 110	4.769×10^{-3}
6 120	5.039×10^{-3}

d) The design collapse strength is obtained by interpolation as 6 119 psi.

H.4.1.3 Multiple pipe sizes

Determine the design collapse strength of P110 HRS product from mill FD00, for a variety of pipe sizes.

The analysis is similar in many respects to the single pipe size case, but the pipe dimensions (average OD and WT) are now generalized by using a range of dataspace positions. Failure probability and design collapse strength (as down-rating factors $k_{e\ des}$ and $k_{y\ des}$) are then calculated for each dataspace position, as described below.

a) D/t is calculated for each dataspace position, using Equations (F.6) and (F.7) with the specified values of f_{ymn}, E and ν. Equations (F.6) and (F.7) cannot be solved directly for D/t for a given value of p_y/p_e, and the solution is therefore obtained either by iteration, or by using a root-solver routine in a mathematical spreadsheet.

The iterative solution for $\log_{10}(p_y/p_e) = -0.5$ is given for illustration. For $D/t = 10.4$:

$$p_y = (2 \times 110\,000/10.4)\,[1 + (0.5/10.4)] = 22\,171 \quad \text{(H.13)}$$

$$p_e = 2 \times 30 \times 10^6/[(1 - 0.28^2) \times 10.4 \times (10.4 - 1)^2] = 70\,847 \quad \text{(H.14)}$$

$$\log_{10}(p_y/p_e) = \log_{10}(22\,171/70\,847) = -0.504\,5 \quad \text{(H.15)}$$

Table H.7 shows the remaining iterations, and Table H.8 the final D/t value for each dataspace position.

Table H.7 — Iteration for D/t

D/t	p_y psi	p_e psi	$\log_{10}(p_y/p_e)$
10.40	22 171	70 847	–0.504 5
10.50	21 950	68 702	–0.495 5
10.44	22 082	69 978	–0.500 9
10.45	22 060	69 764	–0.500 0

Table H.8 — D/t for each dataspace position

$\log_{10}(p_y/p_e)$	D/t	p_y psi	p_e psi
–0.5	10.45	22 060	69 764
–0.3	12.95	17 644	35 205
–0.1	16.10	14 090	17 738
0.1	20.07	11 237	8 926
0.3	25.06	8 954	4 488
0.5	31.35	7 129	2 255

b) The mean outside diameter and wall thickness are obtained as specified value × bias, for a given specified OD; for instance, for 9-5/8 in and $\log_{10}(p_y/p_e) = -0{,}5$:

— mean average outside diameter = 9.625 × 1.007 1 = 9.693 in;

— mean average wall thickness = (9.625/10.45) × 1.006 8 = 0.927 3 in;

— standard deviation of average wall thickness = 0.927 3 × 0.021 7 = 0.020 12 in.

The remainder of the PDF parameters are as before (Table H.5).

c) The nominal load L_{nom} is then calculated for each dataspace position, using Equation (F.5) with the specified values of D, t, f_{ymn}, E and ν (or equivalently the values of p_e and p_y from step a), a decrement factor Ht_{des} obtained as [see Equation (F.4) and Table H.4]:

$$Ht_{des} = (0.127 \times 0.214) + (0.003\,9 \times 5.170) - [0.440 \times (-0.142)] + 0 = 0.113\,2 \quad \text{(H.16)}$$

and initial values for $k_{e\ des}$ and $k_{y\ des}$; 0.825 and 0.91 are usually reasonable choices. Table H.9 shows the results.

NOTE The values of L_{nom} for iterations 2 and 3 are calculated as part of step e), but are given here for the sake of brevity.

Table H.9 — Nominal loads

	L_{nom}		
Iteration	**1**	**2**	**3**
$k_{e\ des}$	0.825	0.825	0.840
$k_{y\ des}$	0.910	0.925	0.925
$\log_{10}(p_y/p_e)$			
–0.5	19 012	19 302	19 328
–0.3	14 440	14 637	14 682
–0.1	10 183	10 282	10 358
0.1	6 251	6 279	6 362
0.3	3 422	3 428	3 483
0.5	1 783	1 785	1 816

d) Predicted failure probability ϕ_f under a deterministic load of L_{nom} is then calculated for each dataspace position, using probabilistic analysis implementing Equation (F.21). ϕ_f is the probability of collapse strength being less than L_{nom}. Figure H.1 shows ϕ_f versus dataspace position, calculated using FORM.

NOTE The curves for iterations 2 and 3 are calculated as part of step e), but are given here for brevity.

e) The best-fit values of $k_{e\ des}$ and $k_{y\ des}$ are then determined by iteration. Figure H.1 shows that ϕ_f for iteration 1 is well below the chosen TRL, with an average of 2.59×10^{-3}. Raising $k_{e\ des}$ will increase L_{nom} in the elastic range, and thus likewise increase ϕ_f. This will tilt the right-hand (elastic) end of the curve upwards. Similarly, increasing $k_{y\ des}$ will tilt the left-hand (yield) end of the curve upwards. It is desired to lift both ends of the curve, but for illustration each will be done one separately. For iteration 2, $k_{y\ des}$ is raised to 0.925; this increases L_{nom} as shown in Table H.9, and ϕ_f as in Figure H.1. The yield end of the curve is now in about the right place. The elastic end is still too low, however, as is the average ϕ_f (3.53×10^{-3}). For iteration 3, $k_{e\ des}$ is increased to 0.84. This gives the best overall fit to the TRL, with an average ϕ_f of 4.83×10^{-3}.

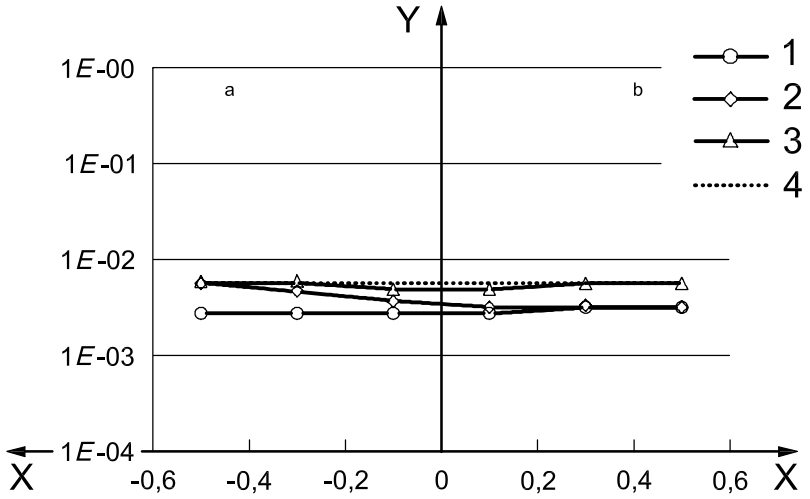

Key

X log (yield/elastic strength)

Y probability of failure

1 iteration 1

2 iteration 2

3 iteration 3

4 target reliability

[a] Yield.

[b] Elastic.

NOTE Manufacturer FD00, P110 seamless HRS.

Figure H.1 — Case-specific calibration for mill FD00 (multiple pipe sizes)

f) The final values of $k_{\text{e des}}$ and $k_{\text{y des}}$ are then used to develop design collapse ratings for the desired sizes and weights, as shown in Table H.10. Equation (F.5) is used, together with the specified values of D, t, f_{ymn}, E and ν, and Ht_{des} from Equation (H.1). The API Bulletin 5C3[2] ratings are given for comparison. Note that the rating for 9-5/8 in 47 lb/ft P110 HRS (6 106 psi) is very slightly lower than the value given by the single-size method [6 119 psi, H.4.1.2 d)]; the difference is because the rating has been calculated as a best fit to the TRL line (Figure H.1), rather than for the exact TRL as before.

Table H.10 — Mill-specific design ratings

Size, weight and grade	API 5C3[2] rating psi	Design rating psi	Increase %
20 in 94 lb/ft P110 HRS	516	590	14.3
13-3/8 in 72 lb/ft P110 HRS	2 880	3 125	8.5
9-5/8 in 47 lb/ft P110 HRS	5 300	6 106	15.2
7 in 32 lb/ft P110 HRS	10 780	11 158	3.5
NOTE The design ratings should not be used for cold rotary straightened pipe.			

H.4.2 Small datasets

Determine the design collapse strength for 9-5/8 in 47 lb/ft P110 HRS from mill FD00, for the actual dataset sizes.

a) Determination of input variable PDF parameters. These are as before (Table H.5), but now the parameters are treated as random variables, rather than deterministic.

b) Sampling uncertainties. Using the methods of H.3.3 gives values as Table H.12.

c) Random realizations of PDF parameters. Table H.11 gives the first and last few realizations. They were obtained using the random deviates generation facility in a mathematical spreadsheet.

Table H.11 — Random realizations of PDF parameters (9-5/8 in 47 lb/ft P110 HRS)

Variable	Parameter	Distribution	Realization					
			1	2	3	…	9 999	10 000
Average OD in	mean	Gaussian	9.692 8	9.692 5	9.692 7		9.693 3	9.695 3
	SD	Gaussian	0.018 71	0.020 82	0.018 19		0.019 08	0.019 03
Average WT in	mean	Gaussian	0.476 2	0.475 8	0.473 4		0.474 1	0.474 2
	SD	Gaussian	0.010 39	0.010 48	0.009 62		0.009 92	0.009 56
Yield stress ksi	mean	Gaussian	126.2	127.0	126.9		127.1	126.9
	SD	Gaussian	4.300	2.839	4.336		4.996	4.911
Ovality %	B	Gaussian	0.262 8	0.267 0	0.276 3		0.271 2	0.276 5
	C	log-normal	3.219	3.229	3.251		3.213	3.240
Eccentricity %	B	Gaussian	5.706	5.739	5.829		5.847	5.543
	C	log-normal	3.524	3.590	3.579		3.438	3.392
Residual stress ksi	mean	Gaussian	−17.69	−17.37	−17.91		−18.31	−18.24
	SD	Gaussian	3.493	3.251	3.559		3.204	3.333
Model uncertainty	mean	Gaussian	0.960 8	0.961 9	0.967 5		0.971 8	0.964 8
	SD	Gaussian	0.048 22	0.047 96	0.058 16		0.049 33	0.056 64

Table H.12 — Sampling uncertainties

Variable	Samples	Gaussian		Two-parameter Weibull		Units
		mean	SD	B	C	
		mean SD	mean SD	mean SD	mean SD	
Average OD	203	9.693 0.001 286	0.018 32 0.000 909			in
Average WT	132	0.475 2 0.000 898	0.010 31 0.000 635			in
Yield stress	46	127.6 0.666 0	4.517 0.470 9			ksi
Ovality	204			0.268 9 0.005 747	3.276 0.041 23	%
Eccentricity	194			5.745 0.117 1	3.510 0.066 34	%
Residual stress	54	−18.12 0.457 8	3.364 0.323 7			ksi
Model uncertainty	75	0.968 1 0.006 070	0.052 57 0.004 292			

d) The predicted failure probability (ϕ_f) is then calculated for each realization. Table H.13 gives ϕ_f for the first and last few realizations, for a deterministic load L_{nom} of 5 960 psi. All values were calculated using FORM.

Table H.13 — Predicted failure probability for each realization (L_{nom} = 5 960 psi)

Realization	ϕ_f
1	1.641×10^{-3}
2	1.488×10^{-3}
3	3.947×10^{-3}
…	…
9 999	1.516×10^{-3}
10 000	3.357×10^{-3}

e) The probability distribution of ϕ_f (Figure H.2) is determined by the counting the number of occurrences of ϕ_f in each interval. The 95 % confidence value is taken; this is obtained by interpolating the cumulative density.

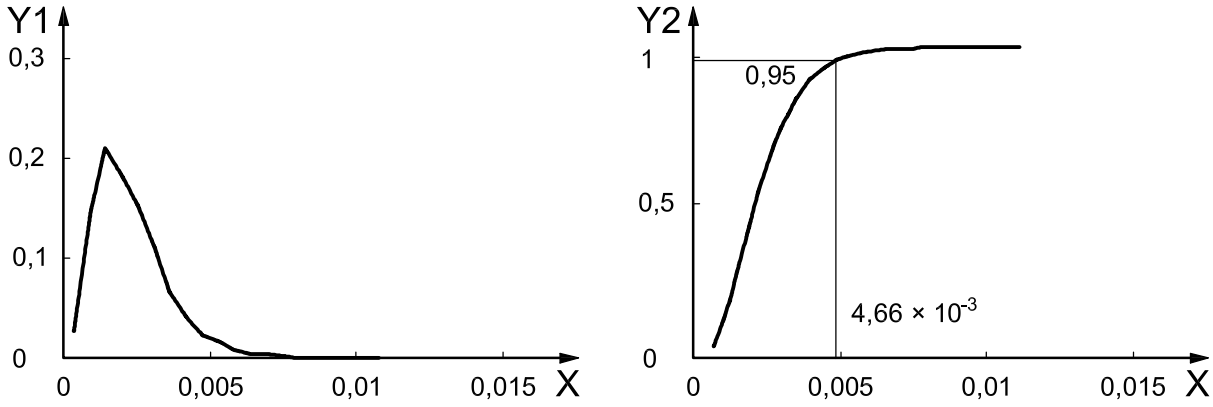

a) Probability distribution function (PDF) **b) Cumulative distribution function (CDF)**

Key

X probability of failure

Y1 probability density

Y2 cumulative probability

NOTE Manufacturer FD00, 9-5/8 in 47 lb/ft P110 HRS.

Figure H.2 — PDF and CDF of predicted failure probability (L_{nom} = 5 960 psi)

f) For L_{nom} = 5 960 psi, the 95 % confidence failure probability ($\phi_{f\ 0.95}$) is 4.66×10^{-3}, Figure H.2. This is slightly too low, and L_{nom} must therefore be increased. Table H.14 shows L_{nom} versus $\phi_{f\ 0.95}$. The design strength is the value of L_{nom} to make $\phi_{f\ 0.95}$ equal the TRL. This is obtained by interpolation as 5 973 psi, some 2.4 % lower than the large-dataset value.

Table H.14 — Case-specific calibration for mill FD00 (9-5/8 in 47 lb/ft P110 HRS) — Small datasets

L_{nom} psi	$\phi_{f\,0,95}$
5 960	4.663×10^{-3}
5 970	4.919×10^{-3}
5 980	5.186×10^{-3}

Figure H.3 shows how collapse rating varies with dataset size, for the hypothetical case of all input variable dataset sizes being equal[87]. The curves are specific to the given case, and should not be used for general guidance.

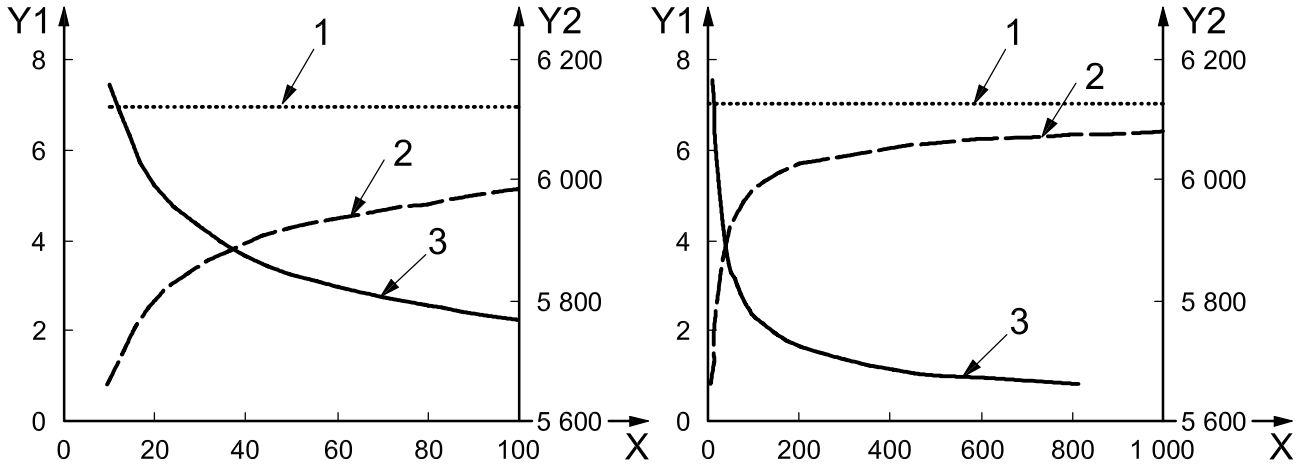

Key

X dataset size

Y1 reduction with respect to large dataset limit, %

Y2 collapse rating, psi

1 large dataset limit

2 rating

3 reduction

Figure H.3 — Reduction in design strength vs. dataset size (mill FD00, 9-5/8 in 47 lb/ft P110 HRS)

Annex I
(informative)

Collapse test procedure

I.1 Introduction

To be acceptable for ISO/API use, collapse tests should be conducted as described below.

I.2 Test specimen

The minimum length of the collapse test specimen should be:

— eight times the specified diameter (D) for specified diameters of 9-5/8 in and below;

— seven times the specified diameter (D) for specified diameters greater than 9-5/8 in.

In addition to the length of the collapse test specimen, additional material should be allocated for the residual stress and tensile test specimens (see Figure I.1).

I.3 Test apparatus

The test apparatus should apply the test pressure to the full specimen length. It should not impose radial or axial restraints on the specimen, either mechanically or hydraulically, and should not apply pressure to the inside surface of the specimen. For combined collapse and axial load tests, the apparatus should maintain the axial load within ±1 % of the target value during application of external pressure.

The test chamber should be equipped with a maximum reading pressure-measuring device which is open to the test chamber during the test. The device should be certified by the manufacturer to be accurate within 0,5 % of the full scale reading.

The pressure-measuring device should be equipped with a damping system to bleed pressure slowly upon specimen collapse. The device should be calibrated at six monthly intervals, or more frequently if there is reason to doubt its accuracy. The error within its working range should not exceed 1 %.

I.4 Measurements prior to collapse testing

I.4.1 General

Pipe geometry, yield stress, and residual stress should be accurately measured prior to collapse testing, as described below.

I.4.2 Pipe geometry

I.4.2.1 General

Average outside diameter, average wall thickness, ovality and eccentricity should be measured at five equally spaced locations, as shown in Figure I.1. Measurements and calculations for each location should be as described in I.4.2.2 to I.4.2.5.

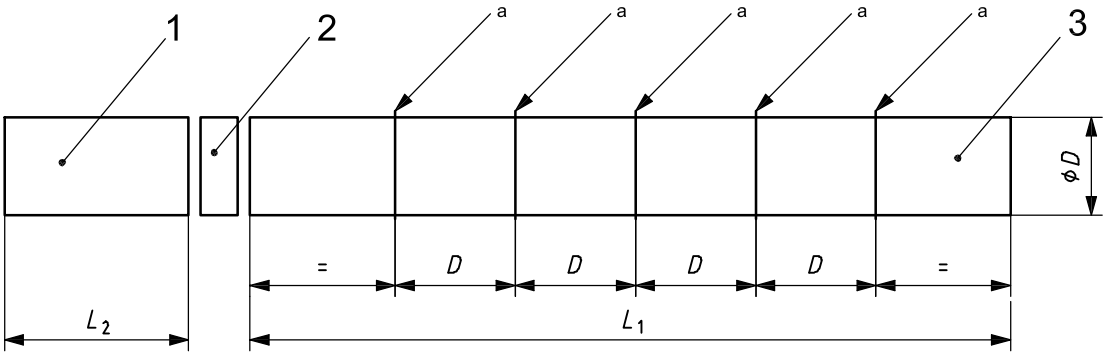

Key

1 residual stress test specimen
2 tensile test specimen
3 collapse test specimen

D outside diameter
L_1 minimum length of collapse test specimen
L_2 minimum length of residual stress test specimen

a Five equally spaced locations at which average outside diameter, average wall thickness and ovality are measured, and eccentricity calculated from wall thickness measurements.

Figure I.1 — Measurements prior to collapse testing

I.4.2.2 Average outside diameter

Average outside diameter should be measured with a pi tape.

I.4.2.3 Average wall thickness

Wall thickness should be measured at eight equally spaced positions (that is, at 45° intervals), and the average taken. Thicknesses should be measured and recorded to a minimum accuracy of 0,1 mm.

I.4.2.4 Ovality

Ovality should be measured with an API ovality gauge or equivalent. Readings should be taken over all circumferential positions: measurements at equally spaced intervals (e.g. 45°) are not acceptable. Ovality should be calculated as 100 $(D_{max} - D_{min})/D_{ave}$, where D_{ave} is the average outside diameter from I.4.2.2.

I.4.2.5 Eccentricity

Eccentricity should be calculated as 100 $(t_{c\ max} - t_{c\ min})/t_{c\ ave}$, where $t_{c\ max}$ and $t_{c\ min}$ are respectively the maximum and minimum wall thicknesses from the eight circumferential measurements of I.4.2.3, and $t_{c\ ave}$ is the average wall thickness.

I.4.3 Yield stress

A tensile test should be conducted for each collapse test sample. The tensile specimen should be taken from pipe adjacent to the end of the collapse test specimen, as shown in Figure I.1. Tensile testing should be in accordance with ISO 11960 or API 5CT.

If the pipe is flame-cut to obtain material for a tensile test specimen, the specimen should not be prepared from areas including the heat-affected zone.

I.4.4 Residual stress

I.4.4.1 Measurement and calculation

Residual stress should be measured for each collapse test sample, using the split ring method. The ring should be taken from pipe adjacent to the end of the collapse test specimen, as shown in Figure I.1. Sample lengths of at least twice the outside diameter are required in order to accurately measure residual stress[94]; shorter samples give lower predicted residual stresses. Accordingly, two alternative approaches may be used, namely:

a) full length ($L/D \geqslant 2$) specimens;

b) shorter specimens ($2 > L/D \geqslant 0{,}5$), with the apparent residual stress corrected using a product-specific calibration curve for the effect of sample length. I.4.4.2 gives instructions for the preparation and use of such curves.

   The calibration curve may be used for all subsequent collapse tests for the given manufacturing process. If any relevant part of the process changes (tempering temperature, straightening method, etc.), testing should be repeated and the curve recalculated.

Testing should be in accordance with ASTM E1928[4], except as noted above. Residual stress, σ_{res}, is calculated as:

$$\sigma_{res} = Et_{c\ ave}(1/D_{bc} - 1/D_{ac})/(1 - \nu^2) \qquad \text{(I.1)}$$

where

D_{ac} is the average outside diameter after cutting;

D_{bc} is the average outside diameter before cutting;

E is Young's modulus, $206{,}9 \times 10^9$ N/m^2 (30×10^6 psi);

$t_{c\ ave}$ is the average actual wall thickness;

ν is Poisson's ratio, 0,28.

This results in a negative residual stress if the pipe springs open, and a positive stress if it springs shut. This is consistent with the sign convention used in Annex F (compression at ID face is negative).

I.4.4.2 Correction for specimen length

I.4.4.2.1 General

Correction curves should be based on test results for a total of twenty specimens of lengths from $0{,}5D$ to $2{,}0D$. The slit ring method should be used, and residual stress should be calculated as described in I.4.4.1. The specimen lengths and cutting sequence should be as shown in Figure I.2. All specimens should be cut from a single pipe, as residual stress is approximately constant along each pipe but varies between pipes.

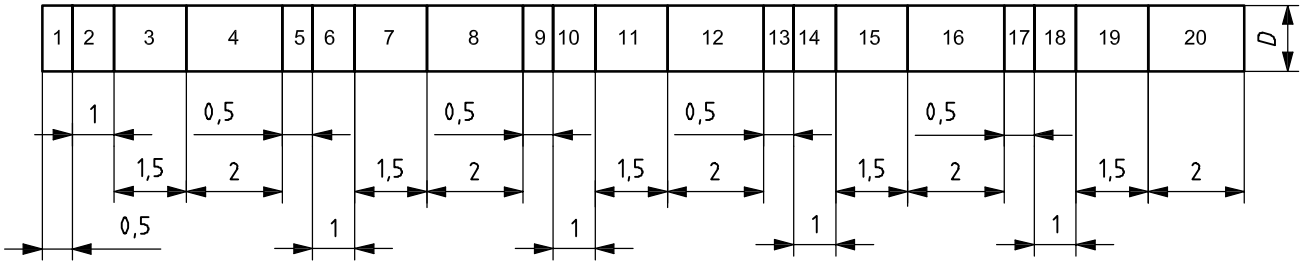

Key

L length of test specimen D outside diameter 1 to 20 order of cutting specimens

Figure I.2 — Order of cutting specimens from test pipe

The mean apparent residual stress should be calculated for each L/D, and divided by the mean residual stress for $L/D = 2$ to determine predicted/actual stress versus specimen length, a plot of which is the correction curve. The line can be assumed to become horizontal at $L/D = 2$. Figure I.3 gives an example of curve preparation. Separate curves should be prepared for each grade and heat treatment type (e.g. normalized N80 and quenched and tempered N80 are separate cases).

I.4.4.2.2 Example of use

A slit ring specimen of length $0.75D$ gives an apparent residual stress of −23.56 ksi. Reference to a correction curve previously prepared for the relevant grade and heat treatment (Figure I.3) gives a correction factor of 0.804. The actual residual stress is therefore −23.56/0.804 = −29.3 ksi. Figure I.3 is for illustration only, and should not be used for any other purpose.

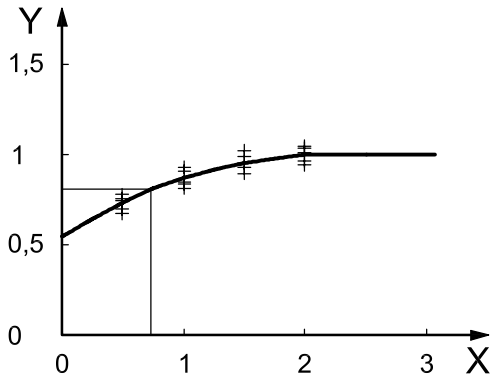

Key

X specimen length/outside diameter

Y predicted residual stress/actual residual stress

For a given grade and heat treatment, slit ring testing of a single pipe gives predicted residual stresses as follows:

	L/D			
	0.5	**1.0**	**1.5**	**2.0**
Predicted residual stress	−27.60 −27.97 −24.66 −25.76 −28.70	−31.28 −33.49 −34.22 −30.91 −29.81	−36.43 −37.54 −35.14 −34.22 −33.12	−37.35 −38.64 −35.33 −34.78 −37.90
Mean	−26.94	−31.94	−35.29	−36.80
Predicted/ actual stress	−26.94/ −36.80	−31.94/ −36.80	−35.29/ −36.80	−36.80/ −36.80
Ratio	0.732	0.868	0.959	1

Figure I.3 — Example of preparation of residual stress correction curve

I.5 Test procedure

The exterior surface of the specimen should be hydraulically loaded at a rate sufficiently slow as to permit reading of the collapse pressure within the specified accuracy. Tests may be conducted either with or without axial stress. If the former, the axial load should be applied first, and held constant during pressure loading.

I.6 Data reporting

The data reported should be as shown in Table I.1. The pipe geometry properties (average outside diameter, average wall thickness, ovality and eccentricity) should be the average of the values for the five circumference locations. Data should be provided in electronic format if at all possible.

Table I.1 — Format for reporting collapse test data

Nominal OD	Nominal weight	Grade	Nominal wall thickness	Forming process [a]	Heat treatment [b]	API yield stress	Average OD [c]	Ovality [c, d]	Average wall thickness [a]	Eccentricity [c, e]	Straightening [f]	Residual stress [g]	L/D [h]	Axial stress [i]	Collapse pressure
in	lb/ft		in			ksi	in	%	in	%		ksi		ksi	ksi
7.000	26.0	P110	0.362	SR	QT	117.9	7.047	0.085	0.364	12.4	CG	–27.9	11.2	12.1	8.17
7.000	26.0	P110	0.362	SR	QT	120.6	7.044	0.241	0.366	6.8	CG	–25.6	11.2	11.4	7.74
7.000	26.0	P110	0.362	SR	QT	118.2	7.046	0.185	0.363	9.0	CG	–28.1	11.2	0	7.57
7.000	26.0	P110	0.362	SR	QT	115.1	7.046	0.170	0.366	22.5	CG	–24.2	11.2	0	7.65
7.000	26.0	P110	0.362	SR	QT	113.4	7.043	0.071	0.363	9.9	CG	–34.7	11.2	0	8.31

NOTE 1 Data may be entered in metric units if desired.

[a] Forming process:

- SP = seamless, pilger mill; SM = seamless, plug mill; SR = seamless, retained or floating mandrel mill; SS = seamless, stretch reduced; SE = seamless, hot expanded.
- WE = welded, electric weld; WL = welded, laser weld; WS = welded, submerged arc weld.

[b] Type of heat treatment/cold working:

- AR = as rolled; CR = control rolled; NR = normalized; NT = normalized and tempered; QT = quenched and tempered; CP = cold worked, pilgered; CD = cold worked, drawn.

[c] Average of values for the circumferences.

[d] Ovality = 100 (maximum OD – minimum OD)/average OD.

[e] Eccentricity = 100 (maximum WT – minimum WT)/average WT.

[f] Type of straightening:

- NS = not straightened; CG = cold gag straightened; CX = cold cross-rolled straightened; CS = cold straightened and stress-relieved; HR = hot rotary straightened.

[g] Compression at ID face is negative. Hence enter residual stress as negative if the pipe springs open after cutting, and positive if it springs shut.

[h] L = specimen length, D = nominal diameter.

[i] Tension is positive.

Annex J
(informative)

Discussion of equations for joint strength

J.1 Introduction

Joint strength is a measure of the structural integrity of a threaded connection, and does not include consideration of leak resistance. For casing applications, where installation of the tubular string is considered permanent, the limit load may be based on either yield or fracture/pull-out of the connector. For tubing applications, where the tubular string may be repeatedly recovered from and re-installed in the wellbore, the limit load is usually based on yield of the connector.

J.2 Design equations for tensile joint strength of API casing connections

J.2.1 General

The following tensile joint strength performance properties apply to casing connections manufactured in accordance with API 5B and ISO 11960 or API 5CT.

J.2.2 Round thread casing joint strength

J.2.2.1 Limit state equation

Round thread casing joint strength is calculated (in USC units) by taking the minimum of the fracture strength and pull-out strength of the connection:

$$P_j = A_{jp} f_{up} \text{ (fracture strength)} \tag{J.1}$$

or

$$P_j = A_{jp} L_{et} [(0.74 D^{-0.59} f_{up})/(0.5 L_{et} + 0.14 D) + f_{yp}/(L_{et} + 0.14 D)] \text{ (pull-out strength)} \tag{J.2}$$

where

$$A_{jp} = \pi/4\ [(D - 0.142\ 5)^2 - d^2] \tag{J.3}$$

and

A_{jp} is the area of the pipe cross section under the last perfect thread, in square inches;

D is the specified pipe outside diameter, in inches;

d is the pipe inside diameter, $d = D - 2t$, in inches;

f_{up} is the tensile strength of a representative tensile specimen from the pipe body, in psi;

f_{yp} is the yield strength of a representative tensile specimen from the pipe body, in psi;

L_{et} is the engaged thread length, [$= L_4 - M$] for nominal make-up, in accordance with API 5B, in inches;

P_j is the joint strength, in lbs;

t is the specified pipe wall thickness, in inches.

J.2.2.2 Design equation

Round thread casing design joint strength is calculated (in USC units) by taking the minimum of the fracture strength and pull-out strength of the connection:

$$P_j = 0.95\, A_{jp} f_{umnp} \text{ (fracture strength)} \quad \text{(J.4)}$$

or

$$P_j = 0.95\, A_{jp} L_{et} [(0{,}74 D^{-0{,}59} f_{umnp})/(0{,}5 L_{et} + 0{,}14 D) + f_{ymnp}/(L_{et} + 0{,}14 D)] \text{ (pull-out strength)} \quad \text{(J.5)}$$

where

$$A_{jp} = \pi/4\, [(D - 0{,}142\,5)^2 - d^2] \quad \text{(J.6)}$$

and

A_{jp} is the area of the pipe cross section under the last perfect thread, in square inches;

D is the specified pipe outside diameter, in inches;

d is the pipe inside diameter, $d = D - 2t$, in inches;

f_{umnp} is the specified minimum tensile strength of the pipe body, in psi;

f_{ymnp} is the specified minimum yield strength of the pipe body, in psi;

L_{et} is the engaged thread length, [$= L_4 - M$] for nominal make-up, in accordance with API 5B, in inches;

P_j is the joint strength, in lbs;

t is the specified pipe wall thickness, in inches.

J.2.2.3 Background

Equations (J.4) and (J.5) apply to both short and long threads and couplings. Equations (J.4) and (J.5) were adopted at the June 1963 API Standardization Conference as reported in API Circular PS 1255. Derivation of the limit state equations is covered in Reference [120]. The equations are based on the results of an API-sponsored test programme consisting of tension tests of 162 joints of round-thread casing in grades K55, N80 and P110, covering a range of wall thicknesses in 114,3 mm, 127,0 mm, 139,7 mm, 168,3 mm, 177,8 mm, 244,5 mm and 273,0 mm diameters, using both short and long threads where called for by the size and grade tested. Fourteen tests failed by fracture of the pipe and 148 tests failed by pull-out. The fracture strength Equation (J.4) agrees satisfactorily with the 14 test fractures. The pull-out strength Equation (J.5) is based on analytical considerations and was adjusted to fit the data by statistical methods. The analytical procedure comprehended coupling properties, but it was found by analysis of the current group of tests that the coupling was non-critical for standard coupling dimensions as listed in API 5B. Subsequent testing established that these equations are also applicable to J55 casing.

The factor 0,95 in Equations (J.4) and (J.5) originates in the statistical error of a multiple-regression equation with adjustment to permit the use of minimum properties in place of average properties.

J.2.2.4 Coupling fracture strength

J.2.2.4.1 Limit state equation

Should the coupling dimensions be such that coupling fracture strength can be lower than either the fracture strength or pull-out strength of the pipe body, the coupling fracture strength can be determined from:

$$P_j = A_{jc} f_{uc} \tag{J.7}$$

where

A_{jc} is the area of the coupling cross section; $A_{jc} = \pi/4\ (W^2 - d_1{}^2)$;

d_1 is the diameter at the root of the coupling thread at the end of the pipe in the power-tight position;

f_{uc} is the tensile strength of a representative tensile specimen from the coupling;

P_j is the joint strength;

W is the specified coupling outside diameter, in accordance with ISO 11960 or API 5CT;

and

$$d_1 = E_1 - (L_1 + A)T_d + H - 2s_{rn} \tag{J.8}$$

where

A is the hand-tight standoff;

E_1 is the pitch diameter at the hand-tight plane, in accordance with API 5B;

H is the thread height of a round thread equivalent Vee thread: 2,199 6 mm (0.086 60 in) for 10 TPI, 2,749 6 mm (0.108 25 in) for 8 TPI;

L_1 is the length from the end of the pipe to the hand-tight plane, in accordance with API 5B;

s_{rn} is the root truncation of the pipe thread of round threads: 0,36 mm (0.014 in) for 10 TPI, 0,43 mm (0.017 in) for 8 TPI;

T_d is the taper (on diameter): 0,062 5 mm/mm (0.062 5 in/in).

J.2.2.4.2 Design equation

Should the coupling dimensions be such that coupling fracture strength can be lower than either the fracture strength or pull-out strength of the pipe thread, the coupling fracture strength (joint strength P_j) can be determined from:

$$P_j = 0{,}95\ A_{jc} f_{umc} \tag{J.9}$$

where

A_{jc} is the area of the coupling cross section; $A_{jc} = \pi/4\ (W^2 - d_1{}^2)$;

d_1 is the diameter at the root of the coupling thread at the end of the pipe in the power-tight position;

f_{umc} is the tensile strength of a representative tensile specimen from the coupling;

W is the specified coupling outside diameter, in accordance with ISO 11960 or API 5CT;

and

$$d_1 = E_1 - (L_1 + A)T_d + H - 2s_{rn} \quad \text{(J.10)}$$

where

A is the hand-tight standoff;

E_1 is the pitch diameter at the hand-tight plane, in accordance with API 5B;

H is the thread height of a round thread equivalent Vee thread: 2,199 6 mm (0.086 60 in) for 10 TPI, 2,749 6 mm (0.108 25 in) for 8 TPI;

L_1 is the length from the end of the pipe to the hand-tight plane, in accordance with API 5B;

S_{rn} is the root truncation of the pipe thread of round threads: 0,36 mm (0.014 in) for 10 TPI, 0,43 mm (0.017 in) for 8 TPI;

T_d is the taper (on diameter): 0,062 5 mm/mm (0.062 5 in/in).

J.2.3 Buttress thread casing joint strength

J.2.3.1 Limit state equation

Buttress thread casing joint strength is calculated by taking the minimum of the pipe thread strength and the coupling thread strength:

$$P_j = A_p f_{up}[1{,}008 - 0{,}039\,6(1{,}083 - f_{yp}/f_{up})D] \text{ (pipe thread strength)} \quad \text{(J.11)}$$

or

$$P_j = A_{jc} f_{uc} \text{ (coupling thread strength)} \quad \text{(J.12)}$$

where

A_{jc} is the area of the coupling cross section; $A_{jc} = \pi/4\ (W^2 - d_1{}^2)$, in square inches;

A_p is the area of the pipe cross section; $A_p = \pi/4\ (D^2 - d^2)$, in square inches;

D is the specified pipe outside diameter, in inches;

d is the pipe inside diameter, $d = D - 2t$, in inches;

d_1 is the diameter at the root of the coupling thread at the end of the pipe in the power-tight position, in inches;

f_{uc} is the tensile strength of a representative tensile specimen from the coupling, in psi;

f_{up} is the tensile strength of a representative tensile specimen from the pipe body, in psi;

f_{yp} is the yield strength of a representative tensile specimen from the pipe body, in psi;

P_j is the joint strength, in lbs;

t is the specified pipe wall thickness;

W is the specified coupling outside diameter, in accordance with ISO 11960 or API 5CT, in inches;

and

$$d_1 = E_7 - (L_7 + I_B)\, T_d + h_B \quad \text{(J.13)}$$

where

E_7 is the pitch diameter, in accordance with API 5B;

h_B is the buttress thread height: 1,575 for SI units, 0.062 for USC units;

I_B is the length from the face of the buttress thread coupling to the base of the triangle in the hand-tight position: 10,16 mm (0.400 in) for Label 1: 4-1/2, 12,70 mm (0.500 in) for sizes between Label 1: 5 and Label 1: 13-3/8, inclusive, and 9,52 mm (0.375 in) for sizes greater than Label 1: 13-3/8;

L_7 is the length of perfect threads, in accordance with API 5B;

T_d is the taper (on diameter).

J.2.3.2 Design equation

Buttress thread casing design joint strength is calculated by taking the minimum of the pipe thread strength and the coupling thread strength:

$$P_j = 0.95 A_p f_{umnp}[1.008 - 0.039\ 6(1.083 - f_{ymnp}/f_{umnp})D] \text{ (pipe thread strength)} \quad \text{(J.14)}$$

or

$$P_j = 0.95 A_{jc} f_{umnc} \text{ (coupling thread strength)} \quad \text{(J.15)}$$

where

A_{jc} is the area of the coupling cross section, $A_{jc} = \pi/4\ (W^2 - d_1{}^2)$, in square inches;

A_p is the area of the pipe cross section, $A_p = \pi/4\ (D^2 - d^2)$, in square inches;

D is the specified pipe outside diameter, in inches;

d is the pipe inside diameter, $d = D - 2t$, in inches;

d_1 is the diameter at the root of the coupling thread at the end of the pipe in the power-tight position, in inches;

f_{umnc} is the specified minimum tensile strength of the coupling, in psi;

f_{umnp} is the specified minimum tensile strength of the pipe body, in psi;

f_{ymnp} is the specified minimum yield strength of the pipe body, in psi;

P_j is the joint strength, in lbs;

t is the specified pipe wall thickness;

W is the specified coupling outside diameter, in accordance with ISO 11960 or API 5CT, in inches;

and

$$d_1 = E_7 - (L_7 + I_B)\, T_d + h_B \quad \text{(J.16)}$$

where

E_7 is the pitch diameter, in accordance with API 5B;

h_B is the buttress thread height: 1,575 for SI units, 0.062 for USC units;

I_B is the length from the face of the buttress thread coupling to the base of the triangle in the hand-tight position: 10,16 mm (0.400 in) for Label 1: 4-1/2, 12,70 mm (0.500 in) for sizes between Label 1: 5 and Label 1: 13-3/8, inclusive, and 9,52 mm (0.375 in) for sizes greater than Label 1: 13-3/8;

L_7 is the length of perfect threads, in accordance with API 5B;

T_d is the taper (on diameter). For buttress threads, T_d is 0,062 5 for sizes Label 1: 13-3/8 and smaller and 0,083 3 for sizes greater than Label 1: 13-3/8.

J.2.3.3 Background

The buttress joint strength equations were adopted at the June 1970 Standardization Conference as reported in API Circular PS-1398. They were based on a regression analysis of 151 tests of buttress thread casing ranging in size from Label 1: 4-1/2 to Label 1: 20 outside diameter and in strength levels from 275,8 MPa to 1034,2 MPa minimum yield. Derivation of the equations is covered in Reference [121].

J.2.4 Extreme-line casing joint strength

J.2.4.1 Limit state equation

Extreme-line casing joint strength is defined by the following expression:

$$P_j = A_{crit} f_u \tag{J.17}$$

where

f_u is the tensile strength of a representative tensile specimen;

A_{crit} is the minimum of:

$\pi/4\ (M^2 - d_b^2)$ if box is critical,

$\pi/4\ (D_p^2 - d_j^2)$ if pin is critical,

$\pi/4\ (D^2 - d^2)$ if pipe is critical;

where

A_x is the maximum diameter at the extreme-line pin seal tangent point;

D is the specified pipe outside diameter;

D_p is the extreme-line pin critical section outside diameter; $D_p = H_x + \delta - \varphi$;

d is the pipe inside diameter, $d = D - 2t$;

d_b is the inside diameter of the critical section of the extreme-line box; $d_b = I_x + 2h_x - \Delta + \theta$;

d_j is the extreme-line specified joint inside diameter, made up;

H_x is the maximum extreme-line root diameter at last perfect pin thread;

h_x is the minimum box thread height for extreme-line casing, as follows:
1,52 mm (0.060 in) for 6 TPI,
2,03 mm (0.080 in) for 5 TPI;

I_x is the minimum extreme-line crest diameter of box thread at Plane H;

M is the specified outside diameter of the extreme-line connection; length from the face of the coupling to the hand-tight plane for line pipe and for round thread casing and tubing, in accordance with API 5B;

O_x is the minimum diameter at the extreme-line box seal tangent point;

P_j is the joint strength;

Δ is the taper drop in extreme-line pin perfect thread length:
6,43 mm (0.253 in) for 6 TPI,
5,79 mm (0.228 in) for 5 TPI;

δ is the extreme-line taper rise between Plane H and Plane J, as follows:
0,89 mm (0.035 in) for 6 TPI,
0,81 mm (0.032 in) for 5 TPI;

φ is ½ the maximum extreme-line seal interference; $\varphi = (A_x - O_x)/2$;

θ is ½ the extreme-line maximum thread interference; $\theta = (H_x - I_x)/2$.

J.2.4.2 Design equation

Extreme-line casing design joint strength is defined by the following expression:

$$P_j = A_{crit} f_{umn} \tag{J.18}$$

where

f_{umn} is the specified minimum tensile strength;

A_{crit} is the minimum of:

$\pi/4\ (M^2 - d_b^2)$ if box is critical,

$\pi/4\ (D_p^2 - d_j^2)$ if pin is critical,

$\pi/4\ (D^2 - d^2)$ if pipe is critical;

where

A_x is the maximum diameter at the extreme-line pin seal tangent point;

D is the specified pipe outside diameter;

D_p is the extreme-line pin critical section outside diameter, $D_p = H_x + \delta - \varphi$;

d is the pipe inside diameter, $d = D - 2t$;

d_b is the inside diameter of the critical section of the extreme-line box, $d_b = I_x + 2h_x - \Delta + \theta$;

d_j is the extreme-line specified joint inside diameter, made up;

H_x is the maximum extreme-line root diameter at last perfect pin thread;

h_x is the minimum box thread height for extreme-line casing, as follows:
1,52 mm (0.060 in) for 6 TPI,
2,03 mm (0.080 in) for 5 TPI;

I_x is the minimum extreme-line crest diameter of box thread at Plane H;

M is the specified outside diameter of the extreme-line connection; length from the face of the coupling to the hand-tight plane for line pipe and for round thread casing and tubing, in accordance with API 5B;

O_x is the minimum diameter at the extreme-line box seal tangent point;

P_j is the joint strength;

Δ is the taper drop in extreme-line pin perfect thread length
6,43 mm (0.253 in) for 6 TPI,
5,79 mm (0.228 in) for 5 TPI;

δ is the extreme-line taper rise between Plane H and Plane J, as follows:
0,89 mm (0.035 in) for 6 TPI,
0,81 mm (0.032 in) for 5 TPI;

φ is ½ the maximum extreme-line seal interference, $\varphi = (A_x - O_x)/2$;

θ is ½ the extreme-line maximum thread interference, $\theta = (H_x - I_x)/2$.

J.2.5 API tubing connections tensile joint strength

J.2.5.1 General

The following tensile joint strength performance properties apply to tubing connections manufactured in accordance with API 5B and ISO 11960 or API 5CT.

J.2.5.2 Non-upset tubing

J.2.5.2.1 General

Non-upset tubing joint strength is calculated as the product of the yield strength and the area of the pipe cross section under the last perfect thread. The areas of the critical sections of regular tubing couplings and special-clearance couplings are, in all instances, greater than the governing critical areas of the pipe part of the joint and do not affect the strength of the joint.

J.2.5.2.2 Limit state equation

The joint strength in tension of non-upset tubing is defined by Equation (J.19):

$$P_j = f_y \{\pi/4 [(D_4 - 2h_s)^2 - d^2]\} \quad \text{(J.19)}$$

where

D is the specified pipe outside diameter;

d is the pipe inside diameter, $d = D - 2t$;

D_4 is the major diameter, in accordance with API 5B;

f_y is the yield strength of a representative tensile specimen;

h_s is the round thread height:
1,312 2 mm (0.055 60 in) for 10 TPI,
1,809 8 mm (0.071 25 in) for 8 TPI;

P_j is the joint strength;

t is the specified pipe wall thickness.

J.2.5.2.3 Design equation

The design joint strength in tension of non-upset tubing is defined by Equation (J.20):

$$P_j = f_{ymn} \{\pi/4 [(D_4 - 2h_s)^2 - d^2]\} \quad \text{(J.20)}$$

where

D is the specified pipe outside diameter;

d is the pipe inside diameter, $d = D - 2t$;

D_4 is the major diameter, in accordance with API 5B;

f_{ymn} is the specified minimum yield strength;

h_s is the round thread height:
1,312 2 mm (0.055 60 in) for 10 TPI,
1,809 8 mm (0.071 25 in) for 8 TPI;

P_j is the joint strength;

t is the specified pipe wall thickness.

J.2.5.3 Upset tubing

J.2.5.3.1 General

Upset tubing joint strength is calculated as the product of the yield strength and the area of the body of the pipe. The area of the section under the last perfect thread of API upset tubing is greater than the area of the body of the pipe. The areas of the critical sections of regular tubing couplings, special-clearance couplings, and the box of integral-joint tubing are, in all instances, greater than the governing critical areas of the pipe part of the joint and do not affect the strength of the joint.

J.2.5.3.2 Limit state equation

The joint strength in tension of upset tubing is defined by Equation (J.21):

$$P_j = f_y [\pi/4 (D^2 - d^2)] \quad \text{(J.21)}$$

where

d is the pipe inside diameter, $d = D - 2t$;

D is the specified pipe outside diameter;

f_y is the yield strength of a representative tensile specimen;

P_j is the joint strength;

t is the specified pipe wall thickness.

J.2.5.3.3 Design equation

The design joint strength in tension of upset tubing is defined by the following expression:

$$P_j = f_{ymn} [\pi/4 (D^2 - d^2)] \quad \text{(J.22)}$$

where

d is the pipe inside diameter; $d = D - 2t$;

D is the specified pipe outside diameter;

f_{ymn} is the specified minimum yield strength;

P_j is the joint strength;

t is the specified pipe wall thickness.

Annex K
(informative)

Tables of calculated performance properties in SI units

K.1 Introduction

All listed values for performance properties in this annex assume a benign environment and material properties conforming to ISO 11960 or API 5CT. Other environments may require additional analyses, such as that outlined in Annex D (informative).

K.2 List of Tables contained in Annex K, and accompanying Notes

Table K.1 — Performance property calculations for external and internal pressure for casing

NOTE 1 All performance properties values in this document assume a benign environment and material properties conforming to ISO 11960 or API 5CT. Other environments may require additional analyses, such as that outlined in Annex D.

NOTE 2 Calculation results for M65 and N80 are repeated for each size and linear mass. The first set represents pipe manufactured using the non-quenched and tempered process. The second set represents pipe manufactured using the quenched and tempered process.

NOTE 3 Calculation results for P110 are repeated for each size and linear mass. The first set represents product inspected to a 12,5 % calibration notch. The second set represents product inspected to a 5 % calibration notch.

NOTE 4 The designation L80* includes grades L80 Type 1 and L80 13Cr.

NOTE 5 The minimum internal yield pressure is the lowest of internal yield pressure of the pipe or the internal yield pressure of the coupling. The internal pressure leak resistance at the E1 plane for round thread casing or at the E7 plane for buttress thread casing may be less than the minimum internal yield pressure for the connection (see Table K.2).

NOTE 6 The collapse resistance values are based on the historical ISO 10400:1993 or API 5C3[2] equations (see Clause 8).

Table K.2 — Performance property calculations for internal pressure leak resistance for casing connections

NOTE 1 All performance properties values in this document assume a benign environment and material properties conforming to ISO 11960 or API 5CT. Other environments may require additional analyses, such as that outlined in Annex D.

NOTE 2 The internal pressure leak resistance at the E1 plane for round thread casing or at the E7 plane for buttress thread casing may be less than the minimum internal yield pressure for the connection (see Table K.1).

Table K.3 — Performance property calculations for axial tension of casing pipe body and connections

NOTE 1 All performance properties values in this document assume a benign environment and material properties conforming to ISO 11960 or API 5CT. Other environments may require additional analyses, such as that outlined in Annex D.

NOTE 2 Calculation results for M65 and N80 are repeated for each size and linear mass. The first set represents pipe manufactured using the non-quenched and tempered process. The second set represents pipe manufactured using the quenched and tempered process. For a particular grade, the axial tension properties are not affected by the heat treat process.

NOTE 3 Calculation results for P110 are repeated for each size and linear mass. The first set represents product inspected to a 12,5 % calibration notch. The second set represents product inspected to a 5 % calibration notch. For a particular grade the axial tension properties are not affected by the different inspection calibration standards.

NOTE 4 The designation L80* includes grades L80 Type 1 and L80 13Cr.

NOTE 5 Some joint strengths for the connections are greater than the corresponding pipe body yield strength.

NOTE 6 For M65 casing, L80 couplings are required. For J55 and K55 casing, the next higher grade coupling is L80. For N80 Q&T casing, the next higher grade coupling is P110. For P110 casing, the next higher grade coupling is Q125. No higher grade couplings have been established for the other grades.

Table K.4 — Performance property calculations for external and internal pressure for tubing

NOTE 1 All performance properties values in this document assume a benign environment and material properties conforming to ISO 11960 or API 5CT. Other environments may require additional analyses, such as that outlined in Annex D.

NOTE 2 Calculation results for N80 are repeated for each size and linear mass. The first set represents pipe manufactured using the non-quenched and tempered process. The second set represents pipe manufactured using the quenched and tempered process.

NOTE 3 Calculation results for P110 are repeated for each size and linear mass. The first set represents product inspected to a 12,5 % calibration notch. The second set represents product inspected to a 5 % calibration notch.

NOTE 4 The designation L80* includes grades L80 Type 1 and L80 13Cr.

NOTE 5 The minimum internal yield pressure is the lowest of internal yield pressure of the pipe or the internal yield pressure of the coupling.

NOTE 6 The collapse resistance values are based on the historical ISO 10400:1993 or API 5C3[2] equations (see Clause 8).

Table K.5 — Performance property calculations for axial tension for tubing pipe body and connections

NOTE 1 All performance properties values in this document assume a benign environment and material properties conforming to ISO 11960 or API 5CT. Other environments may require additional analyses, such as that outlined in Annex D.

NOTE 2 Calculation results for N80 are repeated for each size and linear mass. The first set represents pipe manufactured using the non-quenched and tempered process. The second set represents pipe manufactured using the quenched and tempered process. For a particular grade, the axial tension properties are not affected by the heat treat process.

NOTE 3 Calculation results for P110 are repeated for each size and linear mass. The first set represents product inspected to a 12,5 % calibration notch. The second set represents product inspected to a 5 % calibration notch. For a particular grade, the axial tension properties are not affected by the different inspection calibration standards.

NOTE 4 The designation L80* includes grades L80 Type 1 and L80 13Cr.

Annex L
(informative)

Tables of calculated performance properties in USC units

L.1 Introduction

All listed values for performance properties in this annex assume a benign environment and material properties conforming to ISO 11960 or API 5CT. Other environments may require additional analyses, such as that outlined in Annex D (informative).

L.2 List of Tables contained in Annex L, and accompanying Notes

Table L.1 — Performance property calculations for external and internal pressure for casing

NOTE 1 All performance properties values in this document assume a benign environment and material properties conforming to ISO 11960 or API 5CT. Other environments may require additional analyses, such as that outlined in Annex D.

NOTE 2 Calculation results for M65 and N80 are repeated for each size and weight. The first set represents pipe manufactured using the non-quenched and tempered process. The second set represents pipe manufactured using the quenched and tempered process.

NOTE 3 Calculation results for P110 are repeated for each size and weight. The first set represents product inspected to a 12.5 % calibration notch. The second set represents product inspected to a 5 % calibration notch.

NOTE 4 The designation L80* includes grades L80 Type 1 and L80 13Cr.

NOTE 5 The minimum internal yield pressure is the lowest of internal yield pressure of the pipe or the internal yield pressure of the coupling. The internal pressure leak resistance at the E1 plane for round thread casing or at the E7 plane for buttress thread casing may be less than the minimum internal yield pressure for the connection (see Table L.2).

NOTE 6 The collapse resistance values are based on the historical ISO 10400:1993 or API 5C3[2] equations (see Clause 8).

Table L.2 — Performance property calculations for internal pressure leak resistance for casing connections

NOTE 1 All performance properties values in this document assume a benign environment and material properties conforming to ISO 11960 or API 5CT. Other environments may require additional analyses, such as that outlined in Annex D.

NOTE 2 The internal pressure leak resistance at the E1 plane for round thread casing or at the E7 plane for buttress thread casing may be less than the minimum internal yield pressure for the connection (see Table L.1).

Table L.3 — Performance property calculations for axial tension of casing pipe body and connections

NOTE 1 All performance properties values in this document assume a benign environment and material properties conforming to ISO 11960 or API 5CT. Other environments may require additional analyses, such as that outlined in Annex D.

NOTE 2 Calculation results for M65 and N80 are repeated for each size and weight. The first set represents pipe manufactured using the non-quenched and tempered process. The second set represents pipe manufactured using the quenched and tempered process. For a particular grade, the axial tension properties are not affected by the heat treat process.

NOTE 3 Calculation results for P110 are repeated for each size and weight. The first set represents product inspected to a 12.5 % calibration notch. The second set represents product inspected to a 5 % calibration notch. For a particular grade, the axial tension properties are not affected by the different inspection calibration standards.

NOTE 4 The designation L80* includes grades L80 Type 1 and L80 13Cr.

NOTE 5 Some joint strengths for the connections are greater than the corresponding pipe body yield strength.

NOTE 6 For M65 casing, L80 couplings are required. For J55 and K55 casing, the next higher grade coupling is L80. For N80 Q&T casing, the next higher grade coupling is P110. For P110 casing, the next higher grade coupling is Q125. No higher grade couplings have been established for the other grades.

Table L.4 — Performance property calculations for external & internal pressures for tubing

NOTE 1 All performance properties values in this document assume a benign environment and material properties conforming to ISO 11960 or API 5CT. Other environments may require additional analyses, such as that outlined in Annex D.

NOTE 2 Calculation results for N80 are repeated for each size and weight. The first set represents pipe manufactured using the non-quenched and tempered process. The second set represents pipe manufactured using the quenched and tempered process.

NOTE 3 Calculation results for P110 are repeated for each size and weight. The first set represents product inspected to a 12.5 % calibration notch. The second set represents product inspected to a 5 % calibration notch.

NOTE 4 The designation L80* includes grades L80 Type 1 and L80 13Cr.

NOTE 5 The minimum internal yield pressure is the lowest of internal yield pressure of the pipe or the internal yield pressure of the coupling.

NOTE 6 The collapse resistance values are based on the historical ISO 10400:1993 or API 5C3[2] equations (see Clause 8).

Table L.5 — Performance property calculations for axial tension for tubing pipe body and connections

NOTE 1 All performance properties values in this document assume a benign environment and material properties conforming to ISO 11960 or API 5CT. Other environments may require additional analyses, such as that outlined in Annex D.

NOTE 2 Calculation results for N80 are repeated for each size and weight. The first set represents pipe manufactured using the non-quenched and tempered process. The second set represents pipe manufactured using the quenched and tempered process. For a particular grade, the axial tension properties are not affected by the heat treat process.

NOTE 3 Calculation results for P110 are repeated for each size and weight. The first set represents product inspected to a 12.5 % calibration notch. The second set represents product inspected to a 5 % calibration notch. For a particular grade, the axial tension properties are not affected by the different inspection calibration standards.

NOTE 4 The designation L80* includes grades L80 Type 1 and L80 13Cr.

Bibliography

General

[1] ASTM E1152-95, *Test Method for Determining J-R Curves*

[2] API Bull 5C3, *Bulletin on Formulas and Calculations for Casing, Tubing, Drill Pipe and Line Pipe Properties*, October 1994, 6th edition

[3] API Circular PS-1533, *Equations for the joint strength of threaded line pipe*, developed and presented to the API Committee on Standardization of Tubular Goods by W. O. Clinedinst at the 1976 Standardization Conference

[4] ASTM E1928-99, *Standard Practice for Estimating the Approximate Residual Circumferential Stress in Straight Thin-walled Tubing*, American Society for the Testing of Materials, 1999

[5] BURK, J.D., Fracture Resistance of Casing Steels for Deep Gas Wells, *J. Metals*, January, 1985, pp. 65-70

[6] SHOEMAKER, A.K., *Application of Fracture Mechanics to Oil Country Tubular Goods*, API Pipe Symposium, June 1989

[7] THOMAS, W.H., WILDER, A.B. and CLINEDINST, W.O., *Development of Requirements for Transverse Ductility of Welded Pipe*, presented at the June 1967 API Standardization Conference

Burst

[8] ADAMS, A.J., *Collapse: comparison of direct and synthesis approaches* (2), report prepared by Amerada Hess for API/ISO TC67/SC5/WG2b, January 2000

[9] ANDERSON, T.L., *Fracture Mechanics, Fundamentals and Applications*, second edition, CRC Press, Boca Raton, FL, 1995

[10] BORESI, A.P., SIDEBOTTOM, O.M., *Advanced Mechanics of Materials*, John Wiley and Sons, 1985

[11] BULLOCH, J.H., Stress Corrosion Cracking of Low Alloy Steels in Natural Seawater Environment – The influence of carbon level, *Theoretical and Applied Fracture Mechanics*, **16**, (1991), pp. 1-17

[12] CERNOCKY, E.P., RHODES, P. and MIGLIN, B., *Results of Combined Axial Tension/Compression and Internal Pressure Testing of Mini-Pipe Specimens in H_2S Environment: Discoveries of Material Response to Triaxial Stress with Non-Uniform Exposure to H_2S*, Paper 06130, NACE 2006, March, San Diego CA

[13] CERNOCKY, E.P., AARON, V.D., PASLAY, P.R. and WINK, R.E., *Combined Axial Tension/Compression and Internal Pressure Testing of Mini-Pipe Specimens in H_2S Environment to Determine Three Dimensional (Triaxial) Stress States which Produce Crack Initiation Failure: Explanation of the New Test Fixture, Mini-Pipe Specimen, and Preliminary Test Results*, SPE 97577, 2005

[14] CROLET, J.L. and BONIS, M.R., *Evaluation of the Resistance of Some Highly Alloyed Stainless Steels to Stress Corrosion Cracking in Hot Chloride Solutions under High Pressures of CO_2 and H_2S*, Corrosion/85, Paper 232, NACE International, Houston, TX

[15] FRICK, J.P., *Variations in the Microstructure of Seamless Pipe and their Relationship to Sulfide Stress Cracking*, Corrosion/79, Paper 179, NACE International, Houston, TX

[16] FRICK, J.P., *Variations in environmental cracking resistance of thick-walled low alloy steel tubulars*, Corrosion/88, St Louis, paper 53 (1988), NACE International, Houston, TX

[17] FUNG, Y.C., *Foundations of Solid Mechanics*, Prentice-Hall, 1965

[18] GALAMBOS, T.V. and RAVINDRA, M.K., Properties of steel for use in LRFD, *J. Structural Division*, ASCE, September 1978

[19] GROBNER, P.J., SPONSELLER, D.L. and DIESBURG, D.E., Effect of Molybdenum Content on the Sulfide Stress Cracking Resistance of AISI-Type 4130 Steel with 0.035 % Cb, *Corrosion*, June 1979, pp. 240-249

[20] HIGDON, A., OHLSEN, E.H., STILES, W.B., WEESE, J. A. and RILEY, W.F., Higdon, *Mechanics of Materials*, 3rd edn., John Wiley and Sons, 1976

[21] HUTCHINSON, J.W., Fundamentals of the Phenomenological Theory of Nonlinear Fracture Mechanics, *J. Appl. Mech*., **50**, December 1983, pp. 1042-1051

[22] KAMAT, S.V., MALAKONDAIAH, G., SRINIVAS, M., MARTHANDA MURTHY, J. and RAMA RAO, P., Effect of Alloying Additions on KISSC on Ultrahigh Strength NiSiCr Steel, *Bull. Material Science*, **17**, (6), November 1994, pp. 633-641

[23] KANE, R.D. and GREER, J.B., Sulfide Stress Cracking of High-Strength Steels in Laboratory and Oilfield Environments, *J. Pet. Tech*., November 1977, pp. 1483-1488

[24] KLEVER, F.J., *Formulas for Rupture, Necking, and Wrinkling of OCTG Under Combined Loads*, SPE 102585 presented at the SPE Annual Technical Conference and Exhibition, San Antonio, TX, September 24-27, 2006

[25] KLEVER, F.J. and STEWART, G., *Analytical Burst Strength Prediction of OCTG With and Without Defects*, SPE 48329, 1998

[26] KUMAR, V., GERMAN, M.D. and SHIH, C.F., *An Engineering Approach to Elastic-Plastic Fracture Mechanics*, EPRI Report No. NP-1931, Electric Power Research Institute, Palo Alto, CA, 1981

[27] MACLENNAN, I. and HANCOCK, J.W., Constraint-based Failure Assessment Diagrams, *Int. J. Press. Ves. & Piping*, **64**, 1995, pp. 287-298

[28] MEGUID, S.A., *Engineering Fracture Mechanics*, Elsevier Science Publishers, 1989

[29] PASLAY, P.R., CERNOCKY, E.P. and WINK, R., *Burst pressure prediction of thin-walled, ductile tubulars subjected to axial load*, SPE 48327, 1998

[30] POPOV, E.P., *Introduction to Mechanics of Solids*, Prentice Hall, 1968

[31] SOKOLNIKOFF, I.S., *Mathematical Theory of Elasticity*, McGraw Hill, 1956

[32] STEWART, G. and KLEVER, F.J., *Accounting for Flaws in the Burst Strength of OCTG*, SPE 48330, 1998

[33] SZKLARZ, K.E., *Understanding the Size Effect in NACE Tm0177 Method D (DCB) Testing and Implications for Users*, Corrosion/2001 Paper 1074, NACE International, Houston, TX, 2001

[34] TADA, H., PARIS, P.C. and IRWIN, G.R., *The Stress Analysis of Cracks Handbook*, 2nd edn., Paris Productions In., St. Louis, 1985

[35] TALLIN, A.G., PASLAY, P.R., ONYEWUENYI, O.A., BURRES, C.V. and CERNOCKY, E.P., *The development of a risk-based burst design framework for well casing and tubing*, SPE 48320, 1998

[36] TIMOSHENKO, S.P. and GOODIER, J.N., *Theory of Elasticity*, McGraw Hill, 3rd edn., 1970

[37] WATKINS, M. and VAUGHN, G.A., Effects of H2S Partial Pressure on the Sulfide Stress Cracking Resistance of Steel, *Materials Performance*, January 1986, pp. 44-48

[38] WATKINS, M. and AYER, R., *Microstructure — The critical variable controlling the SSC resistance of low alloy steels*, Corrosion/95, Paper No. 50, NACE International, March 1995

Collapse

[39] ABBASSIAN, F. and PARFITT, S.H.L., Collapse and post collapse behaviour of tubulars: a simple approach, SPE 29458, *Proc. SPE Production Operations Symposium*, Oklahoma City, April 1995

[40] ABRAMOWITZ, M. and STEGUN, I.A., *Handbook of Mathematical Functions*, Dover, 1972

[41] ADAMS, A.J. *et al.,* On the development of reliability-based design rules for casing collapse, SPE 48331, *Proc. SPE Applied Technology Workshop on Risk Based Design of Well Casing and Tubing*, Woodlands, TX, May 1998

[42] ADAMS, A.J. *et al*., On the calibration of design collapse strengths for quenched and tempered pipe, SPE 85112, *SPE Drilling & Completion*, September 2003

[43] ADAMS, A.J., *Collapse: dataset review and production quality statistics*, report prepared for API/ISO TC67/ SC5/WG2b, June 1999

[44] ADAMS, A.J., *Collapse: effect of stress-strain curve shape*, report prepared for API/ISO TC 67/SC 5/WG 2b, September 1999

[45] ADAMS, A.J., *Collapse: comparison of direct and synthesis approaches (2)*, report prepared for API/ISO TC 67/SC 5/WG 2b, January 2000

[46] ADAMS, A.J., *Collapse: trial calibration*, report prepared for API/ISO TC67/SC5/WG2b, April 2000

[47] ADAMS, A.J., *Collapse: trial calibration (2),* report prepared for API/ISO TC67/SC5/WG2b, June 2000

[48] ADAMS, A.J., *Collapse: trial calibration (3),* report prepared for API/ISO TC67/SC5/WG2b, October 2000

[49] ADAMS, A.J., *Collapse: development of non-Q&T ULS model (5),* report prepared for API/ISO TC67/SC5/ WG2b, January 2003

[50] ADAMS, A.J., *Collapse: interim calibration for non-Q&T pipe*, report prepared for API/ISO TC 67/SC 5/WG 2b, May 2003

[51] ADAMS, A.J., *Collapse: design collapse strengths for DIS*, report prepared for API/ISO TC 67/SC 5/WG 2b, June 2003

[52] ANG, A.H-S. and TANG, W.H., *Probability concepts in engineering planning and design, Vol. II: Decision, risk and reliability*, John Wiley, 1984

[53] CALLADINE, C.R., *Theory of shell structures*, Cambridge University Press, 1983

[54] CLINEDINST, W.O., *A rational expression for the critical collapsing pressure of pipe under external pressure, Drilling and Production Practice*, presented at API Chicago meeting.1939, pub. API, 1940

[55] CLINEDINST, W.O., *Development of API collapse pressure equations,* report prepared for the American Petroleum Institute, December 1963

[56] CLINEDINST, W.O., *Collapse Resistance of Pipe*, PhD dissertation, Century University, Los Angeles, California, 1985

[57] CLINEDINST, W.O., *Progress report: round robin collapse test program*, technical note prepared for the American Petroleum Institute, January 1986

[58] DEA(E)-64 project report, *CTR 03: Data analysis*, rev. 02, issued February 1997

[59] DE WINTER, P.E. *et al*., Collapse behaviour of submarine pipelines, in: *Shell structures: stability and strength*, Elsevier, 1985

[60] DITLEVSEN, O. and MADSEN, H.O, *Structural reliability methods*, John Wiley, 1996

[61] EISENHART, C. *et al*., *Techniques of statistical analysis*, McGraw-Hill, 1947

[62] HAAGSMA, S.C. and SCHAAP, D., Collapse resistance of submarine pipelines studied, *Oil and Gas Journal*, February 1981

[63] HOHENBICHLER, M. and RACKWITZ, R., Non-normal dependent vectors in structural safety, *J. Engineering Mechanics Division*, ASCE, **107**, 1981

[64] HOLMQUIST, J.L. and NADAI, A., A theoretical and experimental approach to the problem of collapse of deep-well casing, *Drilling and Production Practice*, 1939, pub. API, 1940

[65] HUANG, N.C. and PATTILLO, P.D., The effect of length:diameter ratio on collapse of casing, Trans. ASME, *J. Pressure Vessel Technology*, **106**, May 1984

[66] Institute of Petroleum Engineering, *Testing of casing under extreme loads*, report prepared at the Technical University of Clausthal for Mannesmann, 1983

[67] ISSA, J.A. and CRAWFORD, D.S., *An improved design equation for tubular collapse*, SPE 26317, Proc. SPE Annual Technical Conference, Houston, TX, October 1993

[68] JIANZENG, H. and TAIHE, S., Equations calculate collapse pressures for casing strings, *Oil and Gas Journal*, January 2001

[69] JOHNSON, N.L. and WELCH, B.L., Applications of the non-central t-distribution, *Biometrika*, **31**, 1939

[70] JU, G.T., *Review of pipe collapse*, presentation made to API/ISO TC67/SC5/WG2b, New Orleans, LA, June 1999

[71] JU, G.T. *et al*., A reliability approach to the design of OCTG tubulars against collapse, SPE 48332*, Proc. SPE Applied Technology Workshop on Risk Based Design of Casing and Tubing*, Woodlands, TX, May 1998

[72] KENDALL, M.G. and STUART, A., *The advanced theory of statistics, Vol. 1: Distribution theory*, Charles Griffin, 1958

[73] KENDRICK, S., The technical basis of the external pressure section of BS 5500, Trans. ASME, *J. Pressure Vessel Technology*, **106**, May 1984

[74] KLEVER, F.J. and TAMANO, T., A new OCTG strength equation for collapse under combined loads, SPE 90904*, Proc. SPE Annual Technical Conference and Exhibition*, Houston, TX, September 2004, and *SPE Drilling & Completion*, September 2006

[75] KURIYAMA, Y. and MIMAKI, T., A new equation for elasto-plastic collapse strength of thick-walled casing, SPE 28327, *Proc. SPE Annual Technical Conference*, New Orleans, LA, September 1994

[76] LENTH, R.V., Cumulative distribution function of the non-central t-distribution, *Statistical algorithms*, **38** (1), 1989

[77] LIEBERMAN, G.J, Tables for one-sided statistical tolerance limits, *Industrial Quality Control*, **14** (10), April 1958

[78] LIU, P.-L. and der KIUREGHIAN, A., Multivariate distribution models with prescribed marginals and covariances, *Prob. Engineering Mechanics*, **1** (2), 1986

[79] MANN, N.R. *et al*., *Methods for Statistical Analysis of Reliability and Life Data*, John Wiley, 1974

[80] MEHDIZADEH, P., Casing collapse performance, Trans. ASME, *J. Engineering for Industry*, **98**, August 1976

[81] MELCHERS, R.E., *Structural reliability analysis and prediction*, 2nd edn., John Wiley, 1999

[82] MURPHEY, C.E. and LANGNER, C.G., Ultimate pipe strength under bending, collapse and fatigue, *Proc. 4th International Symposium on OMAE*, Dallas, TX, February 1985

[83] NATAF, A., Détermination des distributions dont les marges sont données, *Comptes Rendus de l'Académie des Sciences*, **225**, 1962

[84] ADAMS, A.J. *Collapse: effect of input variable cross-correlation*, report prepared for API/ISO TC 67/SC 5/WG 2b, January 2005

[85] ADAMS, A.J. *Collapse: ratings for worst case production*, report prepared for API/ISO TC 67/SC 5/WG 2b, June 2005

[86] ADAMS, A.J. *Collapse: development of non-Q&T ULS model (6),* report prepared for API/ISO TC 67/SC 5/WG 2b, September 2005

[87] ADAMS, A.J. *Collapse: design strength for small datasets*, report prepared for API/ISO TC 67/SC 5/WG 2b, November 2005

[88] Nippon Steel Corp., *Experimental study on the effect of axial loading on collapse resistance of casing*, January 1982

[89] OWEN, D.B., "Tables of factors for one-sided tolerance limits for a normal distribution", Sandia Corporation report, April 1958

[90] PANARELLI, J.E. and HODGE, P.G., Interaction of pressure, end load, and twisting moment for a rigid-plastic circular tube, Trans. ASME, *J. Appl. Mechanics*, September 1963

[91] PATTILLO, P.D. and HUANG, N.C., Collapse of oil well casing with ovality, Trans. ASME, *J. Energy Resources Technol*., **107**, March 1985

[92] RACKWITZ, R., Practical probabilistic approach to design, *Bulletin 112*, Comité Européen du Beton, 1976

[93] RINNE, H., *Taschenbuch der statistik*, Verlag Harri Deutsch, 1997

[94] SACHS, G. and ESPEY, G., *A new method for determination of stress distribution in thin walled tubing*, American Inst. Mining and Met. Engrs. Metals Technology Technical Publication 1384, October 1941; also in Hetenyi, M. (ed.), *Handbook of Experimental Stress Analysis*, John Wiley and Sons, New York, 1957, p. 466

[95] SMALL, N.C., *Plastic collapse of oval straight tubes under external pressure*, ASME publication 77-PVP-57, 1977

[96] SouthWest Research Institute, *Collapse resistance of HC-95 casing*, report prepared for the American Petroleum Institute, ref. 03-6118, November 1982

[97] SouthWest Research Institute, *Collapse resistance of mill selected high collapse grade 95 casing*, report prepared for the American Petroleum Institute, ref. 06-8665, August 1987

[98] STURM, R.G., *A study of the collapsing pressure of thin-walled cylinders*, Bulletin No. 329, University of Illinois Engineering Experiment Station, 1941

[99] Sumitomo Metal Industries report, *On the collapse resistance of commercial casings*, November 1981

[100] Sumitomo Metal Industries Ltd., *Experimental study on the effect of axial loading on collapse resistance of casing*, December 1981

[101] TAMANO, T. *et al.,* A new empirical equation for collapse resistance of commercial casing, *J. Energy Resources Technol.*, ASME, 1983

[102] Tenaris, *Analysis of historical distributions for input parameters of KGT equation*, report prepared for API/ISO TC67/SC5/ WG2B, January 2005

[103] THOFT-CHRISTENSEN, P. and BAKER, M.J., *Structural reliability theory and its applications*, Springer-Verlag, 1982

[104] TIMOSHENKO, S.P. and GERE, J.M., *Theory of elastic stability*, McGraw-Hill International, 2nd edn., 1963

[105] TOKIMASA, K. and TANAKA, K., FEM analysis of the collapse strength of a tube, Trans. ASME, *J. Pressure Vessel Technol.*, May 1986

[106] VERNER, E.A. *et al*., Collapse of thick wall pipe in ultra deep water, *Proc. Conf. on Pipelines in Adverse Environments*, ASCE, San Diego, November 1983

[107] WOLFRAM, S., *Mathematica Technical Manual*, on-line resource at mathworld.wolfram.com, 2005

[108] YEH, M.K. and KYRIAKIDES, S., On the collapse of inelastic thick-walled tubes under external pressure, *Proc. 4th International Symposium on OMAE*, Dallas, TX, February 1985

[109] *Round robin collapse test results of 95 000 psi high collapse casing by four Japanese pipe manufacturers*, report presented to API Standardization Conference, New Orleans, LA, June 1987

[110] Untitled database provided by API manufacturer FD00, 2000

[111] Untitled database provided by API manufacturer HM03, 2002

[112] Untitled database provided by Drilling Engineering Association project DEA-130, 2002

[113] Untitled database provided by Grant Prideco, 2000

[114] *Collapse data of Yawata works*, database provided by Nippon Steel, 1996

[115] Untitled database provided by Nippon Steel, 2000

[116] Untitled database provided by Vallourec and Mannesmann Tubes, 1999

[117] HEBARD, G., reported in Appendix 2-k-4, API Circular PS-1360, Report of the 1968 Pipe Committee meeting

[118] HALD, A., *Statistical Theory With Engineering Applications*, John Wiley & Sons, Inc., New York, 1952

[119] GEORGE, W., Snedecor, *Statistical Methods*, Iowa State College Press, 1956

[120] CLINEDINST, W.O., *Strength of Threaded Joints for Steel Pipe*, Paper No. 64-PET-1 presented at the meeting of the Petroleum Section of ASME in October, 1964

[121] CLINEDINST, W.O., *Buttress Thread Joint Strength*, report shown as Appendix 2-k-6, API Circular PS-1398, June 1970 Standardization Conference

ICS 75.180.10

Price based on 377 pages